UNIVERSITÉ DU QUÉBEC À MONTRÉAL

LES TOURBIÈRES OMBROTROPHES EN TANT QU'ARCHIVES DE LA VARIABILITÉ DES APPORTS DE POUSSIÈRES ATMOSPHÉRIQUES HOLOCÈNES AU QUÉBEC BORÉAL - IMPLICATIONS PALÉOENVIRONNEMENTALES ET PALÉOCLIMATIQUES.

THÈSE

PRÉSENTÉE

COMME EXIGENCE PARTIELLE

DU DOCTORAT EN SCIENCES DE LA TERRE ET DE L'ATMOSPHÈRE

PAR

STEVE PRATTE

JUILLET 2016

REMERCIEMENTS

Je tiens tout d'abord à remercier mes directeurs de thèse Michelle Garneau et François De Vleeschouwer pour leur confiance dans ce projet. Votre disponibilité, votre passion et votre soutien continu au cours de cette thèse sont extrêmement appréciés. Ce fut un privilège de vous côtoyer et de bénificier de votre expertise. Je vous remercie de m'avoir poussé à communiquer dans différents congrès et rencontres, malgré mes réserves. Merci d'avoir cru en moi, surtout quand je doutais. Michelle, merci de constamment t'enquérir du bien-être de tes étudiants, ta générosité est sans limite. Merci François de m'avoir fait voir la valeur du « networking » et de partager ta passion pour la bonne bouffe et le bon vin.

Ma thèse s'étant déroulée en cotutelle avec l'Institut National Polytechnique de Toulouse, il y a de nombreuses personnes que j'aimerais remercier des deux côté de l'Atlantique.

Tout d'abord du côté québécois, j'aimerais souligner le soutien moral, logistique et intellectuel du groupe *Les Tourbeux* en particulier Simon van Bellen, Gabriel Magnan, Antoine Thibault, Hans Asnong, Alexandre Lamarre et Nicole Sanderson. Je tiens à souligner l'excellent travail des assistants de laboratoire ayant contribué à ce projet Julien Baudet-Lancup et Joannie Beaulne. Je suis aussi très reconnaissant envers les chercheurs André Poirier et Bassam Ghaleb. Je vous remercie pour tous vos conseils, pour avoir répondu à mes questions et pour votre aide dans le labo et au spectro. Je tiens aussi à remercier Julien Gogot pour son assitance technique.

Du côté toulousain, je tiens tout particulièrement à remercier Gaël Le Roux et Heleen Vanneste. Vos précieux conseils m'ont probablement permis d'écourter cette thèse de quelques mois. Gaël, un gros *arigato* supplémentaire pour m'avoir inclus dans le projet

J-Peat, ce qui m'a permis de vivre une expérience de terrain extraordinaire au Japon et de participer à la conférence de l'INQUA à Nagoya. J'aimerais aussi saluer le travail exceptionnel que font Marie-Josée Tavella et Virginie Payre-Suc, sans qui Ecolab ne fonctionnerait probablement pas au quart de sa capacité actuelle. Je tiens aussi à remercier Adrien Claustre, Aurélie Lanzanova, David Baqué pour leur aide avec les analyses en spectrométrie de masse.

Je remercie aussi Annick Corrège (Ecolab) et Nicole Turcot (GEOTOP) pour m'avoir aidé avec les nombreuses tâches administratives. La cotutelle est un cauchemar administratif et cela aurait probablement été encore plus pénible sans votre aide. La complexité, le manque d'informations claires et le manque de communication entre les différentes instances est extrêmement frustrant. La thèse en elle-même constitue déjà un processus suffisamment complexe sans que l'addition de procédures admistratives interminables ajoute un stress supplémentaire.

Je voudrais remercier Adrien, Antoine, Juliette et Luiz pour m'avoir hébergé lorsque j'étais sans toit. Je tiens également à remercier Anne pour son accueil et sa gentillesse. Je vous serai toujours reconnaissant à toi et François sans qui mon séjour à Toulouse aurait été beaucoup moins agréable.

Finalement mon parcours menant à ce doctorat n'aurait pas été le même sans le soutien de ma famille. Tout d'abord ma mère, Nicole, qui bien que plus présente de corps l'a toujours été d'esprit et aurait été la première à me pousser dans ce projet. À mon père Christian, ma sœur Sandra et mon frère Simon merci pour votre soutien, pour avoir supporté ma présence inconstante, mais surtout pour me ramener à la « vie normale » quand il le fallait.

Cette thèse a été possible grâce au soutien financier du Fond de recherche du Québec – nature et technologie (FRQNT, dossier 176250), du Conseil national de recherche en sciences naturelles et en génie du Canada (Subvention à la découverte de Michelle

Garneau, CRSNG-SD 250287), du Programme de mobilité Frontenac (Ministère des relations internationales/Consulat Général de France à Québec, dossier 180723), du Programme de formation scientifique dans le Nord de la Commission des affaires polaires (PFSN), ainsi que du Programme de soutien à la mobilité de l'Institut National Polytechnique de Toulouse par le biais de bourses personnelles ou de subventions à mes directeurs de thèse.

AVANT PROPOS

Cette thèse est composée de trois articles, rédigés en anglais, formant chacun un chapitre. Le reste de la thèse est rédigé en français selon les exigences de l'Université du Québec à Montréal. Le premier article, qui s'intitule « Late Holocene atmospheric dust deposition in eastern Canada (St. Lawrence North Shore) » a été accepté pour publication à la revue *The Holocene*, une revue à comité de lecture. Ma directrice de thèse, Michelle Garneau, est deuxième auteure alors que mon directeur, François De Vleeschouwer est troisième auteur. Le deuxième article a été soumis à *Journal of Quaternary Science* (JQS-16-0015), une autre revue à comité de lecture et a pour titre « Geochemical characterization (REE, Nd and Pb isotopes) of atmospheric mineral dust deposited in two maritime peat bogs from the St. Lawrence North Shore (eastern Canada) ». Pour cet article, mon directeur François De Vleeschouwer est le deuxième auteur, alors que ma directrice est troisième auteur. Le troisième article, « Increased atmospheric dust deposition during late Holocene climate instabilities in a boreal bog from north-eastern Canada. », sera soumis prochainement à la revue *Climate of the Past*. Cet article a également été rédigé avec mes directeurs Michelle Garneau et François De Vleeschouwer. Chaque article a été conservé dans son intégralité afin de faciliter la lecture individuelle des chapitres. Ce choix entraîne certaines répétitions notamment dans les sections telles que la méthodologie ou encore les régions et les sites d'étude. Pour chacun des chapitres je suis le principal responsable de la récolte des données, comprenant l'échantillonnage, les analyses de laboratoire, l'interprétation des résultats ainsi que la rédaction. Finalement, une conclusion générale rédigée en français, faisant aussi office de discussion pour l'ensemble des trois chapitres, clôt cette thèse.

TABLE DES MATIÈRES

LISTE DES FIGURES

LISTE DES TABLEAUX

LISTE DES ABRÉVIATIONS ET ACRONYMES

^{14}C	Radiocarbone
^{210}Pb	Isotope Plomb-210
AD	*Anno domini*, années après Jésus-Christ
AMS	Accelerator Mass Spectrometry
BC	Baie-Comeau
BP	Before Present (avant l'actuel i.e. 1950AD)
BSW	Bog Surface Wetness
cal BP	Calibrated years Before Present
CHUR	Chondritic Uniform Reservoir
CRS	Constant Rate of Supply model
DCA	Detrented Correspondance Analysis
HSP	Havre-Saint-Pierre
ICP-MS	Inductively coupled plasma mass spectrometry
IDH	Île du Havre
JTA	July Temperature Anomaly
ka	kiloannum (milliers d'années)

LG2	La Grande 2
LIA	Little Ice Age
MAP	Mean Annual Precipitation
m.a.s.l.	Meter above sea level
MWP	Medieval Warm Period
NAO	North Atlantic Oscillation
PCA	Principal Component Analysis
PVC	Polyvinyl chloride
REE	Rare Earth Elements
RMSEP	Root-Mean-Square Error of Prediction
SD	Standard Deviation
sp.	Specie (singulier)
spp.	Species (pluriel)
UCC	Upper Continental Crust
UOM	Unidentified Organic Matter
WTD	Water Table Depth

RÉSUMÉ

Les poussières atmosphériques jouent un rôle complexe dans le système climatique global étant à la fois un facteur affectant le climat et variant en fonction de ce dernier. Notre compréhension des différentes interactions entre les poussières atmosphériques et le climat est limitée par l'importante variabilité spatiale et temporelle des celles-ci. À l'aide de tourbières ombrotrophes, la variabilité spatiale et temporelle des dépôts de poussières atmosphériques holocènes au Québec boréal fut caractérisée en lien avec les fluctuations climatiques. Les flux de poussières atmosphériques furent reconstruits à l'aide des concentrations en terres rares. Les isotopes du Nd et Pb en combinaison avec les terres rares ont été utilisés afin de déterminer la source des particules déposées dans les tourbières. Afin d'évaluer les liens entre les flux de poussières et la variabilité climatique, les changements temporels dans les flux de poussières et les isotopes du Nd furent comparés à la taille des particules déposées et des reconstitutions écohydrologiques basées sur l'analyse des macrorestes végétaux et des thécamoebiens.

Dans les deux premiers volets de l'étude, les flux de poussières atmosphériques furent reconstruits dans deux tourbières de la région de la Côte-Nord du Québec alors que les particules déposées dans celles-ci furent caractérisées à l'aide des concentrations des terres rares (REE), des isotopes du néodyme et du plomb ainsi que la granulométrie. Les deux profils présentent des valeurs de εNd similaires, ce qui s'explique soit par une source commune des poussières atmosphériques ou encore des sources distinctes, mais possédant des signatures en εNd similaires. Les deux sites étudiés montrent des tendances différentes dans les flux de poussières. La tourbière IDH montre peu de variations dans les flux de poussières, ce qui s'explique en partie par les conditions locales du site d'étude (frange forestière, altitude), qui ont limité les apports de poussières atmosphériques. La tourbière Baie, quant à elle, montre deux périodes de flux de poussières plus élevés soit 1700-1000 et 650-100 cal a BP correspondant à des périodes documentées de refroidissement du climat. Les REE, le εNd et la taille des particules suggèrent qu'au cours des 2000 dernières années, la tourbière de Baie a reçu une proportion accrue de poussières atmosphériques provenant de sources locales. Ces deux périodes ont été identifiées comme étant des épisodes d'instabilité climatique en réponse à une plus grande variabilité des conditions de températures et d'humidité atmosphérique (principalement contrôlée par l'activité solaire). Un changement du régime des vents dans la région a aussi probablement influencé les variations observées.

Dans le troisième chapitre, les mêmes analyses furent réalisées sur une carotte de tourbe prélevée dans une tourbière de la région de la Baie de James, La Grande 2 (LG2). Des

apports accrus de poussières furent observés lors de différentes périodes : 4000 à 3000, 2600 à 2000, 1600 à 1000, 800 à 650 cal a BP et de 1960 à 1990AD. Au moins trois sources distinctes ont contribué aux apports de poussières dans le temps: le sédiment marin à la base de la tourbière, ainsi que la moraine de Sakami, deux sources locales, de même qu'une source probablement plus régionale dont l'origine n'a pas été identifiée. La période allant de 7000 à 4100 cal a BP montre des valeurs près des sources locales (εNd : -36 à -29). Une augmentation graduelle des valeurs de εNd à partir de 4100 cal a BP suggère une diminution des apports locaux de poussières à la faveur d'une source qui n'a pas pu être identifiée.

Dans l'ensemble, la présence de pics de poussières dans deux des trois sites d'étude lors de périodes froides suggère que les flux de poussières seraient un indicateur de conditions froides et sèches au Québec boréal. Ces conditions froides et sèches sont généralement liées à l'intrusion de masses d'air arctique au nord-est du Canada. La présence de certains de ces pics de poussières lors de minima solaires suggère que la variabilité solaireaurait influencé la variabilité climatique. Le fait que les sites de LG2 et Baie montrent des tendances similaires au cours des 2000 dernières années suggère que les deux régions étaient contrôlées par les mêmes processus climatiques.

Mots clés : poussières atmosphériques, terres rares, isotopes du Nd, paléoclimat, tourbières ombrotrophes, Holocène, Québec, forêt boréale

ABSTRACT

Mineral dust plays an important role in the global climate system having effects on the radiation budget and the chemical composition of the atmosphere. Our understanding of the exact role of dust in the Earth's climate system is still poorly constrained mostly due to a lack of data reflecting the high spatial and temporal variability of dust. Using peat bogs, spatial and temporal variability of Holocene dust deposition in boreal Quebec was investigated in relation to climate fluctuations. Dust fluxes were reconstructed using rare earth elements (REE) concentrations in bulk peat, while Nd and Pb isotopes in combination with REE were used to identify the source of dust particles deposited into these bogs. In order to evaluate the relationship between dust fluxes and climate variability, temporal changes in dust flux, and Nd isotopes were compared to dust grain size and ecohydrological reconstructions derived from testate amoebae and plant macrofossils.

In two peat bogs from the North Shore region of the St. Lawrence Estuary (Baie bog) and Gulf (IDH bog), atmospheric dust fluxes were reconstructed using REE concentration while the geochemical composition of deposited dust was characterized using Nd and Pb isotopes combined with REE and grain size. Both peat bogs present similar εNd values, which suggests either a common source or sources with similar signatures in both regions. In terms of dust flux, the two study sites display distinct tendencies. IDH bog show few variations in dust flux, which can be explained by its geographical setting, where a tree fringe and higher altitude likely partially prevent dust from reaching the peat bog. Two dust events were recorded in the Baie bog from 1750 to 1000 cal BP and 600 to 100 cal BP and correspond to documented cold periods. These two periods have been found to occur at the same time as periods of high variability in the macrofossil record (i.e. successive layers dominated by *Sphagnum* or Ericaceae). REE elements, εNd and grain-size distribution suggest that, over the last 2000 years, the Baie bog received more local dust. The two periods were identified as periods of increased local storminess in response to regional hydroclimatic instability and temperature variations mainly controlled by solar activity. These episodes of climatic instability could also have been caused by changes in the wind regime.

The same set of analyses were performed in a third peatland located in the James Bay region, the La Grande 2 bog (LG2). Increases in dust flux were reconstructed from 4000-3000, 2600-2000, 1600-1000, 800-650 cal BP and from 1960-1990AD. The εNd values show a large variability from -37 to -12, identifying a least three sources: local marine sediment, the Sakami moraine and another unidentified source likely from a more regional origin. Between 7000 and 4100 cal BP, εNd values resemble those local

sources (-36 to -29). A gradual increase in εNd signature is observed from 4100 to 1500 cal BP suggesting a decreasing influence of local sources in favor of a yet unidentified source.

The occurrence of increased dust deposition during cold periods in two of the three studied bogs suggests that dust fluxes can be used as an indicator of cold and dry climatic conditions in boreal Quebec. In north-eastern Canada, these cold and dry conditions are usually the results of the intrusion of Arctic air masses. The exact mechanism controlling these incursion is yet unknown, but the similar timing of solar minima and dust peaks suggest that solar irradiance may also have played a role. The fact that both Baie and LG2 sites display similar tendencies during the last 2000 years reveals that both regions were likely controlled by the same climatic processes.

Key words: atmospheric dust, REE, Nd isotopes, paleoclimate, peat bogs, Holocene, Quebec, boreal forest

INTRODUCTION

1. Contexte

Les poussières atmosphériques constituent une composante clé de l'atmosphère et représentent une source importante de matière particulaire. Les poussières minérales constituent l'aérosol le plus abondant comptant pour 40% des émissions globales d'aérosols troposphériques (GIEC, 2013). Les poussières atmosphériques minérales peuvent être de sources naturelles et provenir de l'érosion des roches et des sédiments, du volcanisme, des feux, des aérosols marins de même que des particules cosmogéniques. Les poussières atmosphériques peuvent également être d'origine anthropique et tirer leurs sources entre autres des émissions véhiculaires, des activités minières, des pesticides et du smog. La distinction entre les poussières d'origine naturelle et celles d'origine anthropique peut être difficile à établir (i.e. feux d'origine naturelle vs. provoqués par l'humain ou encore érosion des sols par des processus naturels vs. les activités agricoles). En milieu naturel, les particules fines sont principalement issues de l'érosion de la croûte continentale supérieure, qui constitue l'interface principale entre la géosphère et la biosphère.

Les poussières atmosphériques naturelles jouent un rôle complexe dans le système climatique global étant à la fois un facteur affectant le climat et variant en fonction de ce dernier. Les poussières atmosphériques minérales modifient le budget radiatif global tant par leur capacité de réflexion que d'absorption des rayons (Harrison *et al.*, 2001; Miller et Tegen, 1998) ainsi qu'en tant que noyau de condensation pour les nuages (Yin *et al.*, 2002). « L'année sans été » en 1816, est un exemple de l'impact que les poussières atmosphériques peuvent exercer sur le climat. En effet, les cendres émises

dans l'atmosphère par l'éruption du volcan Pinatubo, aux Philippines, ont affecté plusieurs régions éloignées telles que l'Europe du Nord, le nord-est des États-Unis et l'est du Canada. Suite à cette éruption, les températures moyennes de la saison estivale dans l'ouest et le centre de l'Europe ont considérablement diminué (Oppenheimer, 2003) atteignant des valeurs jusqu'à 3°C inférieures à la moyenne. Les poussières minérales affectent aussi la chimie de l'atmosphère et le cycle biogéochimique de plusieurs éléments (Harrison *et al.*, 2001; Meskhidze *et al.*, 2003). Par exemple, il a été démontré que les poussières sahariennes affectent la nature géochimique des sols des îles Canaries (Menéndez *et al.*, 2007) de même que ceux de la Barbade, des Bahamas et de la Floride (Muhs *et al.*, 2007).

Les poussières atmosphériques minérales sont communément dérivées de la déflation des sols. À l'échelle de la planète, les sols des régions arides et semi-arides constituent la principale source de poussières (Grousset et Biscaye, 2005; Prospero *et al.*, 2002). Les lacs asséchés, les plaines alluviales ainsi que les plaines d'épandage pro-glaciaires représentent aussi des sources importantes de poussières (Prospero *et al.*, 2002). Les principaux facteurs contrôlant la mobilisation des particules incluent la taille des particules de la source, la rugosité de la surface (végétation, topographie et présence de croûte) et le climat (Marticorena *et al.*, 1997). Les principaux facteurs climatiques contrôlant l'émission des particules sont la vitesse du vent et l'humidité des sols (Gillette, 1988). La mobilisation des particules a souvent lieu dans les régions sous l'influence de vents forts. Un niveau élevé de précipitations augmente quant à lui l'humidité et la stabilité du sol par la formation d'une croûte qui le protège contre l'érosion éolienne (Marticorena *et al.*, 1997).

Le transfert des poussières de l'atmosphère vers les surfaces continentales et océaniques (i.e. taux de dépôt) dépend de plusieurs facteurs dont leur concentration dans l'atmosphère, l'intensité des vents les transportant, les précipitations et le couvert végétal (Lawrence et Neff, 2009). Pendant le transport, les particules sont

continuellement « extraites » de l'atmosphère par les processus de dépôt sec et humide. Les particules de la taille des sables et des silts grossiers se déposent généralement par des processus de dépôt sec via des mécanismes gravitationnels (Tegen et Fung, 1994). Les particules de la taille des argiles sont, quant à elles, principalement lessivées par les précipitations (pluie, neige, grêle, dépôt humide), leur taux de transfert vers les sols est donc dépendant du volume total de ces dernières (Tegen et Fung, 1994). Pour ce qui est des particules de la taille des silts, tant les processus de dépôt sec qu'humide constituent des voies de sortie de l'atmosphère. La combinaison de tous ces facteurs fait en sorte que les taux de dépôts de poussières varient de façon importante à des échelles locales à globales.

Notre compréhension de ces différentes interactions avec le climat est limitée par l'importante variabilité spatiale et temporelle des poussières atmosphériques (Harrison *et al.*, 2001). La majorité des études sur les paléo-poussières se concentrent sur les changements entre les périodes glaciaires et interglaciaires puisque le volume de poussières était plus élevé qu'au cours de l'Holocène (Fischer *et al.*, 2007; Lambert *et al.*, 2008). Bien que la variabilité du dépôt de poussières soit d'une amplitude inférieure qu'à l'échelle glaciaire-interglaciaire, la complexité des changements de température et d'humidité au cours de l'Holocène a été suffisamment importante pour affecter la production et le transport des poussières atmosphériques (Wanner *et al.*, 2008). Les projections des différents modèles climatiques suggèrent que certaines régions subiront une augmentation des températures et une diminution des précipitations au cours de prochaines décennies (Diffenbaugh, Giorgi et Pal, 2008; GIEC, 2013). Un tel changement des conditions climatiques résultera probablement en une diminution du couvert végétal entrainant une augmentation du volume de poussières dans l'atmosphère (Pye, 1987). En plus des effets du changement climatique, certaines études montrent que les activités anthropiques, particulièrement au cours des 150 dernières années, ont aussi augmenté le volume et altéré la composition des poussières dans l'atmosphère (Neff *et al.*, 2008; Reynolds *et al.*, 2009). Dans ce contexte, un

nombre plus élevé d'archives de poussières atmosphériques est nécessaire afin de mieux cerner les processus en amont de la production des poussières atmosphériques et les conséquences de la variabilité de ces dernières sur l'environnement.

2. Les archives de poussières atmosphériques

Les glaciers reçoivent des apports éoliens de particules dérivées de l'érosion des sols (De Angelis *et al.*, 1997), d'aérosols marins (Lupker *et al.*, 2010), d'éruptions volcaniques (Abbott et Davies, 2012) et d'activités anthropiques (Boutron, Candelone et Hong, 1995). Les calottes de glace sont limitées géographiquement aux hautes latitudes et à quelques glaciers des basses et moyennes latitudes. Les calottes de glace polaires reçoivent donc des poussières provenant presqu'exclusivement de sources éloignées (Bory, Biscaye et Grousset, 2003; Delmonte *et al.*, 2010). Ainsi, elles enregistrent la variabilité et la magnitude du cycle des poussières à une échelle hémisphérique (Mahowald *et al.*, 2011). Les calottes de glace ont été utilisées pour reconstruire les variations glaciaires-interglaciaires du cycle des poussières sur plusieurs centaines de milliers d'années (Fischer *et al.*, 2007; Petit *et al.*, 1999), permettant d'établir que le volume de poussières atmosphériques était d'au moins un ordre de grandeur plus élevé lors du dernier maximum glaciaire (Late Glacial Maximum : LGM) comparativement à l'Holocène.

Les sédiments marins constituent aussi un type d'archive utile dans l'étude des processus de transport atmosphérique passé (Nakai, Halliday et Rea, 1993). Par contre, les environnements pélagiques sont habituellement caractérisés par des taux de sédimentation faibles, donc par une résolution temporelle plus faible que celle enregistrée dans les calottes de glace. De plus, les apports de matériel non-éolien diluent le signal atmosphérique dans les sédiments marins, ce qui complique l'interprétation de celui-ci (Rea, 1994). Pour cette raison, les sédiments marins offrant

les meilleures conditions pour l'étude des poussières atmosphériques se trouvent loin des sources d'apports fluviaux. A l'instar des calottes de glace, les sédiments marins fournissent des informations sur le transport à longue distance des paléo-poussières (Kohfeld et Harrison, 2001).

Les séquences de loess constituent le principal type d'archive continentale présentement utilisé dans l'étude des paléo-poussières. L'utilité des archives provenant de loess à des échelles glaciaire-interglaciaire et millénaires a déjà été démontré (Mason *et al.*, 2003; Muhs *et al.*, 2008). Par contre, leur interprétation est complexifiée par des processus diagénétiques potentiels ainsi qu'un historique de sources complexes, ce qui limite leur intérêt à des échelles plus fines que celle du millénaire (Kohfeld et Harrison, 2001).

La quantité d'archives continentales de paléo-poussières demeure limitée et couvre des régions restreintes du globe (Kohfeld et Harrison, 2001). Comme mentionné précédemment, les calottes de glace se trouvent principalement aux pôles, alors que les archives de qualité provenant de sédiments marins se trouvent principalement loin des apports fluviaux, donc en océan profond. Dans le cas des loess, ceux-ci sont surtout localisés près de leurs sources soit les déserts. Donc d'autres sources d'information doivent être utilisées afin d'acquérir une vision plus précise des changements de sources, de dépôt et de transport des poussières atmosphériques. Dans ce contexte, les tourbières constituent une alternative afin de pallier cette lacune, plus particulièrement au niveau des reconstitutions holocènes. Avant de discuter des tourbières en tant qu'archives environnementales et de poussières atmosphériques, leur nature et particularités seront brièvement décrites.

3. Les tourbières

Les tourbières couvrent environ 3% de la surface terrestre et sont principalement localisées dans les zones boréales et subarctiques (Tarnocai et Stolbovoy, 2006). Celles-ci occupent une superficie d'environ 1.1 Mkm^2, soit 12% du territoire canadien (Tarnocai *et al.*, 2005). Les tourbières sont des écosystèmes caractérisés par une saturation en eau en raison de nappes phréatiques près de la surface. Ces conditions créent un bilan positif entre la production primaire nette de la végétation et sa décomposition, permettant ainsi une accrétion verticale et latérale de la matière organique dans le temps (Clymo, 1984; Frolking *et al.*, 1998).

Les tourbières peuvent être divisées en deux grandes catégories en lien avec leur développement, leur régime nutritif et leur hydrologie: les tourbières ombrotrophes (communément appelées *bog*) et minérotrophes (communément appelées *fen*). Les tourbières ombrotrophes sont caractérisées par une surface convexe ou bombée, isolée des apports latéraux par ruissellement, et sont alimentées presqu'exclusivement par des apports atmosphériques tels la pluie, la neige ou les poussières (Chambers et Charman, 2004). Ces écosystèmes reçoivent ainsi une quantité limitée de nutriments et possèdent des contenus cendres inférieurs à 5%. Ces faibles apports en nutriments et particules nuisent à la neutralisation des acides produits lors de la décomposition de la matière organique, résultant ainsi en de faibles valeurs de pH (3 à 5.5) (Shotyk, 1988; Steinmann et Shotyk, 1997), La combinaison de conditions anaérobiques ainsi que de faibles pH et apports en nutriments diminue la richesse floristique de ce type de tourbière et résulte généralement en un couvert végétal dominé par les sphaignes, à tout le moins dans l'Hémisphère Nord. Les tourbières minérotrophes reçoivent, quant à elles, tant des apports atmosphériques que des eaux de ruissellement ayant été en contact avec les sols et les roches environnants. Étant alimentées par une quantité plus importante de nutriments, celles-ci sont caractérisées par des valeurs de pH plus élevés

(5.5 à 8.0), une plus grande richesse floristique et des contenus en cendres plus élevés (jusqu'à 35% de la masse sèche) (Shotyk, 1988).

4. Les tourbières en tant qu'archives paléo-environnementales

Les tourbières ombrotrophes constituent d'excellentes archives sédimentaires car elles enregistrent les différents apports provenant de l'atmosphère. Elles sont capables d'enregistrer les changements environnementaux et climatiques à une échelle séculaire et parfois même décennale (Aaby, 1976; Chambers et Charman, 2004). Généralement, les tourbières ombrotrophes sont préférées pour les reconstitutions paléo-environnementales puisque le niveau de leur nappe phréatique est étroitement lié aux conditions atmosphériques (Charman *et al.*, 2009). Plusieurs indicateurs biotiques (thécamoebiens, macrorestes végétaux) et abiotiques (humification, densité sèche, C/N) sont utilisés dans la reconstruction des variations d'humidité de surface de ces écosystèmes (Hughes *et al.*, 2006; Magnan et Garneau, 2014; Mauquoy *et al.*, 2004). Par exemple, à l'aide des macrorestes végétaux de différentes séquences tourbeuses, Barber, Chambers et Maddy (2003) ont reconstruit la variation des conditions d'humidité de surface de tourbières en Irlande et en Angleterre au cours de l'Holocène. Les analyses de thécamoebiens sont souvent combinées à celles des macrorestes végétaux dans les études paléo-environnementales. Comme les assemblages végétaux, les assemblages de thécamoebiens correspondent à une profondeur de nappe phréatique malgré qu'ils répondent plus rapidement que la végétation aux variations de celle-ci (Woodland, Charman et Sims, 1998). La combinaison des macrorestes végétaux, des thécamoebiens et du degré d'humification de la tourbe a permis de montrer l'existence de liens entre l'humidité de surface d'une tourbière de Terre-Neuve et les forçages océaniques et solaires au cours de l'Holocène (Hughes *et al.*, 2006).

En plus de ces indicateurs biologiques classiques, la fraction inorganique contenue dans la tourbe fournit des informations sur l'abondance et la provenance des particules se déposant à la surface des tourbières (Allan *et al.*, 2013; De Vleeschouwer *et al.*, 2014; Sapkota *et al.*, 2007; Shotyk *et al.*, 2002; Vanneste *et al.*, 2015).

5. Les tourbières en tant qu'archives géochimiques

Les tourbières ombrotrophes peuvent être utilisées en tant qu'alternatives aux calottes de glace dans l'étude des apports en particules atmosphériques. Comparativement aux calottes de glace, les tourbières possèdent deux avantages : 1) une plus large distribution géographique et 2) une facilité de datation par les isotopes radioactifs (^{210}Pb, ^{14}C). Puisque la tourbe d'origine ombrotrophe est constituée en grande partie de matière organique, celle-ci permet d'obtenir des chronologies ^{14}C à haute résolution et avec de faibles incertitudes (Charman et Mäkilä, 2003).

Depuis les années 60, un nombre élevé d'études ont utilisé les tourbières en tant qu'archives géochimiques de pollution atmosphérique dans différentes régions d'Europe (De Vleeschouwer *et al.*, 2009; Le Roux *et al.*, 2005; Martinez-Cortizas *et al.*, 2002; Shotyk *et al.*, 1996; Shotyk *et al.*, 1998; Shotyk *et al.*, 2001) et plus récemment d'Amérique du Nord (Givelet, Roos-Barraclough et Shotyk, 2003; Kylander, Weiss et Kober, 2009; Pratte, Mucci et Garneau, 2013; Shotyk et Krachler, 2010). D'autres études se sont plutôt concentrées sur la signature géochimique de séquences tourbeuses lors de la période pré-industrielle (Kylander *et al.*, 2005; Martínez-Cortizas *et al.*, 1999; Roos-Barraclough et Shotyk, 2003; Weiss *et al.*, 2002).

Dans des travaux pionniers sur la géochimie élémentaire de la tourbe, Chapman (1964) a observé une relation entre la quantité de matériel d'origine éolienne et le contenu en Al et Si dans des séquences tourbeuses du nord-est de l'Angleterre. D'une manière similaire, Hölzer et Hölzer (1998) ont utilisé les concentrations en Si et Ti en tant

qu'indicateurs d'érosion des sols dans des profils tourbeux en Allemagne. La concentration de ces éléments lithogéniques dépend du volume et de la nature des particules minérales déposées à la surface des tourbières, ainsi ils reflètent les taux de dépôt de poussières atmosphériques passés.

Au cours des dernières décennies, l'évolution des technologies a permis le développement de nouveaux indicateurs géochimiques autrefois inutilisables en raison de leurs faibles concentrations dans la tourbe. Parmi ceux-ci, les terres rares héritent leur signature chimique de la roche dont ils proviennent suite à l'altération du matériel géologique et ne sont pas significativement affectées par les processus physiques et chimiques au cours de leur transport (McLennan, 1989). Les terres rares peuvent donc être utilisées comme traceurs de source ou éléments de référence dans un large spectre d'études environnementales (Aubert *et al.*, 2006; Chiarenzelli *et al.*, 2001; Greaves, Elderfield et Sholkovitz, 1999). À l'aide des terres rares, il a été révélé que le plateau tibétain a reçu un volume accru de particules provenant du désert de Taklimatan et du plateau de Loess de Chine au cours des 5000 dernières années (Ferrat *et al.*, 2012). Ces apports accrus seraient liés à une intensification des vents associés à la mousson d'hiver d'Asie de l'est et des vents d'ouest (Ferrat et al., 2012). D'une manière similaire, les isotopes radiogéniques, principalement Nd et Pb, ont aussi été utilisés en tant que traceurs de source de poussières atmosphériques puisque leur signature isotopique n'est pas affectée par les processus d'érosion et de transport. Néanmoins, l'analyse des terres rares et des isotopes du néodyme dans les séquences de tourbe est limité, jusqu'à ce jour, à un nombre peu élevé de sites (Allan *et al.*, 2013; Aubert *et al.*, 2006; Le Roux *et al.*, 2012; Vanneste *et al.*, 2015). Malgré leur nombre limité, ces études ont tout de même permis d'identifier des changements importants des taux de dépôt de poussières liés à des variations du climat. Par exemple, l'utilisation de ces indicateurs a permis de retracer l'impact de l'aridification du Sahara sur le volume de poussières en Europe de l'ouest (Le Roux *et al.*, 2012), l'influence des phénomènes El Niño/Oscillation Australe (ENSO) sur le transport de poussières australiennes vers la Nouvelle-Zélande

(Marx, McGowan et Kamber, 2009), l'intensification des vents d'ouest en Terre de Feu lors d'une interruption du réchauffement de l'Antarctique à la transition du dernier maximum glaciaire à l'Holocène (Antarctic Cold Reversal) (Vanneste *et al.*, 2015) ou encore les fluctuations néoglaciaires de l'étendue des glaciers de la Cordillère Darwin au Chili (Vanneste *et al.*, soumis).

6. Objectifs de la thèse

L'objectif principal de cette thèse est de caractériser la variabilité spatiale et temporelle des dépôts poussières atmosphériques naturelles au Québec boréal au cours de l'Holocène en lien avec les fluctuations climatiques. La principale hypothèse qui a été testée est que le climat est le principal facteur contrôlant les changements dans les apports de poussières atmosphériques. Afin de tester cette hypothèse et d'évaluer la variabilité spatiale des dépôts de poussières atmosphériques, une approche multi-sites a été utilisée. Trois tourbières du Québec boréal furent échantillonnées dans trois régions et contextes climatiques différents, soit Baie-Comeau (maritime boréal) et Havre-Saint-Pierre (maritime subarctique), le long de l'Estuaire et du Golfe du Saint-Laurent, et Radisson (continental subarctique), près de la baie de James, dans l'ouest du Québec.

Cette thèse constitue la première étude utilisant les tourbières en tant qu'archives de poussières atmosphériques en Amérique du Nord. De plus, la localisation des sites d'étude à de hautes latitudes a permis l'évaluation du cycle des poussières atmosphériques dans des régions froides et sous-représentées dans l'état actuel de la recherche sur les poussières atmosphériques.

Spécifiquement, les objectifs de la thèse sont de :

1) Reconstituer, à l'aide de la géochimie élémentaire, les variations des apports de poussières atmosphériques dans des tourbières situées dans les portions est et ouest du Québec boréal au cours de l'Holocène moyen et récent;

2) Identifier l'origine des poussières déposées dans ces tourbières, tenter d'en distinguer les sources locales, régionales et de longue-distance et ainsi documenter les processus impliqués dans le transport et les dépôts de ces poussières atmosphériques;

3) Évaluer le lien entre les taux de dépôt de poussières et la variabilité climatique au cours de l'Holocène moyen et récent. Plus précisément, déterminer sous quelles conditions climatiques (conditions froides, chaudes ou sèches, intensité des vents) les pics de poussières atmosphériques ont été produits.

Les objectifs spécifiques n'étant pas exclusifs, ils ne sont pas traités séparément dans les différents chapitres de la thèse, mais plutôt combinés selon les régions d'étude. Ainsi, le premier chapitre traite-t-il de la reconstruction temporelle des apports de poussières et de leur lien avec le climat dans les deux sites de la région de la Côte-Nord, le long de l'Estuaire et du Golfe du Saint-Laurent. Les taux de dépôts de poussières atmosphériques furent reconstruits à l'aide de la somme des concentrations en terres rares. Préalablement, l'immobilité des terres rares dans les séquences de tourbe fut vérifiée à l'aide d'analyses par composantes principales. L'influence climatique sur les apports de poussières a été évaluée en documentant les successions végétales des deux sites d'étude et en comparant avec d'autres archives climatiques régionales déjà publiées.

Le deuxième chapitre se concentre sur l'identification des sources des poussières déposées dans les deux mêmes sites d'étude que dans le premier chapitre. L'origine des poussières atmosphériques a été précisée à l'aide des isotopes du néodyme et du plomb ainsi qu'avec les terres rares. En se concentrant sur les épisodes d'apports accrus de poussières identifiés dans le premier chapitre, les flux de poussières ont été

comparés et combinés avec le εNd ainsi que la granulométrie afin d'extraire des informations supplémentaires sur le climat passé dans la région.

Le chapitre trois intègre les trois objectifs spécifiques de la thèse à partir de l'analyse d'une séquence prélevée dans une tourbière de la région de la rivière La Grande (Radisson), à l'est de la Baie de James. Tout comme pour les chapitres un et deux, les flux de poussières ont été reconstruits à l'aide des concentrations en terres rares et l'origine des poussières déposées à la surface de la tourbière fut identifiée à partir des isotopes du néodyme. Les changements dans les apports de poussières ont été comparés aux changements dans les successions végétales et ceux des thécamoebiens afin d'en extraire des informations sur le climat passé.

Finalement, une comparaison des résultats de reconstruction entre les sites de l'est et de l'ouest du Québec boréal a été réalisée afin de vérifier s'ils étaient soumis ou pas aux mêmes influences climatiques et ainsi évaluer la variabilité spatiale des apports de poussières atmosphériques et du climat à l'échelle du Québec.

7. Références

Aaby, B. (1976). Cyclic climatic variations in climate over the past 5,500 yr reflected in raised bogs. *Nature,* 263(5575), 281-284.

Abbott, P.M. et Davies, S.M. (2012). Volcanism and the Greenland ice-cores: the tephra record. *Earth-Science Reviews,* 115(3), 173-191.

Allan, M., Le Roux, G., Piotrowska, N., Beghin, J., Javaux, E., Court-Picon, M., Mattielli, N., Verheyden, S. et Fagel, N. (2013). Mid and late Holocene dust deposition in western Europe: the Misten peat bog (Hautes Fagnes - Belgium). *Climate of the Past Discussions,* 9(3), 2889-2928.

Aubert, D., Le Roux, G., Krachler, M., Cheburkin, A., Kober, B., Shotyk, W. et Stille, P. (2006). Origin and fluxes of atmospheric REE entering an ombrotrophic peat bog in Black Forest (SW Germany): Evidence from snow, lichens and mosses. *Geochimica et Cosmochimica Acta,* 70(11), 2815-2826.

Barber, K.E., Chambers, F.M. et Maddy, D. (2003). Holocene palaeoclimates from peat stratigraphy: macrofossil proxy climate records from three oceanic raised bogs in England and Ireland. *Quaternary Science Reviews,* 22(5–7), 521-539.

Bory, A.J.M., Biscaye, P.E. et Grousset, F.E. (2003). Two distinct seasonal Asian source regions for mineral dust deposited in Greenland (NorthGRIP). *Geophysical Research Letters,* 30(4).

Boutron, C.F., Candelone, J.-P. et Hong, S. (1995). Greenland snow and ice cores: unique archives of large-scale pollution of the troposphere of the Northern Hemisphere by lead and other heavy metals. *Science of the Total Environment,* 160/161, 233-241.

Chambers, F.M. et Charman, D.J. (2004). Holocene environmental change: contributions from the peatland archive. *The Holocene,* 14(1), 1-6.

Chapman, S.B. (1964). The Ecology of Coom Rigg Moss, Northumberland: II. The Chemistry of Peat Profiles and the Development of the Bog System. *Journal of Ecology,* 52(2), 315-321.

Charman, D.J., Barber, K.E., Blaauw, M., Langdon, P.G., Mauquoy, D., Daley, T.J., Hughes, P.D.M. et Karofeld, E. (2009). Climate drivers for peatland palaeoclimate records. *Quaternary Science Reviews,* 28(19–20), 1811-1819.

Charman, D.J. et Mäkilä, M. (2003). Climate reconstruction from peatlands. *PAGES Newsletter,* 11, 15-17.

Chiarenzelli, J., Aspler, L., Dunn, C., Cousens, B., Ozarko, D. et Powis, K. (2001). Multi-element and rare earth element composition of lichens, mosses, and vascular plants from the Central Barrenlands, Nunavut, Canada. *Applied Geochemistry,* 16(2), 245-270.

Clymo, R.S. (1984). The Limits to Peat Bog Growth. *Philosophical Transactions of the Royal Society of London B: Biological Sciences,* 303(1117), 605-654.

De Angelis, M., Steffensen, J.P., Legrand, M., Clausen, H. et Hammer, C. (1997). Primary aerosol (sea salt and soil dust) deposited in Greenland ice during the

last climatic cycle: Comparison with east Antarctic records. *Journal of Geophysical Research: Oceans,* 102(C12), 26681-26698.

De Vleeschouwer, F., Fagel, N., Cheburkin, A., Pazdur, A., Sikorski, J., Mattielli, N., Renson, V., Fialkiewicz, B., Piotrowska, N. et Le Roux, G. (2009). Anthropogenic impacts in North Poland over the last 1300 years--a record of Pb, Zn, Cu, Ni and S in an ombrotrophic peat bog. *Science of the Total Environment,* 407(21), 5674-5684.

De Vleeschouwer, F., Ferrat, M., McGowan, H., Vanneste, H. et Weiss, D. (2014). Extracting paleodust information from peat geochemistry. *PAGES Magazine,* 22(2), 88-89.

Delmonte, B., Baroni, C., Andersson, P.S., Schoberg, H., Hansson, M., Aciego, S., Petit, J.-R., Albani, S., Mazzola, C., Maggi, V. et Frezzotti, M. (2010). Aeolian dust in the Talos Dome ice core (East Antarctica, Pacific/Ross Sea sector): Victoria Land versus remote sources over the last two climate cycles. *Journal of Quaternary Science,* 25(8), 1327-1337.

Diffenbaugh, N.S., Giorgi, F. et Pal, J.S. (2008). Climate change hotspots in the United States. *Geophysical Research Letters,* 35(16).

Ferrat, M., Langmann, B., Cui, X., Gomes, J. et Weiss, D.J. (2013). Numerical simulations of dust fluxes to the eastern Qinghai-Tibetan Plateau: Comparison of model results with a Holocene peat record of dust deposition. *Journal of Geophysical Research: Atmospheres,* 118(10), 4597-4609.

Ferrat, M., Weiss, D.J., Spiro, B. et Large, D. (2012). The inorganic geochemistry of a peat deposit on the eastern Qinghai-Tibetan Plateau and insights into changing atmospheric circulation in central Asia during the Holocene. *Geochimica et Cosmochimica Acta,* 91(0), 7-31.

Fischer, H., Siggaard-Andersen, M.-L., Ruth, U., Röthlisberger, R. et Wolff, E. (2007). Glacial/interglacial changes in mineral dust and sea-salt records in polar ice cores: Sources, transport, and deposition. *Reviews of Geophysics,* 45(1).

Frolking, S.E., Bubier, J.L., Moore, T.R., Ball, T., Bellisario, L.M., Bhardwaj, A., Carroll, P., Crill, P.M., Lafleur, P.M., McCaughey, J.H., Roulet, N.T., Suyker, A.E., Verma, S.B., Waddington, J.M. et Whiting, G.J. (1998). Relationship between ecosystem productivity and photosynthetically active radiation for northern peatlands. *Global Biogeochemical Cycles,* 12(1), 115-126.

Gillette, D.A. (1988). Threshold friction velocities for dust production for agricultural soils. *Journal of Geophysical Research: Atmospheres,* 93(D10), 12645-12662.

Givelet, N., Roos-Barraclough, F. et Shotyk, W. (2003). Predominant anthropogenic sources and rates of atmospheric mercury accumulation in southern Ontario recorded by peat cores from three bogs: comparison with natural "background" values (past 8000 years). *Journal of Environmental Monitoring,* 5(6), 935-949.

Greaves, M.J., Elderfield, H. et Sholkovitz, E.R. (1999). Aeolian sources of rare earth elements to the Western Pacific Ocean. *Marine Chemistry,* 68(1–2), 31-38.

Groupe d'experts Intergouvernemental sur l'Évolution du Climat (GIEC) (2013). *Changement climatique 2013: les éléments scientifiques.* Contribution du

groupe de travail 1 Contribution au cinquième rapport d'évaluation du Groupe d'experts Intergouvernemental en Évolution du Climat. In: Stocker T.F., Qin, D., Plattner, G.-K., Tignor, M., Allen, S.K., Boschung, J., Nauels, A., Xia, Y., Bex, V., and Midgley, P.M. (eds) Cambridge University Press, Cambridge/New York, pp. 1535.

Grousset, F.E. et Biscaye, P.E. (2005). Tracing dust sources and transport patterns using Sr, Nd and Pb isotopes. *Chemical Geology,* 222(3–4), 149-167.

Harrison, S.P., Kohfeld, K.E., Roelandt, C. et Claquin, T. (2001). The role of dust in climate changes today, at the last glacial maximum and in the future. *Earth-Science Reviews,* 54(1–3), 43-80.

Hölzer, A. et Hölzer, A. (1998). Silicon and titanium in peat profiles as indicators of human impact. *The Holocene,* 8(6), 685-696.

Hughes, P.D.M., Blundell, A., Charman, D.J., Bartlett, S., Daniell, J.R.G., Wojatschke, A. et Chambers, F.M. (2006). An 8500 cal. year multi-proxy climate record from a bog in eastern Newfoundland: contributions of meltwater discharge and solar forcing. *Quaternary Science Reviews,* 25(11–12), 1208-1227.

Kohfeld, K.E. et Harrison, S.P. (2001). DIRTMAP: the geological record of dust. *Earth-Science Reviews,* 54(1–3), 81-114.

Kylander, M., Weiss, D., Martinezcortizas, A., Spiro, B., Garciasanchez, R. et Coles, B. (2005). Refining the pre-industrial atmospheric Pb isotope evolution curve in Europe using an 8000 year old peat core from NW Spain. *Earth and Planetary Science Letters,* 240(2), 467-485.

Kylander, M.E., Weiss, D.J. et Kober, B. (2009). Two high resolution terrestrial records of atmospheric Pb deposition from New Brunswick, Canada, and Loch Laxford, Scotland. *Science of the Total Environment,* 407(5), 1644-1657.

Lambert, F., Delmonte, B., Petit, J.R., Bigler, M., Kaufmann, P.R., Hutterli, M.A., Stocker, T.F., Ruth, U., Steffensen, J.P. et Maggi, V. (2008). Dust-climate couplings over the past 800,000 years from the EPICA Dome C ice core. *Nature,* 452(7187), 616-619.

Lawrence, C.R. et Neff, J.C. (2009). The contemporary physical and chemical flux of aeolian dust: A synthesis of direct measurements of dust deposition. *Chemical Geology,* 267(1–2), 46-63.

Le Roux, G., Aubert, D., Stille, P., Krachler, M., Kober, B., Cheburkin, A., Bonani, G. et Shotyk, W. (2005). Recent atmospheric Pb deposition at a rural site in southern Germany assessed using a peat core and snowpack, and comparison with other archives. *Atmospheric Environment,* 39(36), 6790-6801.

Le Roux, G., Fagel, N., De Vleeschouwer, F., Krachler, M., Debaille, V., Stille, P., Mattielli, N., van der Knaap, W.O., van Leeuwen, J.F.N. et Shotyk, W. (2012). Volcano- and climate-driven changes in atmospheric dust sources and fluxes since the Late Glacial in Central Europe. *Geology,* 40(4), 335-338.

Lupker, M., Aciego, S.M., Bourdon, B., Schwander, J. et Stocker, T.F. (2010). Isotopic tracing (Sr, Nd, U and Hf) of continental and marine aerosols in an 18th century

section of the Dye-3 ice core (Greenland). *Earth and Planetary Science Letters,* 295(1–2), 277-286.

Magnan, G. et Garneau, M. (2014). Evaluating long-term regional climate variability in the maritime region of the St. Lawrence North Shore (eastern Canada) using a multi-site comparison of peat-based paleohydrological records. *Journal of Quaternary Science,* 29(3), 209-220.

Mahowald, N., Albani, S., Engelstaedter, S., Winckler, G. et Goman, M. (2011). Model insight into glacial–interglacial paleodust records. *Quaternary Science Reviews,* 30(7–8), 832-854.

Marticorena, B., Bergametti, G., Gillette, D. et Belnap, J. (1997). Factors controlling threshold friction velocity in semiarid and arid areas of the United States. *Journal of Geophysical Research: Atmospheres,* 102(D19), 23277-23287.

Martinez-Cortizas, A., Garcia-Rodeja, E., Pontevedra Pombal, X., Novoa Munoz, J.C., Weiss, D. et Cheburkin, A. (2002). Atmospheric Pb deposition in Spain during the last 4000 years recorded by two ombrotrophic peat bogs and implications for the use of peat as archive. *Science of the Total Environment,* 292, 33-44.

Martínez-Cortizas, A., Pontevedra-Pombal, X., García-Rodeja, E., Nóvoa-Muñoz, J.C. et Shotyk, W. (1999). Mercury in a Spanish Peat Bog: Archive of Climate Change and Atmospheric Metal Deposition. *Science,* 284(5416), 939-942.

Marx, S.K., McGowan, H.A. et Kamber, B.S. (2009). Long-range dust transport from eastern Australia: A proxy for Holocene aridity and ENSO-type climate variability. *Earth and Planetary Science Letters,* 282(1–4), 167-177.

Mason, J.A., Jacobs, P.M., Hanson, P.R., Miao, X. et Goble, R.J. (2003). Sources and paleoclimatic significance of Holocene Bignell Loess, central Great Plains, USA. *Quaternary Research,* 60(3), 330-339.

Mauquoy, D., van Geel, B., Blaauw, M., Speranza, A. et van der Plicht, J. (2004). Changes in solar activity and Holocene climatic shifts derived from ^{14}C wiggle-match dated peat deposits. *The Holocene,* 14(1), 45-52.

McLennan, S.M. (1989). Rare earth elements in sedimentary rocks; influence of provenance and sedimentary processes. *Reviews in Mineralogy and Geochemistry,* 21(1), 169-200.

Menéndez, I., Díaz-Hernández, J.L., Mangas, J., Alonso, I. et Sánchez-Soto, P.J. (2007). Airborne dust accumulation and soil development in the North-East sector of Gran Canaria (Canary Islands, Spain). *Journal of Arid Environments,* 71(1), 57-81.

Meskhidze, N., Chameides, W.L., Nenes, A. et Chen, G. (2003). Iron mobilization in mineral dust: Can anthropogenic SO2 emissions affect ocean productivity? *Geophysical Research Letters,* 30(21), 2085.

Miller, R.L. et Tegen, I. (1998). Climate Response to Soil Dust Aerosols. *Journal of Climate,* 11(12), 3247-3267.

Muhs, D.R., Bettis, E.A., Aleinikoff, J.N., McGeehin, J.P., Beann, J., Skipp, G., Marshall, B.D., Roberts, H.M., Johnson, W.C. et Benton, R. (2008). Origin and paleoclimatic significance of late Quaternary loess in Nebraska: Evidence from

stratigraphy, chronology, sedimentology, and geochemistry. *Geological Society of America Bulletin,* 120(11-12), 1378-1407.

Muhs, D.R., Budahn, J.R., Prospero, J.M. et Carey, S.N. (2007). Geochemical evidence for African dust inputs to soils of western Atlantic islands: Barbados, the Bahamas, and Florida. *Journal of Geophysical Research: Earth Surface,* 112(F2).

Nakai, S.i., Halliday, A.N. et Rea, D.K. (1993). Provenance of dust in the Pacific Ocean. *Earth and Planetary Science Letters,* 119(1–2), 143-157.

Neff, J.C., Ballantyne, A.P., Farmer, G.L., Mahowald, N.M., Conroy, J.L., Landry, C.C., Overpeck, J.T., Painter, T.H., Lawrence, C.R. et Reynolds, R.L. (2008). Increasing eolian dust deposition in the western United States linked to human activity. *Nature Geoscience,* 1(3), 189-195.

Oppenheimer, C. (2003). Climatic, environmental and human consequences of the largest known historic eruption: Tambora volcano (Indonesia) 1815. *Progress in Physical Geography,* 27(2), 230-259.

Petit, J.R., Jouzel, J., Raynaud, D., Barkov, N.I., Barnola, J.M., Basile, I., Bender, M., Chappellaz, J., Davis, M., Delaygue, G., Delmotte, M., Kotlyakov, V.M., Legrand, M., Lipenkov, V.Y., Lorius, C., Pepin, L., Ritz, C., Saltzman, E. et Stievenard, M. (1999). Climate and atmospheric history of the past 420,000 years from the Vostok ice core, Antarctica. *Nature,* 399(6735), 429-436.

Pratte, S., Mucci, A. et Garneau, M. (2013). Historical records of atmospheric metal deposition along the St. Lawrence Valley (eastern Canada) based on peat bog cores. *Atmospheric Environment,* 79, 831-840.

Prospero, J.M., Ginoux, P., Torres, O., Nicholson, S.E. et Gill, T.E. (2002). Environmental characterization of global sources of atmospheric soil dust identified with the NIMBUS 7 total ozone mapping spectrometer (TOMS) absorbing aerosol product. *Reviews of Geophysics,* 40(1), 1-31.

Pye K. (1987). *Aeolian dust and dust deposits*. Academic Press Inc., London, pp. 325.

Rea, D.K. (1994). The paleoclimatic record provided by eolian deposition in the deep sea: The geologic history of wind. *Reviews of Geophysics,* 32(2), 159-195.

Reynolds, R.L., Mordecai, J.S., Rosenbaum, J.G., Ketterer, M.E., Walsh, M.K. et Moser, K.A. (2009). Compositional changes in sediments of subalpine lakes, Uinta Mountains (Utah): evidence for the effects of human activity on atmospheric dust inputs. *Journal of Paleolimnology,* 44(1), 161-175.

Roos-Barraclough, F. et Shotyk, W. (2003). Millennial-scale records of atmospheric mercury deposition obtained from ombrotrophic and minerotrophic peatlands in the Swiss Jura Mountains. *Environmental Science & Technology,* 37(2), 235-244.

Sapkota, A., Cheburkin, A.K., Bonani, G. et Shotyk, W. (2007). Six millennia of atmospheric dust deposition in southern South America (Isla Navarino, Chile). *The Holocene,* 17(5), 561-572.

Shotyk, W. (1988). Review of the inorganic geochemistry of peats and peatland waters. *Earth-Science Reviews,* 25, 95-176.

Shotyk, W., Cheburkin, A.K., Appleby, P.G., Fankhauser, A. et Kramers, J.D. (1996). Two thousand years of atmospheric arsenic, antimony, and lead deposition recorded in an ombrotrophic peat bog profile, Jura Mountains, Switzerland. *Earth and Planetary Science Letters,* 145(1–4), E1-E7.

Shotyk, W. et Krachler, M. (2010). The isotopic evolution of atmospheric Pb in central Ontario since AD 1800, and its impacts on the soils, waters, and sediments of a forested watershed, Kawagama Lake. *Geochimica et Cosmochimica Acta,* 74(7), 1963-1981.

Shotyk, W., Krachler, M., Martinez-Cortizas, A., Cheburkin, A.K. et Emons, H. (2002). A peat bog record of natural, pre-anthropogenic enrichments of trace elements in atmospheric aerosols since 12 370 ^{14}C yr BP, and their variation with Holocene climate change. *Earth and Planetary Science Letters,* 199(1-2), 21-37.

Shotyk, W., Weiss, D., Appleby, P.G., Cheburkin, A.K., Frei, R., Gloor, M., Kramers, J.D., Reese, S. et Van Der Knaap, W.O. (1998). History of atmospheric lead deposition since 12,370 ^{14}C yr BP from a peat bog, Jura Mountains, Switzerland. *Science,* 281(5383), 1635-1640.

Shotyk, W., Weiss, D., Kramers, J.D., R., F., Cheburkin, A., Gloor, M. et Reese, S. (2001). Geochemistry of the peat bog at Etang de la Gruère, Jura Mountains, Switzerland, and its record of atmospheric Pb and lithogenic trace metals (Sc, Ti, Y, Zr, and REE) since 12,370 ^{14}C yr BP. *Geochimica et Cosmochimica Acta,* 65(14), 2337-2360.

Steinmann, P. et Shotyk, W. (1997). Chemical composition, pH, and redox state of sulfur and iron in complete vertical porewater profiles from two *Sphagnum* peat bogs, Jura Mountains, Switzerland. *Geochimica et Cosmochimica Acta,* 61(6), 1143-1163.

Tarnocai C., Kettles, I.M., et Lacelle. B. (2005). Peatlands of Canada Database Research Branch, Agriculture and Agri-Food Canada, Ottawa, Ontario, Canada, digital database.

Tarnocai, C. et Stolbovoy, V. (2006). Chapter 2: Northern peatlands: their characteristics, development and sensitivity to climate change *Peatlands: Evolution and Records of Environmental and Climate Changes.* (Martini, IP, Martınez Cortizas, A., and Chesworth, W. éd., Vol. 9, p. 17-51). Amsterdam: Elsevier.

Tegen, I. et Fung, I. (1994). Modeling of mineral dust in the atmosphere: Sources, transport, and optical thickness. *Journal of Geophysical Research: Atmospheres,* 99(D11), 22897-22914.

Vanneste, H., De Vleeschouwer, F., Martínez-Cortizas, A., von Scheffer, C., Piotrowska, N., Coronato, A. et Le Roux, G. (2015). Late-glacial elevated dust deposition linked to westerly wind shifts in southern South America. *Scientific Reports,* 5.

Vanneste, H., De Vleeschouwer, F., Bertrand, S., Martinez-Cortizas, A., Vanderstraeten, A., Mattielli, N., Coronato, A., Piotrowska, N., Jeandel, C. et

Le Roux G. (Soumis). Elevated dust deposition in Tierra del Fuego (Chile) resulting from Neoglacial Darwin Cordillera glacier fluctuations. *Journal of Quaternary Science*.

Wanner, H., Beer, J., Bütikofer, J., Crowley, T.J., Cubasch, U., Flückiger, J., Goosse, H., Grosjean, M., Joos, F., Kaplan, J.O., Küttel, M., Müller, S.A., Prentice, I.C., Solomina, O., Stocker, T.F., Tarasov, P., Wagner, M. et Widmann, M. (2008). Mid- to Late Holocene climate change: an overview. *Quaternary Science Reviews,* 27(19–20), 1791-1828.

Weiss, D., Shotyk, W., Rieley, J., Page, S., Gloor, M., Reese, S. et Martinez-Cortizas, A. (2002). The geochemistry of major and selected trace elements in a forested peat bog, Kalimantan, SE Asia, and its implications for past atmospheric dust deposition. *Geochimica et Cosmochimica Acta,* 66(13), 2307-2323.

Woodland, W.A., Charman, D.J. et Sims, P.C. (1998). Quantitative estimates of water tables and soil moisture in Holocene peatlands from testate amoebae. *The Holocene,* 8(3), 261-273.

Yin, Y., Wurzler, S., Levin, Z. et Reisin, T.G. (2002). Interactions of mineral dust particles and clouds: Effects on precipitation and cloud optical properties. *Journal of Geophysical Research: Atmospheres,* 107(D23), 19-14.

CHAPITRE I

LATE HOLOCENE ATMOSPHERIC DUST DEPOSITION IN EASTERN CANADA (ST. LAWRENCE NORTH SHORE)

Steve Pratte[a,b*], Michelle Garneau[a] and François De Vleeschouwer[b]

a GEOTOP, Université du Québec à Montréal, C.P. 8888 Succursale Centre-Ville, Montreal, Canada

b ECOLAB, Université de Toulouse, CNRS, INPT, UPS, France

Sous presse dans *The Holocene* doi : 10.1177/0959683616646185

RÉSUMÉ

À l'aide de la géochimie élémentaire, les apports de poussières atmosphériques minérales furent reconstruits dans deux tourbières (Baie et Île du Hâvre (IDH)) le long de l'Estuaire et du Golfe du Saint-Laurent, dans l'est du Canada. Les éléments terres rares ainsi que d'autre éléments lithogéniques furent mesurés par ICP-AES et Q-ICP-MS dans deux profils de tourbe couvrant les 4000 dernières années. Des analyses en composantes principales réalisées sur les profils géochimiques des deux tourbières montrent que les terres rares affichent le même comportement géochimique que Al, Ti et Zr, tous des éléments conservatifs dans les tourbes. Cette similarité suggère l'immobilité des terres rares dans les séquences de tourbe étudiées et valide leur utilisation en tant qu'indicateur d'apports de poussières atmosphériques minérales. Les flux de poussières, reconstruits à partir de la somme des terres rares, montrent des taux variant entre 0.2 et 3.8 g m^{-2} a^{-1} pour le site de Baie , alors qu'ils sont inférieurs au site IDH avec des valeurs entre 0.1 et 1.2 g m^{-2} a^{-1}. La tourbière Baie a enregistré deux périodes d'apports de poussières accrus, 1750-1000 cal a BP et 600-100 cal a BP, correspondant à des périodes de refroidissement du climat documentées dans la littérature. Ces deux périodes ont été identifiées comme des épisodes d'instabilité climatique pouvant avoir été provoquées par des changements du régime des vents dans la région. Les plus faibles taux de dépôt enregistrés à IDH s'expliquent en partie par l'emplacement du site d'étude, qui a limité les apports de poussières atmosphériques notamment par l'effet protecteur de la frange forestière qui le ceinture.

ABSTRACT

Dust deposition in two ombrotrophic peatlands (Baie and IDH bogs) along the Estuary and Gulf of the St. Lawrence in eastern Canada was reconstructed using elemental geochemistry. The rare earth elements (REE) and other lithogenic element concentrations were measured by ICP-AES and Q-ICP-MS in two peat cores spanning the last 4000 years. Principal component analyses on the geochemical profiles show that REE display the same behavior as Al, Ti, Sc and Zr, all conservative elements, which suggest that REE are immobile in the studied peat bogs and can be used as tracers of dust deposition. Plant macrofossils were also used to infer past environmental and humidity changes. The dust fluxes were reconstructed using the sum of REE (ΣREE). The range of dust deposition varies from 0.2 to 3.8 g m^{-2} a^{-1} in the Baie bog, while the IDH bog shows lower fluxes ranging between 0.1 and 1.2 g m^{-2} a^{-1}. The highest dust fluxes in the Baie bog were recorded from 1750 to 1000 cal BP and 600 to 100 cal BP and occur at the same time as periods of high variability in the macrofossil record (i.e. successive layers dominated by *Sphagnum* or Ericaceae). The timing of these events in the dust and macrofossil records also corresponds to documented cold periods. These two periods have been identified as episodes of climatic instability, which could have been caused by changes in the wind regime.

1.1 Introduction

Mineral dust plays an important role in the global climate system having effects on radiation budgets and the chemical composition of the atmosphere (Goudie and Middleton, 2001; Harrison *et al.*, 2001). Atmospheric mineral dust can affect the biogeochemical cycles of several elements in marine (Meskhidze *et al.*, 2003) and terrestrial environments (Goudie and Middleton, 2001) by supplying nutrients. Fluctuations in atmospheric dust can be indicative of changes in climatic conditions which are related to changes in various factors such as precipitation, temperature, wind regime or vegetation cover.

Paleoclimate records have shown greater dust deposition during glacial compared to interglacial periods. For example, dust deposition was 80 times greater during the Last Glacial Maximum (LGM) in comparison to the Holocene (Fischer *et al.*, 2007). While variations in dust deposition during the Holocene are not of the same magnitude as those occurring on a glacial-interglacial scale, the complex spatial and temporal variability in climate during this period was important enough to affect dust production and transport (Albani *et al.*, 2015; Wanner *et al.*, 2008). Past variability in dust deposition and sources has been reconstructed in a range of archives, for example, ice cores (Albani *et al.*, 2012; Delmonte *et al.*, 2008; Zdanowicz *et al.*, 2000), marine sediments (deMenocal *et al.*, 2000; Rea, 1994), lake sediments (Mischke *et al.*, 2010) and loess deposits (Bettis *et al.*, 2003; Muhs and Budahn, 2006). Despite the importance of atmospheric dust, the number of continental records of their changing rates and sources remains limited.

Recently, there has been an increased interest in using peatlands as archives of past variability in atmospheric dust deposition (De Vleeschouwer *et al.*, 2014). Ombrotrophic peatlands (peat bogs) receive their nutrients and water almost exclusively from atmospheric deposition (Chambers and Charman, 2004). Peatlands present other advantages: they are broadly distributed, hence easily accessible, and

show relatively high accumulation rates allowing high temporal resolution reconstructions. In comparison to ice cores, which record mainly long-range transport of atmospheric particles, peat bogs also record dust inputs from local and regional sources (Le Roux *et al.*, 2012; Marx *et al.*, 2010).

The geochemical analysis of peatland archives has helped to identify changes in dust deposition linked to the Younger Dryas in Switzerland (Le Roux *et al.*, 2012; Shotyk *et al.*, 2001), SE Asia (Weiss *et al.*, 2002) and Tierra del Fuego (Vanneste *et al.*, 2015), the Sahara aridification (Le Roux *et al.*, 2012) and the Little Ice Age (LIA) in Europe (De Vleeschouwer *et al.*, 2009). However, some questions remain as to under which conditions dust events are recorded. De Vleeschouwer *et al.* (2009) observed increases in dust deposition during LIA dry episodes in northern Poland while other studies recorded some peaks during periods of climate instability (wet or dry shifts) (de Jong, Schoning and Björck, 2007; De Vleeschouwer *et al.*, 2012). The timing of some dust deposition episodes with known climatic events can also differ. For example, Le Roux *et al.*, (2012) reported a Saharan dust event at 8.4 decoupled from the 8.2 event, which could have played a role in the onset of the latter. Hence, further research is needed to clarify the dust-climate linkage.

Over North America, continental dust records are scarce and mainly consist of loess deposits from the Great Plains, Mississippi Valley and Alaska (Muhs, 2013), which usually cover glacial-interglacial or millennial time-scales but lack sufficiently high resolution for the Holocene. Furthermore, only a limited number of paleoclimatic studies have been conducted in the peatlands of eastern Canada.

The climate of eastern Canada is currently governed by the relative strength of three major air masses (Bryson, 1966; Bryson and Hare, 1974). Mild, dry Pacific winds enter the region from the west; cold, dry Arctic air arrives from the north and northwest; warm, moist tropical maritime air comes from the south. Eastern Canada Holocene climate history has been characterized by a mid-Holocene thermal maximum (~4000

cal BP; Viau *et al.*, 2006). The proximity of the residual Laurentide Ice Sheet delayed this warm period relative to other regions of boreal North America. Long-term trends in paleohydrology were also linked with other periods of climate change such as the Neoglacial and LIA coolings or the Medieval Warm Period (MWP) (Garneau *et al.*, 2014; Magnan and Garneau, 2014). The climatic studies available in the region have focused on successional vegetation changes and/or surface humidity in relation to climate (Charman *et al.*, 2015; Hughes *et al.*, 2006; Magnan and Garneau, 2014; Magnan, Garneau and Payette, 2014). In Newfoundland, Hughes *et al.* (2006) suggested that bog surface wetness (BSW) over the Holocene was controlled by a combination of oceanic and solar forcing. Magnan and Garneau (2014) reconstructed late Holocene contrasted hydrological responses in peat bogs along the Estuary and the Gulf of the St. Lawrence. They suggested that a greater subarctic influence in the Gulf of the St. Lawrence explained the different responses recorded in each region. These results were based on paleohydrological and paleoecological proxies such as testate amoebae, plant macrofossils and peat humification and interpreted as proxies of surface humidity, although they can also be influenced by temperature (Barber and Langdon, 2007; Lamentowicz *et al.*, 2010) or differential decomposition in the case of humification (Hansson *et al.*, 2013). Furthermore, they may be partially interdependent and can be influenced by site specific factors other than climate (Caseldine *et al.*, 2000; de Jong *et al.*, 2010; Magnan and Garneau, 2014; Sullivan and Booth, 2011). In contrast, dust deposition is independent of bog ecohydrological dynamics and is a function of particle availability and atmospheric transport and deposition (Maher *et al.*, 2010). Accordingly, paleo dust records in eastern Canada may provide complementary information about past climate variations in the region.

The present study is a first attempt to reconstruct dust deposition using two continuous peat bog records from the North Shore of the Gulf and the Estuary of the St. Lawrence, eastern Canada. This paper aims at 1) reconstructing changes in atmospheric dust deposition using lithogenic elements, namely Al, Ti, Sc and rare earth elements (REE);

2) investigating the relationship between dust fluxes and hydroclimatic variability during the late Holocene using plant macrofossil analyses and 3) reconstructing the paleoclimatic events occurring on the North Shore of the St. Lawrence and comparing these with other regional records.

1.2 Material and Methods

1.2.1 Study sites

The Baie peatland (49°04'N, 68°14'W; 1.5 km^2, 15 m.a.s.l.) is a *Sphagnum*-dominated treeless raised bog located on the Manicouagan delta, 20 km southwest of Baie-Comeau, at the eastern end of the Lower St. Lawrence Estuary (Fig. 1.1). The southern border of the peatland (700 m from the coring site) is open towards the coast of the St. Lawrence Estuary, where beaches occupy the coastline. More than 4.5 m of peat has accumulated over marine silt-clay sediments originating from the Laurentian transgression that ended around 4400-4200 cal BP (Bernatchez, 2003; Magnan and Garneau, 2014). Deposits at a higher altitude (> 14 m.a.s.l.) consist of silt-sand deltaic terraces which emerged following the withdrawal of the Goldthwait Sea from 8 ka (Bernatchez, 2003). A closed boreal forest dominated by *Picea mariana*, *Abies balsamea*, and *Betula papyrifera* covers most of the deltaic deposits (Sauvé, 2016).

The bog surface vegetation is dominated by *Sphagnum fuscum, S. capillifolium*, ericaceous shrubs (*Chamaedaphne calyculata, Kalmia angustifolia* and *Rhododendron groenlandicum*) and sparse dwarf *Picea mariana* on the hummock microforms, while the lawn microforms are mainly composed of *S. rubellum*, *Vaccinium oxycoccos*, *Andromeda polifolia* and *Eriophorum* spp.

The Ile du Havre peatland (IDH) (50°13'N, 63°36'W, 0.5 km^2, 31 m.a.s.l.) is a bog, raised at its center, located on a 12 km^2 island two kilometers offshore in the eastern part of the Mingan archipelago in the Gulf of St. Lawrence (Fig. 1.1). Peat accumulated

in a depression over silty-clay sediments. At its deepest part, peat thickness reaches about 6.25 m, accumulated since *ca* 7650 cal BP. The underlying bedrock consists of Ordovician limestone intersected by layers of shale and sandstones from the Mingan formation (Grondin et al., 1980; Poole et al., 1970). The islands of the archipelago are characterized by cuesta landforms with cliffs to the north and gentle slopes towards the south (Grondin et al., 1980). The peatland being located at the north-east side of the island, the surrounding topography is characterized by cliffs and steep slopes. The coastline of the island (600 m away from the peatland) is dominated by pebbles and sandy beaches. A closed forest dominated by *Picea mariana* occupies large parts of the island, while depressions are occupied by peatlands (Grondin et al., 1980).

The peatland is treeless and the dominant plant species are ericaceous shrubs (*Chamaedaphne calyculata*, *Kalmia angustifolia* and *Empetrum nigrum*) along with *Sphagnum fuscum*, *Cladina* spp. and isolated stands of dwarf *Picea mariana*. The hummock microforms at the center of the peatland are dominated by a variable combination of *S. fuscum*, *Cladina* spp., *Empetrum nigrum* and *Rubus chamaemorus*, while hollows are dominated by *S. rubellum* and *Carex limosa*.

1.2.2 Coring and subsampling, bulk density and ash content

A core was retrieved from the deepest part of each peatland, using a stainless steel box corer (10x10 cm width; Jeglum *et al.*, 1992) to sample the upper meter and a Russian sampler (7.5 cm diameter; Jowsey, 1966) for the deeper sections. The cores were collected from two holes approximately 30 cm apart in an overlapping manner to ensure complete stratigraphic recovery. The cores were wrapped in plastic film, transferred into PVC tubes and stored in a freezer (-20°C). In the laboratory, the cores were sliced frozen at 1-cm intervals (Givelet *et al.*, 2004) using a stainless steel band saw at Ecolab (Toulouse, France). Each slice was rinsed with *milliQ* water and the edges of each subsample trimmed away to avoid any contamination from the saw. The

thickness of each slice was then measured again to evaluate the loss from the slicing and correct the mid-point depth of each sample. The slices were then subsampled for each type of analyses. The bulk density of the samples was determined by measuring the volume using a vernier caliper and weighting subsequently the samples fresh and then freeze-dried. The ash content, as a surrogate of the mineral matter content, was obtained by ashing each subsample at 550°C for 6h to remove all organic matter by combustion (Chambers, Beilman and Yu, 2011).

1.2.3 Plant macrofossils

Plant macrofossil analyses were performed at systematic 4-cm intervals and refined (2-cm intervals) where visual changes in the stratigraphy were noted. Subsamples (4 cm^3) were gently boiled in distilled water with addition of 5% KOH and carefully sieved (> 125 µm). Macrofossils were scanned using a binocular microscope (x10-x40) and identified using reference collections (Garneau, 1995; Mauquoy and Van Geel, 2007). Plant macrofossils were expressed as volume percentages (%) representative of cover estimates in a Petri dish (*Sphagnum* remains, ligneous fragments etc.) except seeds, leaf fragments and charcoal fragments, which were reported as numbers (n). *Cenococcum* sclerotia and *Myrica gale* leaves/seeds were scaled from 1 to 5 (1=rare, 5=abundant). *Sphagnum* were determined to the highest taxonomic level possible based on stem and branch leaf characteristics using a photonic microscope (x40-x100). Terminology follows Marie-Victorin (1995) for vascular plants and Crum and Anderson (1979) and Ireland (1982) for bryophytes. Zonation of the macrofossil diagrams was made using constrained cluster analysis by sum-of-square (CONISS) in psimpoll 4.25.

1.2.4 Chronological control

The chronological control of the cores is based on ^{14}C AMS dates and ^{210}Pb measurements. For ^{14}C dating, only aboveground plant macrofossils were selected based on a protocol developed by Mauquoy *et al.* (2004), in order to ensure a better accuracy of dates. Most of the macrofossils consisted of *Sphagnum* spp. stems (Table 1.1). When *Sphagnum* were not sufficient to provide enough material for dating, other types of macrofossils were selected (*Larix laricina* and *Picea mariana* needles, Ericacea leaves, etc.). A total of 24 samples (14 and 11 for Baie and IDH respectively) were submitted to the Keck-CCAMS facility (Irvine, USA) for AMS radiocarbon dating.

Lead-210 activity was determined in the uppermost peat layers after extraction of its granddaughter product, ^{210}Po, from 0.5 g of powdered bulk peat spiked with a ^{209}Po yield tracer following a sequential extraction HNO_3-HCl-HF-H_2O_2 digestion (Ali *et al.*, 2008). Measurements were realized on a α-spectrometer (EGG Ortec 476A) at GEOTOP Research center (UQAM, Montreal). The Constant Rate of Supply (CRS) model was subsequently applied to build ^{210}Pb age-models (Appleby, 2002). The measurement uncertainties (Tables 1.2 and 1.3), corresponding to one-sigma, were calculated from counting statistics. The atmospheric, or excess ($^{210}Pb_{ex}$), is used to determine the chronology of environmental records. Supported ^{210}Pb activity, i.e. produced *in situ*, was estimated by the analysis of deeper samples in each core (Fig. 2) in order to determine at which depth the $^{210}Pb_{ex}$ was not present anymore, hence the limit of the dating technique (Le Roux and Marshall, 2011). Age-depth models were generated by combining both ^{14}C and ^{210}Pb dates using the *BACON* software package (Blaauw and Christen, 2011). The radiocarbon dates were calibrated using the InterCal13 Northern Hemisphere terrestrial calibration curve (Reimer *et al.*, 2013) integrated in the *BACON* package.

1.2.5 Chemical analyses

All geochemical sample preparations were performed under clean laboratory conditions (class 100) using acid-cleaned labware. Approximately 100 mg of powdered peat samples were acid-digested until complete dissolution, using a series of steps (HNO_3 + HF, then H_2O_2) in Savillex® beakers on a hot plate (Le Roux and De Vleeschouwer, 2010). In a number of samples, an additional step involving *aqua regia* was necessary to fully digest the organic matter. The major element (Al, Ti, Ca, Fe, K and Na) analyses were made by ICP-OES at Ecolab laboratory (Toulouse, France) on a Thermo Electron IRIS Intrepid II. The trace element measurements (Sr, Rb, Zr, Sc, Pb, Th, U and REE) were completed on an Agilent Technologies 7500ce Q-ICP-MS at *Observatoire Midi-Pyrénées*, in Toulouse. Prior to ICP-MS analyses, samples were diluted and an In-Re spike was added for internal normalisation process.

The analytical performance was monitored through reference materials (NIST 1515 Apple leaves, NIST 1547 Peach leaves, NIST 1575a Pine needles, GBW07604 Bush branches and leaves, and NIMT/UOE/FM/001 peat). Measurements obtained by ICP-OES were generally within 10% of certified values with the exception of Al concentrations which vary between 6 and 17%. The elements measured by ICP-MS were all within 15% of certified values with the exception of Sc (22%), Lu (19%) and Ce (16%). The reproducibility of digestion procedure was evaluated by repeated analyses of NIST 1515 (n=5), NIST 1547 (n=5), GBW-07063 (n=4) and 10 peat samples (each n=2) and was generally better than 20%. The procedural blanks for the elements analyzed were < 15 ppt for trace elements and < 1 ppm for Al, Ca, Ti, K, and Na.

1.2.6 Dust flux

The rate of deposition of atmospheric dust, i.e. the dust flux, can be calculated using the concentration of a lithogenic element, bulk density of the peat and the rate of peat accumulation. Assuming that "soil dust" contains lithogenic elements in the same concentration as the Earth's crust, the concentration of dust is normalized to the upper continental crust (Wedepohl, 1995). The dust flux was calculated using the sum of REE concentrations ($\mu g\ g^{-1}$) in the bulk peat using the following equation (Shotyk *et al.*, 2002):

$$\text{Dust flux } (g\ m^{-2}\ a^{-1}) = (\Sigma[REE]_{sample}/\Sigma[REE]_{UCC})*PAR*\text{bulk density}*10000.$$

with $\Sigma[REE]_{sample}$ the sum of REE concentrations ($\mu g\ g^{-1}$) in a sample, $\Sigma[REE]_{UCC}$ the sum of REE concentrations in the upper continental crust (144.3 $\mu g\ g^{-1}$; (Wedepohl, 1995), the peat bulk density ($g\ cm^{-3}$) and PAR which is the peat accumulation rate ($cm\ a^{-1}$). The accumulation rate is multiplied by 10000 to obtain a value in m^{-2} instead of cm^{-2}.

1.2.7 Statistics

A principal component analysis (PCA) was performed on the elemental concentrations in each peat profile using SPSS 22.0.0 software. A PCA can help in the inference of the sources and processes affecting the distribution of the chemical elements. The PCA was performed in correlation mode on previously log transformed (log10) and standardized (z-scores) data to avoid scaling effects, using a varimax rotation which is a fixed orthogonal rotation that maximizes the loadings of the variables on the components (Eriksson *et al.*, 1999). The z-scores were calculated as $(X_i-X_{avg})/X_{std}$, where X_i is the variable (i.e. concentration of the element), while X_{avg} and X_{std} are the series average and standard deviation of all samples for the variable X_i. Since we are working with chemical elements, the components will contain elements with similar

records, likely controlled by the same environmental factors. Hence, by using PCA, the chemical signals tend to be clearer and the underlying factors controlling them are more easily identified and interpreted.

1.3 Results

1.3.1 Chronologies

For both cores, the range of calibrated radiocarbon ages of the dated peat layers are presented in Table 1.1, while the supported and unsupported ^{210}Pb activities and CRS modeled ages are reported in Tables 1.2 and 1.3. The age-depth models cover the period of 4500 cal BP to present and 7650 cal BP to present in the Baie and IDH cores respectively (Fig. 1.2). The Baie core reveals a rather constant peat accumulation rate, with a relatively high average value of 1.0 mm a^{-1} from the base of the core to 52 cm below the surface. An important diminution in accumulation rates is registered between 52 cm and 36 cm yielding an average of 0.4 mm a^{-1}. From 36 cm towards the surface, the accumulation rates are much higher and correspond to the acrotelm.

The IDH core displays a mean accumulation rate of 0.4 mm a^{-1} from peat initiation at 623 cm until 554 cm (Fig. 1.2). Accumulation rates are higher between 554 and 452 cm with a mean of 1.1 mm a^{-1}. Between 452 and 70 cm, the IDH core shows a relatively constant accumulation rate of 0.8 mm a^{-1}. As in the Baie core, from 70 cm towards the surface, the accumulation rates are much higher and correspond to the acrotelm.

1.3.2 Plant macrofossils

The main changes in macrofossil composition are reported in Figure 1.3 and Tables 1.4 and 1.5. Following peat inception at ca. 4500 cal BP, the Baie bog displays a high mineral content (ash content > 10%) and a dominance of Cyperaceae (Fig. 1.3; zone

B-1). Zones B-2 (4470-4340 cal BP) and B-3 (4340-3940 cal BP) show high amounts of wet and mineral rich taxa such as *Larix laricina*, *Myrica gale* (B-2), Cyperaceae, brown mosses and *Sphagnum* section *Cuspidata* (B-3). Zone B-4 (3940-2270 cal BP) is characterized by the replacement of *S.* section *Cuspidata* by *S.* section *Sphagnum* at the bottom followed by *Sphagnum* section *Acutifolia*, namely *S. rubellum/capillifolium* to the top of the zone. Zones B-5 (2270-1240 cal BP) is dominated by *S. fuscum* with intermittent layers of Ericaceae/woody debris and unidentified organic matter (UOM) with presence of charcoal layers (130 and 154.1 cm). In zone B-6 (1250-590 cal BP), *S. rubellum/capillifolium* gradually replaces *S. fuscum* to dominate the vegetation assemblages. Similarly to zone B-5, zone B-7 (590 cal BP-1950AD) is characterized by high amounts of *S. fuscum* interspersed with layers of Ericaceae debris and UOM. Finally, in zone B-8 (1950 AD to present), a combination of *S. fuscum* and *S. rubellum/capillifolium* dominates again the vegetation composition.

Ile du Havre peatland initiated at ca. 7650 cal BP over silty-clay sediments. The first three zones, namely IDH-1 (7650-7175 cal BP), IDH-2 (7175-5150 cal BP) and IDH-3 (5150-4750 cal BP), are characterized by minerotrophic taxa dominated by Cyperaceae, *Menyanthes trifoliata*, *Myrica gale*, brown mosses *Cinclidium stygium*, *Calliergon giganteum*, *Scorpidium scorpioïdes* and *Warnstorfia* spp. and other bryophytes such as *Sphagnum teres* and *S.* section *Cuspidata* (Fig. 1.4 and Table 1.5). Zone IDH-4 (4750 to 2910 cal BP) is characterized by a dominance of *Sphagnum fuscum* and *S. rubellum/capillifolium* with high amount of Ericaeae rootlets and wood fragments. In zone IDH-5 (2910-2365 cal BP), *S. rubellum/capillifolium* is the most abundant specie in the assemblages reaching up to 75%. Zone IDH-6 (2365-2000 cal BP), is still dominated by *S. rubellum/capillifolium* but a short period between 2200 and 2000 cal BP is characterized by abundant *Larix laricina* needles and *Myrica gale* leaves. In zone IDH-7 (last 2000 years), *S. fuscum* is the dominant species with relatively high amount of *S. rubellum/capillifolium.*

1.3.3 Principal Component Analyses on elemental geochemistry

Three principal components (PC) were extracted in the Baie record, accounting for 92% of the total variance (Fig. 1.4a). The first PC explains 63% of the variance and is characterized by positive loadings of U, Th, REE, Zr, Sc, Ti, and Al. The factor score profile displays several peaks, mainly between 200-100 cm (1760-1030 cal BP) and 60-25 cm (650 cal BP-1955 AD). PC2 accounts for 20% of the variance and has positive loadings for K, Rb, Na and Pb. The factor scores of PC2 show relatively constant values up to 40 cm, where they increase towards the surface. Rb, Na and K concentrations display low values except at 29.7 cm and near the surface (Fig 1.4). The PC3 explains 9% of the variance and Ca and Sr show high positive loading factors. The factor scores of PC3 show a decreasing trend from the base of the profile until 200 cm, where they increase and remain relatively constant towards the surface.

In the IDH profile, two principal components were extracted, accounting for 90% of the variance (Fig. 1.4b). The first PC explains 70% of the variance and shows high loading factors for all REEs, U, Zr, Al, Sc, Th and Ti. The factor score profile shows a 'see-saw' pattern with several peaks at 400-378 cm (3910 to 3700 cal BP), 335 cm (3130 cal BP), 206 cm (1810 cal BP), 143 cm (875 cal BP) and 40-30 cm (1955AD to 1925AD). The second PC explains 20% of the variability and includes Pb, K, Na, Rb and high negative loadings with Sr, Ca. The factor scores for PC2 display a large peak between 70 cm and 20 cm.

1.3.4 Dust flux

The sum of REE was selected to reconstruct dust fluxes as REEs show very high loading factors in both bog's PC1. With the presence of an aluminum smelter in the region of the Baie bog and a Ti mine close to the IDH bog, these two elements were

not used to reconstruct dust fluxes. Zirconium is known to be enriched in certain mineral phases, mostly zircons (Shotyk *et al.*, 2002) and therefore was not used as well.

If we exclude the basal minerotrophic phase, the dust flux of the Baie profile can mainly be divided into four phases. A first phase from ca. 3800 to ca. 1760 cal BP (Fig. 1.6a), shows a relative stability with fluxes ranging from 0.5 to 1.1 g m^{-2} a^{-1} (mean: 0.81±0.28 g m^{-2} a^{-1}). This period is followed by a period of increased dust fluxes ranging from to 0.68 to 3.81 g m^{-2} a^{-1}, with greater variability (mean: 1.83±0.84 g m^{-2} a^{-1}), between ca. 1760 and ca. 1000 cal BP. From ca. 1000 to ca. 650 cal BP, dust fluxes reach their lowest values in the core (mean: 0.24±0.09 g m^{-2} a^{-1}) followed by a period of high variability with higher fluxes averaging 1.31±0.31 g m^{-2} a^{-1}, which lasted until 1960AD.

The dust flux of the IDH profile shows less variability and a lower rate of particle accumulation (Fig. 1.6a). The profile shows an average dust flux of 0.4 g m^{-2} a^{-1} with four peaks of interest. A peak reaching 2.1 g m^{-2} a^{-1} is observed between ca. 4100 and 3700 cal BP. A second peak reaching 0.9 g m^{-2} a^{-1} is registered at ca. 3130 cal BP. Then the dust flux shows little variability until ca. 875 cal BP where a third peak is observed (1.5 g m^{-2} a^{-1}). After this, the dust flux remains relatively low and stable until 1910AD where it increases again up to 2.7 g m^{-2} a^{-1} and higher fluxes (mean: 1.43±0.85 g m^{-2} a^{-1}) persist until the present-day.

1.4 Discussion

1.4.1 Trophic status of the peatlands

The ombrotrophic conditions of the Baie and IDH cores are confirmed by their ecological and geochemical characteristics. In the Baie bog, Cyperaceae, brown mosses and *Sphagnum* section *Cuspidata*, i.e. species indicative of minerotrophic conditions, dominate the assemblages from the base until 3800 cal BP (Fig 1.3; zones 1 to 3; Table

1.4). Plant macrofossil record (Fig. 1.3) suggests a rapid transition from fen to bog with a persistence of ombrotrophy from 3800 cal BP to the present-day as also reported by Magnan, Garneau and Payette (2014). The ombrotrophy is further confirmed by the low ash content (< 5%) (Tolonen, 1984) in the core above 440 cm (Fig. 1.3).

In the IDH core, the first three zones in figure 1.4 are composed of species typical of minerotrophic conditions, i.e. dominance of Cyperaceae, brown mosses and *Sphagnum teres* (Fig. 1.4 and Table 1.5). Macrofossils and major elements suggest that ombrotrophy was reached at about 445 cm of depth (Fig. 1.4 and 1.5b). The appearance of *Sphagnum fuscum* and *S. rubellum/capillifolium* at the end of zone IDH-3 (5000 cal BP) indicates a transition from a fen to a bog environment (Fig. 1.4 and Table 1.5). The low Sr (< 30 ppm) and Ca values (< 0.5%) (underlying limestone substratum) are also consistent with ombrotrophic conditions (Shotyk *et al.*, 2001). However, the low concentrations of lithogenic elements further down core suggest that their supply was mainly atmospheric approximately 500 years earlier (Fig. 1.5b), which is confirmed by the low ash content (Fig. 1.4).

1.4.2 Paleoenvironmental/paleoclimatic changes from macrofossils

In the Baie macrofossil record (Fig. 1.3), the period between 3800 and 2100 cal BP shows stability with assemblages typical of a lawn microform (*Sphagnum rubellum/capillifolium* and *S.* section *Sphagnum* with Ericaceae rootlets). Between 2100-1250 cal BP (zone B-5) and 500 cal BP to 1950AD (zone B-7), a lower water table probably linked to drier climatic conditions as well as a greater variability in the hydro-climatic conditions are suggested by the changes in vegetation assemblages (*S. fuscum*, several peaks of UOM and Ericaceae and two charcoal layers). The dominance of *S.* section *Acutifolia* almost throughout the core suggests relatively dry conditions over the studied period with substitutions by Ericaceae and UOM indicating even drier periods.

In the IDH ombrotrophic section (Fig. 1.4), zone IDH-4 (4750-2900 cal BP) is characterized by the dominance of *Sphagnum fuscum* and *Sphagnum rubellum/capilifolium* and the presence of Ericaceae rootlets, which indicates drier conditions than in the previous sections. In zones 5 and 6 (2910-2000 cal BP), *S. rubellum/capillifolium* dominates the assemblages, which suggests relatively more humid conditions similar to a lawn microform. A short period between 2200 and 2000 cal BP is characterized by abundant *Larix laricina* needles and *Myrica gale* leaves, which can be explained by more humid conditions or a return to minerotrophic conditions (IDH-6). Over the last 2000 years (IDH-7), little variability is observed in the assemblages in which *S. fuscum* is the dominant species with relatively high amount of *S. rubellum/capillifolium.* The high presence of *S.* section *Acutifolia* and Ericaceae remains in the ombrotrophic section suggests relatively dry conditions over the entire period.

1.4.3 Drivers of the geochemical signal

Principal component analyses were realized in order to identify variables (i.e. chemical elements) with similar behavior and likely to be controlled by the same processes. The PCA analyses focussed on the last 4300 years in the Baie core and 5500 years in the IDH cores. PC1 display high positive loading factors with all lithogenic elements (U, Th, REE, Zr, Sc, Ti, and Al) (Fig. 1.5). The fact that REEs load on the same PC as other lithogenic elements, known for their conservative nature, such as Ti and Sc, confirms that REEs are immobile in the peat column as suggested in Krachler *et al.* (2003) and Aubert *et al.* (2006). Since all lithogenic elements are associated with PC1 in both cores, it reflects the mineral content of the peat from dust deposition, probably derived from soil erosion. In both cores, PC2 shows high loading factors for Na, Rb, K, Pb (Fig. 1.5) and represents a combination of different controlling factors of the geochemical profiles. Lead has a history of anthropogenic use and is known to be

emitted as by-product of human activities. It shows an increase from the beginning of the 19th century and a peak in the 1950-1970's (Gallon *et al.*, 2005; Pratte, Mucci and Garneau, 2013). Elements such as Rb, K and Na are all essential elements known to be bioaccumulated by bog vegetation, which would explain the increase in the factor score at the surface (Damman, 1978; Steinmann and Shotyk, 1997). The presence of a sand layer at 29.7 cm depth in the Baie core likely explains the enrichment in Rb, K, Na but also in other lithogenic elements. Furthermore, the low values, except in the above mentioned layers probably explain the fact that these elements are on the same component as Pb although they normally do not display similar geochemical behaviour in the peat column. Calcium and strontium show high loading factors on the PC3 in the Baie core, while they show high negative loadings with PC2 in the IDH core (Fig. 1.5). Diagenetic processes, such as changes in redox conditions and upward leaching from basal sediments following mineral dissolution, are known to affect the mobility of Ca and Sr in peat (Steinmann and Shotyk, 1997). Both cores show a gradual decrease in Ca and Sr concentrations (less negative values in the case of the IDH core) over time up to the fen to bog transition, which suggests upward leaching from the basal sediments (Shotyk *et al.*, 2001). Hence, PC3 in Baie bog and the Ca and Sr part of PC2 in the IDH core will not be discussed further as they do not provide information about dust deposition or origin.

1.4.4 Paleoclimatic events recorded by the dust records

Period 4100 to 3700 cal BP. Between 4100 and 3700 cal BP, the IDH core displays increased dust fluxes (mean: 0.95±0.76), greater factor scores for PC1 (Fig. 1.5b) and a greater proportion of Ericaceae remains, suggesting slightly drier conditions (Fig 1.6a and c). Although the Baie record covers this time period, it will not be discussed because the dust signal was not solely atmospheric in origin which renders its interpretation difficult in terms of past climate. Several archives recorded a dry episode

at low and mid-latitudes around 4200 cal BP (Booth *et al.*, 2005 and references therein), while the higher latitudes recorded more humid conditions (Yu *et al.*, 2003). Mayewski *et al.* (2004) report a strengthening of the westerlies over North America from 4200 to 3800 cal BP, which is in agreement with studies conducted in eastern North America (Almquist *et al.*, 2001; Jessen *et al.*, 2011). Hence, the combination of drier conditions to the south and increased westerly strength could explain the increased dust deposition in the IDH bog over the period.

Period 3700 to 1750 cal BP. The Baie and IDH records show relative stability in the dust flux at ca. 3800-2000 cal BP (mean: 0.81±0.28 g m^{-2} a^{-1}) and ca. 3700-2000 cal BP (mean: 0.45±0.17 g m^{-2} a^{-1}) respectively, although some slight increases are observed in both records (Fig. 1.6a). The macrofossils composition also shows stability over this period with the dominance of *Sphagnum rubellum/capillifolium* (Fig. 1.3, 1.4 and 1.6b and c). Other regional studies have shown rather stable water table depths (Fig. 1.6d), carbon accumulation rates and summer sea-surface temperature (Fig. 1.6; SST) during this period (Lemay-Tougas, 2014; Magnan and Garneau, 2014; Magnan, Garneau and Payette, 2014). At IDH, a trend toward lower dust deposition is observed from ca. 3600 to ca. 3000 cal BP and, for the same period, higher WTD was reported in a peat bog along the shore of the Gulf of St. Lawrence (Magnan and Garneau, 2014). In the same record, a gradual drying of the peat surface is documented after 3000 cal BP reaching its maximum around 1900 cal BP. Over the same period (3000-1900 cal BP), both dust records do not display significant changes. The macrofossil analyses as well as the low dust fluxes recorded in both Baie and IDH bogs during this period suggest a rather stable wind and climatic regime, which is supported by other records (Fig. 1.6d, f and g) although a number of regional records (Fig 1.5e) suggest a dryer climate in the region of the IDH bog, not recorded by our proxies.

The apparent discrepancies between our dust records and the biological proxies could be explained by their different response time to changes. Furthermore, these proxies

can be controlled by internal processes during certain periods (Sullivan and Booth, 2011). In contrast to the biological proxies, dust deposition is not affected by internal processes, hence, regardless of the geographical scale, it is likely more strongly linked to climate.

Period 1750 to 1000 cal BP. The highest dust fluxes were recorded during the period from 1750 to 1000 cal BP, with values ranging between 1.2 and 3.8 g m^{-2} a^{-1} (mean: 1.83±0.84 g m^{-2} a^{-1}) (Fig. 1.6a), while macrofossils show several changes in species composition (Fig. 1.3 and 1.6b), with several peaks in Ericaceae remains and charcoal horizons. The IDH bog recorded a lower dust flux (mean: 0.39±0.16 g m^{-2} a^{-1}) over the same time period. Although, a relatively warmer climate is suggested from $\Delta^{14}C$ production (Fig 1.6h), the different peaks recorded during this period correspond with periods of higher ^{14}C production, i.e. lower insolation (Bond *et al.*, 2001; Chambers, Ogle and Blackford, 1999). The highest dust flux values in the Baie bog are recorded when summer SST was at its warmest at ca. 1500 cal BP as indicated by a marine core in the St. Lawrence Estuary (Fig. 1.6g; Lemay-Tougas, 2014). Afterwards, a decrease of summer SST and sea-surface salinity (greater precipitation) centered at ca. 1200 cal BP is reported (Lemay-Tougas, 2014).

All the records in Figure 5 agree, that a trend towards more humid conditions occurred around ca. 1750 cal BP. Furthermore, both the Newfoundland (BSW) and the $\Delta^{14}C$ records show greater variability from 1750 cal BP (Fig. 1.6f and h). The same variability is observed for the dust flux and the macrofossil assemblages in the Baie record. Testate amoebae assemblages from records in the Baie-Comeau region also display species associated with periods of high decadal to centennial hydroclimate variations (Magnan and Garneau, 2014). This period is therefore characterized by a certain degree of hydroclimatic instability expressed by high variability of vegetation and testate amoebae assemblages and higher dust loads as in Europe. For example, de Jong *et al.* (2007) noted peaks in aeolian activity during hydrological shifts regardless

of their direction (wet or dry) in South Sweden. In Belgium, De Vleeschouwer *et al.* (2012) also suggested that higher dust loads were favoured by hydroclimatic instabilities (i.e. shift towards wet or dry periods). In these studies, changes in humidity were therefore associated with intensifications in atmospheric circulation (de Jong *et al.*, 2007; De Vleeschouwer *et al.*, 2012). In our records, this hypothesis is supported, especially in the Baie bog, which displays higher dust fluxes during a period where other biological proxies show high variability. Such instability could be explained by a change in atmospheric circulation. Around 1650±200 cal BP, Viau *et al.* (2002) identified a major transition in pollen records of North America (including our study regions) associated with a rearrangement of atmospheric circulation. Furthermore, cooling events during the Late Holocene in eastern Canada were associated with the incursion of Arctic air masses (Carcaillet and Richard, 2000; Girardin *et al.*, 2004), which could partially explain the occurrence of dust peaks with cold events and increased hydroclimatic instability.

'Medieval Warm Period' (MWP). In both study regions, the Medieval Warm Period (roughly 1000-650 cal BP) is characterized by higher WTD around 700 cal BP in peat bogs (Fig. 1.6d and f). Further east, Hughes *et al.* (2006) also reported a wet shift between 900 and 750 cal BP. Arseneault and Payette (1997) reported greater tree growth associated to warmer conditions (1000-800 cal BP) in northern Quebec while Lemay-Tougas (2014) observed slightly cooler and wetter conditions from a record of summer SST (1200-800 cal BP Fig. 1.6g) and sea-surface salinity. Following this period, the summer SST record is characterized by a transition towards a warmer/drier climate. The discrepancies in the age of the different events in the marine record could be ascribed to the lower dating control compared to our record or to slower response of the oceanic system relative to changes. In both Baie and IDH records, a diminution of Ericaceae remains and increase of *Sphagnum rubellum/capillifolium* suggest a slightly wetter climate. This period is also recorded in the dust fluxes and PC1 factor scores (Fig. 1.5) from Baie (mean: 0.24±0.09 g m^{-2} a^{-1}) and IDH (mean: 0.60±0.52 g

m^{-2} a^{-1}), which display lower values, usually typical for a wet period. This has already been observed by Filion (1984), who reported lower aeolian activities in parallel with warmer and/or moister conditions during the same period in Northern Quebec. The 1000-650 cal BP period is therefore characterized by warmer but also wetter conditions.

'Little Ice Age' (LIA). Following the MWP, the Little Ice Age, is characterized by a period of increased dust fluxes in the Baie bog between 650 and 100 cal BP (mean: 1.31±0.31 g m^{-2} a^{-1}), where values reach 2.3 and 1.7 g m^{-2} a^{-1} at 540 and 150 cal BP respectively, while IDH bog shows small peaks around 600-400 cal BP and 200 cal BP (mean: 0.36±0.16 g m^{-2} a^{-1}). Factor scores of PC1 also display higher values during this period in the Baie core but do not show any change in the IDH core (Fig. 1.5). Macrofossil assemblages in both cores suggest dry conditions and display high variability in the Baie core (Fig. 1.3), similar to the previous period of increased dust deposition (1750-1000 cal BP). Previous research in northern Quebec showed a dry shift between 530–350 cal BP (Loisel and Garneau, 2010), while cooling associated with wet shifts were reconstructed in a peatland in Newfoundland around 600 and 200 cal. BP (Fig. 1.6; Hughes *et al.*, 2006). Moreover, Magnan and Garneau (2014) observed differences between the Baie-Comeau and Havre St-Pierre regions, the latter being drier during the LIA (Fig. 1.6) influenced by longer frost duration periods linked to a greater subarctic influence. The timing of the dust peaks during the LIA in the Baie record also corresponds with minima in solar activity ($\Delta^{14}C$). The first peak (650-400 cal BP) encompasses both Spörer and Maunder minima, while the second peak (150-100 cal BP) corresponds with the Dalton minimum. The LIA is therefore characterized by colder conditions, but the wetness probably varied from one region to another, with some places being drier than others in relation to longer frost duration under the influence of arctic air masses.

A more meridional atmospheric circulation or a stronger north polar vortex have been proposed to explain greater dust deposition and colder temperatures in Greenland (GISP2 core) during the LIA (O'Brien *et al.*, 1995). Likewise to the period between 1750 and 1000 cal BP, such a change in atmospheric zonal and meridional circulation may as well have affected mid-and low-latitude circulation, which could explain the increase in dust deposition in our bogs during the LIA. A more meridional circulation could have allowed more frequent intrusion of cold and dry Arctic air masses. This is further confirmed by a transition in North American pollen records during the LIA which would have been provoked by a reorganisation of atmospheric circulation potentially linked to a solar forcing (Viau *et al.*, 2002). The relative agreement between increases in dust deposition in the Baie record and solar minima supports this hypothesis.

Modern Period (1850AD to present). Both peat bogs recorded peaks in dust flux (mean: 0.98±0.42 g m^{-2} a^{-1} and 1.43±0.85 g m^{-2} a^{-1} for Baie and IDH cores respectively) following 1850AD (100 cal BP), which are likely anthropogenic in origin. More precisely a large peak is found in both cores following the 1930s. The North shore was increasingly developed during this period with the development of several towns among them Baie-Comeau, located 20 km north-east from Baie bog, and Havre St-Pierre, two kilometers north of IDH bog on the mainland shore. The land clearance probably increased the amount of dust available for transport and can explain the high fluxes over this period. The construction of hydropower dams (1960-1985AD), and an aluminum smelter, in the region of Baie bog and the development of mining activities, more precisely a Ti mine (1950AD), near IDH bog have most likely contributed to the dust signal recorded in the two regions. The so called "dust bowl", a period of severe drought conditions during the 1930s in the Central US was proposed as a potential contributor to dust deposited in Greenland ice over this period of time (Donarummo, Ram and Stoermer, 2003). However, isotopic analyses (Nd and Pb isotopes) of the mineral fraction in the peat would be needed to verify the presence of dust from Central

US in our peat bogs over this period. The factor scores of PC2 for both cores, which includes Pb, show a sharp increase from 100 cal BP until the 1970s (Fig. 1.5). The timing of this increase in Pb concentrations is in agreement with the historical use of leaded gasoline (Gallon *et al.*, 2005; Pratte *et al.*, 2013) and further confirms that both study regions were impacted by anthropogenic activities over the last century.

1.4.5 Discrepancies between the two records

The two studied peat bogs show differences in the magnitude of the dust signal. A potential explanation would be that both archives record a more regional scale signal or are affected by different air masses since the two sites are found in a zone of mixing air masses (Fig. 1.1). The two study regions are located more than 500 km apart and likely developed in different climatic contexts. Distinct regional signals were already reported by Magnan and Garneau (2014) using testate amoebae, with drier conditions and greater variability on peat bogs near IDH, which are located in the forest tundra ecozone, more exposed and influenced by the Labrador Current (Fig. 1.6).

The discrepancies between the two records could also be, at least partially, ascribed to within-bog spatial heterogeneity. The use of a single core per site could limit the representativeness of the records for the whole bogs as vegetation and micro-topography affect the capture and retention efficiency of atmospheric particles (Bindler *et al.*, 2004). The difference between hummocks and hollows is well established, where hummocks are known to have higher interception of atmospheric particles (Norton, Evans and Kahl, 1997; Oldfield *et al.*, 1995). However, both records were collected onto low hummock microforms with similar plant composition (i.e. *Sphagnum fuscum* and *S. rubellum/capillifolium* dominated), which reduces the potential for the dust flux to be controlled by spatial heterogeneity. Furthermore, both records display similar ^{210}Pb inventories of 0.32 and 0.35 kBq m^{-2} for Baie and IDH respectively, which is similar to the inventory of 0.36 kBq m^{-2} in another record from the Baie bog (Pratte *et*

al., 2013). These similar ^{210}Pb inventories are as expected (Le Roux and Marshall, 2011) given the similar average annual rainfall in both area (1000 mm; Environment Canada, 2010). This suggests that particle deposition has not been overly affected by the micro-topography or vegetation in the present study.

Although previous studies suggest that the Havre St-Pierre region was exposed to a drier and colder climate, the IDH bog did not record any significant increase in dust deposition during these periods, which could be explained by the availability of dust particles. While the peatlands along the coast of the Gulf of St. Lawrence are largely exposed to wind and long freezing seasons (Magnan and Garneau, 2014), the IDH peatland may have been protected by the tree fringe that surrounds its open center, which may have acted as a barrier for dust accumulation. Furthermore, the fact that the peatland is located on an island about two kilometers offshore probably contributed to the lower dust fluxes. For changes in climatic/wind regime to be recorded in peat bogs, specific conditions need to be met. For example, changes in wind regime and climatic conditions were recorded as a result of the presence of sand dunes and/or seashore providing erodible material to certain peat bogs of northern Europe (de Jong *et al.*, 2007; De Vleeschouwer *et al.*, 2009). The same conditions can be applied to Baie bog, which is located near the seashore. Although IDH bog meets similar requirements, it does not record the variations in dust deposition. This discrepancy could be ascribed to the afore-mentioned "isolation" of the peatlands, which would prevent the deposition of a part of the dust.

To summarize, results from the two dust records and comparison with other regional records highlight the importance of local and regional factors on Late Holocene variations in climate and dust deposition in eastern Canada.

1.5 Conclusion

Using peat cores recovered from two peat bogs in the Estuary (Baie) and Gulf (IDH) of the St. Lawrence in eastern Canada, 4000 years of paleodust deposition was reconstructed using REE concentrations. Plant macrofossils and other records of past surface wetness (testate amoeba) from the literature were used to reconstruct hydroclimatic variations over the same period. Principal component analyses showed that REE display the same behavior as other conservative lithogenic elements in the peat column (Ti, Al, Zr), hence they can be used to reconstruct mineral dust deposition in peat. Both cores show periods of increased dust deposition. The Baie bog shows the greatest variability with peaks between 1750-1000 cal BP and 600-100 cal BP. During both periods, comparison with macrofossils assemblages and other surface humidity records suggests periods of climatic instability (wet or dry shift) which affected dust deposition. A reorganisation of atmospheric circulation during these periods is proposed to explain this instability. The agreement between the dust deposition record in the Baie bog and past solar minima suggest that dust deposition increased during cold periods. Over the last 100 years, dust deposition in both peat cores has been affected by anthropogenic activities which increased the atmospheric dust loads through different processes (land clearing, mining, smelting) in both regions.

Aknowledgements

We are grateful to Gaël Le Roux (Ecolab, Toulouse), David Baqué (Ecolab, Toulouse), Aurélie Lanzanova (*Geoscience Environnement Toulouse*) and Bassam Ghaleb (GEOTOP. Montreal, Canada) for their help with major and trace elements analyses and ^{210}Pb dating. Thanks to Gabriel Magnan, Nicole Sanderson, Antoine Thibault and Hans Asnong for help during fieldwork as well as Julien Gogot, Julien Baudet-Lancup and Marie-Josée Tavella for lab assistance. Thanks to *Les Tourbeux* for fruitful discussions. Financial support was provided by Natural Sciences and Engineering

Research Council of Canada (NSERC #250287) discovery grant to MG. Scholarships to SP were provided by the Fonds de Recherche Québec – Nature et Technologie (FRQNT; #176250 and #180723). An additional mobility grant was provided by Institut National Polytechnique de Toulouse ("Soutien à la mobilité" grant to FDV).

1.6 References

Albani, S., Delmonte, B., Maggi, V., Baroni, C., Petit, J.R., Stenni, B., Mazzola, C. and Frezzotti, M. (2012). Interpreting last glacial to Holocene dust changes at Talos Dome (East Antarctica): implications for atmospheric variations from regional to hemispheric scales. *Climate of the Past,* 8(2), 741-750.

Albani, S., Mahowald, N.M., Winckler, G., Anderson, R.F., Bradtmiller, L.I., Delmonte, B., François, R., Goman, M., Heavens, N.G., Hesse, P.P., Hovan, S.A., Kang, S.G., Kohfeld, K.E., Lu, H., Maggi, V., Mason, J.A., Mayewski, P.A., McGee, D., Miao, X., Otto-Bliesner, B.L., Perry, A.T., Pourmand, A., Roberts, H.M., Rosenbloom, N., Stevens, T. and Sun, J. (2015). Twelve thousand years of dust: the Holocene global dust cycle constrained by natural archives. *Climate of the Past,* 11(6), 869-903.

Ali, A.A., Ghaleb, B., Garneau, M., Asnong, H. and Loisel, J. (2008). Recent peat accumulation rates in minerotrophic peatlands of the Bay James region, Eastern Canada, inferred by ^{210}Pb and ^{137}Cs radiometric techniques. *Applied Radiation Isotopes,* 66(10), 1350-1358.

Almquist, H., Dieffenbacher-Krall, A.C., Flanagan-Brown, R. and Sanger, D. (2001). The Holocene record of lake levels of Mansell Pond, central Maine, USA. *The Holocene,* 11(2), 189-201.

Appleby, P.G. (2002). Chronostratigraphic Techniques in Recent Sediments. In: Last, W. and J. Smol (dir.), *Tracking Environmental Change Using Lake Sediments* (Vol. 1, p. 171-203): Springer Netherlands.

Arseneault, D. and Payette, S. (1997). Reconstruction of millenial forest dynamics from tree remains in a subarctic tree line peatland. *Ecology,* 78(6), 1873-1883.

Aubert, D., Le Roux, G., Krachler, M., Cheburkin, A., Kober, B., Shotyk, W. and Stille, P. (2006). Origin and fluxes of atmospheric REE entering an ombrotrophic peat bog in Black Forest (SW Germany): Evidence from snow, lichens and mosses. *Geochimica et Cosmochimica Acta,* 70(11), 2815-2826.

Barber, K.E. and Langdon, P.G. (2007). What drives the peat-based palaeoclimate record? A critical test using multi-proxy climate records from northern Britain. *Quaternary Science Reviews,* 26(25–28), 3318-3327.

Bernatchez, P. (2003). *Évolution littorale holocène et actuelle des complexes deltaïque de Betsiamites et Manicouagan-Outardes: synthèse, processus, causes et perspectives.* (PhD). Université Laval, Québec.

Bettis, E.A.I., Muhs, D.R., Roberts, H.M. and Wintle, A.G. (2003). Last Glacial loess in the conterminous USA. *Quaternary Science Reviews,* 22(18–19), 1907-1946.

Bindler, R., Klarqvist, M., Klaminder, J. and Förster, J. (2004). Does within-bog spatial variability of mercury and lead constrain reconstructions of absolute deposition rates from single peat records? The example of Store Mosse, Sweden. *Global Biogeochemical Cycles,* 18(3), GB3020.

Blaauw, M. and Christen, J.A. (2011). Flexible paleoclimate age-depth models using an autoregressive gamma process. *Bayesian Analysis,* 6, 457-474.

Bond, G., Kromer, B., Beer, J., Muscheler, R., Evans, M.N., Showers, W., Hoffmann, S., Lotti-Bond, R., Hajdas, I. and Bonani, G. (2001). Persistent solar influence on North Atlantic climate during the Holocene. *Science,* 294(5549), 2130-2136.

Booth, R.K., Jackson, S.T., Forman, S.L., Kutzbach, J.E., Bettis, E.A., Kreigs, J. and Wright, D.K. (2005). A severe centennial-scale drought in midcontinental North America 4200 years ago and apparent global linkages. *The Holocene,* 15(3), 321-328.

Bryson, R.A. (1966). Air masses, streamlines and the boreal forest. *Geographical Bulletin,* 8(3), 228-266.

Bryson RA and Hare FK (1974). Climates of North America. In: Bryson RA and Hare FK (eds) *Climates of North America.* Elsevier, 1-47.

Carcaillet, C. and Richard, P.J.H. (2000). Holocene changes in seasonal precipitation highlighted by fire incidence in eastern Canada. *Climate Dynamics,* 16(7), 549-559.

Caseldine, C.J., Baker, A., Charman, D.J. and Hendon, D. (2000). A comparative study of optical properties of NaOH peat extracts: implications for humification studies. *The Holocene,* 10(5), 649-658.

Chambers, F.M., Ogle, M.I. and Blackford, J.J. (1999). Palaeoenvironmental evidence for solar forcing of Holocene climate: linkages to solar science. *Progress in Physical Geography,* 23(2), 181-204.

Chambers, F.M. and Charman, D.J. (2004). Holocene environmental change: contributions from the peatland archive. *The Holocene,* 14(1), 1-6.

Chambers, F.M., Beilman, D.W. and Yu, Z.C. (2011). Methods for determining peat humification and for quantifying peat bulk density, organic matter and carbon content for palaeostudies of climate and peatland carbon dynamics. *Mires and Peat,* 7.

Charman, D.J., Amesbury, M.J., Hinchliffe, W., Hughes, P.D.M., Mallon, G., Blake, W.H., Daley, T.J., Gallego-Sala, A.V. and Mauquoy, D. (2015). Drivers of Holocene peatland carbon accumulation across a climate gradient in northeastern North America. *Quaternary Science Reviews,* 121(0), 110-119.

Crum HA and Anderson LE. (1979–1980). *Mosses of Eastern North America.* New York: Columbia University Press.

Damman, A.W.H. (1978). Distribution and movement of elements in ombrotrophic peat bogs. *Oikos,* 30(3), 480-495.

de Jong, R., Schoning, K. and Björck, S. (2007). Increased aeolian activity during humidity shifts as recorded in a raised bog in south-west Sweden during the past 1700 years. *Clim. Past,* 3(3), 411-422.

de Jong, R., Blaauw, M., Chambers, F., Christensen, T., Vleeschouwer, F., Finsinger, W., Fronzek, S., Johansson, M., Kokfelt, U., Lamentowicz, M., Roux, G., Mauquoy, D., Mitchell, E.D., Nichols, J., Samaritani, E. and Geel, B. (2010). Climate and Peatlands. Dans Dodson, J. (dir.), *Changing Climates, Earth Systems and Society* (p. 85-121): Springer Netherlands.

De Vleeschouwer, F., Piotrowska, N., Sikorski, J., Pawlyta, J., Cheburkin, A., Le Roux, G., Lamentowicz, M., Fagel, N. and Mauquoy, D. (2009). Multiproxy evidence of `Little Ice Age' palaeoenvironmental changes in a peat bog from northern Poland. *The Holocene,* 19(4), 625-637.

De Vleeschouwer, F., Pazdur, A., Luthers, C., Streel, M., Mauquoy, D., Wastiaux, C., Le Roux, G., Moschen, R., Blaauw, M., Pawlyta, J., Sikorski, J. and Piotrowska, N. (2012). A millennial record of environmental change in peat deposits from the Misten bog (East Belgium). *Quaternary International,* 268, 44-57.

De Vleeschouwer, F., Ferrat, M., McGowan, H., Vanneste, H. and Weiss, D. (2014). Extracting paleodust information from peat geochemistry. *PAGES Magazine,* 22(2), 88-89.

Delmonte, B., Andersson, P.S., Hansson, M., Schöberg, H., Petit, J.R., Basile-Doelsch, I. and Maggi, V. (2008). Aeolian dust in East Antarctica (EPICA-Dome C and Vostok): Provenance during glacial ages over the last 800 kyr. *Geophysical Research Letters,* 35(7).

deMenocal, P., Ortiz, J., Guilderson, T., Adkins, J., Sarnthein, M., Baker, L. and Yarusinsky, M. (2000). Abrupt onset and termination of the African Humid Period: rapid climate responses to gradual insolation forcing. *Quaternary Science Reviews,* 19(1–5), 347-361.

Donarummo, J., Ram, M. and Stoermer, E.F. (2003). Possible deposit of soil dust from the 1930's U.S. dust bowl identified in Greenland ice. *Geophysical Research Letters,* 30(6), 1269.

Environment Canada (2010) Canadian Climate Normals 1981-2010. Available at: http://climate.weather.gc.ca/climate_normals/ (accessed 18 January 2016).

Eriksson, L., Johansson, E., N., K.-W. and Wodl, S. (1999). *Introduction to multi-and megavariate data analysis using projection methods (PCA & PLS).* Umeå: Umetrics AB.

Filion, L. (1984). A relationship between dunes, fire and climate recorded in the Holocene deposits of Quebec. *Nature,* 309(5968), 543-546.

Fischer, H., Siggaard-Andersen, M.-L., Ruth, U., Röthlisberger, R. and Wolff, E. (2007). Glacial/interglacial changes in mineral dust and sea-salt records in polar ice cores: Sources, transport, and deposition. *Reviews of Geophysics,* 45(1).

Gallon, C., Tessier, A., Gobeil, C. and Beaudin, L. (2005). Sources and chronology of atmospheric lead deposition to a Canadian Shield lake: Inferences from Pb isotopes and PAH profiles. *Geochimica et Cosmochimica Acta,* 69(13), 3199-3210.

Garneau, M. (1995). *Collection de référence de graines et autres macrofossiles végétaux de taxons provenant du Québec méridional et boréal et de l'Arctique canadien.* Sainte-Foy: Open File 3048, Geological Survey of Canada, Division de la science des terrains.

Garneau, M., van Bellen, S., Magnan, G., Beaulieu-Audy, V., Lamarre, A. and Asnong, H. (2014). Holocene carbon dynamics of boreal and subarctic peatlands from Québec, Canada. *The Holocene,* 24(9), 1043-1053.

Girardin, M.P., Tardif, J., Flannigan, M.D. and Bergeron, Y. (2004). Multicentury reconstruction of the Canadian Drought Code from eastern Canada and its relationship with paleoclimatic indices of atmospheric circulation. *Climate Dynamics,* 23(2), 99-115.

Givelet, N., Le Roux, G., Cheburkin, A., Chen, B., Frank, J., Goodsite, M.E., Kempter, H., Krachler, M., Noernberg, T., Rausch, N., Rheinberger, S., Roos-Barraclough, F., Sapkota, A., Scholz, C. and Shotyk, W. (2004). Suggested protocol for collecting, handling and preparing peat cores and peat samples for physical, chemical, mineralogical and isotopic analyses. *Journal of Environmental Monitoring,* 6(5), 481-492.

Goudie, A.S. and Middleton, N.J. (2001). Saharan dust storms: nature and consequences. *Earth-Science Reviews,* 56(1–4), 179-204.

Grondin P., Blouin, J.-L., and Bouchard, D. (1980). *Étude phyto-écologique de l'archipel de Mingan. Vols. 1-3.* Report for Groupe Dryade, Office de planification et de développement du Québec, Québec.

Hansson, S.V., Rydberg, J., Kylander, M., Gallagher, K. and Bindler, R. (2013). Evaluating paleoproxies for peat decomposition and their relationship to peat geochemistry. *The Holocene,* 23(12), 1666-1671.

Harrison, S.P., Kohfeld, K.E., Roelandt, C. and Claquin, T. (2001). The role of dust in climate changes today, at the last glacial maximum and in the future. *Earth-Science Reviews,* 54(1–3), 43-80.

Hughes, P.D.M., Blundell, A., Charman, D.J., Bartlett, S., Daniell, J.R.G., Wojatschke, A. and Chambers, F.M. (2006). An 8500 cal. year multi-proxy climate record from a bog in eastern Newfoundland: contributions of meltwater discharge and solar forcing. *Quaternary Science Reviews,* 25(11–12), 1208-1227.

Ireland, R.R. (1982) *Moss Flora of the Maritime Provinces*. Ottawa: National Museums of Canada.

Jeglum, J.K., Rothwell, R.L., Berry, G.J. and Smith, G.K.M. (1992). A peat sampler for rapid survey. *Technical Note, Canadian Forestry Service,* 13, 921-932.

Jessen, C.A., Solignac, S., Nørgaard-Pedersen, N., Mikkelsen, N., Kuijpers, A. and Seidenkrantz, M.-S. (2011). Exotic pollen as an indicator of variable atmospheric circulation over the Labrador Sea region during the mid to late Holocene. *Journal of Quaternary Science,* 26(3), 286-296.

Jowsey, P.C. (1966). An improved peat sampler. *New Phytologist,* 65(2), 245-248.

Krachler, M., Mohl, C., Emons, H. and Shotyk, W. (2003). Two thousand years of atmospheric rare earth element (REE) deposition as revealed by an ombrotrophic peat bog profile, Jura Mountains, Switzerland. *Journal of Environmental Monitoring,* 5(1), 111-121.

Lamentowicz, M., van der Knaap, W.O., van Leeuwen, J.F.N., Hangartner, S., Mitchell, E.A.D., Goslar, T., Tinner, W. and Kaminik, C. (2010). A multi-proxy

high-resolution approach to reconstructing past environmental change from an Alpine peat archive. *PAGES News,* 18(1), 13-15.

Lemay-Tougas M (2014). *Changements climatiques le long de la côte nord de l'estuaire du Saint-Laurent Durant l'Holocène : relation entre les conditions hydrographiques et le développement des tourbières ombrotrophes côtières.* MSc Thesis. University of Quebec in Montreal (UQAM), Canada.

Le Roux, G. and De Vleeschouwer, F. (2010). Preparation of peat samples for inorganic geochemistry used as palaeoenvironmental proxies. *Mires and Peat,* 7.

Le Roux, G. and Marshall, W.A. (2011). Constructing recent peat accumulation chronologies using atmospheric fall-out radionuclides. *Mires and Peat,* 7.

Le Roux, G., Fagel, N., De Vleeschouwer, F., Krachler, M., Debaille, V., Stille, P., Mattielli, N., van der Knaap, W.O., van Leeuwen, J.F.N. and Shotyk, W. (2012). Volcano- and climate-driven changes in atmospheric dust sources and fluxes since the Late Glacial in Central Europe. *Geology,* 40(4), 335-338.

Loisel, J. and Garneau, M. (2010). Late Holocene paleoecohydrology and carbon accumulation estimates from two boreal peat bogs in eastern Canada: Potential and limits of multi-proxy archives. *Palaeogeography, Palaeoclimatology, Palaeoecology,* 291(3–4), 493-533.

Magnan, G. and Garneau, M. (2014). Evaluating long-term regional climate variability in the maritime region of the St. Lawrence North Shore (eastern Canada) using a multi-site comparison of peat-based paleohydrological records. *Journal of Quaternary Science,* 29(3), 209-220.

Magnan, G., Garneau, M. and Payette, S. (2014). Holocene development of maritime ombrotrophic peatlands of the St. Lawrence North Shore in eastern Canada. *Quaternary Research,* 82(1), 96-106.

Maher, B.A., Prospero, J.M., Mackie, D., Gaiero, D., Hesse, P.P. and Balkanski, Y. (2010). Global connections between aeolian dust, climate and ocean biogeochemistry at the present day and at the last glacial maximum. *Earth-Science Reviews,* 99(1–2), 61-97.

Marie-Victorin, F. (1995). *Flore laurentienne, Third Edition.* Montreal: Les Presses de l'Université de Montréal.

Marx, S.K., Kamber, B.S., McGowan, H.A. and Zawadzki, A. (2010). Atmospheric pollutants in alpine peat bogs record a detailed chronology of industrial and agricultural development on the Australian continent. *Environmental Pollution,* 158(5), 1615-1628.

Mauquoy, D., van Geel, B., Blaauw, M., Speranza, A. and van der Plicht, J. (2004). Changes in solar activity and Holocene climatic shifts derived from ^{14}C wiggle-match dated peat deposits. *The Holocene,* 14(1), 45-52.

Mauquoy, D. and van Geel, B. (2007). Mire and peat macros. In: Elias, S. A. (dir.), *Encyclopedia of Quaternary Science.* Oxford: Elsevier, 2315-2336.

Mayewski, P.A., Rohling, E.E., Curt Stager, J., Karlén, W., Maasch, K.A., David Meeker, L., Meyerson, E.A., Gasse, F., van Kreveld, S., Holmgren, K., Lee-Thorp, J., Rosqvist, G., Rack, F., Staubwasser, M., Schneider, R.R. and Steig,

E.J. (2004). Holocene climate variability. *Quaternary Research,* 62(3), 243-255.

Meskhidze, N., Chameides, W.L., Nenes, A. and Chen, G. (2003). Iron mobilization in mineral dust: Can anthropogenic SO2 emissions affect ocean productivity? *Geophysical Research Letters,* 30(21), 2085.

Mischke, S., Zhang, C., Börner, A. and Herzschuh, U. (2010). Lateglacial and Holocene variation in aeolian sediment flux over the northeastern Tibetan Plateau recorded by laminated sediments of a saline meromictic lake. *Journal of Quaternary Science,* 25(2), 162-177.

Muhs, D.R. and Budahn, J.R. (2006). Geochemical evidence for the origin of late Quaternary loess in central Alaska. *Canadian Journal of Earth Sciences,* 43(3), 323-337.

Muhs, D.R. (2013). The geologic records of dust in the Quaternary. *Aeolian Research,* 9(0), 3-48.

Norton, S.A., Evans, G.C. and Kahl, J.S. (1997). Comparison of Hg and Pb Fluxes to Hummocks and Hollows of Ombrotrophic Big Heath Bog and to Nearby Sargent Mt. Pond, Maine, USA. *Water, Air, & Soil Pollution,* 100(3), 271-286.

O'Brien, S.R., Mayewski, P.A., Meeker, L.D., Meese, D.A., Twickler, M.S. and Whitlow, S.I. (1995). Complexity of Holocene climate as reconstructed from a Greenland Ice core. *Science,* 270(5244), 1962-1964.

Oldfield F, Richardson N and Appleby PG (1995) Radiometric dating (^{210}Pb, ^{137}Cs, ^{241}Am) of recent ombrotrophic peat accumulation and evidence for changes in mass balance. *The Holocene* (5), 141-148.

Poole, W.H., Sanford, B.V., Williams, H., *et al.* (1970) Geology of southeastern Canada. In: Douglas, R.J.W. (ed) *Geology and economic minerals of Canada.* Ottawa: Geological Survey of Canada, pp. 228-304.

Pratte, S., Mucci, A. and Garneau, M. (2013). Historical records of atmospheric metal deposition along the St. Lawrence Valley (eastern Canada) based on peat bog cores. *Atmospheric Environment,* 79, 831-840.

Rea, D.K. (1994). The paleoclimatic record provided by eolian deposition in the deep sea: The geologic history of wind. *Reviews of Geophysics,* 32(2), 159-195.

Reimer, P.J., Bard, E., Bayliss, A., Beck, J.W., Blackwell, P.G., Bronk Ramsey, C., Buck, C.E., Cheng, H., Edwards, R.L., Friedrich, M., Grootes, P.M., Guilderson, T.P., Haflidason, H., Hajdas, I., Hatté, C., Heaton, T.J., Hoffmann, D.L., Hogg, A.G., Hughen, K.A., Kaiser, K.F., Kromer, B., Manning, S.W., Niu, M., Reimer, R.W., Richards, D.A., Scott, E.M., Southon, J.R., Staff, R.A., Turney, C.S.M. and van der Plicht, J. (2013). IntCal13 and Marine13 Radiocarbon Age Calibration Curves 0–50,000 Years cal BP. *Radiocarbon,* 55(4), 1869-1887.

Sauvé, A. (2016) Reconstitution holocène de la végétation et du climat pour les régions de Baie-Comeau et de Havre-Saint-Pierre, Québec. MSc Thesis, University of Quebec in Montreal (UQAM), Canada.

Shotyk, W., Weiss, D., Kramers, J.D., R., F., Cheburkin, A., Gloor, M. and Reese, S. (2001). Geochemistry of the peat bog at Etang de la Gruère, Jura Mountains, Switzerland, and its record of atmospheric Pb and lithogenic trace metals (Sc, Ti, Y, Zr, and REE) since 12,370 ^{14}C yr BP. *Geochimica et Cosmochimica Acta,* 65(14), 2337-2360.

Shotyk, W., Krachler, M., Martinez-Cortizas, A., Cheburkin, A.K. and Emons, H. (2002). A peat bog record of natural, pre-anthropogenic enrichments of trace elements in atmospheric aerosols since 12 370 ^{14}C yr BP, and their variation with Holocene climate change. *Earth and Planetary Science Letters,* 199(1-2), 21-37.

Steinmann, P. and Shotyk, W. (1997). Geochemistry, mineralogy, and geochemical mass balance on major elements in two peat bog profiles (Jura Mountains, Switzerland). *Chemical Geology,* 138(1–2), 25-53.

Sullivan, M.E. and Booth, R.K. (2011). The potential influence of short-term environmental variability on the composition of testate amoeba communities. *Environmental Microbiology,* 62, 80-93.

Tolonen, K. (1984). Interpretation of changes in the ash content of ombrotrophic peat layers. *Bulletin of the Geological Society of Finland,* 56, 207-219.

Vanneste, H., De Vleeschouwer, F., Martínez-Cortizas, A., von Scheffer, C., Piotrowska, N., Coronato, A. and Le Roux, G. (2015). Late-glacial elevated dust deposition linked to westerly wind shifts in southern South America. *Scientific Reports,* 5

Viau, A.E., Gajewski, K., Fines, P., Atkinson, D.E. and Sawada, M.C. (2002). Widespread evidence of 1500 yr climate variability in North America during the past 14000 yr. *Geology,* 30(5), 455-458.

Viau, A.E., Gajewski, K., Sawada, M.C. and Fines, P. (2006). Millennial-scale temperature variations in North America during the Holocene. *Journal of Geophysical Research: Atmospheres,* 111(D9).

Wanner, H., Beer, J., Bütikofer, J., Crowley, T.J., Cubasch, U., Flückiger, J., Goosse, H., Grosjean, M., Joos, F., Kaplan, J.O., Küttel, M., Müller, S.A., Prentice, I.C., Solomina, O., Stocker, T.F., Tarasov, P., Wagner, M. and Widmann, M. (2008). Mid- to Late Holocene climate change: an overview. *Quaternary Science Reviews,* 27(19–20), 1791-1828.

Wedepohl, K.H. (1995). The composition of the continental crust. *Geochimica et Cosmochimica Acta,* 59(7), 1217-1232.

Weiss, D., Shotyk, W., Rieley, J., Page, S., Gloor, M., Reese, S. and Martinez-Cortizas, A. (2002). The geochemistry of major and selected trace elements in a forested peat bog, Kalimantan, SE Asia, and its implications for past atmospheric dust deposition. *Geochimica et Cosmochimica Acta,* 66(13), 2307-2323.

Yu, Z., Campbell, I.D., Campbell, C., Vitt, D.H., Bond, G.C. and Apps, M.J. (2003). Carbon sequestration in western Canadian peat highly sensitive to Holocene wet-dry climate cycles at millennial timescales. *The Holocene,* 13(6), 801-808.

Zdanowicz, C.M., Zielinski, G.A., Wake, C.P., Fisher, D.A. and Koerner, R.M. (2000). A Holocene Record of Atmospheric Dust Deposition on the Penny Ice Cap, Baffin Island, Canada. *Quaternary Research,* 53(1), 62-69.

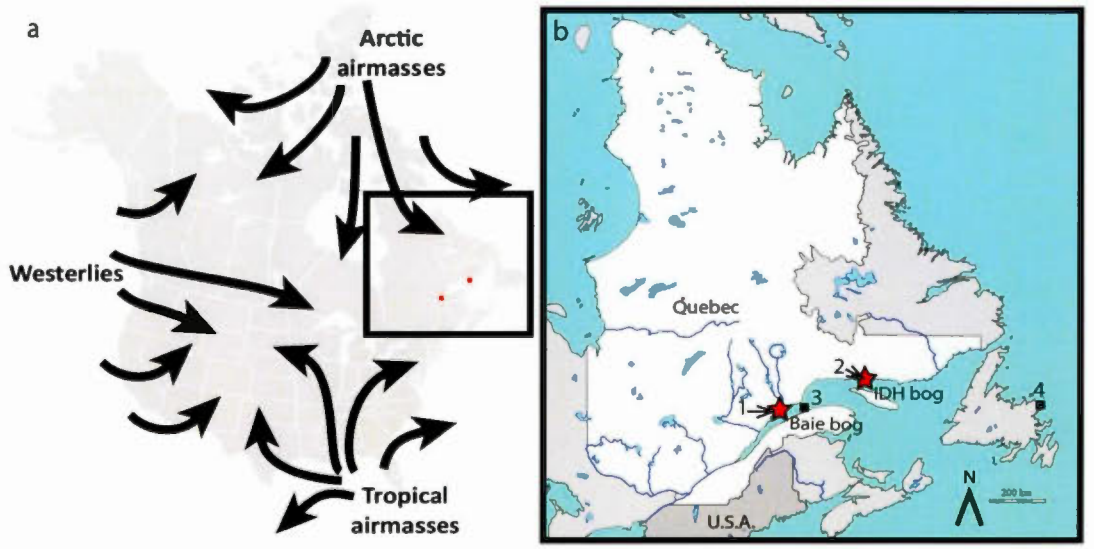

Figure 1.1 Map of North America showing the main air masses over the region (from Bryson, 1966; Bryson and Hare, 1974) (A). Location of the Baie and IDH peatlands (B) and main records discussed in the text including 1) Baie and Lebel bogs (Magnan and Garneau, 2014); 2) Mort and Plaine bogs (Magnan and Garneau, 2014); 3) COR0602-42 marine core (Lemay-Tougas, 2014); 4) Nordan's Pond bog (Hughes *et al.*, 2006).

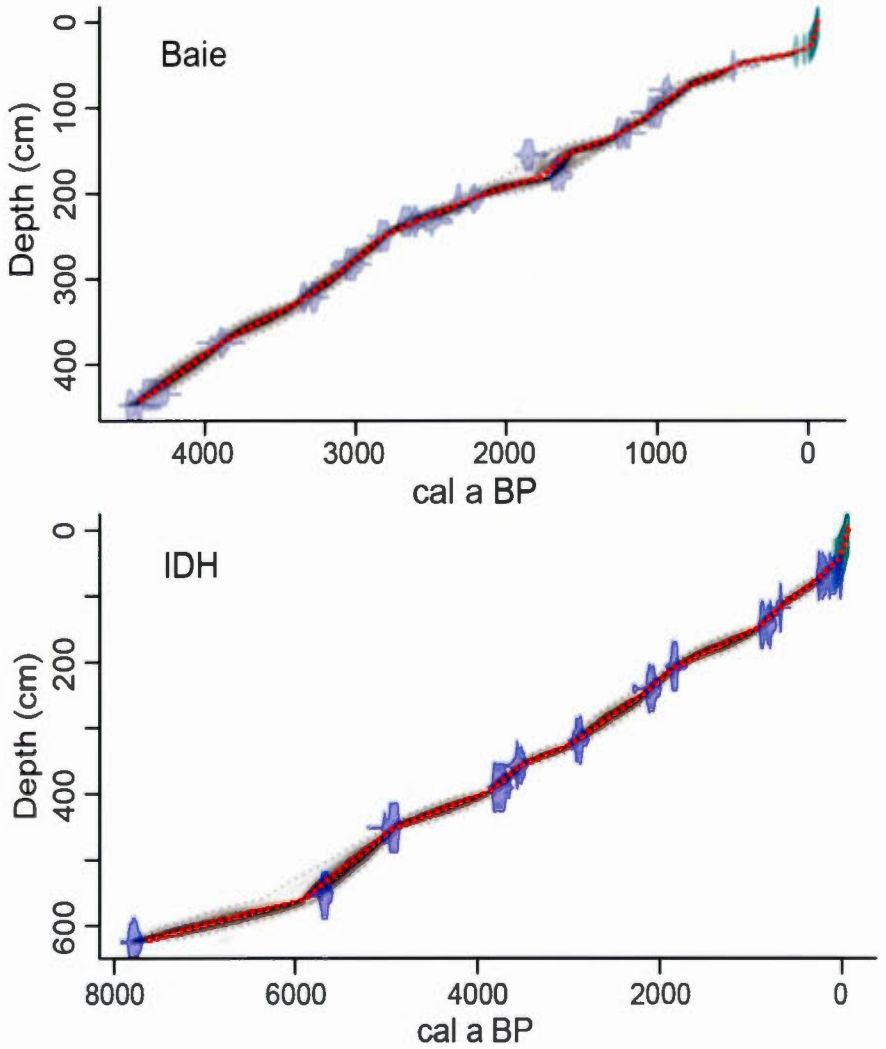

Figure 1.2 Age-depth models for Baie (top) and IDH (bottom) cores constructed using *BACON* software (Blaauw and Christen, 2011) using both ^{210}Pb and ^{14}C dates. The gray bands encompass all possible age-depth models whereas the dotted lines represent the 95% confidence intervals. The red dotted line represents the weighted mean age of each modeled sample. Purple symbols indicate calendar age distribution of ^{14}C dates and light blue symbols show ^{210}Pb ages derived from the CRS model.

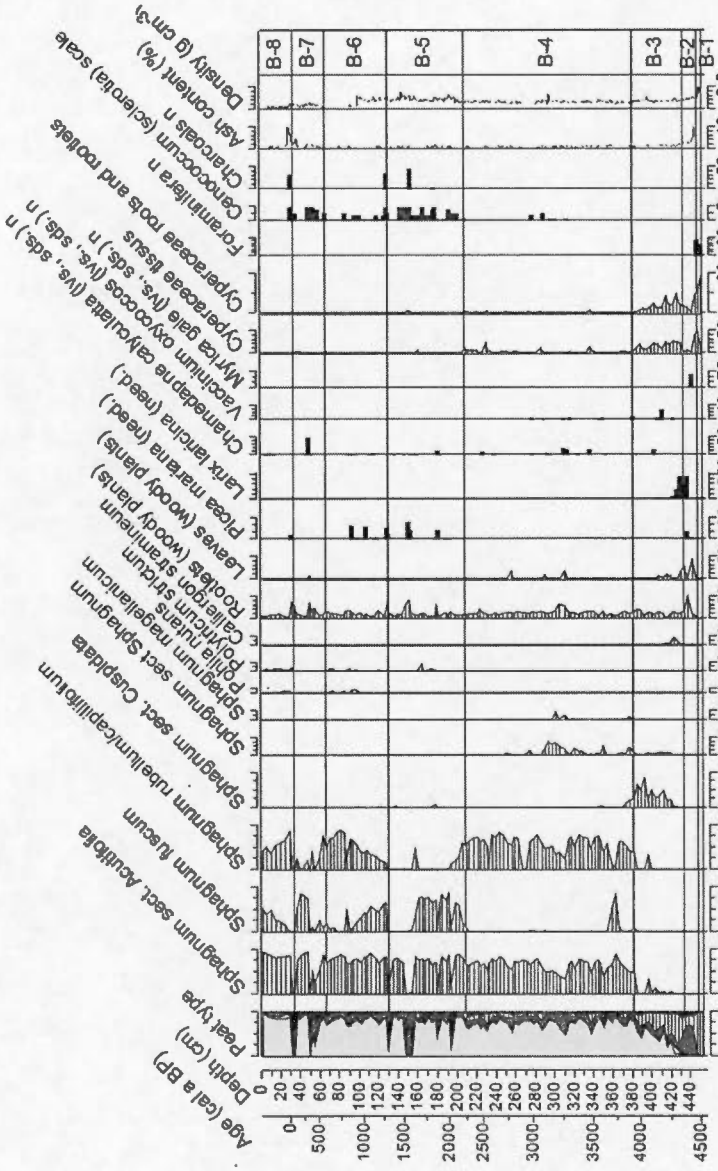

Figure 1.3 Macrofossil diagrams, ash content and bulk density for Baie core. Peat type (%): *Sphagnum* (light grey), other mosses (white), ligneous (dark grey), Cyperaceae (horizontal lines) and unidentified organic matter (black).

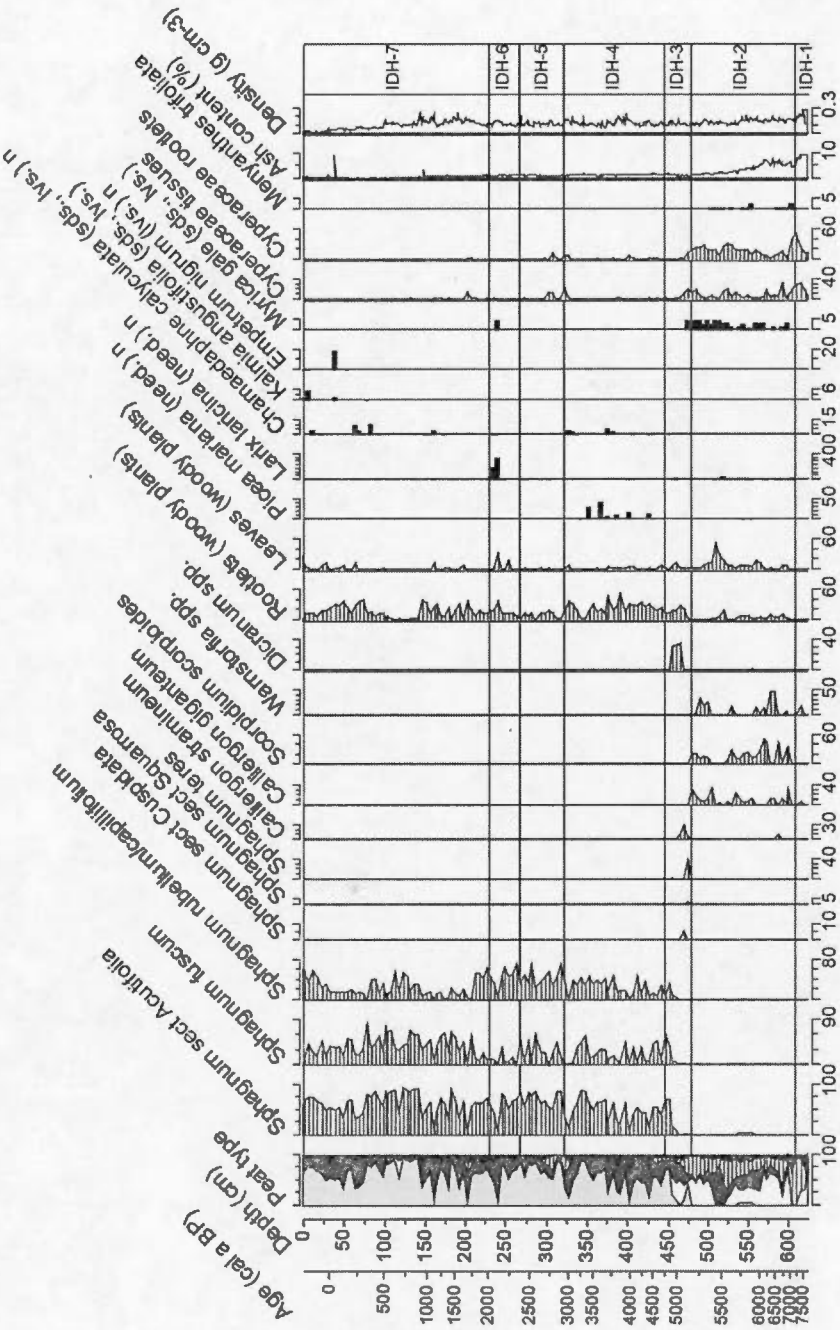

Figure 1.4 Macrofossil diagram, ash content and bulk density for IDH core. Peat type (%): *Sphagnum* (light grey), other mosses (white), ligneous (dark grey), Cyperaceae (horizontal lines) and unidentified organic matter (black).

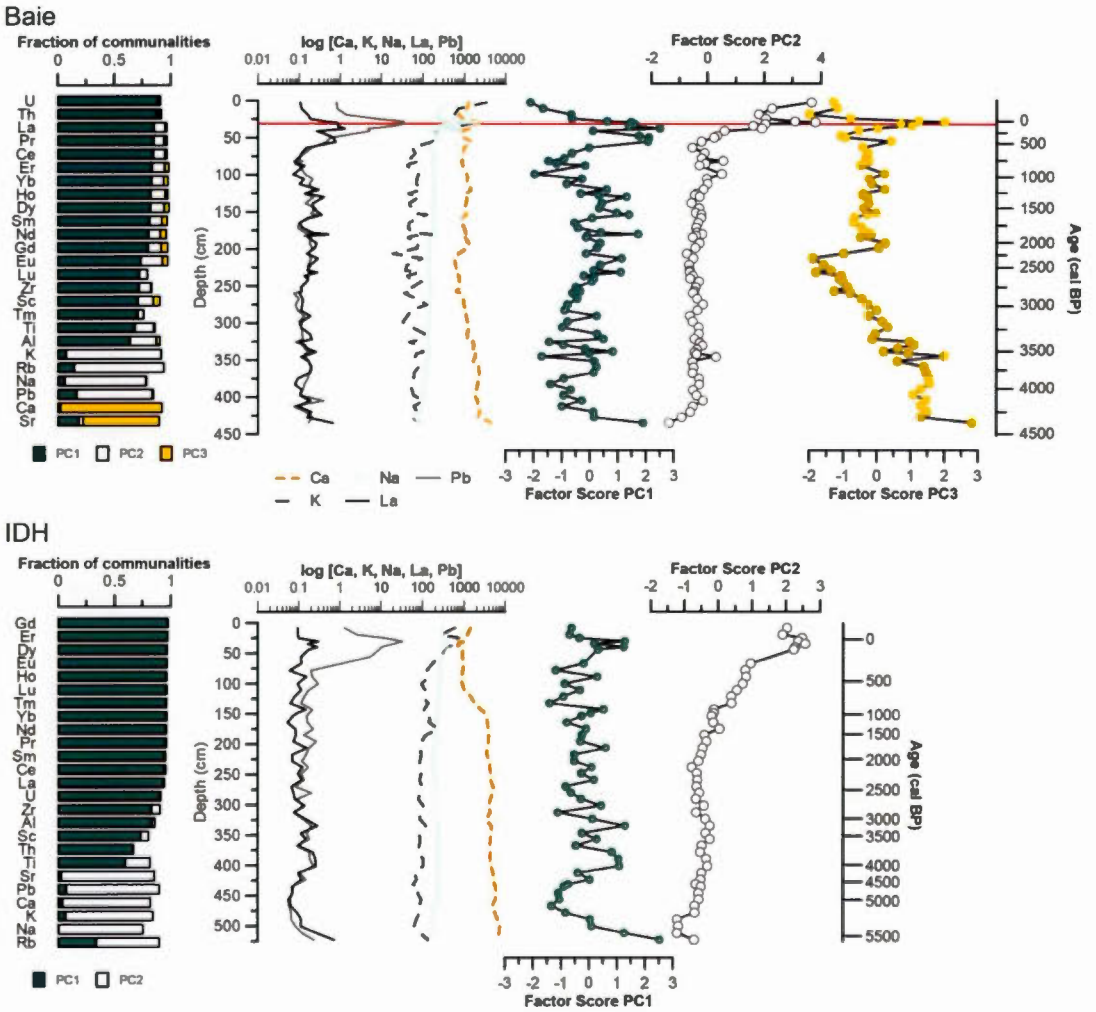

Figure 1.5 Communalities accounting for each element's variance allocated to each principal component, log10 of Ca, Na, K, La and Pb concentrations as well as factor score profiles for each PC for Baie (top) and IDH (bottom) cores. The red line corresponds to a sand layer at 29.7-cm depth in the Baie core.

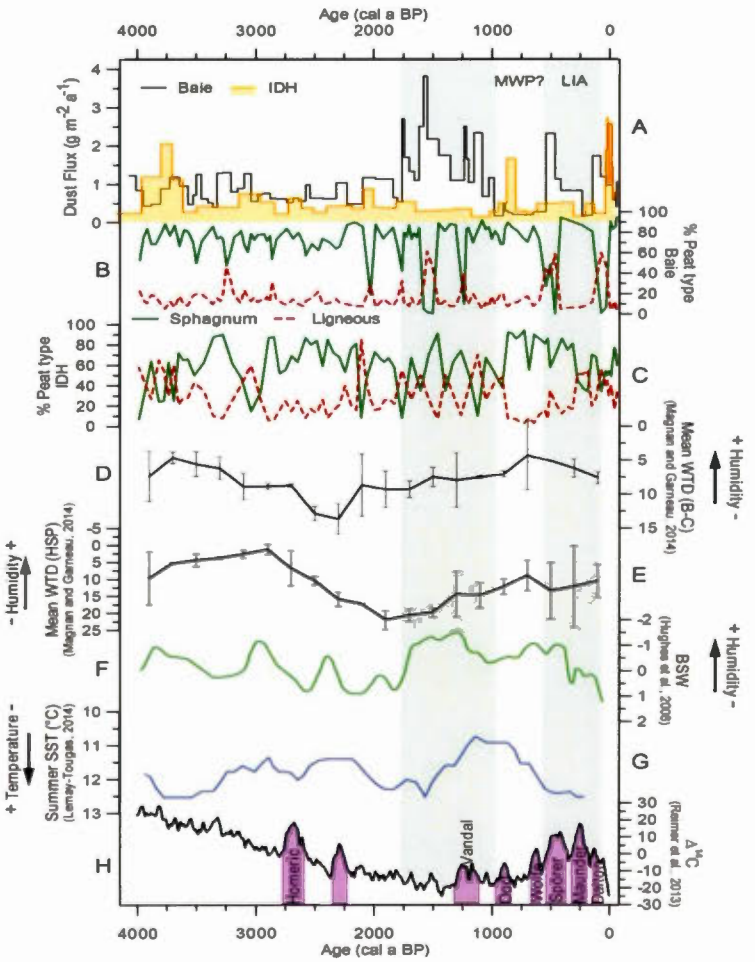

Figure 1.6 a) Atmospheric dust fluxes (g m^{-2} a^{-1}) in Baie and IDH, b) % of *Sphagnum* and Ericaceae in Baie (this study), c) % of *Sphagnum* and Ericaceae in IDH (this study), d) mean water table depth (WTD) for every 200 years from two peatlands in Baie-Comeau (Baie and Lebel; B-C) region (Magnan and Garneau, 2014), e) mean WTD for every 200 years from two peatlands in Havre St-Pierre (Mort and Plaine; HSP) region (Magnan and Garneau, 2014), f) bog surface wetness (BSW) from Newfoundland (Hughes *et al.*, 2006), g) sea surface temperature (SST) from COR0602-42 (Lemay-Tougas, 2014), h) $\Delta^{14}C$ curve (Reimer *et al.*, 2013). The blue areas correspond to periods of increased dust deposition discussed in the text.

Table 1.1 Results of ^{14}C AMS measurements, calibration and description of samples for the Baie and IDH cores.

Site and sample	Depth (cm)	Laboratory number	^{14}C age (BP)	2σ range (cal a BP)	Material dated
Baie					
45	51.6	UCIAMS-129510	425±15	481-513	Charred *Picea mariana* needles
67	79.4	UCIAMS-151367	1015±25	833-971	*Sphagnum* spp. stems
106	105.9	UCIAMS-129511	1120±15	977-1059	*Sphagnum* spp. stems
128	130.0	UCIAMS-129512	1275±15	1181-1271	Charred *Picea mariana* needles
151	155.2	UCIAMS-135384	1905±20	1818-1893	*Sphagnum* spp. stems
173	179.3	UCIAMS-129513	1740±25	1570-1709	*Sphagnum* spp. stems, branches and leaves, charred *Picea mariana* needles
196	206.7	UCIAMS-129514	2250±15	2162-2336	*Sphagnum* spp. stems
217	233.0	UCIAMS-129515	2465±15	2442-2704	*Sphagnum* spp. stems
232	250.2	UCIAMS-129516	2725±15	2779-2853	*Sphagnum* spp. stems
256	283.2	UCIAMS-129517	2900±15	2963-3136	*Sphagnum* spp. stems
286	321.8	UCIAMS-129518	3090±15	3248-3362	*Sphagnum* spp. stems, *Chamaedaphne calyculata* leaf fragments
328	374.8	UCIAMS-129519	3590±15	3842-3961	*Sphagnum* spp. stems, Ericaceae leaf fragments
376	435.3	UCIAMS-129520	3885±15	4250-4409	*Larix laricina* needles
386	447.9	UCIAMS-135385	3995±20	4421-4519	Bulk peat
IDH					
54	69.7	UCIAMS-135378	140±20	8-278	*Sphagnum* spp. stems
116	118.1	UCIAMS-135379	760±20	670-726	*Sphagnum* spp. stems
137	143.6	UCIAMS-151363	905±20	763-910	*Sphagnum* stems, branches and leaves
191	206.8	UCIAMS-151364	1900±20	1815-1896	*Sphagnum* stems
220	240.7	UCIAMS-135380	2120±20	2007-2150	*Larix laricina* needles, *Myrica gale* and *Chamaedaphne calyculata* leaf fragments, *Sphagnum* spp. stems
286	318.9	UCIAMS-135381	2785±20	2804-2951	*Sphagnum* spp. stems
317	357.0	UCIAMS-151365	3320±20	3479-3607	*Sphagnum* spp. stems
345	390.8	UCIAMS-151366	3480±25	3651-3832	*Sphagnum* spp.stems
394	451.7	UCIAMS-135382	4380±20	4857-5033	*Sphagnum* spp. stems

478	554.3	UCIAMS-135383	4960±25	5612-5737	*Larix laricina* needles and seeds, *Myrica gale* and *Chamaedaphne calyculata* leaf fragments
535	624.1	UCIAMS-123619	6950±25	7699-7839	*Carex* spp. seeds

Table 1.2 Results of ^{210}Pb measurements and CRS modelling on Baie core

Sample	Depth (cm)	$^{210}Pb_{tot}$ activity (Bq kg^{-1})	$^{210}Pb_{ex}$ activity (Bq kg^{-1})	CRS ^{210}Pb age (AD)	Uncertainty (a)
Baie 2	1.7	332	316	2010	1
Baie 3	2.9	500	484	2008	1
Baie 4	4.1	257	241	2006	1
Baie 6	6.5	339	323	2003	1
Baie 8	8.9	290	274	2002	1
Baie 10	11	236	221	2001	1
Baie 12	13.4	323	308	1997	1
Baie 14	15.7	358	343	1991	1
Baie 16	17.9	363	347	1987	1
Baie 18	20.3	209	193	1984	2
Baie 20	22.6	268	252	1979	2
Baie 22	24.9	248	232	1974	2
Baie 24	27.3	267	251	1966	2
Baie 26	29.7	237	221	1953	3
Baie 28	32.1	241	225	1921	4
Baie 30	34.5	104	89	1869	8
Baie 32	36.9	32	17		
Baie 34	39.1	16	0		
Baie 36	41.4	15	0		

Table 1.3 Results of ^{210}Pb measurements and CRS modelling on IDH core

Sample	Depth (cm)	$^{210}Pb_{tot}$ Activity (Bq kg^{-1})	$^{210}Pb_{ex}$ activity (Bq kg^{-1})	CRS ^{210}Pb age (AD)	Uncertainty (a)
IDH 1	0.8	449	436	2010	1
IDH 2	2.4	480	468	2006	1
IDH 3	3.6	436	423	2001	1
IDH 5	6.0	388	375	1997	1
IDH 7	8.5	373	360	1993	1
IDH 9	10.9	420	408	1990	1
IDH 11	13.3	227	215	1987	1
IDH 13	15.8	334	321	1983	1
IDH 15	18.4	262	249	1980	1
IDH 17	21.1	261	249	1976	2
IDH 19	23.8	193	180	1973	2
IDH 21	26.4	215	202	1968	2
IDH 23	29.1	267	255	1958	3
IDH 25	32.0	175	162	1948	3
IDH 27	34.7	116	104	1938	4
IDH 29	37.5	62	50	1933	4
IDH 31	40.2	53	40	1928	5
IDH 33	42.9	53	40	1920	5
IDH 35	45.6	55	42	1909	6
IDH 37	48.8	53	41	1891	6
IDH 39	51.2	59	47	1865	7
IDH 41	53.6	39	26		
IDH 43	58.6	14	0		
IDH 45	63..2	13	0		

Table 1.4 Baie macrofossil zonations

Macrofossil zones	Depth (cm)	Main characteristics
B-8	0-33	High presence of *Sphagnum rubellum/capillifolium* up to 60% with lower percentages of *S. fuscum*.
B-7	33-65	Dominance of *S. fuscum* and diminution of *S. rubellum/capillifolium* presence (down to 20%). High presence of *Cenococcum* spp. sclerotia. Presence of charcoal at the transition with zone B-8. Recurrent peaks in UOM and Ericaceae rootlets.
B-6	66-130	Co-dominance of *Sphagnum fuscum* and *S. rubellum/capillifolium*. Presence of *Picea mariana* needles.
B-5	130-209	Dominance of *Sphagnum fuscum* and disappearance of *S. rubellum/capillifolium*. Occurrence of several peaks in UOM (up to 50%) and Ericaceae rootlets. Presence of two charcoal layers at 130 and 154.1 cm. High abundance of *Cenococcum* spp. sclerotia.
B-4	209-382	High presence, reaching up to 84% of *Sphagnum rubellum/capillifolium*. Presence of *Sphagnum* section *Sphagnum* peaking between 295 and 302 cm.
B-3	382-433	High abundance of Cyperaceae and *Calliergon stramineum*. Numerous *Larix laricina* needles at the bottom of the zone. High percentage of *Sphagnum* section *Cuspidata*.
B-2	448-433	High number of *Myrica gale* leaves and *Larix laricina* needles. Up to 50% of Ericaceae rootlets.
B-1	448-453	Presence of Foraminifera tests and high abundance of Cyperaceae remains (more than 80%)

Table 1.5 IDH macrofossil zonations

Macrofossil zones	Depth (cm)	Main characteristics
IDH-7	0-229	Abundant *S. fuscum* and *S. rubellum/capillifolium* together with numerous Ericaceae rootlets.
IDH-6	229-267	Dominance of *S. rubellum/capillifolium*. Peak in *Larix laricina* needles and presence of *Myrica gale* leaves at 230-250 cm.
IDH-5	267-321	Dominance of *Sphagnum fuscum* and *S. rubellum/capillifolium*. High proportion of ericaceous rootlets. Presence of *Picea mariana* needles
IDH-4	321-445	*Sphagnum* peat dominated by *S. fuscum* and *S. rubellum/capillifolium.*
IDH-3	445-478	Peak in *Sphagnum teres* and *Dicranum* spp.at 450-486 cm. Disappearance of brown mosses other than *Dicranum* spp. Presence of *Menyanthes trifoliata* and *Myrica gale*. Important diminution in Cyperaceae.
IDH-2	478-607	Dominance of brown mosses *Calliergon giganteum*, *Scorpidium scorpioides* and *Warnstorfia* spp. Abundant *Larix laricina* needles and *Myrica gale* seeds and leaves. Presence of *Menyanthes trifoliata* seeds.
IDH-1	607-625	High abundance of Cyperaceae and *Bryum* spp. at the base of the section.

CHAPITRE II

GEOCHEMICAL CHARACTERIZATION (REE, ND AND PB ISOTOPES) OF ATMOSPHERIC MINERAL DUST DEPOSITED IN TWO MARITIME PEAT BOGS FROM THE ST. LAWRENCE NORTH SHORE (EASTERN CANADA)

Steve Pratte[a,b*], François De Vleeschouwer[b] and Michelle Garneau[a]

[a] GEOTOP, Université du Québec à Montréal, C.P. 8888 Succursale Centre-Ville, Montreal, Canada

[b] ECOLAB, Université de Toulouse, CNRS, INPT, UPS, France

Article soumis à *Journal of Quaternary Science* (JQS-16-0015)

RÉSUMÉ

La composition géochimique des poussières atmosphériques minérales déposées dans deux tourbières ombrotrophes de l'Estuaire (Baie) et du Golfe (IDH) du Saint-Laurent fût déterminée. Les particules déposées furent caractérisées à l'aide des concentrations des terres rares (REE), des isotopes du néodyme et du plomb ainsi que la granulométrie. Les deux profils présentent des valeurs de εNd similaires, ce qui s'explique soit par une source commune des poussières atmosphériques ou encore des sources distinctes, mais possédant des valeurs de εNd similaires dans les deux régions. La combinaison des données de εNd avec celles des concentrations en REE et de tailles de particules a permis de mieux cerner la source des particules déposées sur les deux sites ainsi que d'inférer les conditions environnementales et climatiques passées. Les REE, le εNd et les tailles de particules suggèrent qu'au cours des 2000 dernières années, la tourbière de Baie a reçu une proportion accrue de poussières atmosphériques provenant de sources locales. Une augmentation de l'instabilité locale en réponse à une instabilité hydroclimatique régionale et une plus grande variabilité des températures (principalement contrôlée par l'activité solaire) sont proposées afin d'expliquer cette quantité accrue de poussières locales. Le même phénomène est observé dans le profil de IDH depuis 620 cal a BP. Cette période correspond au Petit Âge Glaciaire, une période pour laquelle des changements hydro-climatiques et paléo-écologiques ont déjà été documentés dans la région. Bien que les reconstructions des paléo-poussières obtenues s'accordent relativement bien avec les autres reconstructions climatiques de la région, les différences observées entre les deux profils soulignent la structure complexe et variable des changements climatiques et plus particulièrement des dépôts de poussières dans la région au cours de l'Holocène récent.

ABSTRACT

Dust deposited on two ombrotrophic peat bogs (Baie and IDH bogs) of the St. Lawrence Gulf and Estuary north shore was geochemically characterized using REE concentrations, Nd and Pb isotopes along with particle grain size. Both cores display similar εNd values, which suggests either a common source or sources with similar signatures in both regions. Combining Nd isotope data with REE patterns and particle size allowed for better insights into the source of deposited dust and the inference of past environmental and climatic conditions in both regions. REE elements, εNd and grain-size distribution suggest that, over the last 2000 years, the Baie bog received more local dust due to increased local storminess in response to regional hydroclimatic instability and temperature variations mainly controlled by solar activity. The same phenomenon occurred in the IDH bog since 620 cal a BP, i.e. during the Little Ice Age, where hydroclimatic and paleoecological changes have been previously documented. While the dust reconstructions and regional climatic records agree relatively well, the discrepancies between paleodust records highlight the complex and variable structure of late Holocene changes in paleoclimate and more particularly past dust deposition in eastern Canada.

2.1 Introduction

Mineral dust plays a complex role in the climate system acting both as a factor affecting climate and as a function of it. For instance, mineral dust has effects on radiative budgets, chemical processes in the atmosphere and on the biogeochemical cycles of many elements (Goudie and Middleton, 2001; Meskhidze *et al.*, 2003). Reconstruction of past dust composition and fluxes is important in order to increase our understanding of Holocene climate variability and biogeochemical cycles, hence, a greater number of paleo-dust studies are required.

Until recently, paleo-dust studies have mainly focused on ice cores (Gabrielli *et al.*, 2010) and marine sediments (deMenocal *et al.*, 2000), while continental records focused mainly on loess deposits (Muhs, 2013). Similarly to ice cores, ombrotrophic peatlands (peat bogs) are fed exclusively by atmospheric deposition (Chambers and Charman, 2004) and can therefore provide reliable records of changes in aerosol composition over time (De Vleeschouwer *et al.*, 2014). These archives present two main advantages in comparison to ice cores: they are ubiquitous at middle to high latitudes and they are easy to date. The potential of peat bogs for the reconstruction of Holocene climate variability through the use of multiple indicators is well established (de Jong *et al.*, 2010 and references therein). Peat bogs are increasingly being used as archive of atmospheric dust deposition (Allan *et al.*, 2013; De Vleeschouwer *et al.*, 2012; Shotyk *et al.*, 2002; Vanneste *et al.*, 2015).

Rare earth elements (REE) inherit the chemical signature of their source rock during weathering and their relative patterns are not significantly affected by physical and chemical processes during transport (McLennan, 1989). Hence, REE have been used as tracers and reference elements in a broad range of environmental studies (Aubert *et al.*, 2006; Chiarenzelli *et al.*, 2001; Greaves, Elderfield and Sholkovitz, 1999). Radiogenic isotope signatures of sediments, namely Nd and Pb, have also been used as a tool to trace the dust source as their isotopic ratios are unaffected by erosion and

transport. For example, Biscaye *et al.* (1997) used Nd isotopes in combination with Pb and Sr isotopes to show that Asian desert areas were the main source of soil dust deposited over the Greenland ice sheet during the Pleistocene. Peat bog records of temporal variability of REE and Nd isotopes are still limited to a few sites but proved efficient in dust source tracing (Allan *et al.*, 2013; Aubert *et al.*, 2006; Le Roux *et al.*, 2012; Vanneste *et al.*, 2015). For example, using a combination of dust flux and Nd isotope composition, Le Roux *et al.* (2012) demonstrated the importance of Saharan dust as a source over Western Europe during the mid-Holocene.

Most dust reconstruction studies focus on arid regions whereas the higher latitudes have been overlooked. To date, few records of terrestrial dust deposition exist in North America (Muhs, 2013; Neff *et al.*, 2008) and consist mainly of loess deposits. Periods of enhanced dust deposition have been identified for the first time in two peat bogs from eastern Canada, although the source of the dust deposited in these records is yet unknown (Pratte, Garneau and De Vleeschouwer, In press). Using a combination of REE concentrations, Nd and Pb isotopes as well as particle size data analysed from the same peat cores, we aimed at 1) characterizing the geochemistry of atmospheric mineral dust deposited in these peat profiles; 2) identifying potential changes in dust sources and 3) evaluating the links between climate variability (e.g. wind strength, direction) and the dust deposited into the peat bogs.

2.2 Material and Methods

2.2.1 Sites description and sampling

The Baie peatland (49°04'N, 68°14'W; 1.5 km^2; 15 m.a.s.l.) is a *Sphagnum*-dominated raised bog located on the Manicouagan delta, along the coast at the eastern end of the Lower St. Lawrence Estuary (Fig. 2.1). More than 4.5 m of peat accumulated over marine silty-clay sediments originating from the Laurentian transgression from 6500-

4300 cal a BP (Bernatchez, 2003; Magnan and Garneau, 2014). The peatland is open towards the coast of the St. Lawrence Estuary, where beaches occupy the coastline (700 m from the coring site). Deposits at a higher altitude (> 14 m.a.s.l.), onto which soils developed, consist of silt-sand deltaic terraces emerged following the withdrawal of the Goldthwait Sea from 8 ka (Bernatchez, 2003). The regional bedrock is composed of rocks of Paleoproterozoic and Mesoproterozoic age from the Grenville province, mostly gneisses and granites (Fig. 2.1c).

The Ile du Havre peatland (IDH) (50°13'N, 63°36'W, 0.5 km^2; 31 m.a.s.l.) is a raised bog dominated by *Sphagnum* mosses, Ericaceous shrubs and *Cladina* spp. lichens and surrounded by a tree fringe mainly composed of *Picea mariana*. It is located on a 12-km^2 island, two kilometers offshore in the eastern part of the Mingan archipelago in the Gulf of St. Lawrence (Fig. 2.1). Peat started to accumulate at *ca* 7800 cal a BP in a depression over silty-clay sediments (Pratte, Garneau and De Vleeschouwer, In press). At its deepest part, peat thickness reaches about 6.25 m. The islands of the archipelago are characterized by cuesta landforms with cliffs to the north and slopes towards the south (Grondin *et al.*, 1980). The peatland being located at the north-east side of the island, the surrounding topography is characterized by cliffs and steep slopes. The coastline of the island (600 m away from the peatland) is dominated by beaches, which compose the main unconsolidated sediments. The underlying bedrock consists of Ordovician limestone intersected by layers of shale and sandstone from the Mingan formation (Grondin *et al.*, 1980; Poole *et al.*, 1970).

A core was retrieved from the deepest part of each peatland, using a stainless steel Box corer (10x10 cm cross-section; Jeglum *et al.*, 1992) to sample the upper meter and a Russian sampler (7.5 cm diameter; Jowsey, 1966) for the deeper peat sections. The cores were collected from two holes approximately 30 cm apart in an overlapping manner to ensure complete stratigraphic recovery (see De Vleeschouwer, Chambers and Swindles, 2010 for more details). The cores were wrapped in plastic film, transferred into PVC tubes and stored in a freezer (-20°C) until they were sliced frozen

at 1-cm interval (Givelet *et al.*, 2004) using a stainless steel band saw at Ecolab (Toulouse, France).

Bottom sediment samples, from underneath the peatlands, as well as unconsolidated sediments, mineral soils (around Baie bog) and rocks from the surrounding areas (< 10 km) of both study sites were collected (n = 10). The < 63 μm fraction of unconsolidated sediment and soil samples was dried and ground while rocks were cut and fresh material ground.

2.2.2 Chronological control

The construction of the age-depth models for both cores is described in detail in Pratte, Garneau and De Vleeschouwer (In press). In brief, the chronology was constrained by ^{210}Pb activities measured in the uppermost layers of peat (35 and 52 cm for Baie and IDH respectively) by alpha spectrometry at GEOTOP Research center (UQAM, Montreal) and 25 ^{14}C AMS dates (13 and 11 for Baie and IDH respectively) on extracted aboveground plant macrofossils. The ^{14}C dates were processed at Keck-CCAMS facility (Irvine, USA). The constant rate of supply model was applied to derive ^{210}Pb ages of the upper part of the cores (Appleby, 2002). The measurement uncertainties (Tables 2.2 and 2.3), corresponding to one-sigma, were calculated from counting statistics. The atmospheric, or excess ($^{210}Pb_{ex}$), is used to determine the chronology of environmental records. Supported ^{210}Pb activity, i.e. produced *in situ*, was estimated by the analysis of deeper samples in each core in order to determine at which depth the $^{210}Pb_{ex}$ was not present anymore, hence the limit of the dating technique (Le Roux and Marshall, 2011). Age-depth models were generated by combining both ^{14}C and ^{210}Pb dates using the *BACON* software package (Blaauw and Christen, 2011).

2.2.3 Grain-size analyses

Grain-size distribution was determined on the water-insoluble fraction of the bulk peat samples using a Horiba LA-950 laser grain-size analyzer at Ecolab (Toulouse, France). This instrument measures the volume percent of selected bin-size ranges in samples from 0.1 to 3000 μm. Prior to analyses, peat sample were ashed at 550°C for 6h in a muffle furnace. Samples were soaked in deionized water to dissolve potential pseudo-minerals (salts) formed during ashing, and submitted to ultrasounds to separate particles. A number of samples (up to 4 cm) were combined to provide enough material for analyses. The grain-size distribution of the samples was characterized in 70 classes.

2.2.4 Elemental analyses

All geochemical sample preparations were performed under clean laboratory conditions (class 100) using acid-cleaned labware. Approximately 100 mg of powdered peat samples were acid-digested until complete dissolution, using a series of steps (HNO_3 + HF, then H_2O_2) in Savillex® beakers on a hot plate (Le Roux and De Vleeschouwer, 2010). In a number of samples, an additional step involving *aqua regia* was necessary to fully digest the organic matter. The sediments, soil fractions and rock samples were acid digested using a mixture of HNO3 + HF, then HCl on a hot plate (Stevenson, Meng and Hillaire-Marcel, 2008). The major elements (Al and Ti) were analyzed by ICP-OES at Ecolab (Toulouse, France) on a Thermo Electron IRIS Intrepid II. The trace elements (Zr, Sc, Pb and REE) concentrations were measured on an Agilent Technologies 7500ce Q-ICP-MS at *Observatoire Midi-Pyrénées* (Toulouse, France). Prior to ICP-MS analyses, samples were diluted and an In-Re spike was added for internal normalization process.

The analytical performance was monitored through reference materials (NIST 1515 Apple leaves, NIST 1547 Peach leaves, NIST 1575a Pine needles, GBW07604 Bush

branches and leaves, and NIMT/UOE/FM/001 peat). Measurements performed by ICP-OES were generally within 10% of certified values with the exception of Al concentrations which accuracy was between 6 and 17%. The elements measured by ICP-MS were all within 15% of certified values with the exception of Ce (16%) and Lu (19%). The reproducibility of the digestion procedure was evaluated by repeated analyses of NIST 1515 (n = 5), NIST 1547 (n = 5), GBW-07063 (n = 4) and 10 peat samples (each n = 2) and was generally better than 20%. The procedural blanks for the element analyzed were <15 ppt for trace elements and <1 ppm for Al and Ti.

2.2.5 Pb isotopes

After measurement of Pb concentrations, a series of selected sample mother solutions were diluted to 500 $\mu g\ g^{-1}$ for analyses by HR-ICP-MS at the *Observatoire Midi-Pyrénées* (Toulouse, France) (Krachler *et al.*, 2004). Mass bias was controlled and corrected by standard bracketing of a 500 $\mu g\ g^{-1}$ standard solution of SRM 981 between each sample. The $^{206}Pb/^{207}Pb$ ratios obtained for the NIMT peat standard were 1.1772 ± 0.0007 compared to the reported value of 1.1763 ± 0.0004 (Yafa *et al.*, 2004).

2.2.6 Nd isotopes

Peat, rock, unconsolidated sediment and soil samples were prepared for Nd isotopes. Between 100 and 600 mg of dried peat (100 mg for the soil/sediment samples) was placed in oven at 550°C for 6 h, to remove all organic matter by combustion (Chambers, Beilman and Yu, 2011). The resulting ashes were acid-digested in a mixture of 16N HNO_3 and 23N HF in a proportion of 1:4 on a hot plate at 125°C for 48h. To ensure complete dissolution, the residues were re-dissolved in 2 ml of 6N HCl. Residues were dissolved into 1N HNO_3 and Nd was purified by a passage through two sets of columns. Alkalis (e.g. Ca, Rb, Sr) and REE were separated by a passage through

Bio-Rad columns filled with pre-conditioned TRU Spec© resin (50-100 mesh) using dilute HNO_3 (0.05N). This solution was directly loaded onto pre-conditioned and pre-calibrated LN Spec© columns and Nd was isolated sequentially from the other REE using dilute HCl (0.2N). The Nd solution was evaporated and dissolved another time in 2% HNO_3 prior to Nd isotopic measurements.

The Nd isotopic measurements were performed using a MC-ICP-MS (multi-collector inductively coupled plasma mass spectrometer, Nu Plasma II) a GEOTOP-UQAM, in Montreal. Replicate analysis of the JNDi-1 Nd standard (Tanaka *et al.*, 2000) every five samples yielded a $^{143}Nd/^{144}Nd$ value of 0.512084 ± 0.000014 (2σ, n = 16). Mass fractionation was corrected to $^{146}Nd/^{144}Nd$ = 0.7219. Epsilon neodymium (εNd) was calculated according to DePaolo and Wasserburg (1976):

$$\varepsilon Nd = \left(\frac{\left(\frac{143Nd}{144Nd}\right)}{0.512638} - 1 \right) * 10000$$

where 0.512638 corresponds to the chondritic uniform reservoir (CHUR) and represents present-day average earth value (Jacobsen and Wasserburg, 1980).

2.3 Results

2.3.1 Chronology

The results for radiocarbon measurements are presented in Table 2.1, while ^{210}Pb activity and CRS-models are presented in Tables 2.2 and 2.3 for the Baie and IDH cores respectively. Complete details for the measurements and age models are reported

in Pratte, Garneau and De Vleeschouwer (In press). Three periods with different accumulation rates were reconstructed in the Baie core (Fig. 2.2). Most of the core shows a relatively constant accumulation rate, with an average of 1.0 mm a^{-1} from the base to 52-cm depth (4400-400 cal a BP). A second period with lower accumulation rates is found between 52 and 32 cm (400-25 cal a BP: 0.4 mm a^{-1}) while the section between 32 cm and the surface displays values of 2-5 mm a^{-1} and corresponds to the acrotelm, which is composed of poorly decomposed peat and living mosses. In the IDH core, five distinct periods of peat accumulation were identified. From the base of the core to 554 cm (0.5 mm a^{-1}; 7100-5780 cal a BP), from 554 to 452 cm (1.1 mm a^{-1}; 5780-4880 cal a BP), between 452 and 143 cm (0.8 mm a^{-1}; 4880-870 cal a BP), from 143 cm to 45 cm (1.2 mm a^{-1}; 870-35 cal a BP) and from 45 cm to the surface (3-5 mm a^{-1}; 35 cal a BP to present-day), which corresponds to the acrotelm.

2.3.2 Grain-size analyses

The grain-size distribution in the Baie and IDH records are shown in Fig. 2.3. In the Baie record, particles of silt size (2-63 μm) dominate while varying amounts of clay (< 2 μm) and sand (63 μm – 2 mm) particles are present. A relatively constant grain-size distribution is observed during the period 4400-2900 cal a BP (Fig. 2.3), with a median grain-size varying between 7.5 and 11 μm. The median grain-size decreases to an average close to 2 μm between 2820 and 2640 cal a BP. Afterwards, a greater variability in the grain-size distribution is apparent with the occurrence of clays and very fine silts, for short periods of time, and several "peaks" in grain size, displaying distributions that are less well-sorted (Fig. 2.3). The peat layer at 29.7 cm (-5 cal a BP) of depth has a high volume of sand-size particles.

The grain-size distribution in the IDH record is also dominated by silt particles, but there are more clay-sized particles and less sand-sized particles than in the Baie record. From the bottom of the core until 5000 cal a BP, which represents the fen

(minerotrophic) section up to the fen-to-bog transition, the IDH core displays coarser grain-size distribution than the rest of the profile (Fig. 2.3). From 5000 to 4000 cal a BP, the median grain size ranges from 1.2 to 2.9 μm, while it shows more variability with values of 1.5-5.8 μm between 4000-2100 cal a BP. The grain-size decreases to values of 0.5-3 μm between 2100-1500 cal a BP. From 1500 cal a BP towards the surface, the grain size of dust varies considerably with values ranging between 2.3 and 10 μm. The peat layer at 40.1 cm (110 cal a BP), is characterized by the presence of sand particles up to 2 mm.

2.3.3 REE content

All REE display similar depth profiles in each core and vary in parallel with other lithogenic elements such as Ti or Zr. This similar chemical behaviour was confirmed by PCA analyses performed on the elemental profiles in both cores (Pratte, Garneau and De Vleeschouwer, In press). Lanthanum content ranges between 0.07 and 8.2 μg g^{-1} in the Baie core, while it ranges between 0.05 and 19.8 μg g^{-1} in the IDH core (Fig. 2.4). In both cores, the highest REE concentrations and ΣREE/Ti ratios are found at the base, in the minerotrophic and fen-to-bog transition (FBT) sections (455-380 cm in Baie and 623-500 cm in IDH). Individual REE profiles decrease gradually up to 435 cm and 500 cm of depth in the Baie and IDH cores, respectively. In the Baie core, REE concentrations and La/Sm ratios remain relatively low and constant between 435 and 235 cm (4300-2600 cal a BP) as well as between 112 and 70 cm (1075-640 cal a BP). They increase two- to fivefold, between 235 and 112 cm (2600-1075 cal a BP) and up to tenfold from 70 to 25 cm (640 to -25 cal a BP), while La/Sm ratios remain around 0.9 for the former and increase to values near 1.4 in the latter sections.

In the IDH core, apart from two periods when REE concentrations increased threefold between 413-313 cm (4170-2830 cal a BP) and 67-25 cm (1750 to -20 cal a BP), most of the REE concentrations are low and constant (Fig. 2.4). These changes in REE

concentrations are not reflected in the profiles of ΣREE/Ti and La/Sm ratios as they display small variability throughout the ombrotrophic section (500-20 cm). From 20 cm depth to the surface, the ΣREE/Ti ratios decrease gradually.

2.3.4 Nd and Pb isotopes

The εNd values range between -12.6 and -22.3 and from -11.8 to -21.0 in the Baie and IDH cores respectively, while the $^{206}Pb/^{207}Pb$ ratios vary between 1.168 and 1.215 in the Baie core and 1.122 and 1.253 in the IDH core (Tables 2.4 and 2.5). Bottom sediments at the base of each core yielded εNd values of -21.3 and -19.2 and $^{206}Pb/^{207}Pb$ values of 1.123 and 1.138 in Baie and IDH respectively. Epsilon Nd values in the Baie core are at their highest (less negative) between 390 and 225 cm (4000-2500 cal a BP), with εNd of -12.6 to -13.3, while $^{206}Pb/^{207}Pb$ ratios of 1.201-1.215 are observed (Fig. 2.4). From 225 cm to the top of the core (2000 cal a BP to present-day), εNd values show more variability and more negative values (between –13.4 and -15.2). The $^{206}Pb/^{207}Pb$ ratios also display slightly more variability than the preceding period with ratios ranging between 1.188 and 1.206. Over the last 100 years, the $^{206}Pb/^{207}Pb$ ratios decrease to reach their minimum value of 1.168 near the surface.

The minerotrophic section of the IDH core has the most negative εNd values. At the base, εNd values reach -21.3 at 620 cm (6975 cal a BP) and they increase towards the fen-to-bog transition, reaching -17.9 at 500 cm (5330 cal a BP) (Fig. 2.4). A second section of the core from 470 to 111 cm (5050-620 cal a BP) shows relatively stable εNd values ranging between -11.8 and -12.5 with a level (290.7 cm) yielding a value of -13.2. From 111 cm towards the surface (620 cal a BP to the present-day), the εNd values decrease and display slightly more variability with values between -12.8 and -15.1. A similar trend is observed for the $^{206}Pb/^{207}Pb$ ratios, i.e. less radiogenic ratios in the minerotrophic section (1.12) with a gradual increase towards the FBT (1.18-1.20). Stable $^{206}Pb/^{207}Pb$ ratios (1.193-1.208) are also observed between 5330 and 620 cal a

BP. A sample at 67.1cm of depth (200 cal a BP) yielded a ratio of 1.25. Afterwards, $^{206}Pb/^{207}Pb$ ratios decrease towards the surface to reach a minimum of 1.167.

2.4 Discussion

2.4.1 REE distribution patterns

The REE content of peat samples and surrounding soils, unconsolidated sediments and rocks, normalized to the Upper Continental Crust (UCC; Wedepohl, 1995), are shown in Fig. 2.5. Both Baie and IDH peat bogs have relatively homogeneous crustal-normalized REE patterns. In the vicinity of the Baie bog, unconsolidated sediments from the beach are characterized by a flat pattern without Eu anomaly. On the other hand, deltaic deposits, onto which soils developed, display slightly higher HREE content and positive Eu anomaly (Fig. 2.5). In the Baie bog, the samples in the fen section (447-435 cm) have a negative Eu anomaly and lower HREE than LREE, when compared to the FBT (435-380 cm) and bog samples (380 cm to the surface). This can be explained by the contribution from the bottom mineral sediments and local rocks such as gneisses. The other samples (FBT and bog) display an increasing influence of local sediments/soils with less negative (FBT) or no Eu anomaly (bog). The REE patterns in the bog section reflect a mixture of particles from the local soils and the beach. Over the last 1700 years, some samples (Fig. 2.5; Baie 'events') received a greater proportion of particles from the local soil as shown by the positive Eu anomaly. A greater number of these samples is found over the last 600 years, which comprises the Little Ice Age (LIA) period.

The REE for the local beach near IDH peatland show a flat pattern with a slight negative Eu anomaly and enrichment in HREE, while the limestone also displays a negative Eu anomaly along with a MREE and HREE enrichment (Fig. 2.5). Peat samples from the fen section (624-605 cm) have a negative Eu anomaly with an

enrichment in LREE. This reflects the contribution from the bottom sediments and the local limestone. The rather flat patterns of the FBT (605-523 cm) and bog (523 cm-surface) samples reflect the increasing proportion of particles from the beach over the bottom sediments.

2.4.2 Dust sources

As mentioned previously, REE in the ombrotrophic section of each core vary in parallel with conservative elements such as Ti, Zr or Al (Pratte, Garneau and De Vleeschouwer, In press), which confirms that REE are immobile and preserved in the peat column, therefore their concentrations are controlled by atmospheric deposition from local and/or regional sources (Aubert *et al.*, 2006; Kylander *et al.*, 2007).

Usually, the REE composition and isotopic signature of dust is inherited from its source rock, allowing its fingerprinting (Aubert *et al.*, 2006; Grousset and Biscaye, 2005; Kylander *et al.*, 2007). To identify the origin of the dust deposited in Baie and IDH bogs, all peat samples and potential local and regional sources were plotted on a $^{206}Pb/^{207}Pb$ vs εNd diagram (Fig. 2.6). The εNd exhibits a wide range in both cores, between -22 and -12, which suggests contrasting sources over the studied period. Figure 2.6 shows that samples from the minerotrophic and FBT have lower εNd (-22 to -17 and -21 to -17 in Baie and IDH respectively) and $^{206}Pb/^{207}Pb$ (1.12-1.17 for Baie and 1.12-1.18 for IDH) signatures. The lower εNd values in the fen section of each core is linked with a significant enrichment in Nd content (Fig. 2.7). This is in agreement with the εNd values obtained from bottom sediments of Baie (-21) and IDH (-19) as well as the grain-size distribution, which shows the presence of larger particles unlikely to have been transported over long distance (Fig. 2.3). The bottom sediments at both sites represent a mixture of several sources that likely explains the variability of the εNd of both fen sections. In the vicinity of Baie bog, soils that developed over deltaic

sediments, and beach sands exhibit εNd values of -17 and -19 respectively, while sandy beach sediments around IDH display a value of -19.

The ombrotrophic sections of the Baie and IDH cores, which received particles of atmospheric origin only, possess a similar range of εNd and $^{206}Pb/^{207}Pb$ values (Fig. 2.6), although the εNd values for IDH are slightly less negative (-11.8 to -13.1) than Baie (-12.6 to -15) before 650 cal a BP. The overlapping εNd values of both cores with those from the Appalachians (Fagel *et al.*, 2002) and St. Lawrence Gulf sediments (Farmer, Barber and Andrews, 2003) could be explained by a common source for particles deposited in each peatland. More likely, the similar εNd values in both cores could be explained by regional sources with similar Nd isotopic ratios as suggested by the fact that rocks in each region display similar εNd values (Dickin, 2000; Dickin and Higgins, 1992). Similarly, $^{206}Pb/^{207}Pb$ ratios show more radiogenic values over the same period (1.19-1.21) and fall within the range of reported values for natural sources (Gallon *et al.*, 2005; Kylander *et al.*, 2010; Wedepohl, 1995).

The lack of isotopic data for the region and the fact that the currently available data display similar isotopic signatures prevent the identification of single sources for particles being deposited in the Baie and IDH bogs. However, when REE patterns are taken into account with εNd, we can reasonably conclude that the particles deposited on both sites come from a mixture of sources. Local sediments such as soils and beach sands are a likely source, while the similarity of the Gulf of the St. Lawrence sediments, also representing a mixture of sources, and Appalachians εNd signatures, suggest that regional sources also contribute. Futhermore, a shift in the Nd isotopic data is linked with the transition from fen to bog conditions in both cores (Fig. 2.7) suggesting that at least three sources must be invoked to explain the variability in εNd.

The gradual decrease in $^{206}Pb/^{207}Pb$ during the recent years (Fig. 2.4) is due to anthropogenic impacts, likely from leaded gasoline emissions. The isotopic ratios in both cores (1.16-1.17) are in agreement with those obtained from another core in the

Baie bog (Pratte, Mucci and Garneau, 2013). Since AD 1950 (20 cm-surface), the ΣREE/Ti have decreased gradually in the IDH core (Fig. 2.4), which suggests a change in the source of the deposited dust in the region. This could be explained by the presence of a Ti mine (Lac Tio mine) and shipping facilities, which started operating in 1950, in the port of Havre-Saint-Pierre, located 2 km north of the study site.

2.4.3 Climate-related changes in the dust signal

The temporal εNd evolution can be used to retrieve information about past climate variations when combined with other proxies. Here, we integrate elemental (in the form of dust flux and REE patterns) and isotopic geochemical data as well as grain size to track past climatic influences registered in both records. To extract the climate signal from dust, REE concentrations were used to derive dust fluxes (Chapter 1: Pratte, Garneau and De Vleeschouwer, In press). Then, the dust-rich events previously identified, were analyzed for Nd isotopic composition and compared with local and regional sources. Finally, these changes are interpreted in terms of local or regional environmental changes.

Based on the εNd record, the Baie bog can be divided into three intervals (Fig. 2.8; B-1: 4400-3800 cal a BP, B-2: 3270-2300 cal a BP and B-3: 2000 cal a BP-present). The interval 4400-3800 cal a BP (zone 1) comprises the minerotrophic phase and hence represents a local signal combining both atmospheric and lateral inputs. The influence of the bottom sediments and local bedrock on the εNd signal decreases towards the FBT as shown by the increasing values (Fig. 2.7 and 2.8). The REE patterns for the fen and FBT phases agree with the εNd signal as it displays a decreasing influence of the bottom sediments and local rocks in favour of particles from local mineral soils and the nearby beach (Fig. 2.5).

The second interval, covering the period of 3270-2600 cal BP (B-2), has the highest εNd values of the record (Fig. 2.8). The dust flux displays a relative stability and the grain size does as well apart for the period of 2800-2600 cal a BP, where it possesses the lowest particle size in the record (Fig. 2.3). In the REE patterns (Fig. 2.5) no distinction can be made between this period and the following one (last 2000 years). A testate amoebae record from the same bog shows relatively high and constant water-table depth (WTD) over this period, suggesting wetter hydroclimatic conditions (Fig. 2.8; Magnan and Garneau, 2014). A pollen-based reconstruction of July temperature anomaly in Baie peatland reports slightly cooler conditions from 4000 cal a BP (Sauvé, 2016) while Viau and Gajewski (2009) reconstructed warmer but wetter conditions for northern Quebec. We hypothesize that the change in Nd values and particles size reflects more humid and, more importantly, stable conditions, which may have reduced the local dust load in favour of more regional sources, especially during the 2800-2600 cal a BP interval. The REE pattern of the samples over that period reveals that local sources were still contributing to a certain extent.

The interval covering the last 2000 years (B-3) is marked by more negative εNd values, greater and more variable dust flux and particle grain size (Fig. 2.3 and 2.8). The lower εNd values and greater particle size suggest a greater proportion of particles originating from a local source. This is further confirmed by the REE patterns that reflect a mixture between the local mineral soils and the beach (i.e. bog in Fig. 2.5). Although not of the same amplitude as the dust flux, the εNd record for this period displays greater variability. This high variability was also observed in the WTD reconstruction from Magnan and Garneau (2014) (Fig. 2.8). Hydroclimatic instability has been reported to affect dust loads through increased storminess (de Jong, Schoning and Björck, 2007; De Vleeschouwer *et al.*, 2009). Decreasing July temperature anomalies over the last 2000 years also suggest a climatic "deterioration", shortly interrupted around 1.100 cal a BP (Viau and Gajewski, 2009). An agreement between the dust flux record and solar minima (Reimer *et al.*, 2013) was noted for the Baie bog (Pratte, Garneau and De

Vleeschouwer, In press). Hence, over the last 2000 years, the dust εNd signature, particle size and flux all point towards increased local storminess, which deposited a greater proportion of particles from local sources in response to regional (hydrology) and global (temperature; i.e. solar minima) events. This is especially true for the last ca 600 years, when distinct events (Fig. 2.8; red lines) with REE patterns closer to the signature of the local soils where recorded (Fig. 2.5).

A closer look at the εNd record of IDH bog reveals three intervals: 7100-5000 cal (I-1) a BP, 5000-620 cal a BP (I-2) and 410 cal a BP to the present day (I-3). The interval 7100-5000 cal a BP (I-1) represents the minerotrophic and FBT sections with values typical for the local sources, mostly brought to the peatland by lateral inputs. As in the Baie core, the gradual increase in εNd and $^{206}Pb/^{207}Pb$ values towards the top of the minerotrophic section is explained by the gradual isolation of the peat surface from the local runoff and the proportionally increasing importance of atmospheric particles, from sources such as beach sands, on the isotopic signatures (Fig. 2.4, 2.7 and 2.8). This is confirmed by the REE pattern of the FBT transition samples, which has values more similar to the beach than the bottom sediments and limestone (Fig. 2.5).

In the second interval (I-2: 5000-620 cal a BP), the εNd profile mirrors the REE dust flux, i.e. it shows relatively constant values (mean: -12.3±0.3). The grain-size record displays a similar pattern (Fig. 2.3). A WTD record from a core collected 5 km north of IDH bog (Plaine bog) displays large hydrological variations over the same period (Magnan and Garneau, 2014), which are not reflected in any proxy from IDH bog. The geographical setting (on an island, protected by a forest fringe, higher elevation) of the IDH bog was invoked as a factor reducing the amount of dust being deposited on the site and explaining the low dust flux (Pratte, Garneau and De Vleeschouwer, In press). While the "isolation" of IDH probably contributes to the stability of the dust record, it cannot explain alone the εNd values. The nearly constant εNd signal either means that dust has a single source within that timespan or that the εNd values of the surrounding

geological formations are not diagnostic. Nevertheless, the similarity of the REE pattern of the peat samples for the period to those of the beach suggests a dominant local source.

The last interval, covering 620 cal a BP to the present (I-3), has more negative εNd values and greater particle size (~10μm) suggesting a greater proportion of local dust sources. While the REE patterns (Fig. 2.5) reveal that atmospheric particles from local source (beach) are an important source, they do not display distinct patterns when compared to the previous period (5000-620 cal a BP). The dust flux increases slightly over the period as well (Fig. 2.8). Reconstructed WTD on the continental shore suggests wetter and colder conditions on the coast (Magnan and Garneau, 2014). Furthermore, Viau and Gajewski (2009) report that northern Quebec was the coldest Canadian region during the LIA. Similarly to the Baie bog, the εNd values and the particles size of the dust deposited onto the IDH bog indicate locally increased wind intensity.

As previously hypothesized, the distinct geographical settings of Baie and IDH bogs might explain the difference in the timing of changes between their records. The changes recorded in the Baie core between 2000 and 1000 cal a BP, might not have been significant enough to be recorded in the IDH site considering its geomorphic setting. Comparatively, changes occurring during the LIA would have been more important, since they were recorded by the IDH record. This is in agreement with what is known about the LIA climatic deterioration, which affected North America on a large scale (Viau and Gajewski, 2009; Wanner *et al.*, 2011). More records from the coast would be needed to verify whether the different dust signal recorded in the IDH bog is representative of the regional dust signal.

2.5 Conclusion

The dust deposited on two peat bogs of the north shore of the Estuary and Gulf of the St. Lawrence was geochemically characterized using REE concentrations, Nd and Pb isotopes. Both cores show distinct REE content, εNd and $^{206}Pb/^{207}Pb$ signatures between minerotrophic and ombrotrophic sections. Baie and IDH bogs display similar εNd values, which either suggests a common source or similar εNd signature for regional sources. While the similar range of εNd values between potential sources prevents a definitive identification of the origin for the dust deposited on both peat bogs, the REE patterns and grain-size distribution reveal that local soils and beach sands are likely sources.

The evolution of the isotopic signal, in combination with the REE patterns, the grain-size distribution and the dust flux, was used to retrieve information on past environmental and climatic conditions in the region. Both sites display signals similar to the bottom sediments and local bedrock during their respective minerotrophic phase, likely overprinting the atmospheric signal. Apart from the minerotrophic phases, the two sites registered two intervals with contrasting εNd values. The IDH bog has a nearly constant εNd signature between 5000 and 620 cal a BP, which suggests a particular source that has not yet been identified. From 3270-2600 cal a BP, the Baie bog shows more regional dust supplies during a more stable climatic phase. The more humid and stable climate reduced particle availability locally in favour of a more regional signal. REE patterns, grain-size distribution and, to a certain extent, εNd values indicate that a greater proportion of local dust has been deposited over the last 2000 years in the Baie core and the last 600 years in the IDH core, respectively. These inputs are related to increased local storminess (i.e. wind intensity) in response to greater instability in the hydroclimatic conditions on a regional scale and cold events (solar minima) on a more global scale. Over the last century, anthropogenic activities (mining, leaded gasoline) have affected the dust cycle in the region. While these changes agree reasonably well with regional records, the discrepancies between both

paleodust records highlight the complex and variable structure of the late-Holocene changes in climate and atmospheric dust.

Acknowledgments

We are grateful to Gaël Le Roux (*Ecolab*, Toulouse), Marie-Jo Tavella (*EcoLab*, Toulouse), David Baqué (*Ecolab*, Toulouse), Aurélie Lanzanova (*Geoscience Environnement Toulouse*), André Poirier (GEOTOP-UQAM, Canada) and Bassam Ghaleb (GEOTOP-UQAM, Canada) for their help with major and trace elements analyses, Nd and Pb isotopes and ^{210}Pb dating. Thanks to Gabriel Magnan, Nicole Sanderson, Antoine Thibault and Hans Asnong for help during fieldwork as well as Julien Gogot for lab assistance. Thanks to *Les Tourbeux* for fruitful discussions. Financial support was provided by Natural Sciences and Engineering Research Council of Canada (NSERC; #250287) discovery grant to MG. Scholarships to SP were provided by the Fonds de Recherche Québec – Nature et Technologie (FRQNT; #176250 and #180723). An additional mobility grant was provided by *Institut National Polytechnique de Toulouse* ("*Soutien à la mobilité*" grant to FDV).

2.6 References

Allan, M., Le Roux, G., Piotrowska, N., Beghin, J., Javaux, E., Court-Picon, M., Mattielli, N., Verheyden, S. and Fagel, N. (2013). Mid and late Holocene dust deposition in western Europe: the Misten peat bog (Hautes Fagnes - Belgium). *Climate of the Past Discussion,* 9(3), 2889-2928.

Appleby, P.G. (2002). Chronostratigraphic Techniques in Recent Sediments. In: Last, W. and J. Smol (dir.), *Tracking Environmental Change Using Lake Sediments* (Vol. 1, p. 171-203): Springer Netherlands.

Aubert, D., Le Roux, G., Krachler, M., Cheburkin, A., Kober, B., Shotyk, W. and Stille, P. (2006). Origin and fluxes of atmospheric REE entering an ombrotrophic peat bog in Black Forest (SW Germany): Evidence from snow, lichens and mosses. *Geochimica et Cosmochimica Acta,* 70(11), 2815-2826.

Bernatchez, P. (2003). *Évolution littorale holocène et actuelle des complexes deltaïques de Betsiamites et Manicouagan-Outardes: synthèse, processus, causes et perspectives.* (PhD). Université Laval, Québec.

Biscaye, P.E., Grousset, F.E., Revel, M., Van der Gaast, S., Zielinski, G.A., Vaars, A. and Kukla, G. (1997). Asian provenance of glacial dust (stage 2) in the Greenland Ice Sheet Project 2 Ice Core, Summit, Greenland. *Journal of Geophysical Research: Oceans,* 102(C12), 26765-26781.

Blaauw, M. and Christen, J.A. (2011). Flexible paleoclimate age-depth models using an autoregressive gamma process. *Bayesian Analysis,* 6, 457-474.

Chambers, F.M. and Charman, D.J. (2004). Holocene environmental change: contributions from the peatland archive. *The Holocene,* 14(1), 1-6.

Chambers, F.M., Beilman, D.W. and Yu, Z.C. (2011). Methods for determining peat humification and for quantifying peat bulk density, organic matter and carbon content for palaeostudies of climate and peatland carbon dynamics. *Mires and Peat,* 7.

Chiarenzelli, J., Aspler, L., Dunn, C., Cousens, B., Ozarko, D. and Powis, K. (2001). Multi-element and rare earth element composition of lichens, mosses, and vascular plants from the Central Barrenlands, Nunavut, Canada. *Applied Geochemistry,* 16(2), 245-270.

de Jong, R., Schoning, K. and Björck, S. (2007). Increased aeolian activity during humidity shifts as recorded in a raised bog in south-west Sweden during the past 1700 years. *Climate of the Past,* 3(3), 411-422.

de Jong, R., Blaauw, M., Chambers, F., Christensen, T., Vleeschouwer, F., Finsinger, W., Fronzek, S., Johansson, M., Kokfelt, U., Lamentowicz, M., Roux, G., Mauquoy, D., Mitchell, E.D., Nichols, J., Samaritani, E. and Geel, B. (2010). Climate and Peatlands. In: Dodson, J. (dir.), *Changing Climates, Earth Systems and Society*: Springer Netherlands.

De Vleeschouwer, F., Piotrowska, N., Sikorski, J., Pawlyta, J., Cheburkin, A., Le Roux, G., Lamentowicz, M., Fagel, N. and Mauquoy, D. (2009). Multiproxy evidence

of `Little Ice Age' palaeoenvironmental changes in a peat bog from northern Poland. *The Holocene,* 19(4), 625-637.

De Vleeschouwer, F., Chambers, F.M. and Swindles, G.T. (2010). Coring and subsampling of peatlands for palaeoenvironmental research. *Mires and Peat,* 7.

De Vleeschouwer, F., Pazdur, A., Luthers, C., Streel, M., Mauquoy, D., Wastiaux, C., Le Roux, G., Moschen, R., Blaauw, M., Pawlyta, J., Sikorski, J. and Piotrowska, N. (2012). A millennial record of environmental change in peat deposits from the Misten bog (East Belgium). *Quaternary International,* 268, 44-57.

De Vleeschouwer, F., Ferrat, M., McGowan, H., Vanneste, H. and Weiss, D. (2014). Extracting paleodust information from peat geochemistry. *PAGES Magazine,* 22(2), 88-89.

deMenocal, P., Ortiz, J., Guilderson, T., Adkins, J., Sarnthein, M., Baker, L. and Yarusinsky, M. (2000). Abrupt onset and termination of the African Humid Period: rapid climate responses to gradual insolation forcing. *Quaternary Science Reviews,* 19(1–5), 347-361.

DePaolo, D.J. and Wasserburg, G.J. (1976). Nd isotopic variations and petrogenetic models. *Geophysical Research Letters,* 3(5), 249-252.

Dickin, A.P. and Higgins, M.D. (1992). Sm/Nd evidence for a major 1.5 Ga crust-forming event in the central Grenville province. *Geology,* 20(2), 137-140.

Dickin, A.P. (2000). Crustal formation in the Grenville Province: Nd-isotope evidence. *Canadian Journal of Earth Sciences,* 37(2-3), 165-181.

Fagel, N., Innocent, C., Gariepy, C. and Hillaire-Marcel, C. (2002). Sources of Labrador Sea sediments since the last glacial maximum inferred from Nd-Pb isotopes. *Geochimica et Cosmochimica Acta,* 66(14), 2569-2581.

Farmer, G.L., Barber, D. and Andrews, J. (2003). Provenance of Late Quaternary ice-proximal sediments in the North Atlantic: Nd, Sr and Pb isotopic evidence. *Earth and Planetary Science Letters,* 209(1–2), 227-243.

Gabrielli, P., Wegner, A., Petit, J.R., Delmonte, B., De Deckker, P., Gaspari, V., Fischer, H., Ruth, U., Kriews, M., Boutron, C., Cescon, P. and Barbante, C. (2010). A major glacial-interglacial change in aeolian dust composition inferred from Rare Earth Elements in Antarctic ice. *Quaternary Science Reviews,* 29(1–2), 265-273.

Gallon, C., Tessier, A., Gobeil, C. and Beaudin, L. (2005). Sources and chronology of atmospheric lead deposition to a Canadian Shield lake: Inferences from Pb isotopes and PAH profiles. *Geochimica et Cosmochimica Acta,* 69(13), 3199-3210.

Givelet, N., Le Roux, G., Cheburkin, A., Chen, B., Frank, J., Goodsite, M.E., Kempter, H., Krachler, M., Noernberg, T., Rausch, N., Rheinberger, S., Roos-Barraclough, F., Sapkota, A., Scholz, C. and Shotyk, W. (2004). Suggested protocol for collecting, handling and preparing peat cores and peat samples for physical, chemical, mineralogical and isotopic analyses. *Journal of Environmental Monitoring,* 6(5), 481-492.

Goudie, A.S. and Middleton, N.J. (2001). Saharan dust storms: nature and consequences. *Earth-Science Reviews,* 56(1–4), 179-204.

Greaves, M.J., Elderfield, H. and Sholkovitz, E.R. (1999). Aeolian sources of rare earth elements to the Western Pacific Ocean. *Marine Chemistry,* 68(1–2), 31-38.

Grousset, F.E. and Biscaye, P.E. (2005). Tracing dust sources and transport patterns using Sr, Nd and Pb isotopes. *Chemical Geology,* 222(3–4), 149-167.

Jacobsen, S.B. and Wasserburg, G.J. (1980). Sm-Nd isotopic evolution of chondrites. *Earth and Planetary Science Letters,* 50(1), 139-155.

Jeglum, JK, Rothwell, RL, Berry, GJ and Smith, G.K.M. (1992). A peat sampler for rapid survey. Technical note, *Canadian Forestry Service* 13: 921–932.

Jowsey PC. (1966) An improved peat sampler. *New Phytologist* 65: 245-248.

Krachler, M., Le Roux, G., Kober, B. and Shotyk, W. (2004). Optimising accuracy and precision of lead isotope measurement (^{206}Pb, ^{207}Pb, ^{208}Pb) in acid digests of peat with ICP-SMS using individual mass discrimination correction. *Journal of Analytical Atomic Spectrometry,* 19(3), 354-361.

Kylander, M.E., Klaminder, J., Bindler, R. and Weiss, D.J. (2010). Natural lead isotope variations in the atmosphere. *Earth and Planetary Science Letters,* 290(1-2), 44-53.

Kylander, M.E., Muller, J., Wüst, R.A.J., Gallagher, K., Garcia-Sanchez, R., Coles, B.J. and Weiss, D.J. (2007). Rare earth element and Pb isotope variations in a 52 kyr peat core from Lynch's Crater (NE Queensland, Australia): Proxy development and application to paleoclimate in the Southern Hemisphere. *Geochimica et Cosmochimica Acta,* 71(4), 942-960.

Le Roux, G. and De Vleeschouwer, F. (2010). Preparation of peat samples for inorganic geochemistry used as palaeoenvironmental proxies. *Mires and Peat,* 7.

Le Roux, G. and Marshall, W.A. (2011). Constructing recent peat accumulation chronologies using atmospheric fall-out radionuclides. *Mires and Peat,* 7.

Le Roux, G., Fagel, N., De Vleeschouwer, F., Krachler, M., Debaille, V., Stille, P., Mattielli, N., van der Knaap, W.O., van Leeuwen, J.F.N. and Shotyk, W. (2012). Volcano- and climate-driven changes in atmospheric dust sources and fluxes since the Late Glacial in Central Europe. *Geology,* 40(4), 335-338.

Magnan, G. and Garneau, M. (2014). Evaluating long-term regional climate variability in the maritime region of the St. Lawrence North Shore (eastern Canada) using a multi-site comparison of peat-based paleohydrological records. *Journal of Quaternary Science,* 29(3), 209-220.

McLennan, S.M. (1989). Rare earth elements in sedimentary rocks; influence of provenance and sedimentary processes. *Reviews in Mineralogy and Geochemistry,* 21(1), 169-200.

Meskhidze, N., Chameides, W.L., Nenes, A. and Chen, G. (2003). Iron mobilization in mineral dust: Can anthropogenic SO2 emissions affect ocean productivity? *Geophysical Research Letters,* 30(21), 2085.

Muhs, D.R. (2013). The geologic records of dust in the Quaternary. *Aeolian Research,* 9, 3-48.

Neff, J.C., Ballantyne, A.P., Farmer, G.L., Mahowald, N.M., Conroy, J.L., Landry, C.C., Overpeck, J.T., Painter, T.H., Lawrence, C.R. and Reynolds, R.L. (2008). Increasing eolian dust deposition in the western United States linked to human activity. *Nature Geoscience,* 1(3), 189-195.

Pratte, S., Garneau, M. and De Vleeschouwer, F. (In press). Late Holocene atmospheric dust deposition in eastern Canada (St. Lawrence North Shore). *The Holocene*

Pratte, S., Mucci, A. and Garneau, M. (2013). Historical records of atmospheric metal deposition along the St. Lawrence Valley (eastern Canada) based on peat bog cores. *Atmospheric Environment,* 79, 831-840.

Reimer, P.J., Bard, E., Bayliss, A., Beck, J.W., Blackwell, P.G., Bronk Ramsey, C., Buck, C.E., Cheng, H., Edwards, R.L., Friedrich, M., Grootes, P.M., Guilderson, T.P., Haflidason, H., Hajdas, I., Hatté, C., Heaton, T.J., Hoffmann, D.L., Hogg, A.G., Hughen, K.A., Kaiser, K.F., Kromer, B., Manning, S.W., Niu, M., Reimer, R.W., Richards, D.A., Scott, E.M., Southon, J.R., Staff, R.A., Turney, C.S.M. and van der Plicht, J. (2013). IntCal13 and Marine13 Radiocarbon Age Calibration Curves 0–50,000 Years cal BP. *Radiocarbon,* 55(4), 1869-1887.

Shotyk, W., Krachler, M., Martinez-Cortizas, A., Cheburkin, A.K. and Emons, H. (2002). A peat bog record of natural, pre-anthropogenic enrichments of trace elements in atmospheric aerosols since 12 370 ^{14}C yr BP, and their variation with Holocene climate change. *Earth and Planetary Science Letters,* 199(1-2), 21-37.

Stevenson, R.K., Meng, X.W. and Hillaire-Marcel, C. (2008). Impact of melting of the Laurentide Ice Sheet on sediments from the upper continental slope off southeastern Canada: evidence from Sm–Nd isotopes. *Canadian Journal of Earth Sciences,* 45(11), 1243-1252.

Tanaka, T., Togashi, S., Kamioka, H., Amakawa, H., Kagami, H., Hamamoto, T., Yuhara, M., Orihashi, Y., Yoneda, S., Shimizu, H., Kunimaru, T., Takahashi, K., Yanagi, T., Nakano, T., Fujimaki, H., Shinjo, R., Asahara, Y., Tanimizu, M. and Dragusanu, C. (2000). JNdi-1: a neodymium isotopic reference in consistency with LaJolla neodymium. *Chemical Geology,* 168(3–4), 279-281.

Vanneste, H., De Vleeschouwer, F., Martínez-Cortizas, A., von Scheffer, C., Piotrowska, N., Coronato, A. and Le Roux, G. (2015). Late-glacial elevated dust deposition linked to westerly wind shifts in southern South America. *Scientific Reports,* 5

Viau, A.E. and Gajewski, K. (2009). Reconstructing Millennial-Scale, Regional Paleoclimates of Boreal Canada during the Holocene. *Journal of Climate,* 22(2), 316-330.

Wanner, H., Solomina, O., Grosjean, M., Ritz, S.P. and Jetel, M. (2011). Structure and origin of Holocene cold events. *Quaternary Science Reviews,* 30(21–22), 3109-3123.

Wedepohl, K.H. (1995). The composition of the continental crust. *Geochimica et Cosmochimica Acta,* 59(7), 1217-1232.

Yafa, C., Farmer, J.G., Graham, M.C., Bacon, J.R., Barbante, C., Cairns, W.R.L., Bindler, R., Renberg, I., Cheburkin, A., Emons, H., Handley, M.J., Norton, S.A., Krachler, M., Shotyk, W., Li, X.D., Martinez-Cortizas, A., Pulford, I.D., MacIver, V., Schweyer, J., Steinnes, E., Sjobakk, T.E., Weiss, D., Dolgopolova, A. and Kylander, M. (2004). Development of an ombrotrophic peat bog (low ash) reference material for the determination of elemental concentrations. *Journal of Environmental Monitoring,* 6(5), 493-501.

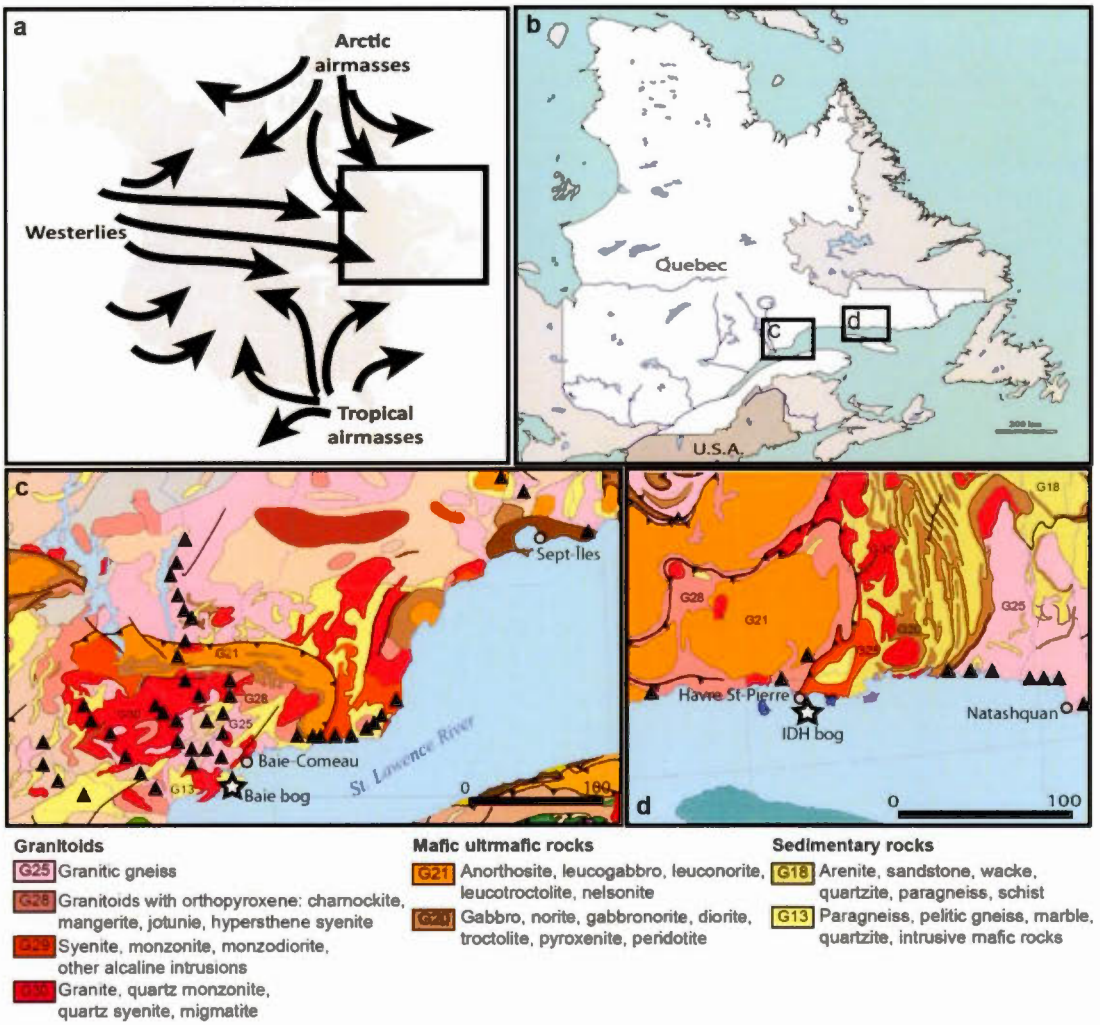

Figure 2.1 Map of the study region : (a) Map of North America showing the main air masses over the region; (b) map of Quebec with the location of the two study areas; (c) location of the Baie bog (star) in the Baie-Comeau region; (d) and location of the IDH bog (star) in the Havre Saint-Pierre region. Grey dots represent towns. Triangles correspond to rock analyzed for $^{143}Nd/^{144}Nd$ by Dickin and Higgins (1992) and Dickin (2000).

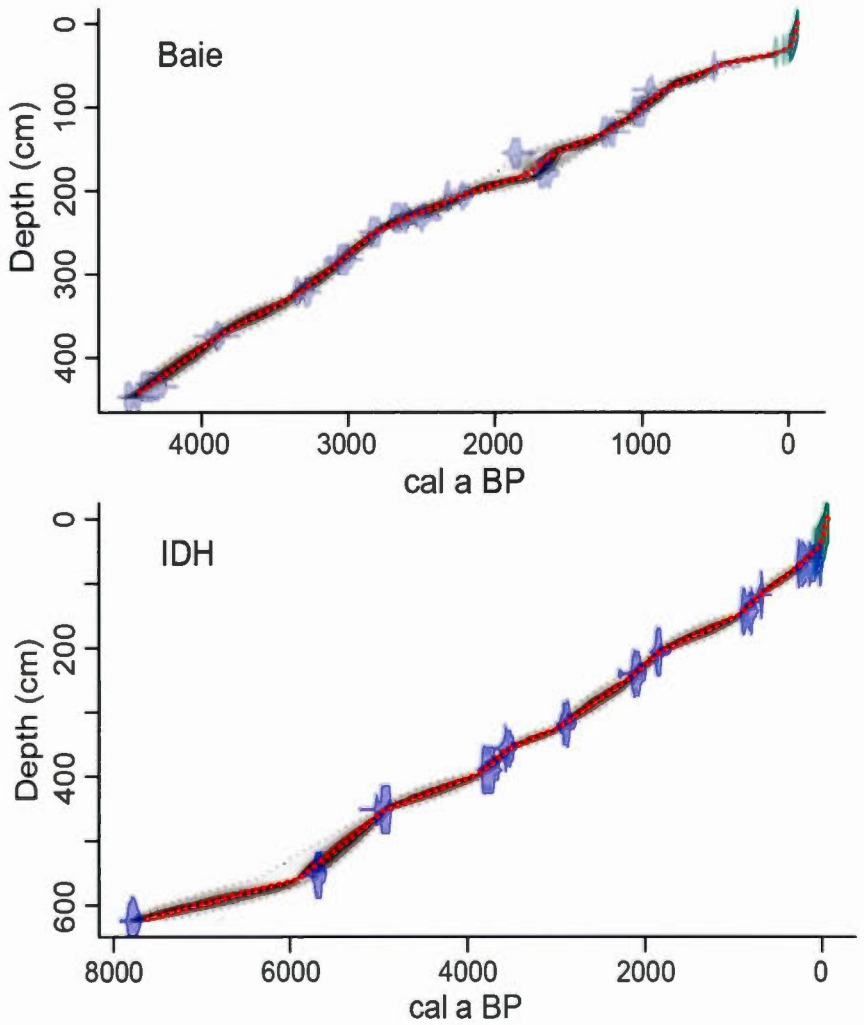

Figure 2.2 Age-depth models for Baie (top) and IDH (bottom) cores constructed using *BACON* software (Blaauw and Christen, 2011) using both ^{210}Pb and ^{14}C dates. The gray bands encompass all possible age-depth models whereas the dotted lines represent the 95% confidence intervals. The red dotted line represents the weighted mean age of each modeled sample. Purple symbols indicate calendar age distribution of ^{14}C dates and light blue symbols show ^{210}Pb ages derived from the CRS model.

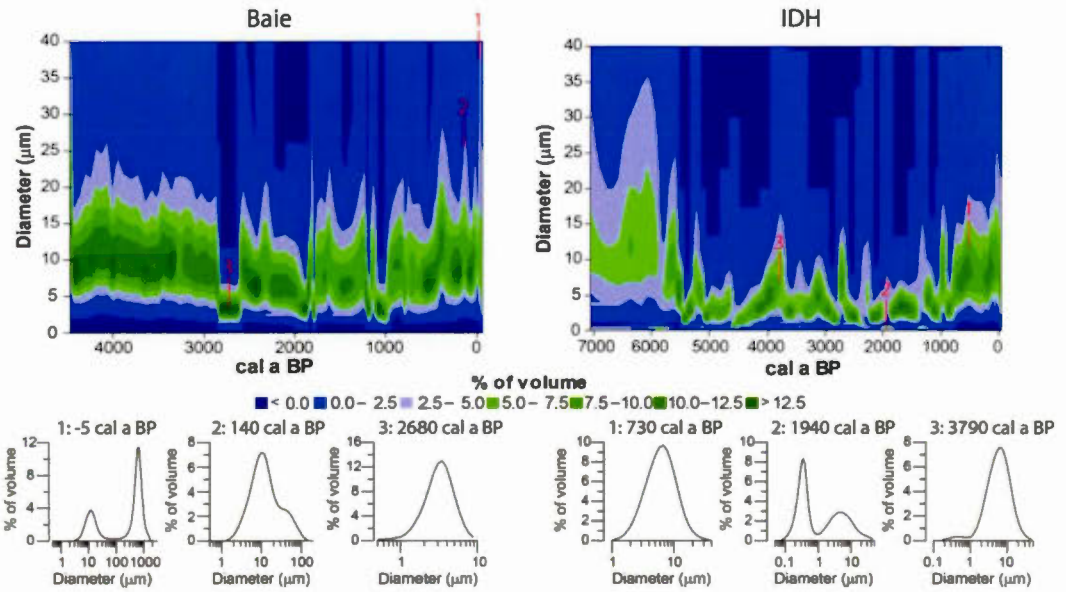

Figure 2.3 Grain-size distribution of water insoluble inorganic fraction from (A) the Baie core and (B) the IDH core. Number 1 to 3 for both core: grain-size distribution of selected samples.

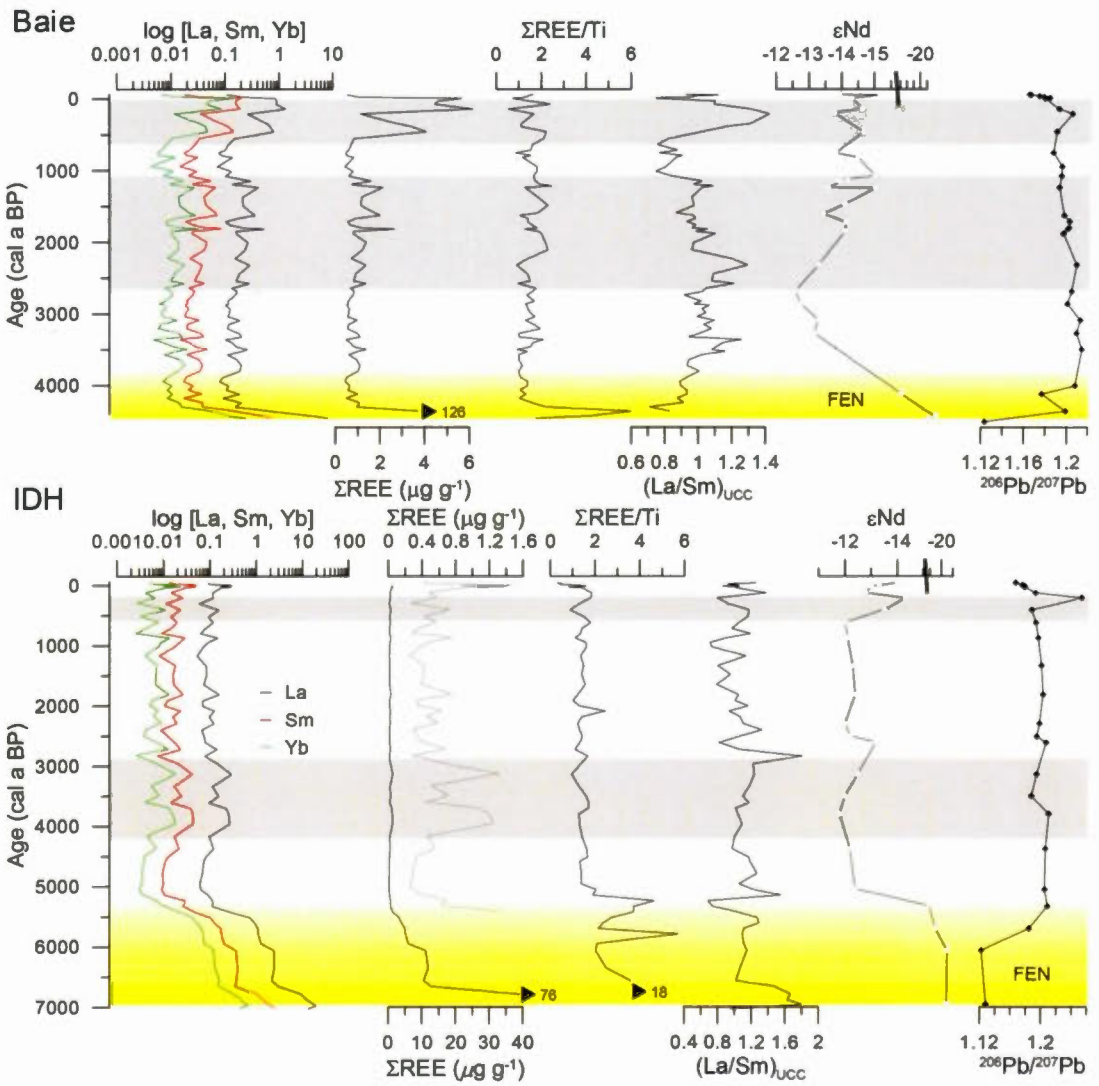

Figure 2.4 La, Sm, Yb (log scale) and ΣREE concentrations, ΣREE/Ti, La/Sm normalized to UCC, εNd and $^{206}Pb/^{207}Pb$ vs. age for Baie (top) and IDH (bottom) cores. Grey areas represent periods of higher elemental concentrations. Yellow areas represent the minerotrophic section (fen) of each core. Black arrows represent maximum values at the bottom of the cores.

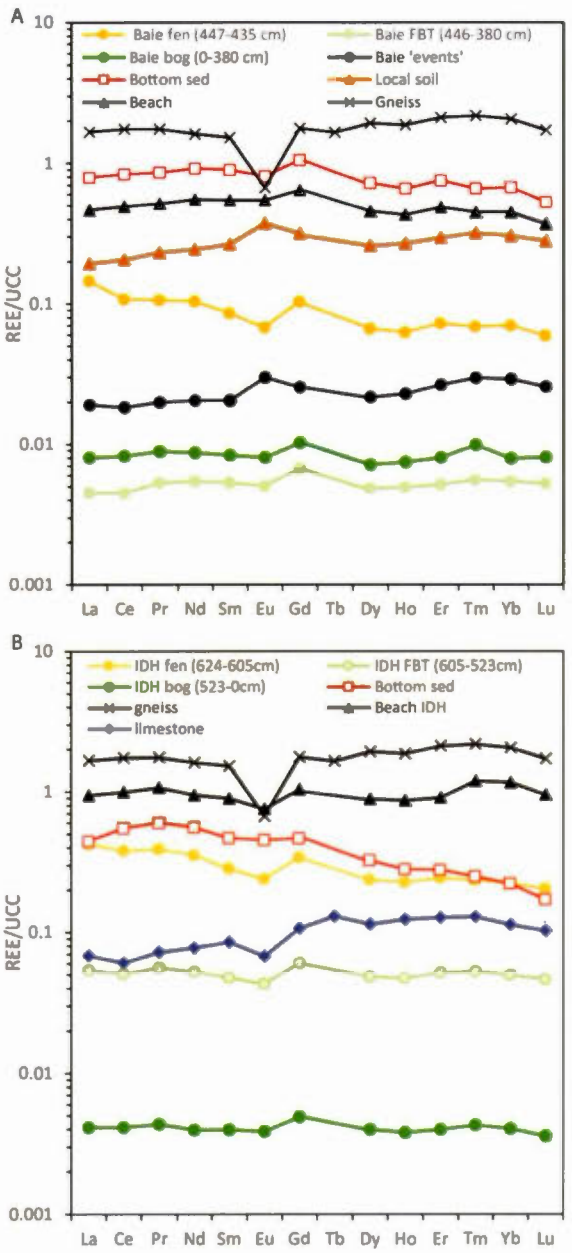

Figure 2.5 UCC-normalized (Wedepohl, 1995) REE patterns for (A) the Baie core and (B) the IDH core. Circles: Mean values for different portion of each core (fen; FBT; bog); squares: basal sediments underneath each core; triangles: local soils and beach; diamonds: limestone; crosses: mean regional gneisses (GEOROC, 2003).

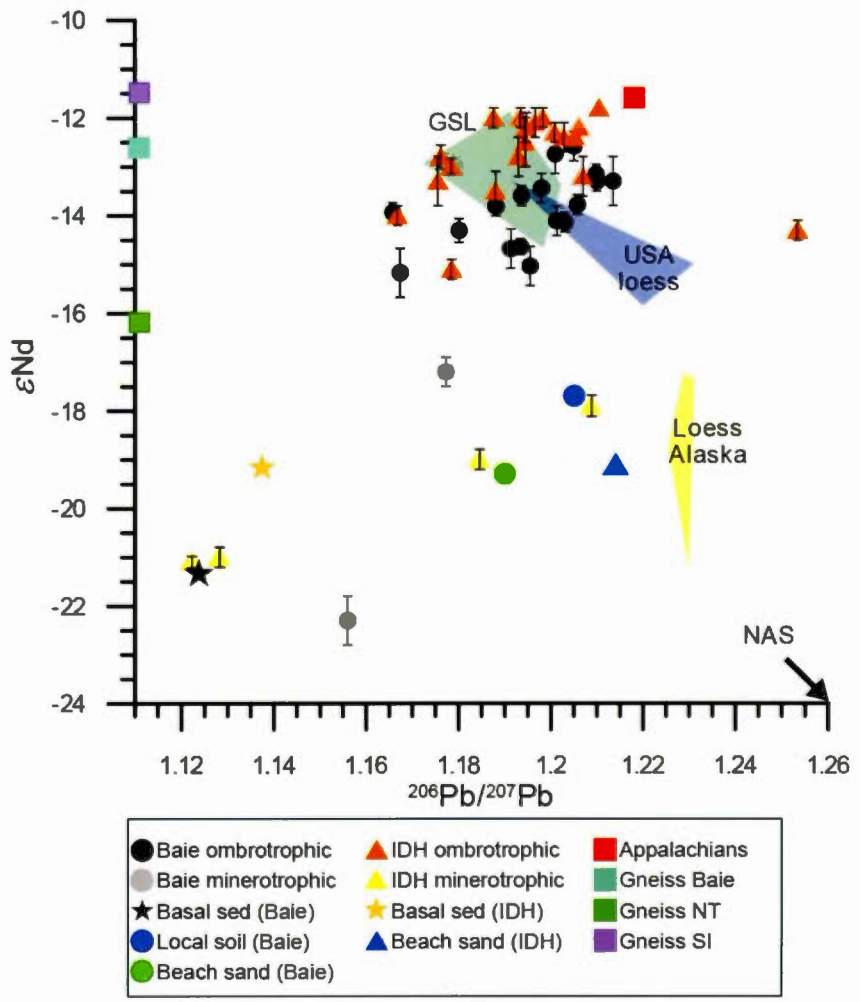

Figure 2.6 εNd vs. $^{206}Pb/^{207}Pb$ for Baie (circles) and IDH (triangles) peat samples. Basal sediments, local soils, beach sand are from this study. Alaskan loess (yellow) and USA loess (blue) areas are from Biscaye *et al.* (1997). Gulf of St. Lawrence samples (GSL; dark green) from Farmer *et al.* (2003) and North American Shield (NAS) from Fagel *et al.* (2002). Squares: potential isotope signature of local (mean gneisses Baie region, Dickin and Higgins (1992); mean gneisses from Sept-Îles (SI) and mean gneisses from Natashquan (NT), Dickin (2000)) and regional (Appalachian (Pan-African crust, Fagel *et al.* (2002). Note that samples with no $^{206}Pb/^{207}Pb$ data are fixed on the left along the y-axis.

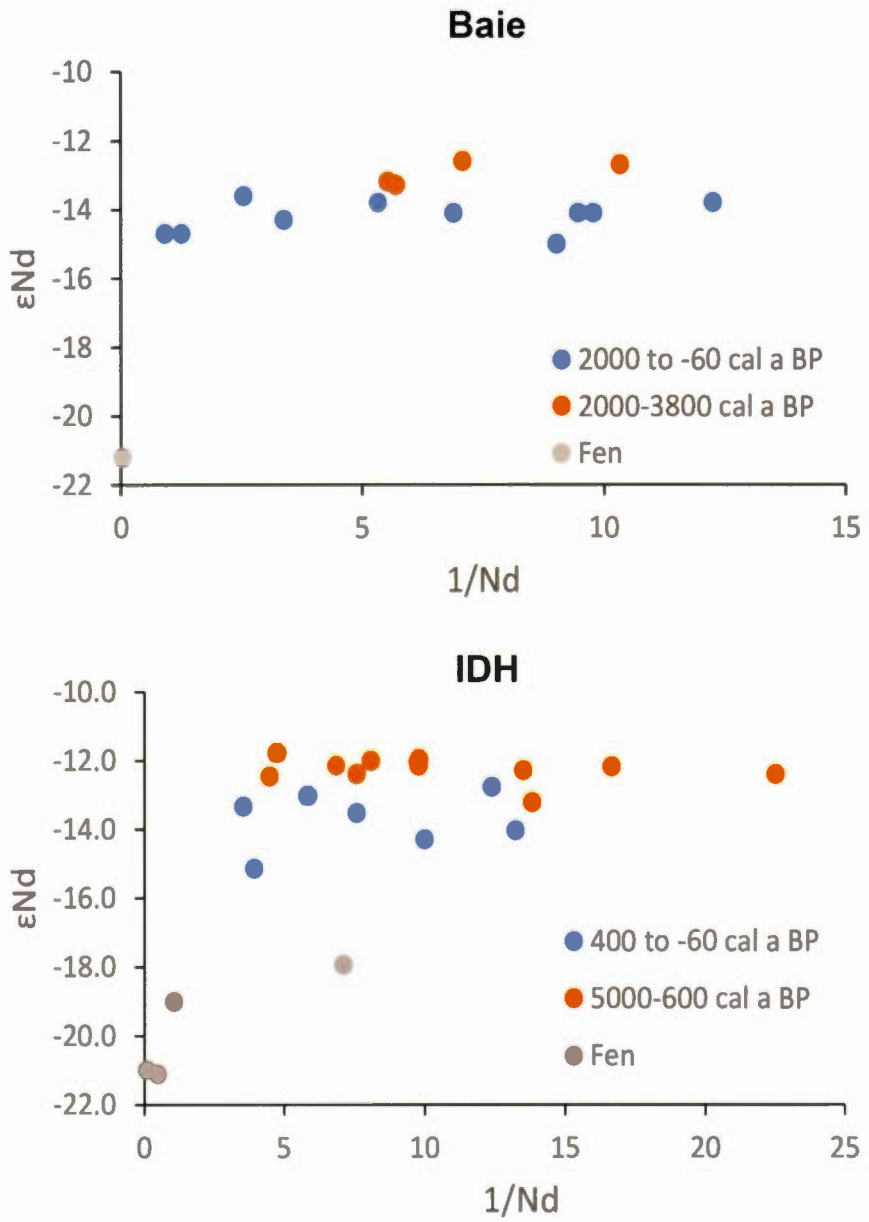

Figure 2.7 Binary diagram of 1/Nd content and εNd for Baie (top) and IDH (bottom) cores.

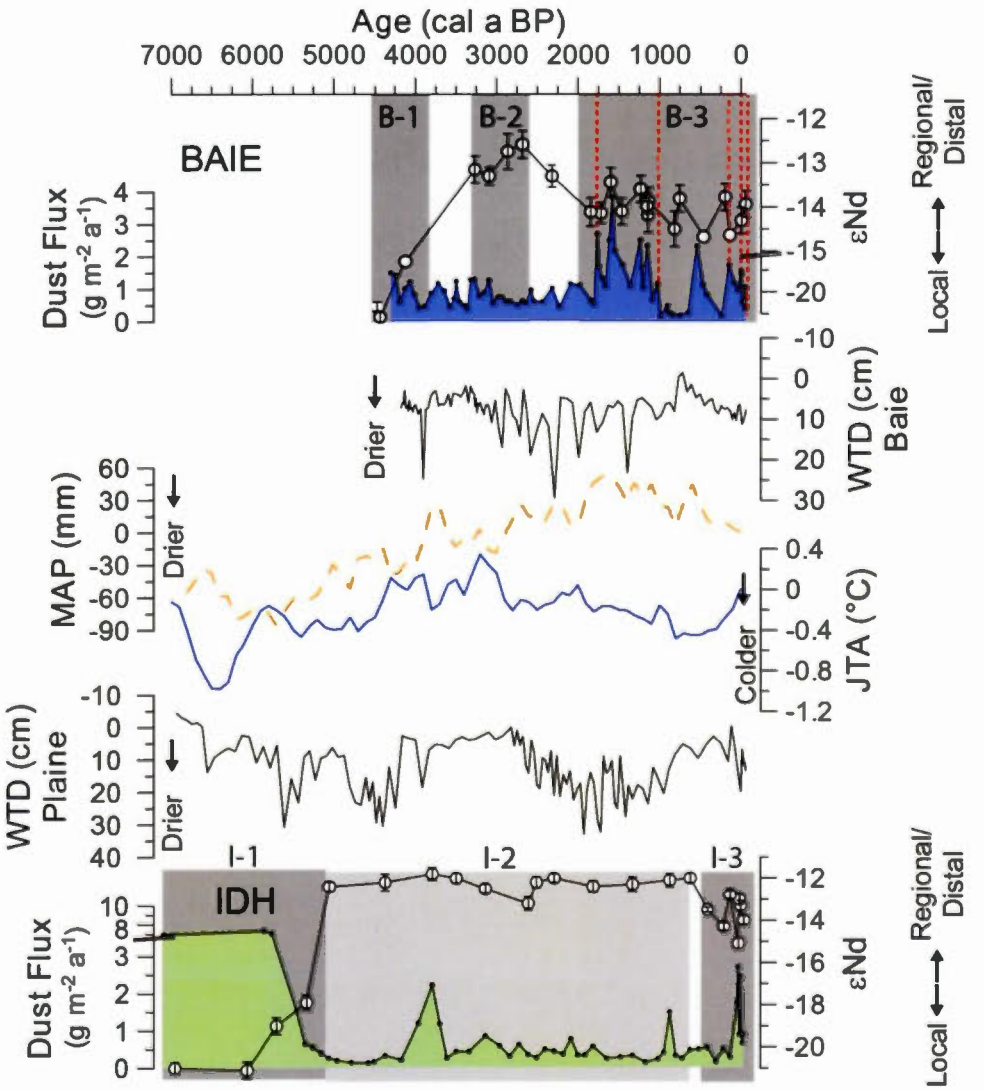

Figure 2.8 Nd isotope composition, evolution of REE-dust flux (Pratte, Garneau and De Vleeschouwer, In press) for Baie (top, blue) and IDH (bottom, green) bogs compared with regional records. Water table depth (WTD) reconstructions for Baie and Plaine are from (Magnan and Garneau, 2014). Mean annual precipitation (MAP; blue dash line) and mean July temperature anomalies (orange) in northern Quebec from Viau and Gajewski (2009). Red dashed lines represent Baie samples with REE patterns closer to local soils (see "Baie events"; Fig. 2.5). Grey areas represents climatic periods discussed in section 2.4.3.

Table 2.1 Results of ^{14}C AMS measurements, calibration and description of samples for Baie and IDH cores.

Site and sample	Depth (cm)	Laboratory number	^{14}C age (BP)	2σ range (cal a BP)	Material dated
Baie					
45	51.6	UCIAMS-129510	425±15	481-513	Charred *Picea mariana* needles
67	79.4	UCIAMS-151367	1015±25	833-971	*Sphagnum* spp. stems
106	105.9	UCIAMS-129511	1120±15	977-1059	*Sphagnum* spp. stems
128	130.0	UCIAMS-129512	1275±15	1181-1271	Charred *Picea mariana* needles
151	155.2	UCIAMS-135384	1905±20	1818-1893	*Sphagnum* spp. stems
173	179.3	UCIAMS-129513	1740±25	1570-1709	*Sphagnum* spp. stems, branches and leaves, charred *Picea mariana* needles
196	206.7	UCIAMS-129514	2250±15	2162-2336	*Sphagnum* spp. stems
217	233.0	UCIAMS-129515	2465±15	2442-2704	*Sphagnum* spp. stems
232	250.2	UCIAMS-129516	2725±15	2779-2853	*Sphagnum* spp. stems
256	283.2	UCIAMS-129517	2900±15	2963-3136	*Sphagnum* spp. stems
286	321.8	UCIAMS-129518	3090±15	3248-3362	*Sphagnum* spp. stems, *Chamaedaphne calyculata* leaf fragments
328	374.8	UCIAMS-129519	3590±15	3842-3961	*Sphagnum* spp. stems, Ericaceae leaf fragments
376	435.3	UCIAMS-129520	3885±15	4250-4409	*Larix laricina* needles
386	447.9	UCIAMS-135385	3995±20	4421-4519	Bulk peat
IDH					
54	69.7	UCIAMS-135378	140±20	8-278	*Sphagnum* spp. stems
116	118.1	UCIAMS-135379	760±20	670-726	*Sphagnum* spp. stems
137	143.6	UCIAMS-151363	905±20	763-910	*Sphagnum* stems, branches and leaves
191	206.8	UCIAMS-151364	1900±20	1815-1896	*Sphagnum* stems
220	240.7	UCIAMS-135380	2120±20	2007-2150	*Larix laricina* needles, *Myrica gale* and *Chamaedaphne calyculata* leaf fragments, *Sphagnum* spp. stems
286	318.9	UCIAMS-135381	2785±20	2804-2951	*Sphagnum* spp. stems
317	357.0	UCIAMS-151365	3320±20	3479-3607	*Sphagnum* spp. stems
345	390.8	UCIAMS-151366	3480±25	3651-3832	*Sphagnum* spp.stems
394	451.7	UCIAMS-135382	4380±20	4857-5033	*Sphagnum* spp. stems

478	554.3	UCIAMS-135383	4960±25	5612-5737	*Larix laricina* needles and seeds, *Myrica gale* and *Chamaedaphne calyculata* leaf fragments
535	624.1	UCIAMS-123619	6950±25	7699-7839	*Carex* spp. seeds

Table 2.2 Results of ^{210}Pb measurements and CRS modelling on the Baie core.

Sample	Depth (cm)	$^{210}Pb_{tot}$ activity (Bq kg^{-1})	$^{210}Pb_{ex}$ activity (Bq kg^{-1})	CRS ^{210}Pb age (AD)	Uncertainty (a)
Baie 2	1.7	332	316	2010	1
Baie 3	2.9	500	484	2008	1
Baie 4	4.1	257	241	2006	1
Baie 6	6.5	339	323	2003	1
Baie 8	8.9	290	274	2002	1
Baie 10	11	236	221	2001	1
Baie 12	13.4	323	308	1997	1
Baie 14	15.7	358	343	1991	1
Baie 16	17.9	363	347	1987	1
Baie 18	20.3	209	193	1984	2
Baie 20	22.6	268	252	1979	2
Baie 22	24.9	248	232	1974	2
Baie 24	27.3	267	251	1966	2
Baie 26	29.7	237	221	1953	3
Baie 28	32.1	241	225	1921	4
Baie 30	34.5	104	89	1869	8
Baie 32	36.9	32	17		
Baie 34	39.1	16	0		
Baie 36	41.4	15	0		

Table 2.3 Results of ^{210}Pb measurements and CRS modelling on the IDH core.

Sample	Depth (cm)	$^{210}Pb_{tot}$ Activity (Bq kg^{-1})	$^{210}Pb_{ex}$ activity (Bq kg^{-1})	CRS ^{210}Pb age (AD)	Uncertainty (a)
IDH 1	0.8	449	436	2010	1
IDH 2	2.4	480	468	2006	1
IDH 3	3.6	436	423	2001	1
IDH 5	6.0	388	375	1997	1
IDH 7	8.5	373	360	1993	1
IDH 9	10.9	420	408	1990	1
IDH 11	13.3	227	215	1987	1
IDH 13	15.8	334	321	1983	1
IDH 15	18.4	262	249	1980	1
IDH 17	21.1	261	249	1976	2
IDH 19	23.8	193	180	1973	2
IDH 21	26.4	215	202	1968	2
IDH 23	29.1	267	255	1958	3
IDH 25	32.0	175	162	1948	3
IDH 27	34.7	116	104	1938	4
IDH 29	37.5	62	50	1933	4
IDH 31	40.2	53	40	1928	5
IDH 33	42.9	53	40	1920	5
IDH 35	45.6	55	42	1909	6
IDH 37	48.8	53	41	1891	6
IDH 39	51.2	59	47	1865	7
IDH 41	53.6	39	26		
IDH 43	58.6	14	0		
IDH 45	63..2	13	0		

Table 2.4 Nd isotopic data, εNd and $^{206}Pb/^{207}Pb$ for the Baie core.

Sample	Depth (cm)	$^{143}Nd/^{144}Nd$	±2se	εNd	$^{206}Pb/^{207}Pb$	±2se
Baie 3	2.9	0.511924	0.000019	-13.9	1.1657	0.0002
Baie 10	11.0	0.511860	0.000024	-15.2	1.1673	0.0011
Baie 17	19.1	-	-	-	1.1748	0.0006
Baie 22	24.9	-	-	-	1.1792	0.0009
Baie 25	28.5	-	-	-	1.1846	0.0001
Baie 26	29.7	0.511905	0.000006	-14.3	1.1800	0.0009
Baie 26*		0.511912	0.000006	-14.2	1.1803	0.0001
Baie 33	38.0	0.511888	0.000010	-14.6	1.1933	0.0003
Baie 33		*0.511881*	*0.000021*	*-14.8*	*1.1981*	*0.0007*
Baie 36	41.4	0.511932	0.000010	-13.8	1.2057	0.0007
Baie 48	55.7	0.511886	0.000010	-14.7	1.1912	0.0016
Baie 69	81.8	0.511930	0.000008	-13.8	1.1880	0.0005
Baie 74	87.9	0.511894	0.000007	-14.5	-	-
Baie 112	112.5	0.511867	0.000014	-15.0	1.1954	0.0011
Baie 118	119.1	0.511927	0.000007	-13.9	-	-
Baie 119	120.1	0.511911	0.000005	-14.2	-	-
Baie 119		*0.511897*	*0.000008*	*-14.4*	-	-
Baie 120	121.2	0.511921	0.000010	-14.0	-	-
Baie 120		*0.511909*	*0.000007*	*-14.2*	-	-
Baie 128	130.0	0.511941	0.000005	-13.6	1.1936	0.0006
Baie 129	131.1	0.511867	0.000009	-15.0	-	-
Baie 141	144.1	0.511914	0.000005	-14.1	-	-
Baie 148	151.9	0.511949	0.000006	-13.4	-	-
Baie 148		*0.511946*	*0.000007*	*-13.5*	-	-
Baie 150	154.1	-	-	-	1.1979	0.0011
Baie 160	165.1	0.511913	0.000009	-14.1	1.2029	0.0005
Baie 172	178.3	-	-	-	1.2023	0.0001
Baie 174	180.4	-	-	-	1.2011	0.0003
Baie 175	181.5	0.511915	0.000016	-14.1	-	-
Baie 178	184.8	-	-	-	1.1971	0.0006
Baie 201	213.2	0.511954	0.000007	-13.3	1.2098	0.0012
Baie 223	240.3	0.511993	0.000008	-12.6	1.2049	0.0008
Baie 236	257.3	0.511985	0.000012	-12.7	1.2008	0.0008
Baie 262	290.7	0.511956	0.000011	-13.3	1.2134	0.0011
Baie 281	315.1	0.511964	0.000007	-13.2	1.2097	0.0008
Baie 299	338.8	-	-	-	1.2148	0.0006
Baie 340	390.2	-	-	-	1.2082	0.0004
Baie 352	404.9	0.511754	0.000009	-17.9	1.1772	0.0007
Baie 376	435.3	-	-	-	1.1992	0.0003
Baie 383	444.1	0.511494	0.000009	-22.3	1.1562	0.0009
Bottom sed.		0.511544	0.000020	-21.3	1.123	0.0001
Bottom sed.		*0.511554*	*0.000022*	*-21.2*	*1.1316*	*0.0003*
Local soil		0.511729	0.000008	-17.7	1.2058	0.0012
Local soil		*0.511730*	*0.000008*	*-17.7*	*1.2061*	*0.0008*
Beach		0.5116865	0.000009	-19.2	1.1909	0.0009

*Duplicate analysis; italic: replicate analysis

Table 2.5 Nd isotopic data, εNd and $^{206}Pb/^{207}Pb$ for the IDH core.

Sample	Depth (cm)	$^{143}Nd/^{144}Nd$	±2se	εNd	$^{206}Pb/^{207}Pb$	±2se
IDH 7	8.5	0.511919	0.000017	-14.0	1.1668	0.0004
IDH 24	30.5	0.511954	0.000009	-13.3	1.1755	0.0007
IDH 24		*0.511982*	*0.000019*	*-12.8*	*1.1761*	*0.0012*
IDH 27	34.7	0.511971	0.000006	-13.0	1.1785	0.0003
IDH 31	40.2	0.511862	0.000007	-15.1	1.1784	0.0001
IDH 43	56.1	0.511984	0.000009	-12.8	1.1929	0.0001
IDH 52	67.1	0.511905	0.000007	-14.3	1.2533	0.0011
IDH 70	89.0	0.511945	0.000010	-13.5	1.1880	0.0005
IDH 110	111.0	0.512025	0.000010	-12.0	1.1934	0.0004
IDH 137	143.1	0.512015	0.000012	-12.1	1.1965	0.0012
IDH 164	175.1	0.512008	0.000013	-12.3	1.2008	0.0003
IDH 191	206.8	0.512002	0.000008	-12.4	1.2028	0.0010
IDH 236	259.4	0.512021	0.000013	-12.0	1.1982	0.0006
IDH 254	280.5	0.512013	0.000021	-12.2	1.1946	0.0012
IDH 263	290.7	0.511961	0.000014	-13.2	1.2069	0.0003
IDH 299	335.0	0.511999	0.000005	-12.5	1.1944	0.0008
IDH 317	357.0	0.512022	0.000007	-12.0	1.1876	0.0008
IDH 344	389.6	0.512034	0.000006	-11.8	1.2104	0.0005
IDH 371	423.8	0.512015	0.000010	-12.2	1.2062	0.0006
IDH 407	467.3	0.512002	0.000019	-12.4	1.2052	0.0011
IDH 434	500.5	0.511718	0.000011	-17.9	1.2088	0.0009
IDH 470	545.0	0.511664	0.000006	-19.0	1.1846	0.0014
IDH 470		*0.511658*	*0.000006*	*-19.1*	-	-
IDH 493	572.5	0.511556	0.000014	-21.1	1.1223	0.0002
IDH 493		*0.511550*	*0.000014*	*-21.2*	-	-
IDH 532	620.2	0.511563	0.000011	-21.0	1.1283	0.0004
IDH 532		*0.511549*	*0.000046*	*-21.3*	-	-
Bottom sed.		0.511655	0.000007	-19.2	1.1376	0.0008
Beach		0.511658	0.000015	-19.1	1.2143	0.0009

italic: replicate analyses

CHAPITRE III

INCREASED ATMOSPHERIC DUST DEPOSITION DURING LATE HOLOCENE CLIMATIC INSTABILITIES IN A BOREAL PEAT BOG FROM NORTH-EASTERN CANADA

Steve Pratte[a,b,*], Michelle Garneau[a], François De Vleeschouwer[b]

[a] GEOTOP, Université du Québec à Montréal, C.P. 8888, Succ. Centre-Ville, Montreal, Quebec, Canada, H3C 3P8.

[b] ECOLAB, Université de Toulouse, CNRS, INPT, UPS, France

Article soumis à *Palaeogeography, Palaeoclimatology, Palaeoecology*

RÉSUMÉ

Les variations des apports de poussières atmosphériques dans le nord-est du Canada furent reconstruites à l'aide de la géochimie élémentaire dans une séquence tourbeuse de la région de la Baie de James. Les concentrations en terres rares (REE) et en éléments lithogéniques ainsi que la signature isotopique du néodyme furent mesurés par spectrométrie de masse avec les méthodes de Q-ICP-MS, ICP-OES et MC-ICP-MS respectivement. Une analyse par composante principale effectuée sur les profils de concentration des divers éléments mesurés montre que les REE se comportent de façon similaire aux autres éléments lithogéniques, tels que Al et Ti. Ceci suggère que les REE ne sont pas remobilisés dans les séquences de tourbe et qu'ils peuvent ainsi être utilisés en tant qu'indicateurs d'apports de poussières atmosphériques. Des analyses de macrorestes végétaux et de thécamoebiens furent aussi réalisées afin de reconstruire la succession végétale et les conditions d'humidité de surface. Les flux de poussières reconstruits varient entre 0.1 et 18 g m^{-2} a^{-1}. Des apports accrus de poussières furent observés lors de différentes périodes : 4000 à 3000, 2600 à 2000, 1600 à 1000, 800 à 650 cal a BP et de 1960 à 1990AD. Les valeurs de εNd montrent un large spectre allant de -37 à -12. Au moins trois sources distinctes constituent les apports de poussières dans le temps: les sédiments marins à la base de la tourbière, la moraine de Sakami ainsi qu'une source probablement plus régionale dont l'origine reste non-identifiée. La période allant de 7000 à 4100 cal a BP montre des valeurs de εNd plus négative entre -36 et -29. Une augmentation graduelle des valeurs de εNd à partir de 4100 cal a BP suggère une diminution des apports locaux de poussières à la faveur d'une source non identifiée. À partir de 1500 cal a BP, les valeurs de εNd demeurent relativement stables autour de -12 à -15. La majorité des périodes d'apports accrus de poussières identifiées correspondent à des périodes documentées comme étant froides et sèches, probablement liées à des intrusions de masses d'air arctiques. La présence de certains

de ces pics de poussières lors de minima solaires suggère que la variabilité solaire a aussi joué un rôle dans les fluctuations climatiques de la région.

ABSTRACT

Dust deposition in north-eastern Canada was estimated from the geochemical signature of an ombrotrophic peatland. The rare earth elements and other lithogenic elements, as well as Nd isotopes were measured by Q-ICP-MS, ICP-OES and MC-ICP-MS, respectively along a 4.20 m peat core covering the last 7000 years. A principal component analysis performed on the geochemical dataset shows that REEs display the same chemical behavior as other lithogenic elements such as Al and Ti, which suggests that they are immobile in the peat column and can be used as tracers of dust deposition. Plant macrofossils and testate amoebae were also used to reconstruct past ecohydrological conditions. The range of dust deposition varies from 0.1 to 18 g m^{-2} a^{-1}. Increases in dust flux were observed from 4000-3000, 2600-2000, 1600-1000, 800-650 cal a BP and from 1960-1990AD. The εNd values show a large variability from -37 to -12, identifying a least three sources: local marine sediments, the Sakami moraine and another unidentified source likely from a more regional origin. Between 7000 and 4100 cal a BP, the εNd values varied from -36 to -29, while they gradually increased from 4100 cal a BP until 1500 cal a BP, suggesting proportionnally less dust from local source(s) is deposited in favor of more regional source(s). From 1500 cal a BP, εNd values remained relatively stable around -15 and -12. Most of the dust peaks correspond to documented cold and dry periods likely linked to intrusion of arctic air masses. The occurrence of some peaks during solar minima suggests that insolation played a role in the climatic variations of the region.

3.1 Introduction

Mineral dust plays an important role in the global climate system, having effect on radiation budgets, the chemical composition of the atmosphere and affecting marine and terrestrial biogeochemical cycles by supplying nutrients (Harrison *et al.*, 2001). Mineral dust not only affects climate but is also a function of it, i.e. fluctuations in atmospheric dust production, transport and deposition are sensitive to climatic variations (Martini and Martinez-Cortizas, 2006).

Paleo-climate records have shown greater dust deposition during glacial compared to interglacial phases (Fischer *et al.*, 2007). Thus, dust is both a driver and a passive recorder of past climate conditions. However, our understanding of the exact role of dust in the Earth's climate system is still poorly constrained mostly due to a lack of data reflecting its high spatial and temporal variability (Harrison *et al.*, 2001). Paleo-dust deposition reconstructions using environmental archives provide a mean of assessing temporal and spatial dust variability under different climatic conditions (Biscaye *et al.*, 1997; deMenocal *et al.*, 2000; Mischke *et al.*, 2010; Zdanowicz *et al.*, 2000).

At present, the spatial coverage of paleo-dust records from continental archives is sparse and focuses on arid regions whereas the higher latitudes have been overlooked (Kohfeld and Harrison, 2001). Peatlands are continental archives of particular interest in this context because they are broadly distributed, especially in the higher latitudes, and usually show high accumulation rates, allowing high temporal resolution reconstructions. Peat bogs are hydrologically isolated, i.e. they receive their water and nutrients from precipitation (rain, snow, fog, dust) (Chambers and Charman, 2004) and as such their surface wetness is closely linked to atmospheric conditions (Aaby, 1976; Barber, 1993). In comparison to ice cores, which record mainly long-range transport of atmospheric particles, peat bogs also record dust inputs from local and regional sources (Le Roux *et al.*, 2012; Marx, McGowan and Kamber, 2009).

Apart from pollen, which has often been used as past paleo-ecological and paleo-climatic indicators, there are a number of other climate indicators incorporated in peat sequences. Macrofossil (Barber, Chambers and Maddy, 2003), peat humification (Chambers, Beilman and Yu, 2011) and testate amoebae (Booth, 2002; Charman, 2001; Mitchell, Charman and Warner, 2008) analyses provide reliable reconstructions of past ecohydrological changes in peat bogs. While the validity of the past climate signals derived from these proxies has been confirmed (Barber and Langdon, 2007; Charman et al., 2009; Charman *et al.*, 2004), previous studies have also highlighted some limitations (Caseldine *et al.*, 2000; de Jong *et al.*, 2010; Hansson *et al.*, 2013; Sullivan and Booth, 2011), suggesting a multi-proxy approach is needed to improve the interpretation. In addition to those usual biological proxies, the inorganic fraction of peat also provides information on past abundance and provenance of atmospheric mineral dust which affects the Earth's climate system (Goudie and Middleton, 2001; Kohfeld and Harrison, 2001).

Despite the potential of peat bogs as dust archives, the number of studies reconstructing past climate using inorganic geochemistry in peat profiles remains limited, although their use has increased over the recent years. For example, peat cores were successfully used to identify changes in dust deposition linked to the Younger Dryas in Switzerland (Le Roux *et al.*, 2012; Shotyk *et al.*, 2001) and SE Asia (Weiss *et al.*, 2002), the impact of Sahara aridification on the atmospheric dust load in western Europe (Allan et al., 2013; Le Roux *et al.*, 2012) as well as a strengthening of the westerlies during the Antarctic Cold Reversal in Tierra del Fuego (Vanneste *et al.*, 2015). Such studies highlight the importance of peat investigation for a better understanding of the role of dust on the Holocene climate variability.

To date, few continental records of dust deposition exist in North America and focus mainly on loess deposits (Muhs, 2013) which apart certain number of studies (Mason *et al.*, 2008; Miao *et al.*, 2007), usually lack resolution for the Holocene. Furthermore,

multi-proxy paleo-environmental and paleo-climatic studies in north-east American peat bogs involving inorganic geochemistry are scarce and mostly focus on elemental pollution (Givelet, Roos-Barraclough and Shotyk, 2003; Pratte, Mucci and Garneau, 2013; Roos-Barraclough et al., 2006; Shotyk and Krachler, 2010).

In this study we aim to use past atmospheric dust flux derived from REE concentrations to reconstruct potential climatic events during the mid- and late Holocene in a peat bog from the James Bay lowlands, north-eastern Canada. We use the Nd isotopic signature of these the deposited particles to attempt to decipher their source. Other proxies (plant macrofossils, testate amoebae) are also used to picture the local paleo-climatic and paleo-environmental conditions and investigate the relationship between dust flux and climatic variability. Furthermore, the high-latitude location of the study site allows the investigation of the dust cycle in a cold region, which are, as mentioned previously, underrepresented.

3.2 Material and Methods

3.2.1 Site description and sampling

The study site is located along the course of the *La Grande* River in a depression of the Precambrian Shield (Fig. 3.1). The Wisconsinan glaciation ended around 8000 BP in the region (Dyke and Prest, 1987) and was followed by the invasion of the Tyrell Sea around 7.8 BP (Hillaire-Marcel, 1976). Hence, Quaternary deposits such as glacial tills, littoral sands and marine clays are present regionally. Among these deposits, the Sakami moraine constitutes an important feature of the landscape (Fig. 3.1b) and is located about 500 m east of the sampling site. The Sakami moraine was deposited following a stillstand in the drainage of Lake Agassiz-Ojibway around 8.47 ka (Hardy et al., 1982; Hillaire-Marcel et al., 1981; Lajeunesse, 2008).

The climate in the region is considered as continental subarctic, with mean annual temperature of -3°C, mean July temperature of 24°C and mean January temperature of -23°C (Environment Canada, 2010). Mean annual precipitation is 684 mm of which one third falls as snow.

The LG2 peatland (53°; 77°44'W; 1.7 km^2; 172 m a.s.l.) is part of a wide bog complex located approximately 90 km east of James Bay. The majority of the complex consists of ombrotrophic peat dominated by *Sphagnum fuscum* and *S. capillifolium*, ericaceous shrubs (*Chamaedaphne calyculata*, *Rhododendron groendlandicum* and *Kalmia polifolia*), lichens (*Cladina* spp.) and sparse *Picea mariana* and *Larix laricina*.

Two cores were retrieved from the deepest section of the peatland, using a stainless steel box corer (8x8 cm width; Jeglum *et al.* (1992) to sample the upper meter and a Russian sampler (7.5 cm diameter; (Jowsey, 1966)) for the deeper sections. The cores were collected from two holes approximately 30 cm apart in an overlapping manner to ensure complete stratigraphic recovery (De Vleeschouwer, Chambers and Swindles, 2010). The cores were wrapped in plastic film, transferred into polyvinyl chloride tubes and stored in a freezer (-20°C) until preparation. The cores were sliced frozen using a stainless steel band saw at *Ecolab* (*Université de Toulouse*, France) at 1-cm interval (Givelet *et al.*, 2004). The thickness of each slice was then measured again to evaluate the loss from the slicing and correct the mid-point depth of each sample. The edges of each subsample were trimmed away to avoid any contamination from the saw. The slices were then subsampled for each type of analyses.

Till samples from the Sakami moraine were collected as potential dust source. Littoral sands, also located in the vicinity of the LG2 peatland, were collected for the same purpose.

3.2.2 Chronological control

The chronological control of the core is based on a combination of ^{210}Pb and ^{14}C AMS dates. Lead-210 activity was determined in the upper 30-cm of peat after extraction of its grand-daughter product, ^{210}Po, from 0.5 g of powdered bulk peat spiked with ^{209}Po yield tracer following a sequential extraction HNO_3:HCl (3:1)-HF-H_2O_2 digestion. Measurements were obtained using a α-spectrometer (EGG Ortec 476A) at GEOTOP Research center (UQAM, Montreal). The Constant Rate of Supply (CRS) model was subsequently applied to build ^{210}Pb age-models (Appleby, 2002). The measurement uncertainties (Table 3.1), corresponding to one-sigma, were calculated from counting statistics. The atmospheric, or excess ($^{210}Pb_{ex}$), is used to determine the chronology of environmental records. Supported ^{210}Pb activity, i.e. produced *in situ*, was estimated by the analysis of deeper samples in each core in order to determine at which depth the $^{210}Pb_{ex}$ was not present anymore, hence the limit of the dating technique (Le Roux and Marshall, 2011).

Radiocarbon ages were obtained from selected plant macrofossils based on a protocol developed by Mauquoy *et al.* (2004). To ensure a better accuracy of dates, only aboveground plant macrofossils were selected. The majority of the macrofossils consisted of *Sphagnum* spp. stems (Tables 1 and 2). When *Sphagnum* were not sufficient to provide enough material for dating, other types of macrofossils were selected (*Larix laricina* and *Picea mariana* needles, Ericaceae leaves, etc.). All samples were submitted to an acid-alkaly-acid washing treatment, drying, combustion and graphitisation (Piotrowska, 2013) at the GADAM Centre (Gliwice, Poland). Radiocarbon concentrations were measured at Rafter Radiocarbon Laboratory (Lower Hutt, New Zealand) and DirectAMS Laboratory (Bothel, USA) following established protocols (Donahue, Linick and Jull, 1990).

Age-depth models were generated by combining both ^{14}C and ^{210}Pb dates using the *BACON* software package (Blaauw and Christen, 2011). The radiocarbon dates were

calibrated using the InterCal13 Northern Hemisphere terrestrial calibration curve (Reimer *et al.*, 2013) integrated in the *BACON* package. The surface age was fixed at -63 cal a BP (i.e. AD 2013, the age of core extraction).

3.2.3 Bulk density, ash content and grain size

The bulk density of the samples was determined by measuring the volume using a vernier caliper and weighting subsequently the samples fresh and then freeze-dried. The ash content, as a surrogate of the mineral matter content, was obtained by ashing each subsample at 550°C for 6h to remove all organic matter by combustion (Chambers, Beilman and Yu, 2011).

Grain-size distribution was determined on the water insoluble inorganic fraction of bulk peat samples using a Horiba LA-950 laser grain-size analyser at Ecolab. The inorganic fraction was obtained from a selection of ash samples resulting from the ash content analyses. To dissolve pseudo-minerals (salts) potentially formed during the ashing process, each sample was dissolved in MQ water and subjected to a 3-minute ultrasonic treatment to separate particles. A number of 70 size classes were used to characterize the grain-size distribution of the samples. When volume was unsufficient, contiguous samples were combined (116-162 cm: 3 samples per analyse and 203-284 cm: 2 samples per analyses) to ensure enough material for analyses.

3.2.4 Plants macrofossil and testate amoebae analyses

Plant macrofossil analyses were performed at 4-cm intervals and refined (2-cm intervals) were visual changes in the stratigraphy were noted. Subsamples (4 cm^3) were gently boiled in distilled water with addition of 5% KOH and carefully rinsed through a 125-µm sieve. Macrofossils were scanned using a binocular microscope (x10-x40)

and identified using reference collections (Garneau, 1995; Mauquoy and van Geel, 2007). Vegetation types were expressed as volume percentages (%) representative of cover estimates in a chequered Petri dish (*Sphagnum* remains, ligneous fragments, etc.) or counted (seeds, leaf fragments, etc.), which were reported as the number (n) present in each subsample. *Sphagnum* were determined to the highest taxonomic level possible based on branch and stem leaf characteristics using a microscope (x40-x100). Terminology follows Marie-Victorin (1995) for vascular plants and Crum and Andersen (1979) and Ireland (1982) for bryophytes.

Testate amoebae analyses were conducted at 4-cm intervals and refined (2-cm intervals) in sections with lower rate of peat accumulation. The analyses were mostly restricted to the ombrotrophic section (*Sphagnum*-dominated) of the core with some samples from the fen-bog transition. Subsamples (1 cm^3) were extracted and treated following standard procedures (Booth, 2011), with addition of *Lycopodium* spores to calculate concentrations. Only the size fraction between 300 and 15 µm was analysed. A hundred tests were identified using an optical microscope at 400x magnification following the taxonomy of Charman, Hendon and Woodland (2000) with modifications from Booth and Sullivan (2007). Fossil assemblages with less than 40 specimens (n=3) are shown in the diagrams but were excluded from the WTD reconstruction since they may be unreliable.

Using a transfer function based on 206 modern assemblages (Lamarre *et al.*, 2013), a paleo-hydrological reconstruction was carried out with C2. A weighted average tolerance down-weighted (WA-tol) model with classical deshrinking was used to infer past WTDs. This model has the best performance statistics in cross-validation for the prediction of WTD (r^2 = 0.84; RMSEP = 5.28 cm). Sample-specific error ranges for the reconstructed WTD were calculated using bootstrapping (1000 cycles).

3.2.5 Major and trace elements analyses

All geochemical sample preparations were performed under clean laboratory conditions (class 100) using acid-cleaned labware. About 100 mg of powdered peat samples and the < 63-μm fraction of sediment samples were acid-digested until complete dissolution, using a series of steps (HNO_3 + HF, H_2O_2) in Savillex® beakers on a hot plate (Le Roux and De Vleeschouwer, 2010). In a number of samples, an additional step involving *aqua regia* was necessary due to higher organic content. Selected major elements concentrations (Al, Ti, Ca, Fe and Na) were measured at Ecolab laboratory (Toulouse, France) on a Thermo Electron IRIS Intrepid II ICP-OES. Selected trace element measurements (Sr, Zr, Sc, Hf, Th, U and REE) were completed on an Agilent Technologies 7500ce Q-ICP-MS at *Observatoire Midi-Pyrénées* in Toulouse, France. Prior to ICP-MS analyses, samples were diluted and an In-Re spike was added for internal normalisation process. The analytical performance was monitored through reference materials NIST 1515 Apple leaves, NIST 1547 Peach leaves, NIST 1575a Pine needles and GBW07604 (GSV-7) Bush branches and leaves. Replicate analyses were generally within 10% of each other. The blanks for all elements considered here are < 0.01%.

3.2.6 Nd isotope analyses

Peat and sediment samples were prepared for Nd isotopes. Between 100 and 600 mg of dried peat (100 mg for sediments) was placed in oven at 550 °C for 6 h, to remove all organic matter by combustion (Chambers, Beilman and Yu, 2011). The resulting ashes were acid-digested in a mixture of concentrated HNO_3 and HF. To ensure complete dissolution, concentrated HCl was added and samples were evaporated. Residues were dissolved into 1N HNO_3 and Nd was purified by a passage through two sets of columns. Alkalis (e.g. Ca, Rb, Sr) and REE were separated by a passage through Bio-Rad columns filled with preconditioned TRU Spec© resin (50-100 mesh). After

repeated column cleaning using 1N HNO_3, the REE were collected by passing 1.75 ml of 0.05N HNO_3. This solution was directly loaded onto pre-conditioned and pre-calibrated LN Spec© and sequentially eluted using 0.2N HCl. The Nd solutions were evaporated and dissolved another time in 2% HNO_3 prior to Nd isotopic measurements.

The Nd isotopic measurements were made on a Nu Plasma II MC-ICP-MS (multi-collector inductively coupled plasma mass spectrometer) at GEOTOP-UQAM, in Montreal, Quebec. Replicate analysis of the JNDi-1 Nd standard (Tanaka *et al.*, 2000) every five samples yielded a $^{143}Nd/^{144}Nd$ value of 0.512084 ± 0.000014 (2σ, n = 16). Mass fractionation was corrected to $^{146}Nd/^{144}Nd$ = 0.7219. Epsilon neodymium (εNd) was calculated according to DePaolo and Wasserburg (1976)

$$\varepsilon Nd = \left(\frac{\left(\frac{143Nd}{144Nd}\right)}{0.512638} - 1 \right) * 10000$$

where 0.512638 corresponds to the chondritic uniform reservoir (CHUR) and represents present-day average Earth value (Jacobsen and Wasserburg, 1980).

3.2.7 Statistical analyses

A principal component analysis (PCA) was performed on the elemental concentrations using SPSS 22.0.0 software to help identify the sources and processes affecting the distribution of the chemical elements in both peat profiles. The PCA was realised in correlation mode on previously log transformed (log10) and standardized (z-scores) data to avoid scaling effects, using a varimax rotation which is a fixed orthogonal rotation that maximizes the loadings of the variables on the components (Eriksson *et*

al., 1999). The z-scores were calculated as $(X_i-X_{avg})/X_{std}$, where X_i is the variable (i.e. concentration of the element), while X_{avg} and X_{std} are the series average and standard deviation of all samples for the variable X_i. Elements with similar records load onto the same principal component and are most likely controlled by the same environmental factors. Hence, the chemical signals tend to be clearer and the underlying factors controlling them are more easily identified and interpreted.

Detrended correspondence analysis (DCA) was applied to the fossil dataset to explore the testate amoeba associations using CANOCO 5.0 (detrending by segments, down-weighting of rare species). For the same purpose, a PCA was applied to the macrofossil dataset. The axis 1 and 2 scores derived from the DCA and the PCA were used in combination with testate amoebae and macrofossil assemblages as well as inferred WTD to define the diagram zones.

3.2.8 Dust flux

The rate of deposition of atmospheric dust, i.e. the dust flux, can be calculated using the concentration of a lithogenic element, peat bulk density and peat accumulation rate. Assuming that "soil dust" contains lithogenic elements in the same concentration as the Earth's crust, the concentration of dust is normalized to the upper continental crust (Wedepohl, 1995). The dust accumulation rate, i.e. dust flux, was calculated based on the REE concentrations in the bulk samples using the following formula (Shotyk *et al.*, 2002):

$$\text{Dust flux (g m}^{-2}\text{ a}^{-1}) = [\Sigma\text{REE}]_{sample}/[\ \Sigma\text{REE}]_{UCC} \times \text{bulk density} \times \text{PAR} \times 10000$$

where $[\Sigma\text{REE}]_{sample}$ is the sum of REE concentrations in a sample, $[\Sigma\text{REE}]_{UCC}$ is the sum of REE concentrations in the upper continental crust (144.3 ug g^{-1}; Wedepohl, 1985) and PAR is the peat accumulation rate.

3.3 Results

3.3.1 Chronology

The supported, unsupported ^{210}Pb activities and the CRS-modelled ages for LG2 core are presented in Table 3.1 while the range of calibrated radiocarbon ages are presented in Table 3.2. Peat accumulation started around 7080 cal a BP (Fig. 3.2; Table 3.2), which is in good agreement with another core collected on the same peatland, for which an age of 7010 cal a BP was obtained (Beaulieu-Audy *et al.*, 2009). Chronology shows a relatively rapid rate of peat accumulation during the first 700 years with a mean of 0.8 (± 0.02) mm a^{-1}. Between 3040 and 840 cal a BP, mean peat accumulation rate is around 0.5 mm a^{-1}. From 840 cal a BP, peat accumulation rates decrease to reach their lowest values between 640 and 150 cal a BP with a mean value of 0.2 mm a^{-1}. In the upper 26 cm, the accumulation rates are much higher and correspond to the acrotelm, characterized by fresh undecomposed peat and living mosses.

3.3.2 Bulk density and ash content

The density of the peat in the LG2 core ranges between 0.04 to 0.25 g cm^{-3} (Fig. 3.3). The ash content varies between 0.04 and 12%. In the lower peat section (below 250 cm) the ash content decreases progressively towards the top of the section along with the density (minerotrophic section). The density remains relatively stable between 250 and 130 cm, while it oscillates between 0.08 and 0.2 g cm^{-3} higher in the core. Similarly, ash content remains low above 250 cm with the exception of the top 40 cm, where two peaks are found (40-20 cm and 5-cm of depth).

3.3.3 Ecohydrological reconstruction and ordination of the fossil assemblages

The results of the plant macrofossil and testate amoeba analyses are presented in Figure 3.4. The main features of the identified zones are described in Table 3.3. Stratigraphic analyses show that brown mosses and herbaceous species started accumulating at *ca.* 7080 cal a BP (zone 1). The top of the zone (4400 cal a BP) is characterized by the presence of *Sphagnum* section *Cuspidata* and several species of testate amoebae of which *Amphitrema wrightianum*, *Centropyxis aculeata*, *C. platystoma*, *Heleopera sphagni* are dominant in certain layers. From 249 cm to 132 cm (zone 2: 4400-2700 cal a BP), *S. fuscum* dominates the macrofossil assemblages while testate amoebae are dominated by *A. flavum*. From 2700 cal a BP (zone 3), WTD show a greater variability driven by a greater number of testate amoeba species in the assemblages (*A. flavum*, *A. muscorum*, *Amphitrema wrightianum* and *Difflugia pristis*), while the macrofossil assemblages remain stable with a dominance of *S. fuscum*. This trend is accentuated between 1470 cal a BP and 1930AD (zones 4, 5 and 6) through several shifts in testate amoeba (*Hyalosphenia subflava*, *Arcella discoides*, *Difflugia pristis* and *D. pulex*) and macrofossil (*S. fuscum*, Herbaceae, UOM, charcoals) assemblages. Well-preserved *S. fuscum* accumulated since 1930AD, while *Nebela militaris* and *Hyalosphenia elegans* constitute the main species in the testate amoeba assemblages.

Results of the DCA on the testate amoeba assemblages and PCA on plant macrofossils are presented in figure 3.5. The DCA shows a relatively good separation of testate amoeba species (Fig. 3.5a). The ordination along axis 1 reveals a distinction between species from zone 1 (higher values) on the right and those from the other zones further on the left (lower values). Species such as *Arcella discoides*, *Hyalosphenia subflava*, *Difflugia pristis* and *D. pulex* display lower values (left end) of the axis while *Centropyxis aculeata*, *C. cassis*, *C. platystoma* and *Heleopera petricola* show higher values (right end). Axis 1 is taken to represent the distinction between the minerotrophic (right end) and ombrotrophic parts of the LG2 core (see DCA axis 1 in Fig. 3.4). The ordination along axis 2 shows that species found in zones 4 and 6 (mostly

Arcella discoides and *Hyalosphenia subflava*) have higher values (top end) while species found in samples close to the surface (*Nebela militaris*, *Euglypha rotunda*, *E. strigosa*, *E. turberculata* and *Hyalosphenia elegans*) display lower values (bottom end). With the exception of *N. militaris* and *H. elegans*, the presence of those species is usually < 5%. The species found at the top end of axis 2, namely *A. discoides* and *H. subflava*, are often found in combination in fossil samples and were associated with periods of high decadal to centennial hydroclimatic variability (Magnan and Garneau, 2014; Sullivan and Booth, 2011).

The PCA ordination of the plant macrofossil assemblages (Fig. 3.5b) shows a similar pattern as the testate amoebae, i.e. species from the deeper sections of the core (Herbaceae, brown mosses) show positive values on axis 1 and species from other zones (*Sphagnum fuscum*, *S. capillifolium* and ligneous remains) have negative values (Fig. 3.5). Hence, as for the testate amoebae ordination, axis 1 represents the separation between ombrotrophic and minerotrophic sections of the core.

3.3.4 Elemental concentrations and principal component analyses

The REE display very similar concentration profiles to Al and Ti in the LG2 core (Fig. 3.3). Lanthanum is reported as light REE, Sm as middle REE and Yb as heavy REE. "Peaks" in REE and lithogenic element (Al and Ti) concentrations are observed at *ca.* 6050-5650, 3750-3050, 2650-1750, 1450-1050 and 700 to -27 cal a BP. The REE/Ti ratio displays values greater than 10 before 6750 cal a BP. Between 6750 and 3750 cal a BP, REE/Ti range between 4 and 10, while they decrease to values of one to two from ca. 3500 cal a BP towards the top of the core.

The results of the principal component analysis are shown in Figure 3.6. Three principal components, explaining 93% of the variance, were extracted from the geochemical dataset. The first principal component (PC1) accounts for 70% of the total

variance and includes REE, Y, U, Th, Zr, Ti and Al. The second component (PC2) explains 14% of the total variance and comprises Sr, Ca and Na. PC3 explains 9% of the total variance and includes Pb.

3.3.5 Grain size

The grain-size distribution of LG2 samples are presented in Figure 3.7. Silts dominate (2-63 μm) but sand particles (> 63 μm) are also present throughout the core, while clays (< 2 μm) are only found in certain levels covering the last 3000 years. From the bottom of the core to *ca.* 5000 cal a BP, the grain-size distribution displays a high variability with median grain size between 6 and 20 μm. An increase in grain size up to 80 μm is observed between 325 and 331 cm (5890-5750 cal a BP). From 4800 to 2500 cal a BP, the median grain size ranges between 12 and 16.6 μm. Other peaks in grain size are found around 2100 cal a BP, between 1430 and 1150 cal a BP (up to 58 μm) and from 260 cal a BP to 1977AD. Between those peaks, grain size distribution is dominated by fine silts.

3.3.6 Dust flux

The dust flux ranges between 0.12 and 2.5 g m^{-2} a^{-1} over the last 4000 years (Fig. 3.7). The samples older than 4000 years also show high values. However, this period corresponds to the fen section, which receives both atmospheric and lateral (i.e streams/surficial weathering) mineral inputs. The dust flux in the ombrotrophic section can be divided into five periods of increased dust deposition. From 4000-3300 cal a BP, the dust flux increases to reach maxima of 1.9 g cm^{-2} a^{-1} and 1.7 g cm^{-2} a^{-1} at 3800 and 3400 cal a BP respectively. Between 2650 and 2000 cal a BP, the average dust flux is around 1.7 g cm^{-2} a^{-1} and reaches 2.3 g cm^{-2} a^{-1} at 2200 cal a BP. Another dust peak is observed from 1600 to 1000 cal a BP with values up to 1.2 g cm^{-2} a^{-1}, while a slight

increase of the dust flux to 1.0 g cm^{-2} a^{-1} is found between 800-600 cal a BP. Finally, a sharp increase in dust fluxes is observed from 25 cal a BP (1925AD) to the present-day with values up to 18.4 g cm^{-2} a^{-1} in 1986AD. Between these periods of increased dust deposition, the dust flux values range between 0.1 and 0.4 g cm^{-2} a^{-1}.

3.3.7 Nd Isotopes

The LG2 εNd signatures display a large spectrum from -37 to -12 (Table 3.4 and Fig. 3.7), with some temporal trends. Peat samples between 7000 and 4100 cal a BP have a εNd ranging between -36 and -29 with an excursion of -22 corresponding with a dust peak at 5800 cal a BP. From 4100 to 1500 cal a BP, εNd increases gradually from -29 to -14. The εNd values are more stable between 1500 and 25 cal a BP ranging between -15 and -12. From 1975AD to the present-day, εNd samples display values from -27 to -19. Sediments from the bottom of the core have a εNd of -37, while the Sakami moraine samples have a signature of -25 and some littoral sands a value of -27.

3.4 Discussion

3.4.1 Major processes controlling the geochemical signal

A PCA was realized in order to reduce the dimension of the geochemical dataset and explain as much variability as possible with fewer components (Jolliffe, 2002; Reimann *et al.*, 2008). This allows the identification of variables (i.e. chemical elements) with similar behavior and likely to be controlled by the same processes. PC1 displays high positive loading factors with all lithogenic elements (Y, REE, U, Th, Hf, Zr, Ti, and Al) (Fig. 3.6). The fact that REE load on the same PC as other lithogenic elements, known for their conservative nature, such as Ti and Al, confirms that REE are immobile in the peat column as suggested in Krachler *et al.* (2003) and Aubert *et*

al. (2006). Since all lithogenic elements are associated with PC1, they reflects the mineral content of the peat from dust deposition, probably derived from soil erosion. The principal component analysis extracted a second component, PC2, which is considered to represent diagenetic processes as it is linked to Ca, Sr and Na which are known to be mobile in peat (Shotyk, 1997; Steinmann and Shotyk, 1997). PC2 will not be discussed further as it does not provide any information about dust deposition or sources. A third component was extracted by the PCA and displays high loading factor for Pb. Lead has a history of anthropogenic use and is known to be emitted as by-product of human activities. Hence, PC3 is taken to represent pollution and will also not be further be discussed.

3.4.2 Dust source

With the exception of a sample with a value of -22, the minerotrophic samples have much more negative εNd values (-29 to -36) than the ombrotrophic section (-12 to -20) (Fig. 3.7a). The εNd values of the minerotrophic section are in agreement with the range of local sources identified. Effectively, the marine sediments from the bottom of the core have yielded εNd values of -37, while samples from the Sakami moraine and littoral sands collected in the vicinity of the study site have values of -26 and -27 respectively (Table 3.4). Hence, the minerotrophic section represents a mixture between particles from local sources such as the bottom sediments and the Sakami moraine which is located about 500 m east of the study site.

Samples from the ombrotrophic section (younger than 4100 cal a BP) display a distinct isotopic signature (Fig 3.7a). The gradual increase in εNd values between 4100 and 1500 cal a BP (Fig 3.7a), suggests a decreasing proportion of particles from local sources is deposited onto LG2 bog. No local or regional source with a signature similar to these late Holocene samples has been identified. Either this means that the dust deposited at the surface of the LG2 bog comes from a more distal source or that a

mixture of sources contribute to the dust signal. The relative stability of the εNd signature and the REE/Ti (Fig. 3.4) in the ombrotrophic samples over the last 1500 years suggests that dust comes from a single source. The dust source could also be local in origin since, for example, moraine are highly heterogeneous in nature and hence, could have a highly variable εNd signature. The return to more negative εNd values (-19 to -27) in the most recent samples suggests that local sources have contributed to the dust supply onto the LG2 bog over the last 25 years. This can be explained by the recent anthropogenic activities in the region. The James Bay road (800 m from the coring site) and a series of hydro-power dams were built in the region during late 1970's and 1980's, which most likely released large amounts of dust in the atmosphere locally.

3.4.3 Paleoecological succession

Macrofossil analyses reveal that the LG2 core was dominated by minerotrophic conditions before 4400 cal a BP. Herbaceae, brown mosses (*Scorpidium scorpioides* and *Calliergon giganteum*), *Sphagnum teres* and *Myrica gale*, all species indicative of minerotrophic conditions, dominate the assemblages in zone 1, while *Sphagnum fuscum* appears in the assemblages from 4400-2700 cal a BP (zone 2; Fig. 3.4). The timing of the fen to bog transition is more recent than another core collected on the same peatland (5500 cal a BP; Beaulieu-Audy *et al.*, 2009). The dominance of *Archerella flavum* and *Sphagnum fuscum* throughout zone 2, suggests stable and less humid conditions than in the previous zone, although conditions remain rather humid as shown by the WTD (Fig 3.4). Zone 3 (2700-1470 cal a BP) is characterized by unstable hydroclimatic conditions as shown by the frequent changes in WTD and testate amoeba assemblages. The high presence of *Hyalosphenia subflava* and *Arcella discoides* in zone 4 (1470-1175 cal a BP) along with the replacement of *S. fuscum* by Herbaceae reveals an important hydroclimatic change on the site. In fossil assemblages,

A. discoides is often found with dry-indicating species such as *H. subflava* and associated with periods of high decadal to centennial hydroclimate variability (Magnan and Garneau, 2014; Sullivan and Booth, 2011). The climatic instability is further evidenced by the composition of zone 5 and 6. Zone 5 (1125-475 cal a BP) shows a return of *S. fuscum* dominance along with *Difflugia pristis*. Zone 6 (475 cal a BP-1932AD) is dominated by similar assemblages as zone 4, which suggests similar condition as those reconstructed between 1600 and 1000 cal a BP, although Herbaceae are less present. Finally, zone 8 corresponds roughly to the acrotelm, where a greater diversity of testate amoebae species is found. The high presence of *Nebela militaris* suggests contemporaneous "dry" climatic conditions (WTD: 15 to 25 cm of depth).

3.4.4 Comparison of the LG2 record with documented climatic periods in NE Canada

The main trends in dust deposition and paleo-hydrology in LG2 core correspond with documented climatic periods in NE Canada and over the northern hemisphere. An increase in the dust flux reaching 1.8 g m^{-2} a^{-1} is found between 4000 and 3300 cal a BP, while the macrofossil and testate amoeba assemblages indicate rather stable conditions in terms of humidity (Fig. 3.4 and 3.7b). Many climatic studies have documented a cooler climate starting between 4000 and 3000 cal a BP. Viau *et al.* (2002) reported a widespread cooling throughout North America (Neoglacial cooling) starting around 4000 cal a BP in response to decreasing solar insolation (Kutzbach, 1981). Several short periods of increased dune activity are reported a 100 km north of our study region (Fig. 3.7; Filion, 1984). Regional increases in lake level suggests that this period may have been characterized by humid climatic conditions (Miousse, Bhiry and Lavoie, 2003; Payette and Filion, 1993). However, proxies do not agree as whether this cooling period was dry or humid.

Between 2600 and 2000 cal a BP, the dust flux increases to reach values greater than 2 g m^{-2} a^{-1} at 2300 cal a BP (Fig. 3.7a). Low water table depths are reconstructed at the

start of the period (2600 cal a BP), while higher WTD are recorded at the end. In other peatlands of the James Bay region, dry surface conditions were recorded after 3000 cal a BP (van Bellen, Garneau and Booth, 2011). Van Bellen, Garneau and Booth (2011) recorded unstable hydroclimatic conditions over the last 3000 years when compared to the mid-Holocene (7000-4000 cal a BP). This is in agreement with the LG2 record which shows greater variability in the testate amoebae and macrofossil assemblages as well as dust fluxes over the last 4000 years. Glacier advances were identified worldwide between 3000 and 2300 cal a BP (Grove; 2004). The recorded dust peak occurred at the end of a cold period according to Wanner *et al.* (2011) and is found at the transition to a warm period commonly known as the Roman Warm Period (RWP; Viau and Gajewski, 2009; Wang, Surge and Walker, 2013). Viau and Gajewski (2009) reconstructed warmer January temperatures in northern Quebec (Fig. 3.7e). Hence, this period represents a transition in the climatic conditions from a cold to a warmer period.

Between 1600 and 1000 cal a BP (Fig. 3.7a), the dust flux displays high values (average: 1.62 g m^{-2} a^{-1}) at the same time as a change in the testate amoebae and macrofossil assemblages (Fig. 3.4). Dry shifts were observed in other peatlands of the region between 1400 and 1000 cal a BP (Loisel and Garneau, 2010; van Bellen, Garneau and Booth, 2011) and an increase in dust deposition was also recorded in a peat bog from the North Shore of the St. Lawrence Estuary over the same period (1750 to 1000 cal a BP; Chapter 1). This period corresponds to an increase in sand dunes activity, fire events (Filion *et al.*, 1991) and more frequent low lake levels (Payette and Filion, 1993) in northern Quebec. A cold period centered around 1550 cal a BP was identified in climatic records world-wide (Fig. 3.7; Wanner *et al.*, 2011). The Vandal solar minimum also occurred during this time frame. Altogether, these changes point to a climatic deterioration with cold and dry conditions.

While an increase in dust deposition is not visible during most of the Little Ice Age (LIA) at LG2, a small increase in dust flux (1.0 g m^{-2} a^{-1}) is registered between 800 and

650 cal a BP (Fig. 3.7a). A WTD drawdown expressed by a dominance of *Hyalosphenia subflava* and a presence of *Arcella discoides* is observed. The macrofossil assemblages show an increase in the amount of Herbaceae remnants (Fig 3.4). A dry shift was recorded during this period in the region (Loisel and Garneau, 2010; van Bellen, Garneau and Booth, 2011), while an increase in dune activity has been reported further north during the LIA (Filion, 1984). The timing of the dust peak also corresponds with the Wolfe solar minimum and the start of a cold event covering the LIA (Wanner *et al.*, 2011). In Quebec, permafrost aggradation have been reported around 800 and 450-400 cal a BP (Bhiry and Robert, 2006). Although the dust flux shows only a small peak, the observations for this period indicate that the climatic conditions were most likely cold and dry. The very low peat accumulation rates during this period (0.2 mm a^{-1}) associated with short growing seasons prevented the incorporation of the dust signal.

3.4.5 Paleoclimatic interpretation of the LG2 dust records

The main dust deposition and paleohydrological trends and linkages with documented mid- to late Holocene climate changes suggest a climatic control on the dust cycle in the region. The agreement between the dust flux and the paleohydrological and paleoenvironmental proxies (testate amoebae and macrofossils) as well as the documented climate changes confirms the increase in dust deposition during cold periods. Furthermore, the majority of the studies recorded dry climatic conditions during those periods (Filion, 1984; Filion *et al.*, 1991; Loisel and Garneau, 2010; van Bellen, Garneau and Booth, 2011).

In north-eastern Canada, climatic cooling is usually associated with the incursion of dry Arctic air masses (Carcaillet and Richard, 2000; Girardin *et al.*, 2004). Such incursion of dry and cold air masses reduces snow cover and results in more particles available for deflation through a greater exposition of the surfaces. Snow cover also

influences bog surface wetness (BSW) by controlling frost penetration through the peat layers and constitutes an important water supply in spring. Such influence of reduced snow cover are evidenced by important palsa formation between 1500 and 1000 cal a BP and during the LIA a hundred kilometers north of the region (Asselin and Payette, 2006; Couillard and Payette, 1985) and permafrost aggradation in the region (Thibault and Payette, 2009).

In LG2, the co-dominance of *Hyalosphenia subflava* (dry optima) and *Arcella discoides* (wet optima) between 1600 and 1000 cal a BP as well as during the LIA, suggests high seasonal to annual hydrological variability (Magnan and Garneau, 2014; Sullivan and Booth, 2011; van Bellen, Garneau and Booth, 2011). The occurrence of dust peaks during periods of increased hydroclimatic instability is documented on the North Shore of the St. Lawrence Estuary (Chapter 1; Pratte, Garneau and De Vleeschouwer, In press) as well as in Belgium (De Vleeschouwer *et al.*, 2012), Poland (De Vleeschouwer *et al.*, 2009) and South Sweden (de Jong, Schoning and Björck, 2007). The occurrence some dust peaks during solar minima (1000-1600 and 800-650 cal a BP) suggests that insolation may also be a controlling factor of the climate variability in the region.

While the fact that the source of the dust deposited over the last 4000 years (Fig. 3.7a) cannot be precisely identified prevents the determination of the prevailing wind direction, some information can still be extracted. The stable εNd signature suggests that no important change in the atmospheric circulation over the region has occurred during this period. However, when looking at the grain-size distribution (Fig. 3.7f), a period of stability is notable until *ca.* 2800 cal a BP. Afterwards, the grain-size distribution displays greater variability. Such a change in grain-size distribution can either be explained by changes in dust source or wind intensity. Since the εNd and REE/Ti values (Fig 3.3 and 3.7a) are rather stable in this portion of the core, the latter explanation is the most probable. No clear pattern is visible in the timing of the changes in particle grain size. Certain peaks in grain size occur at the same time as periods of increased dust deposition (1600-1000 cal a BP), while others are found during periods

of low dust deposition (2600-2000 cal a BP). Further investigation, for example through mineralogical analyses, is needed to better understand the controlling factor underneath these variations in dust deposition.

3.5 Conclusion

Elemental concentrations in a 4.1 m long peat section from the LG2 bog, in the James Bay lowlands (north-eastern Canada), allow for the reconstruction of variations in dust deposition over the late Holocene. Testate amoebae have been used to reconstruct past local hydrological conditions, while plant macrofossils were analysed to establish past vegetation succession. A principal component analysis showed that REE display the same behavior as other conservative lithogenic elements in the peat column (Ti, Al, Zr), hence they can be used to reconstruct mineral dust deposition. Several periods of increased dust deposition were identified: from 4000-3300 cal a BP, 2600-2000 cal a BP, 1600-1000 cal a BP, 800-650 cal a BP and 1960-1990AD. The increase in dust deposition between 1960 and 1990AD is linked to human activities. The development of a series of hydropower dams in the region in the 1970s likely modified the atmospheric dust load in the region. The εNd values show a large variability from -37 to -12, identifying a least three sources: local marine sediments, the Sakami moraine and another unidentified source likely from a more regional origin. After 4000 cal a BP, the contribution of local (marine sediments, Sakami moraine) dust particles decreases in favor of another source. The εNd and REE/Ti signatures remain stable from 1500 cal ry BP until 1975AD, which suggest that a single source contribute to the dust signal. From 1975AD, human activities release local dust with more negative signatures in the atmosphere. The occurrence of most dust events with documented cold periods and dry/instable events reconstructed from the testate amoebae and macrofossil assemblages suggest a link with intrusions of arctic air masses.

Aknowledgements

We are grateful to Gaël Le Roux (Ecolab, Toulouse), David Baqué (Ecolab, Toulouse), Aurélie Lanzanova (*Geoscience Environnement Toulouse*), André Poirier (GEOTOP, Montreal, Canada) and Bassam Ghaleb (GEOTOP) for their help with major and trace elements analyses, Nd isotopes and ^{210}Pb dating. Thanks to Gabriel Magnan and Antoine Thibault for help during fieldwork as well as Julien Gogot, Joannie Beaulne and Marie-Josée Tavella for lab assistance. Thanks to *Les Tourbeux* for fruitful discussions. Financial support was provided by Natural Sciences and Engineering Research Council of Canada (NSERC; #250287) discovery grant to MG. Scholarships to SP were provided by the Fonds de Recherche Québec – Nature et Technologie (FRQNT; #176250 and #180723). A grant was also provided by the Northern Scientific Training Program (NSTP) to SP. An additional mobility grant (*Soutien à la mobilité*) was provided by *Institut National Polytechnique de Toulouse* to FDV and SP.

3.6 References

Aaby, B. (1976). Cyclic climatic variations in climate over the past 5,500 yr reflected in raised bogs. *Nature,* 263(5575), 281-284.

Allan, M., Le Roux, G., Piotrowska, N., Beghin, J., Javaux, E., Court-Picon, M., Mattielli, N., Verheyden, S. and Fagel, N. (2013). Mid and late Holocene dust deposition in western Europe: the Misten peat bog (Hautes Fagnes - Belgium). *Climate of the Past Discussion,* 9(3), 2889-2928.

Appleby, P.G. (2002). Chronostratigraphic techniques in recent sediments. In: Last, W. and J. Smol (dir.), *Tracking Environmental Change Using Lake Sediments* (Vol. 1, p. 171-203): Springer Netherlands.

Asselin, H. and Payette, S. (2006). Origin and long-term dynamics of a subarctic tree line. *Ecoscience,* 13(2), 135-142.

Aubert, D., Le Roux, G., Krachler, M., Cheburkin, A., Kober, B., Shotyk, W. and Stille, P. (2006). Origin and fluxes of atmospheric REE entering an ombrotrophic peat bog in Black Forest (SW Germany): Evidence from snow, lichens and mosses. *Geochimica et Cosmochimica Acta,* 70(11), 2815-2826.

Barber, K.E. (1993). Peatlands as scientific archives of past biodiversity. *Biodiversity & Conservation,* 2(5), 474-489.

Barber, K.E., Chambers, F.M. and Maddy, D. (2003). Holocene palaeoclimates from peat stratigraphy: macrofossil proxy climate records from three oceanic raised bogs in England and Ireland. *Quaternary Science Reviews,* 22(5–7), 521-539.

Barber, K.E. and Langdon, P.G. (2007). What drives the peat-based palaeoclimate record? A critical test using multi-proxy climate records from northern Britain. *Quaternary Science Reviews,* 26(25–28), 3318-3327.

Beaulieu-Audy, V., Garneau, M., Richard, P.J.H. and Asnong, H. (2009). Holocene palaeoecological reconstruction of three boreal peatlands in the La Grande Rivière region, Québec, Canada. *The Holocene,* 19(3), 459-476.

Bhiry, N. and Robert, É.C. (2006). Reconstruction of changes in vegetation and trophic conditions of a palsa in a permafrost peatland, subarctic Québec, Canada. *Ecoscience,* 13(1), 56-65.

Biscaye, P.E., Grousset, F.E., Revel, M., Van der Gaast, S., Zielinski, G.A., Vaars, A. and Kukla, G. (1997). Asian provenance of glacial dust (stage 2) in the Greenland Ice Sheet Project 2 Ice Core, Summit, Greenland. *Journal of Geophysical Research: Oceans,* 102(C12), 26765-26781.

Blaauw, M. and Christen, J.A. (2011). Flexible paleoclimate age-depth models using an autoregressive gamma process. *Bayesian Analysis,* 6, 457-474.

Booth, R. and Sullivan, M. (2007). *Key of testate amoebae inhabiting Sphagnum-dominated peatlands with an emphasis on taxa preserved in Holocene sediments*. Earth and Environmental Science Department, Lehigh University, Bethlehem, PA.

Booth, R.K. (2002). Testate amoebae as paleoindicators of surface-moisture changes on Michigan peatlands: modern ecology and hydrological calibration. *Journal of Paleolimnology,* 28(3), 329-348.

Carcaillet, C. and Richard, P.J.H. (2000). Holocene changes in seasonal precipitation highlighted by fire incidence in eastern Canada. *Climate Dynamics,* 16(7), 549-559.

Caseldine, C.J., Baker, A., Charman, D.J. and Hendon, D. (2000). A comparative study of optical properties of NaOH peat extracts: implications for humification studies. *The Holocene,* 10(5), 649-658.

Chambers, F.M. and Charman, D.J. (2004). Holocene environmental change: contributions from the peatland archive. *The Holocene,* 14(1), 1-6.

Chambers, F.M., Beilman, D.W. and Yu, Z.C. (2011). Methods for determining peat humification and for quantifying peat bulk density, organic matter and carbon content for palaeostudies of climate and peatland carbon dynamics. *Mires and Peat,* 7.

Charman, D.J., Hendon, D. and Woodland, W.A. (2000). *The identification of testate amoebae (Protozoa: Rhizopoda) in peats*. London: Quaternary Research Association.

Charman, D.J. (2001). Biostratigraphic and palaeoenvironmental applications of testate amoebae. *Quaternary Science Reviews,* 20(16–17), 1753-1764.

Charman, D.J., Brown, A.D., Hendon, D. and Karofeld, E. (2004). Testing the relationship between Holocene peatland palaeoclimate reconstructions and instrumental data at two European sites. *Quaternary Science Reviews,* 23(1–2), 137-143.

Charman, D.J., Barber, K.E., Blaauw, M., Langdon, P.G., Mauquoy, D., Daley, T.J., Hughes, P.D.M. and Karofeld, E. (2009). Climate drivers for peatland palaeoclimate records. *Quaternary Science Reviews,* 28(19–20), 1811-1819.

Couillard, L. and Payette, S. (1985). Évolution holocène d'une tourbière à pergélisol (Québec nordique). *Canadian Journal of Botany,* 63(6), 1104-1121.

Crum, H.A. and Anderson L.E. (1979–1980). *Mosses of Eastern North America*. New York: Columbia University Press.

de Jong, R., Schoning, K. and Björck, S. (2007). Increased aeolian activity during humidity shifts as recorded in a raised bog in south-west Sweden during the past 1700 years. *Climate of the Past,* 3(3), 411-422.

de Jong, R., Blaauw, M., Chambers, F., Christensen, T., De Vleeschouwer, F., Finsinger, W., Fronzek, S., Johansson, M., Kokfelt, U., Lamentowicz, M., Roux, G., Mauquoy, D., Mitchell, E.D., Nichols, J., Samaritani, E. and van Geel, B. (2010). Climate and Peatlands. Dans Dodson, J. (dir.), *Changing Climates, Earth Systems and Society* (p. 85-121): Springer Netherlands.

De Vleeschouwer, F., Piotrowska, N., Sikorski, J., Pawlyta, J., Cheburkin, A., Le Roux, G., Lamentowicz, M., Fagel, N. and Mauquoy, D. (2009). Multiproxy evidence of `Little Ice Age' palaeoenvironmental changes in a peat bog from northern Poland. *The Holocene,* 19(4), 625-637.

De Vleeschouwer, F., Chambers, F.M. and Swindles, G.T. (2010). Coring and subsampling of peatlands for palaeoenvironmental research. *Mires and Peat,* 7.

De Vleeschouwer, F., Pazdur, A., Luthers, C., Streel, M., Mauquoy, D., Wastiaux, C., Le Roux, G., Moschen, R., Blaauw, M., Pawlyta, J., Sikorski, J. and Piotrowska, N. (2012). A millennial record of environmental change in peat deposits from the Misten bog (East Belgium). *Quaternary International,* 268(0), 44-57.

deMenocal, P., Ortiz, J., Guilderson, T., Adkins, J., Sarnthein, M., Baker, L. and Yarusinsky, M. (2000). Abrupt onset and termination of the African Humid Period: rapid climate responses to gradual insolation forcing. *Quaternary Science Reviews,* 19(1–5), 347-361.

DePaolo, D.J. and Wasserburg, G.J. (1976). Nd isotopic variations and petrogenetic models. *Geophysical Research Letters,* 3(5), 249-252.

Donahue, D.J., Linick, T.W. and Jull, A.J.T. (1990). Isotope-Ratio and background corrections for accelerator mass spectrometry radiocarbon measuments. *Radiocarbon,* 32, 135-142.

Dyke, A.S. and Prest, V.K. (1987). Late Wisconsinan and Holocene history of the Laurentide ice sheet. *Géographie physique et Quaternaire,* 41(2), 237-263.

Eriksson, L., Johansson, E., Kettapeh-Wold, S. and Wold, S. (1999). *Introduction to multi-and megavariate data analysis using projection methods (PCA & PLS).* Umeå: Umetrics AB.

Environment Canada (2010). Canadian Climate Normals 1981-2010. Retrieved 27 October 2015 from http://climate.weather.gc.ca/climate_normals/.

Filion, L. (1984). A relationship between dunes, fire and climate recorded in the Holocene deposits of Quebec. *Nature,* 309(5968), 543-546.

Filion, L., Saint-Laurent, D., Desponts, M. and Payette, S. (1991). The late Holocene record of aeolian and fire activity in northern Québec, Canada. *The Holocene,* 1(3), 201-208.

Fischer, H., Siggaard-Andersen, M.-L., Ruth, U., Röthlisberger, R. and Wolff, E. (2007). Glacial/interglacial changes in mineral dust and sea-salt records in polar ice cores: Sources, transport, and deposition. *Reviews of Geophysics,* 45(1).

Garneau, M. (1995). *Collection de référence de graines et autres macrofossiles végétaux de taxons provenant du Québec méridional et boréal et de l'Arctique canadien.* Open File 3048. Geological Survey of Canada, Division de la science des terrains.

Girardin, M.P., Tardif, J., Flannigan, M.D. and Bergeron, Y. (2004). Multicentury reconstruction of the Canadian Drought Code from eastern Canada and its relationship with paleoclimatic indices of atmospheric circulation. *Climate Dynamics,* 23(2), 99-115.

Givelet, N., Roos-Barraclough, F. and Shotyk, W. (2003). Predominant anthropogenic sources and rates of atmospheric mercury accumulation in southern Ontario recorded by peat cores from three bogs: comparison with natural "background" values (past 8000 years). *Journal of Environmental Monitoring,* 5(6), 935-949.

Givelet, N., Le Roux, G., Cheburkin, A., Chen, B., Frank, J., Goodsite, M.E., Kempter, H., Krachler, M., Noernberg, T., Rausch, N., Rheinberger, S., Roos-Barraclough, F., Sapkota, A., Scholz, C. and Shotyk, W. (2004). Suggested protocol for collecting, handling and preparing peat cores and peat samples for physical, chemical, mineralogical and isotopic analyses. *Journal of Environmental Monitoring,* 6(5), 481-492.

Goudie, A.S. and Middleton, N.J. (2001). Saharan dust storms: nature and consequences. *Earth-Science Reviews,* 56(1–4), 179-204.

Grove, J. (2004). *Little Ice Ages: Ancient and Modern*. Routledge, New York.

Hansson, S.V., Rydberg, J., Kylander, M., Gallagher, K. and Bindler, R. (2013). Evaluating paleoproxies for peat decomposition and their relationship to peat geochemistry. *The Holocene,* 23(12), 1666-1671.

Harrison, S.P., Kohfeld, K.E., Roelandt, C. and Claquin, T. (2001). The role of dust in climate changes today, at the last glacial maximum and in the future. *Earth-Science Reviews,* 54(1–3), 43-80.

Hillaire-Marcel, C. (1976). La déglaciation et le relèvement isostatique sur la côte est de la Baie d'Hudson. *Cahiers de Géographie du Québec,* 20(50), 185-220.

Hillaire-Marcel, C., Occhietti, S. and Vincent, J.-S. (1981). Sakami moraine, Québec: a 500 km-long moraine without climatic control. *Geology* 9, 210–214.

Ireland, R.R. 1982. *Moss Flora of the Maritime Provinces*. National Museums of Canada: Ottawa.

Jacobsen, S.B. and Wasserburg, G.J. (1980). Sm-Nd isotopic evolution of chondrites. *Earth and Planetary Science Letters,* 50(1), 139-155.

Jeglum, J.K., Rothwell, R.L., Berry, G.J. and Smith, G.K.M. (1992). A peat sampler for rapid survey. *Technical Note, Canadian Forestry Service,* 13, 921-932.

Jolliffe, I.T. (2002). *Principal Component Analysis*. Springer, New York.

Jowsey, P.C. (1966). An improved peat sampler. *New Phytologist,* 65(2), 245-248.

Kohfeld, K.E. and Harrison, S.P. (2001). DIRTMAP: the geological record of dust. *Earth-Science Reviews,* 54(1–3), 81-114.

Krachler, M., Mohl, C., Emons, H. and Shotyk, W. (2003). Two thousand years of atmospheric rare earth element (REE) deposition as revealed by an ombrotrophic peat bog profile, Jura Mountains, Switzerland. *Journal of Environmental Monitoring,* 5(1), 111-121.

Kutzbach, J.E. (1981). Monsoon climate of the early Holocene: climate experiment with the Earth's orbital parameters for 9000 years ago. *Science,* 214(4516), 59-61.

Lajeunesse, P. (2008). Early Holocene deglaciation of the eastern coast of Hudson Bay. *Geomorphology* 99, 341-352.

Lamarre, A., Magnan, G., Garneau, M. and Boucher, É. (2013). A testate amoeba-based transfer function for paleohydrological reconstruction from boreal and subarctic peatlands in northeastern Canada. *Quaternary International,* 306, 88-96.

Laterreur, N. (2008). *Structuration relationnelle et intégration de données multi-sources caractérisant les bassins tourbeux de la région de la rivière La Grande (Baie James)*. M.Sc. Thesis. Department of Geography, Montreal: Université du Québec à Montréal.

Le Roux, G. and De Vleeschouwer, F. (2010). Preparation of peat samples for inorganic geochemistry used as palaeoenvironmental proxies. *Mires and Peat,* 7.

Le Roux, G. and Marshall, W.A. (2011). Constructing recent peat accumulation chronologies using atmospheric fall-out radionuclides. *Mires and Peat,* 7.

Le Roux, G., Fagel, N., De Vleeschouwer, F., Krachler, M., Debaille, V., Stille, P., Mattielli, N., van der Knaap, W.O., van Leeuwen, J.F.N. and Shotyk, W. (2012). Volcano- and climate-driven changes in atmospheric dust sources and fluxes since the Late Glacial in Central Europe. *Geology,* 40(4), 335-338.

Loisel, J. and Garneau, M. (2010). Late Holocene paleoecohydrology and carbon accumulation estimates from two boreal peat bogs in eastern Canada: Potential and limits of multi-proxy archives. *Palaeogeography, Palaeoclimatology, Palaeoecology,* 291(3–4), 493-533.

Magnan, G. and Garneau, M. (2014). Evaluating long-term regional climate variability in the maritime region of the St. Lawrence North Shore (eastern Canada) using a multi-site comparison of peat-based paleohydrological records. *Journal of Quaternary Science,* 29(3), 209-220.

Marie-Victorin, F. (1995). *Flore laurentienne, Third Edition*. Montreal: Les Presses de l'Université de Montréal.

Marx, S.K., McGowan, H.A. and Kamber, B.S. (2009). Long-range dust transport from eastern Australia: A proxy for Holocene aridity and ENSO-type climate variability. *Earth and Planetary Science Letters,* 282(1–4), 167-177.

Martini P. and Martinez-Cortizas A. (eds) (2006). *Peatlands - Evolution and Records of Environmental and Climate Changes*. Developments in Earth Surface Processes. Vol. 9. Elsevier. 606pp.

Mason, J.A., Miao, X., Hanson, P.R., Johnson, W.C., Jacobs, P.M. and Goble, R.J. (2008). Loess record of the Pleistocene–Holocene transition on the northern and central Great Plains, USA. *Quaternary Science Reviews,* 27(17–18), 1772-1783.

Mauquoy, D., van Geel, B., Blaauw, M., Speranza, A. and van der Plicht, J. (2004). Changes in solar activity and Holocene climatic shifts derived from ^{14}C wiggle-match dated peat deposits. *The Holocene,* 14(1), 45-52.

Mauquoy, D. and van Geel, B. (2007).| Mire and peat macros. In: Elias, S. A. (dir.), *Encyclopedia of Quaternary Science*. Oxford: Elsevier, 2315-2336.

Miao, X., Mason, J.A., Swinehart, J.B., Loope, D.B., Hanson, P.R., Goble, R.J. and Liu, X. (2007). A 10,000 year record of dune activity, dust storms, and severe drought in the central Great Plains. *Geology,* 35(2), 119-122.

Miousse, L., Bhiry, N. and Lavoie, M. (2003). Isolation and water-level fluctuations of Lake Kachishayoot, Northern Québec, Canada. *Quaternary Research,* 60(2), 149-161.

Mischke, S., Zhang, C., Börner, A. and Herzschuh, U. (2010). Late Glacial and Holocene variation in aeolian sediment flux over the northeastern Tibetan Plateau recorded by laminated sediments of a saline meromictic lake. *Journal of Quaternary Science,* 25(2), 162-177.

Mitchell, E.D., Charman, D. and Warner, B. (2008). Testate amoebae analysis in ecological and paleoecological studies of wetlands: past, present and future. *Biodiversity and Conservation,* 17(9), 2115-2137.

Muhs, D.R. (2013). The geologic records of dust in the Quaternary. *Aeolian Research,* 9(0), 3-48.

Payette, S. and Filion, L. (1993). Holocene water-level fluctuations of a subarctic lake at the tree line in northern Québec. *Boreas,* 22(1), 7-14.

Piotrowska, N. (2013). Status report of AMS sample preparation laboratory at GADAM Centre, Gliwice, Poland. *Nuclear Instruments and Methods in Physics Research Section B: Beam Interactions with Materials and Atoms,* 294, 176-181.

Pratte, S., Garneau, M. and De Vleeschouwer, F. (In press). Late-Holocene atmospheric dust deposition in eastern Canada (St. Lawrence North Shore). *The Holocene.*

Pratte, S., Mucci, A. and Garneau, M. (2013). Historical records of atmospheric metal deposition along the St. Lawrence Valley (eastern Canada) based on peat bog cores. *Atmospheric Environment,* 79(0), 831-840.

Reimann, C., Filzmoser, P., Garret, R. and Dutter, R. (2008). *Statistical Data Analysis Explained: Applied Environmental Statistics with R.* John Wiley & Sons Ltd, Chichester.

Reimer, P.J., Bard, E., Bayliss, A., Beck, J.W., Blackwell, P.G., Bronk Ramsey, C., Buck, C.E., Cheng, H., Edwards, R.L., Friedrich, M., Grootes, P.M., Guilderson, T.P., Haflidason, H., Hajdas, I., Hatté, C., Heaton, T.J., Hoffmann, D.L., Hogg, A.G., Hughen, K.A., Kaiser, K.F., Kromer, B., Manning, S.W., Niu, M., Reimer, R.W., Richards, D.A., Scott, E.M., Southon, J.R., Staff, R.A., Turney, C.S.M. and van der Plicht, J. (2013). IntCal13 and Marine13 Radiocarbon Age Calibration Curves 0–50,000 Years cal BP. *Radiocarbon,* 55(4), 1869-1887.

Roos-Barraclough, F., Givelet, N., Cheburkin, A.K., Shotyk, W. and Norton, S.A. (2006). Use of Br and Se in peat to rconstruct the natural and anthropogenic fluxes of atmospheric Hg: A 10000-Year record from Caribou Bog, Maine. *Environmental Science & Technology,* 40(10), 3188-3194.

Shotyk, W. (1997). Atmospheric deposition and mass balance of major and trace elements in two oceanic peat profiles, northern Scotland and Shetland Islands. *Chemical Geology,* 138, 55-72.

Shotyk, W., Weiss, D., Kramers, J.D., R., F., Cheburkin, A., Gloor, M. and Reese, S. (2001). Geochemistry of the peat bog at Etang de la Gruère, Jura Mountains, Switzerland, and its record of atmospheric Pb and lithogenic trace metals (Sc,

Ti, Y, Zr, and REE) since 12,370 ^{14}C yr BP. *Geochimica et Cosmochimica Acta,* 65(14), 2337-2360.

Shotyk, W., Krachler, M., Martinez-Cortizas, A., Cheburkin, A.K. and Emons, H. (2002). A peat bog record of natural, pre-anthropogenic enrichments of trace elements in atmospheric aerosols since 12 370 ^{14}C yr BP, and their variation with Holocene climate change. *Earth and Planetary Science Letters,* 199(1-2), 21-37.

Shotyk, W. and Krachler, M. (2010). The isotopic evolution of atmospheric Pb in central Ontario since AD 1800, and its impacts on the soils, waters, and sediments of a forested watershed, Kawagama Lake. *Geochimica et Cosmochimica Acta,* 74(7), 1963-1981.

Steinmann, P. and Shotyk, W. (1997). Geochemistry, mineralogy, and geochemical mass balance on major elements in two peat bog profiles (Jura Mountains, Switzerland). *Chemical Geology,* 138(1–2), 25-53.

Sullivan, M.E. and Booth, R.K. (2011). The potential influence of short-term environmental variability on the composition of testate amoeba communities. *Environmental Microbiology,* 62, 80-93.

Tanaka, T., Togashi, S., Kamioka, H., Amakawa, H., Kagami, H., Hamamoto, T., Yuhara, M., Orihashi, Y., Yoneda, S., Shimizu, H., Kunimaru, T., Takahashi, K., Yanagi, T., Nakano, T., Fujimaki, H., Shinjo, R., Asahara, Y., Tanimizu, M. and Dragusanu, C. (2000). JNdi-1: a neodymium isotopic reference in consistency with LaJolla neodymium. *Chemical Geology,* 168(3–4), 279-281.

Thibault, S. and Payette, S. (2009). Recent permafrost degradation in bogs of the James Bay area, northern Quebec, Canada. *Permafrost and Periglacial Processes,* 20(4), 383-389.

van Bellen, S., Garneau, M. and Booth, R.K. (2011). Holocene carbon accumulation rates from three ombrotrophic peatlands in boreal Quebec, Canada: Impact of climate-driven ecohydrological change. *The Holocene,* 21(8), 1217-1231.

Vanneste, H., De Vleeschouwer, F., Martínez-Cortizas, A., von Scheffer, C., Piotrowska, N., Coronato, A. and Le Roux, G. (2015). Late-glacial elevated dust deposition linked to westerly wind shifts in southern South America. *Scientific Reports,* 5

Viau, A.E., Gajewski, K., Fines, P., Atkinson, D.E. and Sawada, M.C. (2002). Widespread evidence of 1500 yr climate variability in North America during the past 14000 yr. *Geology,* 30(5), 455-458.

Viau, A.E. and Gajewski, K. (2009). Reconstructing millennial-scale, regional paleoclimates of boreal Canada during the Holocene. *Journal of Climate,* 22(2), 316-330.

Wang, T., Surge, D. and Walker, K.J. (2013). Seasonal climate change across the Roman Warm Period/Vandal Minimum transition using isotope sclerochronology in archaeological shells and otoliths, southwest Florida, USA. *Quaternary International,* 308–309, 230-241.

Wanner, H., Solomina, O., Grosjean, M., Ritz, S.P. and Jetel, M. (2011). Structure and origin of Holocene cold events. *Quaternary Science Reviews,* 30(21–22), 3109-3123.

Weiss, D., Shotyk, W., Rieley, J., Page, S., Gloor, M., Reese, S. and Martinez-Cortizas, A. (2002). The geochemistry of major and selected trace elements in a forested peat bog, Kalimantan, SE Asia, and its implications for past atmospheric dust deposition. *Geochimica et Cosmochimica Acta,* 66(13), 2307-2323.

Zdanowicz, C.M., Zielinski, G.A., Wake, C.P., Fisher, D.A. and Koerner, R.M. (2000). A Holocene record of atmospheric dust deposition on the Penny Ice Cap, Baffin Island, Canada. *Quaternary Research,* 53(1), 62-69.

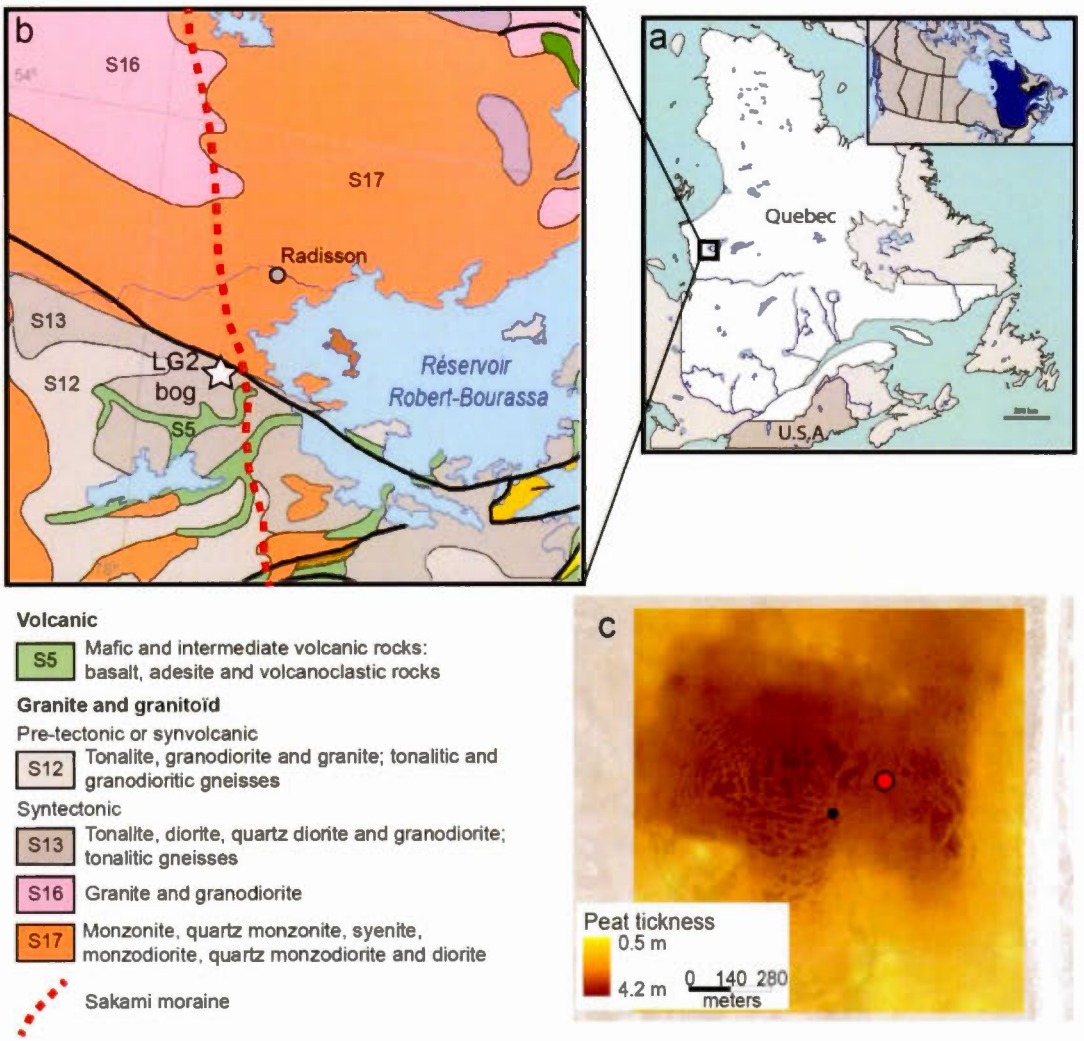

Figure 3.1 (a) Location of the La Grande region in Quebec, (b) Main geological units in the study region and location of the LG2 peatland (star) and (c) map of the LG2 peat bog modified from Laterreur (2008). Colors indicate peat thickness. The red dot shows the location of LG2 core, while the black dot corresponds to the location of another core studied by Beaulieu-Audy *et al.* (2009).

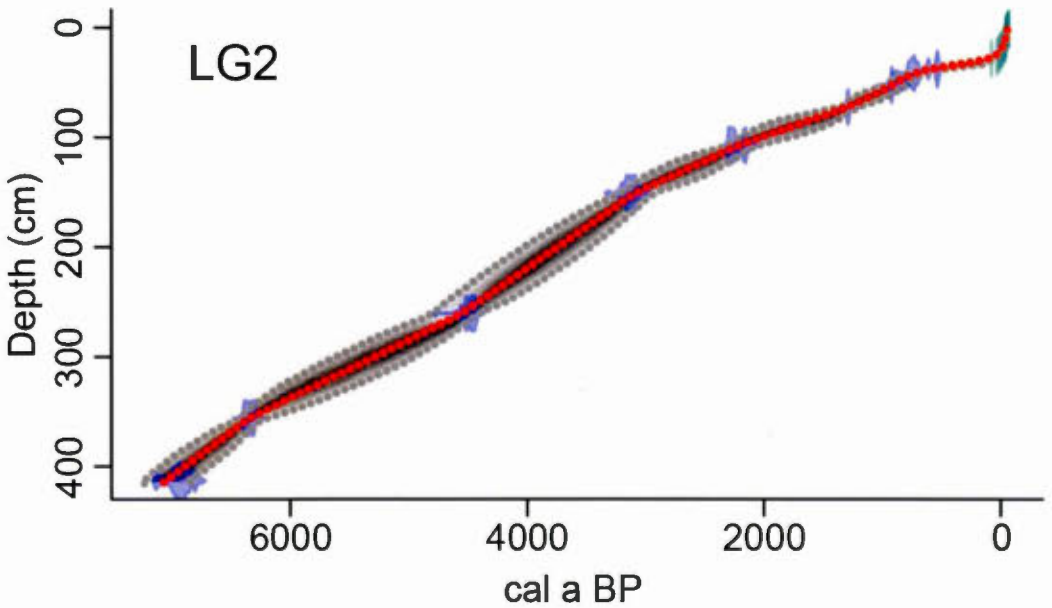

Figure 3.2 Age-depth models for LG2 core. The gray bands encompass all possible age-depth models whereas the dotted lines represent the 95% confidence intervals. Blue symbols indicate calendar age distribution of ^{14}C dates and light blue symbols show ^{210}Pb ages derived from the CRS model. The red dotted line represents the weighted mean age of the model.

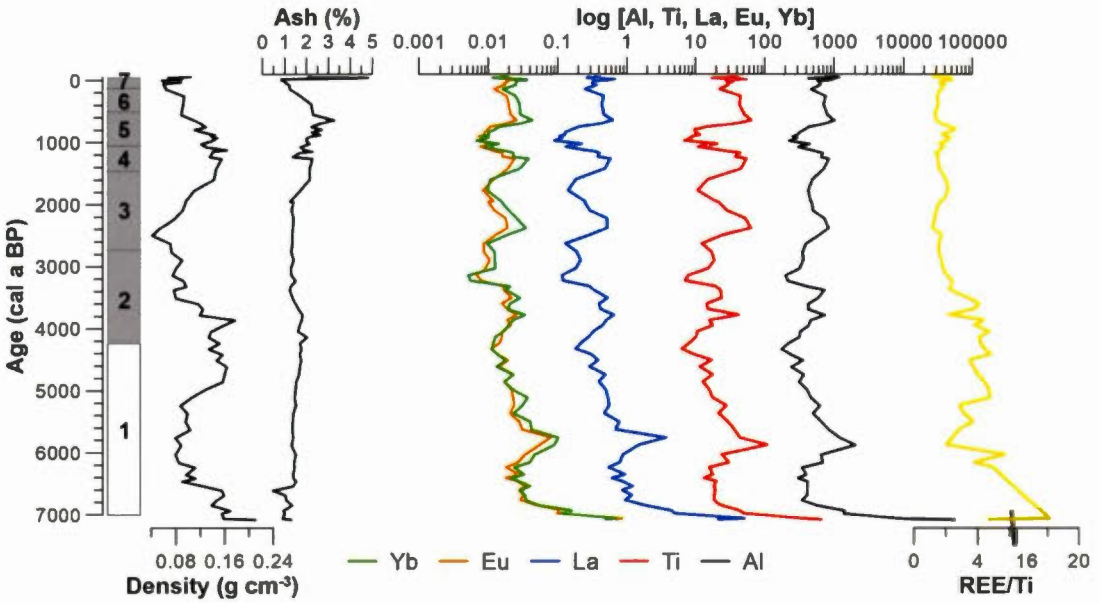

Figure 3.3 Bulk density, ash, log10 of Al, Ti, La, Eu and Yb concentrations and REE/Ti vs. age. The numbered boxes (1-8) correspond to zones identified in Fig. 3.4.

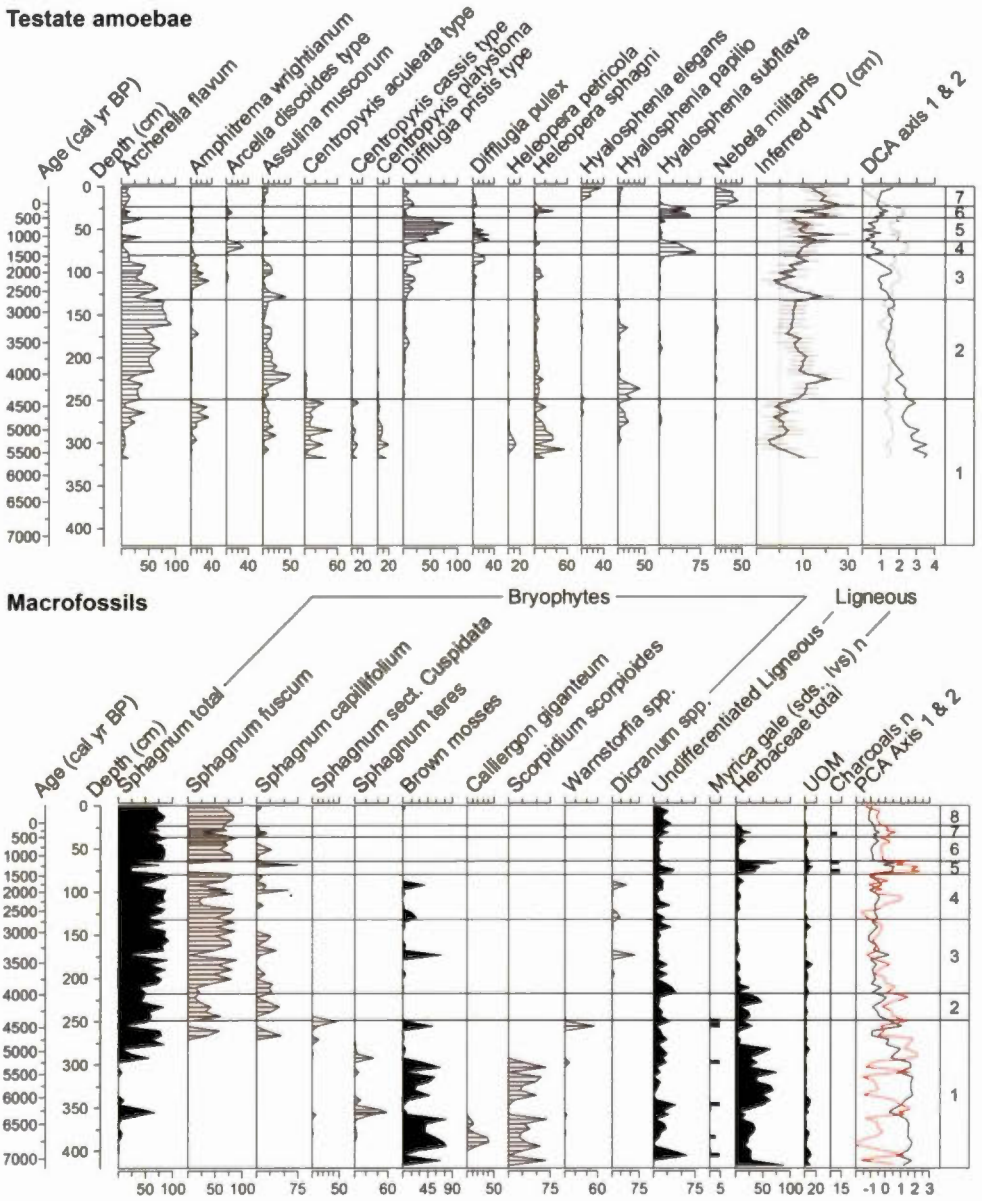

Figure 3.4 Top: summary of testate amoebae, inferred water table depths (WTD) and DCA axis 1 (black) and 2 (grey). Bottom: plant macrofossil records and PCA axis 1 (black) and 2 (red) scores for LG2 core. Testate amoebae are expressed as percentage values of the total counts. Plant macrofossils are expressed as volume percentages and counts (n).

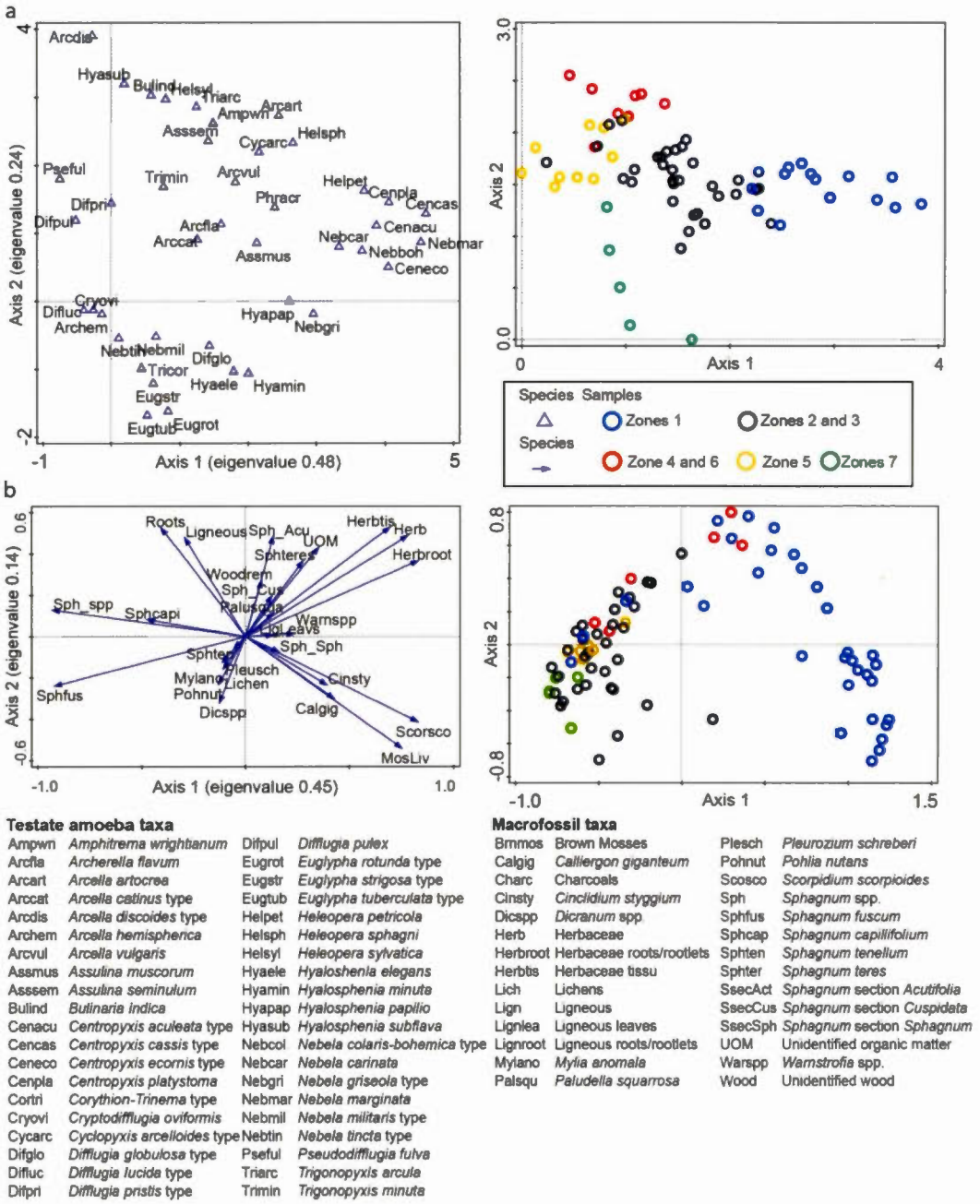

Figure 3.5 DCA ordination of the testate amoebae dataset (a) and PCA ordination of the macrofossil dataset (b): species (left) and samples (right).

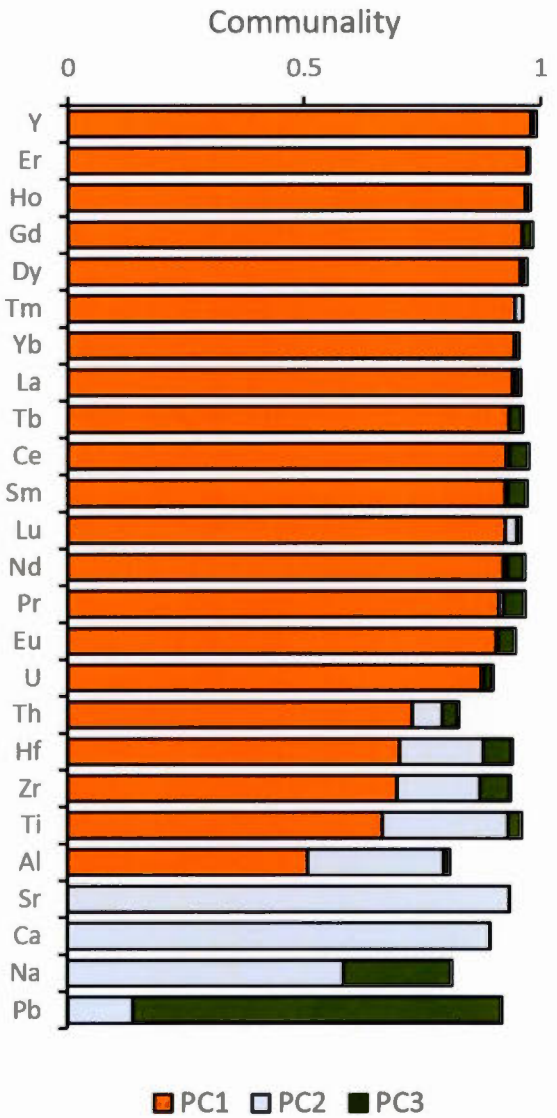

Figure 3.6 Plot of the importance of each principal component in explaining the variance of the elements of interest (the communality corresponds to the total variance of an element explained by the extracted components).

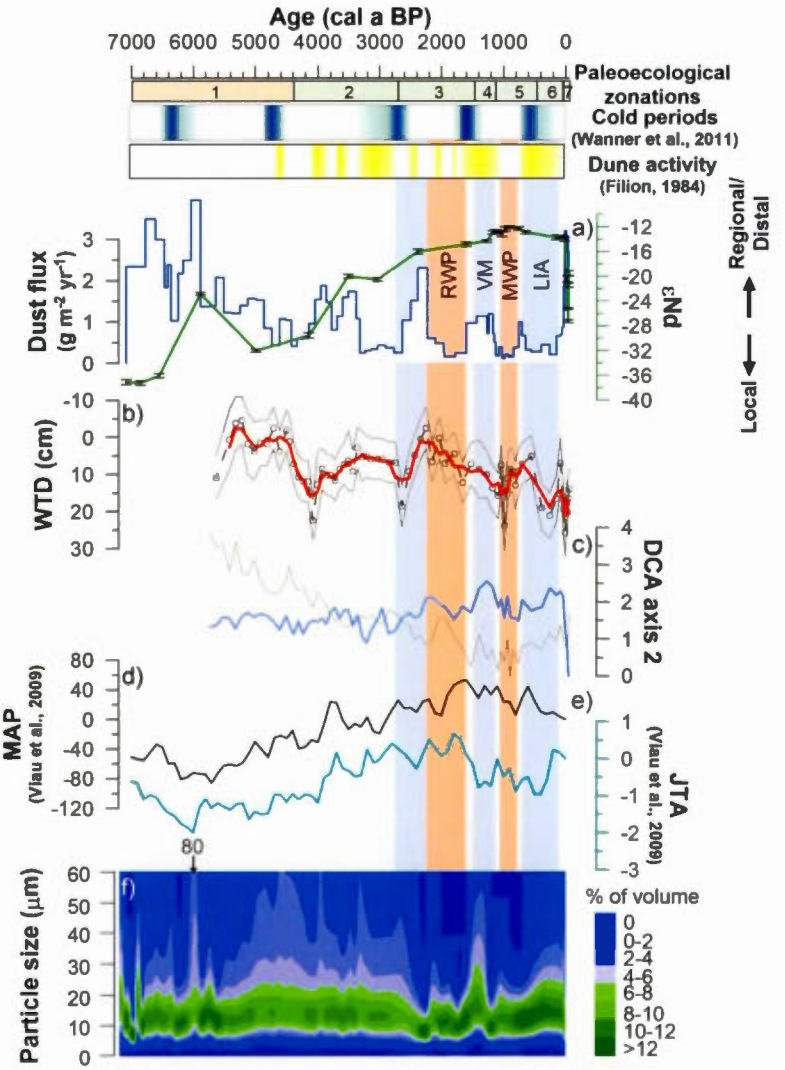

Figure 3.7 a) Dust flux from REE elements (blue) and εNd values (green); b) water table depth reconstruction (WTD; dashed line), three point running mean of WTD (red line); c) testate amoebae DCA axis 1 (grey line) and 2 (pale blue line) from LG2 core; d) mean annual precipitations anomaly (MAP) and e) January temperature anomaly (JTA) for northern Quebec (Viau et al., 2009); f) Grain-size distribution from LG2 core. LIA: Little Ice Age; MWP: Medieval Warm Period; VM: Vandal Minimum; RWP: Roman Warm Period. Cold periods from (Wanner *et al.*, 2011); Periods of aeolian activity (Filion, 1984).

Table 3.1 Results of ^{210}Pb measurements and CRS modelling for the LG2 core

Sample	Depth (cm)	^{210}Pb Activity (Bq kg^{-1})	$^{210}Pb_{ex}$ activity (Bq kg^{-1})	CRS ^{210}Pb age (AD)	Age (cal a BP)	Uncertainty (a)
LG2 2	1.7	606	593	2009	-59	0.2
LG2 3	2.9	815	802	2002	-52	0.5
LG2 4	4.1	731	718	1996	-46	0.7
LG2 6	6.5	767	754	1989	-39	1.1
LG2 8	8.9	189	176	1987	-37	1.3
LG2 10	11.3	118	105	1986	-36	1.4
LG2 12	13.8	333	320	1982	-32	1.5
LG2 14	16.2	499	486	1972	-22	1.9
LG2 16	18.8	416	403	1960	-10	2.6
LG2 18	21.3	291	278	1944	6	3.2
LG2 20	23.8	160	147	1932	18	4
LG2 22	26.2	116	104	1914	36	5
LG2 24	28.5	115	103	1867	83	7.5
LG2 26	30.9	51	38			
LG2 28	33.3	13	0			

Table 3.2 Results of ^{14}C AMS measurements, calibration and description of samples for the LG2 core.

Sample	Depth (cm)	Laboratory number	^{14}C age (BP)	2σ range (cal a BP)	Material dated
LG2C1 32	38.1	GdA-4092	542±26	517-631	*Sphagnum* spp. stems
LG2C1 36	43.2	GdA-3750	837±27	692-788	*Sphagnum* spp. stems
LG2C1 43	52.7	GdA-4093	995±24	802-960	*Sphagnum* spp. stems
LG2C1 59	72.9	GdA-4094	1376±25	1275-1331	*Sphagnum* spp. stems
LG2C2 109	107.7	GdA-4095	2187±25	2129-2308	*Sphagnum* spp. stems
LG2C2 144	151.3	GdA-3884	2963±32	3005-3214	*Sphagnum* spp. stems
LG2C2 224	260.6	GdA-3752	4027±31	4422-4569	*Sphagnum* spp. stems
LG2C2 295	356.3	GdA-3885	5560±34	6296-6403	*Sphagnum teres* stems
LG2C2 338	413.6	GdA-3754	6073±50	6791-7155	Mosses remains

Table 3.3 Zonation details of LG2 core

Zone	Depth (cm)	Age (cal a BP/AD)	Description
1	416-249	7030-4400	High presence of brown mosses and Herbaceae. Relatively high amounts of *Sphagnum teres*. High abundance of *Amphitrema wrightianum*, *Centropyxis aculeata* and *Heleopera sphagni*.
2	240-132	4400-2700	High abundance of *A. flavum*, *A. muscorum* and *S. fuscum*.
3	132-80	2700-1470	Gradual decrease in *A. flavum* and *A. muscorum*. High presence of *Amphitrema wrightianum* and gradual increase in *Difflugia pristis*. Dominance of *S. fuscum* with occasional peaks in *Dicranum* spp.
4	80-64	1470-1125	Dominance of *Hyalosphenia subflava* and Herbaceae. High presence of *Arcella discoides*. Presence of charcoal.
5	64-37	1125-475	Dominance of *Difflugia pristis* and *S. fuscum*. Presence of two peaks of *A. flavum* at both end of the zone. Presence of *D. pristis*.
6	37-24	475-1932AD	Dominance of *H. subflava*. High presence of *S. fuscum* and Herbaceae. Presence of *A. discoides*, *Heleopera sphagnii* and charcoal.
7	24-0	1932AD-present	Dominance of *S. fuscum*, *Nebela militaris* and *Hyalosphenia elegans*.

Table 3.4 Nd isotopic data and εNd

Sample	Depth (cm)	$^{143}Nd/^{144}Nd$	±2se	εNd
LG2-3	2.9	0.511640	0.000008	-19.5
LG2-5	5.3	0.511540	0.000009	-21.4
LG2-8	8.9	0.511241	0.000009	-27.2
LG2-10	11.3	0.511344	0.000009	-25.2
LG2-13	15.0	0.511592	0.000007	-20.4
LG2-20	23.8	0.511922	0.000006	-14.0
LG2-23	27.4	0.511942	0.000005	-13.6
LG2-26	30.9	0.511935	0.000008	-13.7
LG2-33	39.4	0.511978	0.000006	-12.9
LG2-36	43.2	0.512008	0.000007	-12.3
LG2-43	52.7	0.512019	0.000007	-12.1
LG2-46	56.6	0.512006	0.000007	-12.3
LG2-48	59.2	0.511959	0.000012	-13.2
LG2-52	64.3	0.511981	0.000007	-12.8
LG2-54	66.8	0.511976	0.000005	-12.9
LG2-58	71.6	0.511905	0.000006	-14.3
LG2-68	84.7	0.511877	0.000011	-14.8
LG2-117	116.3	0.511817	0.000007	-16.0
LG2-142	148.6	0.511587	0.000010	-20.5
LG2-167	183.0	0.511613	0.000006	-20.0
LG2-202	230.2	0.511124	0.000010	-29.5
LG2-242	284.6	0.510998	0.000009	-32.0
LG2-277	331.4	0.511470	0.000018	-22.8
LG2-277		*0.511479*	*0.000011*	*-22.6*
LG2-307	372.7	0.510792	0.000016	-36.0
LG2-307		*0.510811*	*0.000013*	*-35.6*
LG2-326	397.4	0.510731	0.000011	-37.2
LG2-326		*0.510750*	*0.000009*	*-36.8*
Sources				
Bottom sed		0.510738	0.000007	-37.1
Bottom sed.		*0.510740*	*0.000014*	*-37.0*
Sakami-1		0.511322	0.000012	-25.7
Sakami-1		*0.511327*	*0.000011*	*-25.6*
RadSed-12		0.511261	0.000008	-26.9

CONCLUSION

Cette thèse visait à caractériser la variabilité spatiale et temporelle des dépôts holocènes de poussières atmosphériques au Québec boréal en lien avec les fluctuations climatiques. Trois tourbières s'étant développées dans trois contextes climatiques différents : Baie-Comeau (boréal maritime), Havre-Saint-Pierre (subarctique maritime) et Radisson (subarctique continental) furent échantillonnées. La géochimie élémentaire, par le biais des éléments lithogéniques et des terres rares, fut utilisée afin de reconstituer les apports de poussières atmosphériques minérales dans les tourbières sélectionnées. L'isotopie du néodyme fut combinée aux patrons de terres rares afin de mieux cerner l'origine des poussières déposées dans les tourbières. Finalement, des analyses de macrorestes végétaux, de thécamoebiens et de granulométrie furent effectuées dans le but d'évaluer le lien entre les changements des dépôts de poussières et les variations paléoécologiques et paléoclimatiques au cours de l'Holocène moyen et récent.

1. Reconstruction des dépôts atmosphériques de poussières

Avant de reconstruire les dépôts de poussières atmosphériques, l'immobilité des terres rares dans les sites d'étude sélectionnés a été démontrée par le biais des analyses par composantes principales (ACP; Chapitres 1 et 3). Bien que l'immobilité des terres rares dans les profils de tourbe ait préalablement été démontré (Aubert *et al.*, 2006; Krachler *et al.*, 2003), il est préférable de confirmer leur caractère conservatif au cas par cas afin de s'assurer de leur représentativité en tant qu'indicateurs d'apports de poussières atmosphériques. Dans le cas des tourbières du Québec boréal, le fait que les terres rares

se trouvent sur la même composante principale que d'autres éléments lithogéniques tels que Al, Ti et Zr, dont l'immobilité dans les séquences de tourbe a déjà été démontrée (Shotyk *et al.*, 2001; Weiss *et al.*, 2002) suggère qu'elles présentent un comportement chimique semblable à ces derniers en contexte tourbeux.

La reconstruction des flux de poussières atmosphériques par le biais de la somme des terres rares a permis d'identifier plusieurs phases d'apports accrus de poussières atmosphériques. Plus spécifiquement, les tourbières La Grande 2 (Baie James; 53°; 77°44'W) et Baie (Baie-Comeau; 49°04'N, 68°14'W) montrent le plus de variations dans les flux de poussières, ce qui confirme leur utilité en tant qu'archives atmosphériques d'apports de particules minérales. Dans le cas de la tourbière IDH (Havre-Saint-Pierre; 50°13'N, 63°36'W), cette dernière montre peu de variations de flux parmi ses horizons à l'exception de la période entre 4100 et 3700 cal a BP. Le peu de variabilité enregistrée est probablement attribuable à l'emplacement du site, ce qui sera discuté dans la prochaine section.

2. Influence du site d'étude

La sélection du site joue un rôle important dans la validité des séquences de tourbe en tant qu'archives de poussières atmosphériques. Le cas de la tourbière de l'Île du Havre en est un exemple. Les tourbières Baie et LG2 se sont développées sous des conditions plus propices à l'enregistrement des apports de poussières. Les effets des variations du régime des vents et du climat ont été enregistrées dans ces deux sites en raison de la présence de la moraine de Sakami (LG2) et du littoral du St-Laurent (Baie) fournissant du matériel pouvant facilement être érodé et transporté. La tourbière Baie est située près du littoral et le paysage végétal est ouvert alors que celle de LG2 se trouve à environ à 500 m à l'ouest de la moraine de Sakami. Malgré le fait que des plages soient localisées près de la tourbières IDH, cette dernière est située à une altitude plus élevée

(alt. 31 m.) que les plages (alt.1 m.) et elle est protégée par une frange forestière qui la ceinture. Ces éléments constituent de toute évidence des barrières naturelles qui ont intercepté une partie des poussières atmosphériques atteignant le site. Le rôle de la végétation dans l'interception et les dépôts de mercure a déjà été établi (Rydberg *et al.*, 2010). Bien que les poussières atmosphériques n'aient pas exactement le même comportement que les polluants atmosphériques, une dynamique similaire peut expliquer le peu de variabilité enregistré dans le profil IDH.

3. Sources des poussières atmosphériques

La source des poussières déposées à la surface des tourbières a pu être précisée à l'aide des isotopes du néodyme et des patrons de terres rares. Dans les trois sites d'étude, la portion minérotrophe, c'est-à-dire celle recevant tant des apports atmosphériques que les eaux de ruissellement sur les versants, montrent des valeurs de εNd distinctes de la portion ombrotrophe (Chapitres 2 et 3). Dans les trois cas, la signature isotopique du néodyme et les partons de REE de la partie minérotrophe ont permis d'obtenir une fourchette de valeurs en accord avec celles des sources locales (roches et sédiments meubles). Ceci s'explique par le fait que les apports de particules ne sont pas uniquement atmosphériques, i.e. les tourbières minérotrophes sont aussi affectées par des eaux de ruissellement ayant été en contact avec les roches et le substrat minéral environnant. Par exemple, les valeurs de εNd de moins de -30 correspondent généralement à des roches peu radiogéniques, comme d'anciens cratons. Effectivement, la région de La Grande est composée de roches d'âge archéen, donc peu radiogéniques (<-20; McCulloch et Wasserburg, 1978), ce qui explique les signatures très négatives retrouvées dans certains échantillons de ce site.

Dans les sections ombrotrophes, couvrant les 4000 à 5000 dernières années, les valeurs de εNd deviennent plus positives que dans la section minérotrophe suggérant des

apports autres que les sources locales. Le nombre limité de sources identifiées a empêché l'identification précise de la ou des source(s) des particules déposées dans les différentes tourbières. La similitude des valeurs de εNd pour les sites de Baie et LG2 entre environ 1700 et 100 cal a BP pourrait signifier qu'ils ont reçu des particules d'une ou des source(s) commune(s). Par contre, la présence de roches possédant des valeurs semblables à celles de la tourbière Baie suggère plutôt une ou plusieurs sources locales ou régionales. De plus, les patrons de terres rares montrent que les sources de poussières locales sont relativement importantes pendant la même période, ce qui suggère que les dépôts de poussières ont pu être contrôlés par des processus locaux d'origine climatique ou qu'ils constituent une réponse locale à des processus de plus grande échelle. Un échantillonnage plus approfondi des sources potentielles pourra, dans le futur, permettre d'affiner la signature des sources locales et ainsi déterminer laquelle des deux hypothèses est la plus plausible.

4. Liens entre les poussières et le climat régional

Plusieurs études conduites dans l'est et le nord-est du Canada montrent une relative stabilité climatique jusqu'à 4000 à 3000 cal a BP alors qu'une plus grande variabilité a été enregistrée au cours des 2500 à 2000 dernières années (Fig. C.1). Cette variabilité est visible dans les carottes des tourbières Baie et LG2 lorsque les conditions hydroclimatiques reconstruites à partir de l'analyse des thécamoebiens et les flux de poussières sont combinées. Toutes deux montrent des alternances de périodes froides et sèches de même que chaudes et humides. Un nombre élevé de reconstitutions climatiques, incluant la présente étude, suggèrent des conditions froides au Petit Âge Glaciaire (*ca* 700-100 cal a BP; (Desponts et Payette, 1993; Filion, 1984; Filion *et al.*, 1991; Loisel et Garneau, 2010; Magnan et Garneau, 2014; Pratte, Garneau et De Vleeschouwer, In press; van Bellen, Garneau et Booth, 2011) ainsi qu'entre 1500 et 1100 cal aBP (Filion, 1984; Morin et Payette, 1988; Pratte, Garneau et De

Vleeschouwer, sous presse; Viau et Gajewski, 2009). Plusieurs de ces mêmes études révèlent des conditions plus chaudes à l'Optimum Climatique Médiéval (*ca* 1100-800 cal a BP; Filion, 1984; Hughes *et al.*, 2006; Naulier *et al.*, 2015; Pratte, Garneau et De Vleeschouwer, sous presse; Viau et Gajewski, 2009). Pour ce qui est des conditions d'humidité, le patron est moins clair et les reconstitutions régionales montrent plus de variabilité (Fig. C.1). Certaines tendances peuvent tout de même être extraites : le Petit Âge Glaciaire semble avoir été sec (Desponts et Payette, 1993; Loisel et Garneau, 2010; van Bellen, Garneau et Booth, 2011) et l'Optimum Climatique Médiéval plus humide (Filion, 1984; Filion *et al.*, 1991; Ouzilleau Samson, Bhiry et Lavoie, 2010).

La présence de pics de poussières lors de périodes froides suggère que les flux seraient un indicateur de conditions froides et sèches dans l'aire couverte par l'étude. La concordance entre les épisodes accrus de dépôts de poussières, la présence d'assemblages de thécamoebiens typiques d'instabilité hydroclimatique et la formation de pergélisol (Asselin et Payette, 2006; Couillard et Payette, 1985) dans le nord-est du Canada supportent cette hypothèse. Ces conditions froides et sèches ont été liées à l'intrusion de masses d'air arctique dans le nord-est du Canada (Carcaillet et Richard, 2000; Girardin *et al.*, 2004), ce qui suggère des changements dans la circulation atmosphérique.

Le fait que les sites de LG2 et Baie montrent des tendances similaires au cours des 2000 dernières années suggère que les deux régions étaient contrôlées par les mêmes processus climatiques. Un contrôle à plus large échelle est révélé par le fait que plusieurs périodes d'apports prononcés de poussières à LG2 (Fig. C.1 : II, III et IV) et Baie (I, II et III) coïncident avec des minima solaires (Bond *et al.*, 2001). Cela suggère que l'insolation joue aussi un rôle dans les processus climatiques contrôlant les flux de poussières.

5. Impact des activités humaines sur le cycle des poussières atmosphériques

L'augmentation des flux de poussières atmosphériques au cours de dernières décennies dans les trois sites d'études révèle une influence probable des activités humaines sur le volume de poussières émis dans chacune des régions. L'influence des activités humaines telles que la déforestation ou les activités minières sur les flux de poussières a déjà été observée principalement en Europe (De Vleeschouwer *et al.*, 2012; Fagel *et al.*, 2014), où les populations humaines ont modifié le paysage depuis plusieurs millénaires. Les activités humaines ont aussi entrainé des changements dans la source des poussières. Par exemple, la tourbière LG2 a enregistré un retour vers des valeurs de εNd plus négatives au cours des dernières années probablement lié à la construction des centrales hydro-électriques dans la région. Ces activités ont favorisé une plus grande proportion de poussières de source locale émises dans l'atmosphère. D'une façon similaire, un changement dans les valeurs de REE/Ti dans la tourbière IDH a eu lieu au même moment que l'ouverture de la mine de titane à 40 km à l'intérieur des terres et de la construction du quai de chargement directement sur la côte située à deux kilomètres du site d'étude.

6. Recommandations et perspectives futures

Les résultats de cette thèse confirment les reconstructions climatiques qui ont précédemment été réalisées dans le nord du Québec. L'analyse des flux de poussières reconstruits par le biais de la géochimie élémentaire représente un outil qui, à notre connaissance, n'a jamais été utilisé en milieu tourbeux dans cette partie de l'Amérique du Nord. La thèse a permis d'approfondir significativement les connaissances sur les liens entre le climat et les variations des dépôts de poussières atmosphériques. Les données recueillies permettent d'obtenir un premier tableau des facteurs contrôlant ces

variations. Cette étude ouvre de nouvelles perspectives dans la compréhension de la dynamique hydroclimatique et atmosphérique de la région boréale nord-américaine.

Les similitudes entre les sites de La Grande 2 et Baie suggèrent que les deux régions ont été influencées par des processus climatiques similaires, du moins au cours des 2000 dernières années. Il serait donc intéressant d'augmenter le nombre de sites au Québec, mais aussi d'étendre la couverture spatiale à d'autres régions d'Amérique du Nord, par exemple en se rapprochant des sources du sud-ouest américain. Afin d'atteindre ce but, l'inclusion d'autres types d'archives telles que les sédiments lacustres et les lœss serait nécessaire puisque les tourbières sont rares ou même absentes dans certaines de ces régions.

L'étude de la source des particules déposées sur les tourbières sélectionnées a permis d'établir que plusieurs sources contribuent au signal isotopique du εNd, dont certaines n'ont pas été identifiées. L'une des prochaines étapes dans l'étude des poussières atmosphériques en Amérique du Nord sera de mieux cerner la source des poussières se déposant dans les différentes régions du continent. Pour cela, des analyses isotopiques devront être effectuées sur un plus grand nombre de sources potentielles (roches, sédiments meubles, loess, etc). Effectivement, en Amérique du Nord les analyses isotopiques de sources de poussières se limitent à quelques analyses sur des lœss du sud-ouest américain et d'Alaska. De plus, la réalisation d'analyses minéralogiques sur les particules déposées dans les tourbières contribuerait à une meilleure identification des sources. Finalement, une fois ces étapes franchies, il serait intéressant de coupler les données obtenues avec de la modélisation des trajectoires de vent (i.e. *backtrajectories*). Cela permettrait d'approfondir notre compréhension des processus atmosphériques impliqués dans le cycle des poussières en Amérique du Nord.

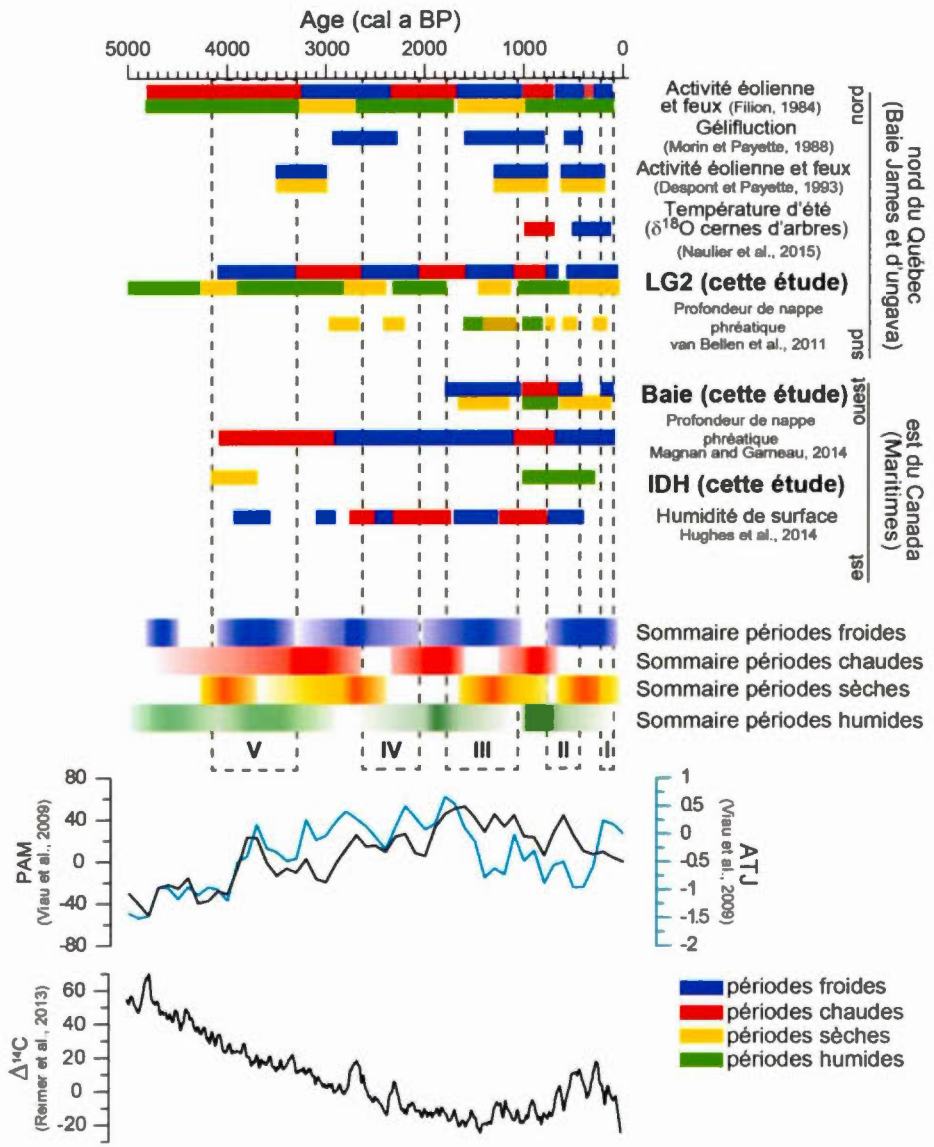

Figure C.1 Comparaison des phases climatiques enregistrées dans les trois sites d'études avec celles d'autres archives du nord du Québec et de l'est du Canada. Précipitations annuelles moyennes (PAM) et anomalies de température de juillet (ATJ) pour le nord du Québec (Viau et Gajewski, 2009); courbe de production de $\Delta^{14}C$ (Reimer *et al.*, 2013). Boîtes pointillées : pics de poussières identifiés dans les trois sites d'étude.

RÉFÉRENCES

Aaby, B. (1976). Cyclic climatic variations in climate over the past 5,500 yr reflected in raised bogs. *Nature,* 263(5575), 281-284.

Abbott, P.M. et Davies, S.M. (2012). Volcanism and the Greenland ice-cores: the tephra record. *Earth-Science Reviews,* 115(3), 173-191.

Albani, S., Delmonte, B., Maggi, V., Baroni, C., Petit, J.R., Stenni, B., Mazzola, C. and Frezzotti, M. (2012). Interpreting last glacial to Holocene dust changes at Talos Dome (East Antarctica): implications for atmospheric variations from regional to hemispheric scales. *Climate of the Past,* 8(2), 741-750.

Albani, S., Mahowald, N.M., Winckler, G., Anderson, R.F., Bradtmiller, L.I., Delmonte, B., François, R., Goman, M., Heavens, N.G., Hesse, P.P., Hovan, S.A., Kang, S.G., Kohfeld, K.E., Lu, H., Maggi, V., Mason, J.A., Mayewski, P.A., McGee, D., Miao, X., Otto-Bliesner, B.L., Perry, A.T., Pourmand, A., Roberts, H.M., Rosenbloom, N., Stevens, T. and Sun, J. (2015). Twelve thousand years of dust: the Holocene global dust cycle constrained by natural archives. *Climate of the Past,* 11(6), 869-903.

Allan, M., Le Roux, G., Piotrowska, N., Beghin, J., Javaux, E., Court-Picon, M., Mattielli, N., Verheyden, S. and Fagel, N. (2013). Mid and late Holocene dust deposition in western Europe: the Misten peat bog (Hautes Fagnes - Belgium). *Climate of the Past Discussion,* 9(3), 2889-2928.

Ali, A.A., Ghaleb, B., Garneau, M., Asnong, H. and Loisel, J. (2008). Recent peat accumulation rates in minerotrophic peatlands of the Bay James region, Eastern Canada, inferred by ^{210}Pb and ^{137}Cs radiometric techniques. *Applied Radiation Isotopes,* 66(10), 1350-1358.

Almquist, H., Dieffenbacher-Krall, A.C., Flanagan-Brown, R. and Sanger, D. (2001). The Holocene record of lake levels of Mansell Pond, central Maine, USA. *The Holocene,* 11(2), 189-201.

Appleby, P.G. (2002). Chronostratigraphic techniques in recent sediments. Dans: Last, W. and J. Smol (dir.), *Tracking Environmental Change Using Lake Sediments* (Vol. 1, p. 171-203): Springer Netherlands.

Arseneault, D. and Payette, S. (1997). Reconstruction of millenial forest dynamics from tree remains in a subarctic tree line peatland. *Ecology,* 78(6), 1873-1883.

Asselin, H. et Payette, S. (2006). Origin and long-term dynamics of a subarctic tree line. *Ecoscience,* 13(2), 135-142.

Aubert, D., Le Roux, G., Krachler, M., Cheburkin, A., Kober, B., Shotyk, W. et Stille, P. (2006). Origin and fluxes of atmospheric REE entering an ombrotrophic peat

bog in Black Forest (SW Germany): Evidence from snow, lichens and mosses. *Geochimica et Cosmochimica Acta,* 70(11), 2815-2826.

Barber, K.E. (1993). Peatlands as scientific archives of past biodiversity. *Biodiversity & Conservation,* 2(5), 474-489.

Barber, K.E., Chambers, F.M. and Maddy, D. (2003). Holocene palaeoclimates from peat stratigraphy: macrofossil proxy climate records from three oceanic raised bogs in England and Ireland. *Quaternary Science Reviews,* 22(5–7), 521-539.

Barber, K.E. and Langdon, P.G. (2007). What drives the peat-based palaeoclimate record? A critical test using multi-proxy climate records from northern Britain. *Quaternary Science Reviews,* 26(25–28), 3318-3327.

Beaulieu-Audy, V., Garneau, M., Richard, P.J.H. and Asnong, H. (2009). Holocene palaeoecological reconstruction of three boreal peatlands in the La Grande Rivière region, Québec, Canada. *The Holocene,* 19(3), 459-476.

Bernatchez, P. (2003). *Évolution littorale holocène et actuelle des complexes deltaïques de Betsiamites et Manicouagan-Outardes: synthèse, processus, causes et perspectives.* (PhD). Université Laval, Québec.

Bettis, E.A.I., Muhs, D.R., Roberts, H.M. and Wintle, A.G. (2003). Last Glacial loess in the conterminous USA. *Quaternary Science Reviews,* 22(18–19), 1907-1946.

Bhiry, N. and Robert, É.C. (2006). Reconstruction of changes in vegetation and trophic conditions of a palsa in a permafrost peatland, subarctic Québec, Canada. *Ecoscience,* 13(1), 56-65.

Bindler, R., Klarqvist, M., Klaminder, J. and Förster, J. (2004). Does within-bog spatial variability of mercury and lead constrain reconstructions of absolute deposition rates from single peat records? The example of Store Mosse, Sweden. *Global Biogeochemical Cycles,* 18(3), GB3020.

Biscaye, P.E., Grousset, F.E., Revel, M., Van der Gaast, S., Zielinski, G.A., Vaars, A. and Kukla, G. (1997). Asian provenance of glacial dust (stage 2) in the Greenland Ice Sheet Project 2 Ice Core, Summit, Greenland. *Journal of Geophysical Research: Oceans,* 102(C12), 26765-26781.

Blaauw, M. and Christen, J.A. (2011). Flexible paleoclimate age-depth models using an autoregressive gamma process. *Bayesian Analysis,* 6, 457-474.

Bond, G., Kromer, B., Beer, J., Muscheler, R., Evans, M.N., Showers, W., Hoffmann, S., Lotti-Bond, R., Hajdas, I. et Bonani, G. (2001). Persistent solar influence on North Atlantic climate during the Holocene. *Science,* 294(5549), 2130-2136.

Booth, R.K. (2002). Testate amoebae as paleoindicators of surface-moisture changes on Michigan peatlands: modern ecology and hydrological calibration. *Journal of Paleolimnology,* 28(3), 329-348.

Booth, R.K., Jackson, S.T., Forman, S.L., Kutzbach, J.E., Bettis, E.A., Kreigs, J. and Wright, D.K. (2005). A severe centennial-scale drought in midcontinental North America 4200 years ago and apparent global linkages. *The Holocene,* 15(3), 321-328.

Booth, R. and Sullivan, M. (2007). *Key of testate amoebae inhabiting Sphagnum-dominated peatlands with an emphasis on taxa preserved in Holocene*

sediments. Earth and Environmental Science Department, Lehigh University, Bethlehem, PA.

Bory, A.J.M., Biscaye, P.E. et Grousset, F.E. (2003). Two distinct seasonal Asian source regions for mineral dust deposited in Greenland (NorthGRIP). *Geophysical Research Letters,* 30(4).

Boutron, C.F., Candelone, J.-P. et Hong, S. (1995). Greenland snow and ice cores: unique archives of large-scale pollution of the troposphere of the Northern Hemisphere by lead and other heavy metals. *Science of the Total Environment,* 160/161, 233-241.

Bryson, R.A. (1966). Air masses, streamlines and the boreal forest. *Geographical Bulletin,* 8(3), 228-266.

Bryson, R.A. and Hare, F.K. (1974). Climates of North America. In: Bryson, R.A. and Hare, F.K. (eds) *Climates of North America.* Elsevier, 1-47.

Carcaillet, C. et Richard, P.J.H. (2000). Holocene changes in seasonal precipitation highlighted by fire incidence in eastern Canada. *Climate Dynamics,* 16(7), 549-559.

Caseldine, C.J., Baker, A., Charman, D.J. and Hendon, D. (2000). A comparative study of optical properties of NaOH peat extracts: implications for humification studies. *The Holocene,* 10(5), 649-658.

Chambers, F.M., Ogle, M.I. and Blackford, J.J. (1999). Palaeoenvironmental evidence for solar forcing of Holocene climate: linkages to solar science. *Progress in Physical Geography,* 23(2), 181-204.

Chambers, F.M. and Charman, D.J. (2004). Holocene environmental change: contributions from the peatland archive. *The Holocene,* 14(1), 1-6.

Chambers, F.M., Beilman, D.W. and Yu, Z.C. (2011). Methods for determining peat humification and for quantifying peat bulk density, organic matter and carbon content for palaeostudies of climate and peatland carbon dynamics. *Mires and Peat,* 7.

Chapman, S.B. (1964). The ecology of Coom Rigg Moss, Northumberland: II. The chemistry of peat profiles and the development of the bog system. *Journal of Ecology,* 52(2), 315-321.

Charman, D.J., Hendon, D. and Woodland, W.A. (2000). *The identification of testate amoebae (Protozoa: Rhizopoda) in peats*. London: Quaternary Research Association.

Charman, D.J. (2001). Biostratigraphic and palaeoenvironmental applications of testate amoebae. *Quaternary Science Reviews,* 20(16–17), 1753-1764.

Charman, D.J. et Mäkilä, M. (2003). Climate reconstruction from peatlands. *PAGES Newsletter,* 11, 15-17.

Charman, D.J., Brown, A.D., Hendon, D. and Karofeld, E. (2004). Testing the relationship between Holocene peatland palaeoclimate reconstructions and instrumental data at two European sites. *Quaternary Science Reviews,* 23(1–2), 137-143.

Charman, D.J., Barber, K.E., Blaauw, M., Langdon, P.G., Mauquoy, D., Daley, T.J., Hughes, P.D.M. and Karofeld, E. (2009). Climate drivers for peatland palaeoclimate records. *Quaternary Science Reviews,* 28(19–20), 1811-1819.

Charman, D.J., Amesbury, M.J., Hinchliffe, W., Hughes, P.D.M., Mallon, G., Blake, W.H., Daley, T.J., Gallego-Sala, A.V. and Mauquoy, D. (2015). Drivers of Holocene peatland carbon accumulation across a climate gradient in northeastern North America. *Quaternary Science Reviews,* 121(0), 110-119.

Chiarenzelli, J., Aspler, L., Dunn, C., Cousens, B., Ozarko, D. and Powis, K. (2001). Multi-element and rare earth element composition of lichens, mosses, and vascular plants from the Central Barrenlands, Nunavut, Canada. *Applied Geochemistry,* 16(2), 245-270.

Clymo, R.S. (1984). The Limits to peat bog growth. *Philosophical Transactions of the Royal Society of London B: Biological Sciences,* 303(1117), 605-654.

Couillard, L. et Payette, S. (1985). Évolution holocène d'une tourbière à pergélisol (Québec nordique). *Canadian Journal of Botany,* 63(6), 1104-1121.

Crum, H.A. and Anderson, L.E. (1979–1980). *Mosses of Eastern North America*. New York: Columbia University Press.

Damman, A.W.H. (1978). Distribution and movement of elements in ombrotrophic peat bogs. *Oikos,* 30(3), 480-495.

De Angelis, M., Steffensen, J.P., Legrand, M., Clausen, H. et Hammer, C. (1997). Primary aerosol (sea salt and soil dust) deposited in Greenland ice during the last climatic cycle: Comparison with east Antarctic records. *Journal of Geophysical Research: Oceans,* 102(C12), 26681-26698.

de Jong, R., Schoning, K. and Björck, S. (2007). Increased aeolian activity during humidity shifts as recorded in a raised bog in south-west Sweden during the past 1700 years. *Climate of the Past,* 3(3), 411-422.

de Jong, R., Blaauw, M., Chambers, F., Christensen, T., De Vleeschouwer, F., Finsinger, W., Fronzek, S., Johansson, M., Kokfelt, U., Lamentowicz, M., Roux, G., Mauquoy, D., Mitchell, E.D., Nichols, J., Samaritani, E. and van Geel, B. (2010). Climate and Peatlands. Dans: Dodson, J. (dir.), *Changing Climates, Earth Systems and Society* (p. 85-121): Springer Netherlands.

Delmonte, B., Andersson, P.S., Hansson, M., Schöberg, H., Petit, J.R., Basile-Doelsch, I. and Maggi, V. (2008). Aeolian dust in East Antarctica (EPICA-Dome C and Vostok): Provenance during glacial ages over the last 800 kyr. *Geophysical Research Letters,* 35(7).

Delmonte, B., Baroni, C., Andersson, P.S., Schoberg, H., Hansson, M., Aciego, S., Petit, J.-R., Albani, S., Mazzola, C., Maggi, V. et Frezzotti, M. (2010). Aeolian dust in the Talos Dome ice core (East Antarctica, Pacific/Ross Sea sector): Victoria Land versus remote sources over the last two climate cycles. *Journal of Quaternary Science,* 25(8), 1327-1337.

deMenocal, P., Ortiz, J., Guilderson, T., Adkins, J., Sarnthein, M., Baker, L. and Yarusinsky, M. (2000). Abrupt onset and termination of the African Humid

Period: rapid climate responses to gradual insolation forcing. *Quaternary Science Reviews,* 19(1–5), 347-361.

DePaolo, D.J. and Wasserburg, G.J. (1976). Nd isotopic variations and petrogenetic models. *Geophysical Research Letters,* 3(5), 249-252.

Desponts, M. et Payette, S. (1993). The Holocene dynamics of jack pine at its northern range limit in Quebec. *The Journal of Ecology,* 81(4), 719-727.

De Vleeschouwer, F., Piotrowska, N., Sikorski, J., Pawlyta, J., Cheburkin, A., Le Roux, G., Lamentowicz, M., Fagel, N. and Mauquoy, D. (2009). Multiproxy evidence of `Little Ice Age' palaeoenvironmental changes in a peat bog from northern Poland. *The Holocene,* 19(4), 625-637.

De Vleeschouwer, F., Chambers, F.M. and Swindles, G.T. (2010). Coring and subsampling of peatlands for palaeoenvironmental research. *Mires and Peat,* 7.

De Vleeschouwer, F., Pazdur, A., Luthers, C., Streel, M., Mauquoy, D., Wastiaux, C., Le Roux, G., Moschen, R., Blaauw, M., Pawlyta, J., Sikorski, J. et Piotrowska, N. (2012). A millennial record of environmental change in peat deposits from the Misten bog (East Belgium). *Quaternary International,* 268, 44-57.

De Vleeschouwer, F., Ferrat, M., McGowan, H., Vanneste, H. and Weiss, D. (2014). Extracting paleodust information from peat geochemistry. *PAGES Magazine,* 22(2), 88-89.

Dickin, A.P. and Higgins, M.D. (1992). Sm/Nd evidence for a major 1.5 Ga crust-forming event in the central Grenville province. *Geology,* 20(2), 137-140.

Dickin, A.P. (2000). Crustal formation in the Grenville Province: Nd-isotope evidence. *Canadian Journal of Earth Sciences,* 37(2-3), 165-181.

Diffenbaugh, N.S., Giorgi, F. et Pal, J.S. (2008). Climate change hotspots in the United States. *Geophysical Research Letters,* 35(16).

Donahue, D.J., Linick, T.W. and Jull, A.J.T. (1990). Isotope-ratio and background corrections for accelerator mass spectrometry radiocarbon measuments. *Radiocarbon,* 32, 135-142.

Donarummo, J., Ram, M. and Stoermer, E.F. (2003). Possible deposit of soil dust from the 1930's U.S. dust bowl identified in Greenland ice. *Geophysical Research Letters,* 30(6), 1269.

Dyke, A.S. and Prest, V.K. (1987). Late Wisconsinan and Holocene history of the Laurentide ice sheet. *Géographie physique et Quaternaire,* 41(2), 237-263.

Eriksson, L., Johansson, E., N., K.-W. and Wodl, S. (1999). *Introduction to multi-and megavariate data analysis using projection methods (PCA & PLS)*. Umeå: Umetrics AB.

Environment Canada (2010). Canadian Climate Normals 1981-2010. Retrieved 27 October 2015 from http://climate.weather.gc.ca/climate_normals/.

Fagel, N., Innocent, C., Gariepy, C. and Hillaire-Marcel, C. (2002). Sources of Labrador Sea sediments since the last glacial maximum inferred from Nd-Pb isotopes. *Geochimica et Cosmochimica Acta,* 66(14), 2569-2581.

Fagel, N., Allan, M., Le Roux, G., Mattielli, N., Piotrowska, N. et Sikorski, J. (2014). Deciphering human–climate interactions in an ombrotrophic peat record: REE,

Nd and Pb isotope signatures of dust supplies over the last 2500 years (Misten bog, Belgium). *Geochimica et Cosmochimica Acta,* 135(0), 288-306.

Farmer, G.L., Barber, D. and Andrews, J. (2003). Provenance of Late Quaternary ice-proximal sediments in the North Atlantic: Nd, Sr and Pb isotopic evidence. *Earth and Planetary Science Letters,* 209(1–2), 227-243.

Ferrat, M., Weiss, D.J., Spiro, B. et Large, D. (2012). The inorganic geochemistry of a peat deposit on the eastern Qinghai-Tibetan Plateau and insights into changing atmospheric circulation in central Asia during the Holocene. *Geochimica et Cosmochimica Acta,* 91(0), 7-31.

Ferrat, M., Langmann, B., Cui, X., Gomes, J. et Weiss, D.J. (2013). Numerical simulations of dust fluxes to the eastern Qinghai-Tibetan Plateau: Comparison of model results with a Holocene peat record of dust deposition. *Journal of Geophysical Research: Atmospheres,* 118(10), 4597-4609.

Filion, L. (1984). A relationship between dunes, fire and climate recorded in the Holocene deposits of Quebec. *Nature,* 309(5968), 543-546.

Filion, L., Saint-Laurent, D., Desponts, M. et Payette, S. (1991). The late Holocene record of aeolian and fire activity in northern Québec, Canada. *The Holocene,* 1(3), 201-208.

Fischer, H., Siggaard-Andersen, M.-L., Ruth, U., Röthlisberger, R. and Wolff, E. (2007). Glacial/interglacial changes in mineral dust and sea-salt records in polar ice cores: Sources, transport, and deposition. *Reviews of Geophysics,* 45(1).

Frolking, S.E., Bubier, J.L., Moore, T.R., Ball, T., Bellisario, L.M., Bhardwaj, A., Carroll, P., Crill, P.M., Lafleur, P.M., McCaughey, J.H., Roulet, N.T., Suyker, A.E., Verma, S.B., Waddington, J.M. et Whiting, G.J. (1998). Relationship between ecosystem productivity and photosynthetically active radiation for northern peatlands. *Global Biogeochemical Cycles,* 12(1), 115-126.

Gabrielli, P., Wegner, A., Petit, J.R., Delmonte, B., De Deckker, P., Gaspari, V., Fischer, H., Ruth, U., Kriews, M., Boutron, C., Cescon, P. and Barbante, C. (2010). A major glacial-interglacial change in aeolian dust composition inferred from Rare Earth Elements in Antarctic ice. *Quaternary Science Reviews,* 29(1–2), 265-273.

Gallon, C., Tessier, A., Gobeil, C. and Beaudin, L. (2005). Sources and chronology of atmospheric lead deposition to a Canadian Shield lake: Inferences from Pb isotopes and PAH profiles. *Geochimica et Cosmochimica Acta,* 69(13), 3199-3210.

Garneau, M. (1995). *Collection de référence de graines et autres macrofossiles végétaux de taxons provenant du Québec méridional et boréal et de l'arctique canadien.* Open File 3048. Geological Survey of Canada, Division de la science des terrains.

Garneau, M., van Bellen, S., Magnan, G., Beaulieu-Audy, V., Lamarre, A. and Asnong, H. (2014). Holocene carbon dynamics of boreal and subarctic peatlands from Québec, Canada. *The Holocene,* 24(9), 1043-1053.

Gillette, D.A. (1988). Threshold friction velocities for dust production for agricultural soils. *Journal of Geophysical Research: Atmospheres,* 93(D10), 12645-12662.

Girardin, M.P., Tardif, J., Flannigan, M.D. et Bergeron, Y. (2004). Multicentury reconstruction of the Canadian Drought Code from eastern Canada and its relationship with paleoclimatic indices of atmospheric circulation. *Climate Dynamics,* 23(2), 99-115.

Givelet, N., Roos-Barraclough, F. and Shotyk, W. (2003). Predominant anthropogenic sources and rates of atmospheric mercury accumulation in southern Ontario recorded by peat cores from three bogs: comparison with natural "background" values (past 8000 years). *Journal of Environmental Monitoring,* 5(6), 935-949.

Givelet, N., Le Roux, G., Cheburkin, A., Chen, B., Frank, J., Goodsite, M.E., Kempter, H., Krachler, M., Noernberg, T., Rausch, N., Rheinberger, S., Roos-Barraclough, F., Sapkota, A., Scholz, C. and Shotyk, W. (2004). Suggested protocol for collecting, handling and preparing peat cores and peat samples for physical, chemical, mineralogical and isotopic analyses. *Journal of Environmental Monitoring,* 6(5), 481-492.

Goudie, A.S. and Middleton, N.J. (2001). Saharan dust storms: nature and consequences. *Earth-Science Reviews,* 56(1–4), 179-204.

Greaves, M.J., Elderfield, H. and Sholkovitz, E.R. (1999). Aeolian sources of rare earth elements to the Western Pacific Ocean. *Marine Chemistry,* 68(1–2), 31-38.

Grondin, P., Blouin, J.-L., and Bouchard, D. (1980). *Étude phyto-écologique de l'archipel de Mingan. Vols. 1-3.* Report for Groupe Dryade, Office de planification et de développement du Québec, Québec.

Groupe d'experts Intergouvernemental sur l'Évolution du Climat (GIEC) (2013). *Changement climatique 2013: les éléments scientifiques.* Contribution du groupe de travail 1 Contribution au cinquième rapport d'évaluation du Groupe d'experts Intergouvernemental en Évolution du Climat. In: Stocker T.F., Qin, D., Plattner, G.-K., Tignor, M., Allen, S.K., Boschung, J., Nauels, A., Xia, Y., Bex, V., and Midgley, P.M. (eds) Cambridge University Press, Cambridge/New York, pp. 1535.

Grousset, F.E. and Biscaye, P.E. (2005). Tracing dust sources and transport patterns using Sr, Nd and Pb isotopes. *Chemical Geology,* 222(3–4), 149-167.

Grove, J. (2004). *Little Ice Ages: Ancient and Modern.* Routledge, New York.

Hansson, S.V., Rydberg, J., Kylander, M., Gallagher, K. and Bindler, R. (2013). Evaluating paleoproxies for peat decomposition and their relationship to peat geochemistry. *The Holocene,* 23(12), 1666-1671.

Harrison, S.P., Kohfeld, K.E., Roelandt, C. and Claquin, T. (2001). The role of dust in climate changes today, at the last glacial maximum and in the future. *Earth-Science Reviews,* 54(1–3), 43-80.

Hillaire-Marcel, C. (1976). La déglaciation et le relèvement isostatique sur la côte est de la Baie d'Hudson. *Cahiers de Géographie du Québec,* 20(50), 185-220.

Hillaire-Marcel, C., Occhietti, S. and Vincent, J.-S. (1981). Sakami moraine, Québec: a 500 km-long moraine without climatic control. *Geology* 9, 210–214.

Hölzer, A. et Hölzer, A. (1998). Silicon and titanium in peat profiles as indicators of human impact. *The Holocene,* 8(6), 685-696.

Hughes, P.D.M., Blundell, A., Charman, D.J., Bartlett, S., Daniell, J.R.G., Wojatschke, A. and Chambers, F.M. (2006). An 8500 cal. year multi-proxy climate record from a bog in eastern Newfoundland: contributions of meltwater discharge and solar forcing. *Quaternary Science Reviews,* 25(11–12), 1208-1227.

Ireland, R.R. 1982. *Moss Flora of the Maritime Provinces*. National Museums of Canada: Ottawa.

Jacobsen, S.B. and Wasserburg, G.J. (1980). Sm-Nd isotopic evolution of chondrites. *Earth and Planetary Science Letters,* 50(1), 139-155.

Jeglum, J.K., Rothwell, R.L., Berry, G.J. and Smith, G.K.M. (1992). A peat sampler for rapid survey. *Technical Note, Canadian Forestry Service,* 13, 921-932.

Jessen, C.A., Solignac, S., Nørgaard-Pedersen, N., Mikkelsen, N., Kuijpers, A. and Seidenkrantz, M.-S. (2011). Exotic pollen as an indicator of variable atmospheric circulation over the Labrador Sea region during the mid to late Holocene. *Journal of Quaternary Science,* 26(3), 286-296.

Jolliffe, I.T. (2002). *Principal Component Analysis*. Springer, New York.

Jowsey, P.C. (1966). An improved peat sampler. *New Phytologist,* 65(2), 245-248.

Kohfeld, K.E. and Harrison, S.P. (2001). DIRTMAP: the geological record of dust. *Earth-Science Reviews,* 54(1–3), 81-114.

Krachler, M., Mohl, C., Emons, H. and Shotyk, W. (2003). Two thousand years of atmospheric rare earth element (REE) deposition as revealed by an ombrotrophic peat bog profile, Jura Mountains, Switzerland. *Journal of Environmental Monitoring,* 5(1), 111-121.

Krachler, M., Le Roux, G., Kober, B. and Shotyk, W. (2004). Optimising accuracy and precision of lead isotope measurement (^{206}Pb, ^{207}Pb, ^{208}Pb) in acid digests of peat with ICP-SMS using individual mass discrimination correction. *Journal of Analytical Atomic Spectrometry,* 19(3), 354-361.

Kylander, M., Weiss, D., Martinez-Cortizas, A., Spiro, B., Garciasanchez, R. et Coles, B. (2005). Refining the pre-industrial atmospheric Pb isotope evolution curve in Europe using an 8000 year old peat core from NW Spain. *Earth and Planetary Science Letters,* 240(2), 467-485.

Kylander, M.E., Muller, J., Wüst, R.A.J., Gallagher, K., Garcia-Sanchez, R., Coles, B.J. and Weiss, D.J. (2007). Rare earth element and Pb isotope variations in a 52 kyr peat core from Lynch's Crater (NE Queensland, Australia): Proxy development and application to paleoclimate in the Southern Hemisphere. *Geochimica et Cosmochimica Acta,* 71(4), 942-960.

Kylander, M.E., Weiss, D.J. et Kober, B. (2009). Two high resolution terrestrial records of atmospheric Pb deposition from New Brunswick, Canada, and Loch Laxford, Scotland. *Science of the Total Environment,* 407(5), 1644-1657.

Kylander, M.E., Klaminder, J., Bindler, R. and Weiss, D.J. (2010). Natural lead isotope variations in the atmosphere. *Earth and Planetary Science Letters,* 290(1-2), 44-53.

Kutzbach, J.E. (1981). Monsoon Climate of the Early Holocene: Climate Experiment with the Earth's Orbital Parameters for 9000 Years Ago. *Science,* 214(4516), 59-61.

Lajeunesse, P. (2008). Early Holocene deglaciation of the eastern coast of Hudson Bay. *Geomorphology* 99, 341-352.

Lamarre, A., Magnan, G., Garneau, M. and Boucher, É. (2013). A testate amoeba-based transfer function for paleohydrological reconstruction from boreal and subarctic peatlands in northeastern Canada. *Quaternary International,* 306, 88-96.

Lambert, F., Delmonte, B., Petit, J.R., Bigler, M., Kaufmann, P.R., Hutterli, M.A., Stocker, T.F., Ruth, U., Steffensen, J.P. et Maggi, V. (2008). Dust-climate couplings over the past 800,000 years from the EPICA Dome C ice core. *Nature,* 452(7187), 616-619.

Lamentowicz, M., van der Knaap, W.O., van Leeuwen, J.F.N., Hangartner, S., Mitchell, E.A.D., Goslar, T., Tinner, W. and Kaminik, C. (2010). A multi-proxy high-resolution approach to reconstructing past environmental change from an Alpine peat archive. *PAGES News,* 18(1), 13-15.

Laterreur, N. (2008). *Structuration relationnelle et intégration de données multi-sources caractérisant les bassins tourbeux de la région de la rivière La Grande (Baie James).* M.Sc. Thesis. Department of Geography, Montreal: Université du Québec à Montréal.

Lawrence, C.R. et Neff, J.C. (2009). The contemporary physical and chemical flux of aeolian dust: A synthesis of direct measurements of dust deposition. *Chemical Geology,* 267(1–2), 46-63.

Lemay-Tougas M (2014). *Changements climatiques le long de la côte nord de l'estuaire du Saint-Laurent Durant l'Holocène : relation entre les conditions hydrographiques et le développement des tourbières ombrotrophes côtières.* MSc Thesis. University of Quebec in Montreal (UQAM), Canada.

Le Roux, G., Aubert, D., Stille, P., Krachler, M., Kober, B., Cheburkin, A., Bonani, G. et Shotyk, W. (2005). Recent atmospheric Pb deposition at a rural site in southern Germany assessed using a peat core and snowpack, and comparison with other archives. *Atmospheric Environment,* 39(36), 6790-6801.

Le Roux, G. and De Vleeschouwer, F. (2010). Preparation of peat samples for inorganic geochemistry used as palaeoenvironmental proxies. *Mires and Peat,* 7.

Le Roux, G. and Marshall, W.A. (2011). Constructing recent peat accumulation chronologies using atmospheric fall-out radionuclides. *Mires and Peat,* 7.

Le Roux, G., Fagel, N., De Vleeschouwer, F., Krachler, M., Debaille, V., Stille, P., Mattielli, N., van der Knaap, W.O., van Leeuwen, J.F.N. and Shotyk, W. (2012). Volcano- and climate-driven changes in atmospheric dust sources and fluxes since the Late Glacial in Central Europe. *Geology,* 40(4), 335-338.

Loisel, J. et Garneau, M. (2010). Late Holocene paleoecohydrology and carbon accumulation estimates from two boreal peat bogs in eastern Canada: Potential

and limits of multi-proxy archives. *Palaeogeography, Palaeoclimatology, Palaeoecology,* 291(3–4), 493-533.

Lupker, M., Aciego, S.M., Bourdon, B., Schwander, J. et Stocker, T.F. (2010). Isotopic tracing (Sr, Nd, U and Hf) of continental and marine aerosols in an 18th century section of the Dye-3 ice core (Greenland). *Earth and Planetary Science Letters,* 295(1–2), 277-286.

Magnan, G. et Garneau, M. (2014). Evaluating long-term regional climate variability in the maritime region of the St. Lawrence North Shore (eastern Canada) using a multi-site comparison of peat-based paleohydrological records. *Journal of Quaternary Science,* 29(3), 209-220.

Magnan, G., Garneau, M. and Payette, S. (2014). Holocene development of maritime ombrotrophic peatlands of the St. Lawrence North Shore in eastern Canada. *Quaternary Research,* 82(1), 96-106.

Maher, B.A., Prospero, J.M., Mackie, D., Gaiero, D., Hesse, P.P. and Balkanski, Y. (2010). Global connections between aeolian dust, climate and ocean biogeochemistry at the present day and at the last glacial maximum. *Earth-Science Reviews,* 99(1–2), 61-97.

Mahowald, N., Albani, S., Engelstaedter, S., Winckler, G. et Goman, M. (2011). Model insight into glacial–interglacial paleodust records. *Quaternary Science Reviews,* 30(7–8), 832-854.

Marie-Victorin, F. (1995). *Flore laurentienne, Third Edition*. Montreal: Les Presses de l'Université de Montréal.

Marx, S.K., McGowan, H.A. and Kamber, B.S. (2009). Long-range dust transport from eastern Australia: A proxy for Holocene aridity and ENSO-type climate variability. *Earth and Planetary Science Letters,* 282(1–4), 167-177.

Marx, S.K., Kamber, B.S., McGowan, H.A. and Zawadzki, A. (2010). Atmospheric pollutants in alpine peat bogs record a detailed chronology of industrial and agricultural development on the Australian continent. *Environmental Pollution,* 158(5), 1615-1628.

Marticorena, B., Bergametti, G., Gillette, D. et Belnap, J. (1997). Factors controlling threshold friction velocity in semiarid and arid areas of the United States. *Journal of Geophysical Research: Atmospheres,* 102(D19), 23277-23287.

Martinez-Cortizas, A., Garcia-Rodeja, E., Pontevedra Pombal, X., Novoa Munoz, J.C., Weiss, D. et Cheburkin, A. (2002). Atmospheric Pb deposition in Spain during the last 4000 years recorded by two ombrotrophic peat bogs and implications for the use of peat as archive. *Sci Total Environ,* 292, 33-44.

Martínez-Cortizas, A., Pontevedra-Pombal, X., García-Rodeja, E., Nóvoa-Muñoz, J.C. et Shotyk, W. (1999). Mercury in a Spanish Peat Bog: Archive of Climate Change and Atmospheric Metal Deposition. *Science,* 284(5416), 939-942.

Martini P. and Martinez-Cortizas A. (eds), (2006). *Peatlands - Evolution and Records of Environmental and Climate Changes*. Developments in Earth Surface Processes. Vol. 9. Elsevier. 606pp.

Mason, J.A., Jacobs, P.M., Hanson, P.R., Miao, X. et Goble, R.J. (2003). Sources and paleoclimatic significance of Holocene Bignell Loess, central Great Plains, USA. *Quaternary Research,* 60(3), 330-339.

Mason, J.A., Miao, X., Hanson, P.R., Johnson, W.C., Jacobs, P.M. and Goble, R.J. (2008). Loess record of the Pleistocene–Holocene transition on the northern and central Great Plains, USA. *Quaternary Science Reviews,* 27(17–18), 1772-1783.

Mauquoy, D., van Geel, B., Blaauw, M., Speranza, A. and van der Plicht, J. (2004). Changes in solar activity and Holocene climatic shifts derived from ^{14}C wiggle-match dated peat deposits. *The Holocene,* 14(1), 45-52.

Mauquoy, D. and van Geel, B. (2007). Mire and Peat Macros. Dans Elias, S. A. (dir.), *Encyclopedia of Quaternary Science* (p. 2315-2336). Oxford: Elsevier.

Mayewski, P.A., Rohling, E.E., Curt Stager, J., Karlén, W., Maasch, K.A., David Meeker, L., Meyerson, E.A., Gasse, F., van Kreveld, S., Holmgren, K., Lee-Thorp, J., Rosqvist, G., Rack, F., Staubwasser, M., Schneider, R.R. and Steig, E.J. (2004). Holocene climate variability. *Quaternary Research,* 62(3), 243-255.

McLennan, S.M. (1989). Rare earth elements in sedimentary rocks; influence of provenance and sedimentary processes. *Reviews in Mineralogy and Geochemistry,* 21(1), 169-200.

McCulloch, M.T. et Wasserburg, G.J. (1978). Sm-Nd and Rb-Sr Chronology of Continental Crust Formation. *Science,* 200(4345), 1003-1011.

Menéndez, I., Díaz-Hernández, J.L., Mangas, J., Alonso, I. et Sánchez-Soto, P.J. (2007). Airborne dust accumulation and soil development in the North-East sector of Gran Canaria (Canary Islands, Spain). *Journal of Arid Environments,* 71(1), 57-81.

Meskhidze, N., Chameides, W.L., Nenes, A. and Chen, G. (2003). Iron mobilization in mineral dust: Can anthropogenic SO2 emissions affect ocean productivity? *Geophysical Research Letters,* 30(21), 2085.

Miao, X., Mason, J.A., Swinehart, J.B., Loope, D.B., Hanson, P.R., Goble, R.J. and Liu, X. (2007). A 10,000 year record of dune activity, dust storms, and severe drought in the central Great Plains. *Geology,* 35(2), 119-122.

Miller, R.L. et Tegen, I. (1998). Climate Response to Soil Dust Aerosols. *Journal of Climate,* 11(12), 3247-3267.

Miousse, L., Bhiry, N. and Lavoie, M. (2003). Isolation and water-level fluctuations of Lake Kachishayoot, Northern Québec, Canada. *Quaternary Research,* 60(2), 149-161.

Mischke, S., Zhang, C., Börner, A. and Herzschuh, U. (2010). Late Glacial and Holocene variation in aeolian sediment flux over the northeastern Tibetan Plateau recorded by laminated sediments of a saline meromictic lake. *Journal of Quaternary Science,* 25(2), 162-177.

Mitchell, E.D., Charman, D. and Warner, B. (2008). Testate amoebae analysis in ecological and paleoecological studies of wetlands: past, present and future. *Biodiversity and Conservation,* 17(9), 2115-2137.

Morin, H. and Payette, S. (1988). Holocene gelifluction in a snow-patch environment at the Forest-Tundra Transition along the eastern Hudson Bay Coast, Canada. *Boreas,* 17(1), 79-88.

Muhs, D.R. and Budahn, J.R. (2006). Geochemical evidence for the origin of late Quaternary loess in central Alaska. *Canadian Journal of Earth Sciences,* 43(3), 323-337.

Muhs, D.R., Budahn, J.R., Prospero, J.M. et Carey, S.N. (2007). Geochemical evidence for African dust inputs to soils of western Atlantic islands: Barbados, the Bahamas, and Florida. *Journal of Geophysical Research: Earth Surface,* 112(F2).

Muhs, D.R., Bettis, E.A., Aleinikoff, J.N., McGeehin, J.P., Beann, J., Skipp, G., Marshall, B.D., Roberts, H.M., Johnson, W.C. et Benton, R. (2008). Origin and paleoclimatic significance of late Quaternary loess in Nebraska: Evidence from stratigraphy, chronology, sedimentology, and geochemistry. *Geological Society of America Bulletin,* 120(11-12), 1378-1407.

Muhs, D.R. (2013). The geologic records of dust in the Quaternary. *Aeolian Research,* 9(0), 3-48.

Nakai, S.i., Halliday, A.N. et Rea, D.K. (1993). Provenance of dust in the Pacific Ocean. *Earth and Planetary Science Letters,* 119(1–2), 143-157.

Naulier, M., Savard, M.M., Bégin, C., Gennaretti, F., Arseneault, D., Marion, J., Nicault, A. et Bégin, Y. (2015). A millennial summer temperature reconstruction for northeastern Canada using oxygen isotopes in subfossil trees. *Climate of the Past,* 11(9), 1153-1164.

Neff, J.C., Ballantyne, A.P., Farmer, G.L., Mahowald, N.M., Conroy, J.L., Landry, C.C., Overpeck, J.T., Painter, T.H., Lawrence, C.R. and Reynolds, R.L. (2008). Increasing eolian dust deposition in the western United States linked to human activity. *Nature Geoscience,* 1(3), 189-195.

Norton, S.A., Evans, G.C. and Kahl, J.S. (1997). Comparison of Hg and Pb fluxes to hummocks and hollows of ombrotrophic Big Heath Bog and to Nearby Sargent Mt. Pond, Maine, USA. *Water, Air, & Soil Pollution,* 100(3), 271-286.

O'Brien, S.R., Mayewski, P.A., Meeker, L.D., Meese, D.A., Twickler, M.S. and Whitlow, S.I. (1995). Complexity of holocene climate as reconstructed from a Greenland ice core. *Science,* 270(5244), 1962-1964.

Oldfield F, Richardson N and Appleby PG (1995) Radiometric dating (^{210}Pb, ^{137}Cs, ^{241}Am) of recent ombrotrophic peat accumulation and evidence for changes in mass balance. *The Holocene,* 5(2), 141-148.

Oppenheimer, C. (2003). Climatic, environmental and human consequences of the largest known historic eruption: Tambora volcano (Indonesia) 1815. *Progress in Physical Geography,* 27(2), 230-259.

Ouzilleau Samson, D., Bhiry, N. et Lavoie, M. (2010). Late-Holocene palaeoecology of a polygonal peatland on the south shore of Hudson Strait, northern Québec, Canada. *The Holocene,* 20(4), 525-536.

Payette, S. and Filion, L. (1993). Holocene water-level fluctuations of a subarctic lake at the tree line in northern Québec. *Boreas,* 22(1), 7-14.

Petit, J.R., Jouzel, J., Raynaud, D., Barkov, N.I., Barnola, J.M., Basile, I., Bender, M., Chappellaz, J., Davis, M., Delaygue, G., Delmotte, M., Kotlyakov, V.M., Legrand, M., Lipenkov, V.Y., Lorius, C., Pepin, L., Ritz, C., Saltzman, E. et Stievenard, M. (1999). Climate and atmospheric history of the past 420,000 years from the Vostok ice core, Antarctica. *Nature,* 399(6735), 429-436.

Piotrowska, N. (2013). Status report of AMS sample preparation laboratory at GADAM Centre, Gliwice, Poland. *Nuclear Instruments and Methods in Physics Research Section B: Beam Interactions with Materials and Atoms,* 294, 176-181.

Poole, W.H., Sanford, B.V., Williams, H, *et al.* (1970) Geology of southeastern Canada. In: Douglas RJW (ed) *Geology and economic minerals of Canada.* Ottawa: Geological Survey of Canada, pp. 228-304.

Pratte, S., Mucci, A. and Garneau, M. (2013). Historical records of atmospheric metal deposition along the St. Lawrence Valley (eastern Canada) based on peat bog cores. *Atmospheric Environment,* 79, 831-840.

Pratte, S., Garneau, M. et De Vleeschouwer, F. (In press). Late Holocene atmospheric dust deposition in eastern Canada (St. Lawrence North Shore). *The Holocene*

Prospero, J.M., Ginoux, P., Torres, O., Nicholson, S.E. et Gill, T.E. (2002). Environmental characterization of global sources of atmospheric soil dust identified with the NIMBUS 7 total ozone mapping spectrometer (TOMS) absorbing aerosol product. *Reviews of Geophysics,* 40(1), 1-31.

Pye K. (1987). *Aeolian dust and dust deposits*. Academic Press Inc., London, pp. 325.

Rea, D.K. (1994). The paleoclimatic record provided by eolian deposition in the deep sea: The geologic history of wind. *Reviews of Geophysics,* 32(2), 159-195.

Reimann, C., Filzmoser, P., Garret, R. and Dutter, R. (2008). *Statistical Data Analysis Explained: Applied Environmental Statistics with R*. John Wiley & Sons Ltd, Chichester.

Reimer, P.J., Bard, E., Bayliss, A., Beck, J.W., Blackwell, P.G., Bronk Ramsey, C., Buck, C.E., Cheng, H., Edwards, R.L., Friedrich, M., Grootes, P.M., Guilderson, T.P., Haflidason, H., Hajdas, I., Hatté, C., Heaton, T.J., Hoffmann, D.L., Hogg, A.G., Hughen, K.A., Kaiser, K.F., Kromer, B., Manning, S.W., Niu, M., Reimer, R.W., Richards, D.A., Scott, E.M., Southon, J.R., Staff, R.A., Turney, C.S.M. et van der Plicht, J. (2013). IntCal13 and Marine13 Radiocarbon Age Calibration Curves 0–50,000 Years cal BP. *Radiocarbon,* 55(4), 1869-1887.

Reynolds, R.L., Mordecai, J.S., Rosenbaum, J.G., Ketterer, M.E., Walsh, M.K. et Moser, K.A. (2009). Compositional changes in sediments of subalpine lakes,

Uinta Mountains (Utah): evidence for the effects of human activity on atmospheric dust inputs. *Journal of Paleolimnology,* 44(1), 161-175.

Roos-Barraclough, F. et Shotyk, W. (2003). Millennial-Scale records of atmospheric mercury deposition obtained from ombrotrophic and minerotrophic peatlands in the Swiss Jura Mountains. *Environmental Science & Technology,* 37(2), 235-244.

Roos-Barraclough, F., Givelet, N., Cheburkin, A.K., Shotyk, W. and Norton, S.A. (2006). Use of Br and Se in peat to reconstruct the natural and anthropogenic fluxes of atmospheric Hg: A 10000-year record from Caribou Bog, Maine. *Environmental Science & Technology,* 40(10), 3188-3194.

Rydberg, J., Karlsson, J., Nyman, R., Wanhatalo, I., Näthe, K. et Bindler, R. (2010). Importance of vegetation type for mercury sequestration in the northern Swedish mire, Rödmossamyran. *Geochimica et Cosmochimica Acta,* 74(24), 7116-7126.

Sauvé, A. (2016). Reconstitution holocène de la végétation et du climat pour les régions de Baie-Comeau et de Havre-Saint-Pierre, Québec. MSc Thesis, University of Quebec in Montreal (UQAM), Canada.

Sapkota, A., Cheburkin, A.K., Bonani, G. et Shotyk, W. (2007). Six millennia of atmospheric dust deposition in southern South America (Isla Navarino, Chile). *The Holocene,* 17(5), 561-572.

Shotyk, W. (1988). Review of the inorganic geochemistry of peats and peatland waters. *Earth-Science Reviews,* 25, 95-176.

Shotyk, W., Cheburkin, A.K., Appleby, P.G., Fankhauser, A. et Kramers, J.D. (1996). Two thousand years of atmospheric arsenic, antimony, and lead deposition recorded in an ombrotrophic peat bog profile, Jura Mountains, Switzerland. *Earth and Planetary Science Letters,* 145(1–4), E1-E7.

Shotyk, W. (1997). Atmospheric deposition and mass balance of major and trace elements in two oceanic peat profiles, northern Scotland and Shetland Islands. *Chemical Geology,* 138, 55-72.

Shotyk, W., Weiss, D., Appleby, P.G., Cheburkin, A.K., Frei, R., Gloor, M., Kramers, J.D., Reese, S. et Van Der Knaap, W.O. (1998). History of atmospheric Lead deposition Since 12,370 ^{14}C yr BP from a peat bog, Jura Mountains, Switzerland. *Science,* 281(5383), 1635-1640.

Shotyk, W., Weiss, D., Kramers, J.D., R., F., Cheburkin, A., Gloor, M. et Reese, S. (2001). Geochemistry of the peat bog at Etang de la Gruère, Jura Mountains, Switzerland, and its record of atmospheric Pb and lithogenic trace metals (Sc, Ti, Y, Zr, and REE) since 12,370 ^{14}C yr BP. *Geochimica et Cosmochimica Acta,* 65(14), 2337-2360.

Shotyk, W., Krachler, M., Martinez-Cortizas, A., Cheburkin, A.K. and Emons, H. (2002). A peat bog record of natural, pre-anthropogenic enrichments of trace elements in atmospheric aerosols since 12 370 ^{14}C yr BP, and their variation with Holocene climate change. *Earth and Planetary Science Letters,* 199(1-2), 21-37.

Shotyk, W. and Krachler, M. (2010). The isotopic evolution of atmospheric Pb in central Ontario since AD 1800, and its impacts on the soils, waters, and sediments of a forested watershed, Kawagama Lake. *Geochimica et Cosmochimica Acta,* 74(7), 1963-1981.

Steinmann, P. and Shotyk, W. (1997). Geochemistry, mineralogy, and geochemical mass balance on major elements in two peat bog profiles (Jura Mountains, Switzerland). *Chemical Geology,* 138(1–2), 25-53.

Steinmann, P. et Shotyk, W. (1997). Chemical composition, pH, and redox state of sulfur and iron in complete vertical porewater profiles from two *Sphagnum* peat bogs, Jura Mountains, Switzerland. *Geochimica et Cosmochimica Acta,* 61(6), 1143-1163.

Stevenson, R.K., Meng, X.W. and Hillaire-Marcel, C. (2008). Impact of melting of the Laurentide Ice Sheet on sediments from the upper continental slope off southeastern Canada: evidence from Sm–Nd isotopes. *Canadian Journal of Earth Sciences,* 45(11), 1243-1252.

Sullivan, M.E. and Booth, R.K. (2011). The potential influence of short-term environmental variability on the composition of testate amoeba communities. *Environmental Microbiology,* 62, 80-93.

Tanaka, T., Togashi, S., Kamioka, H., Amakawa, H., Kagami, H., Hamamoto, T., Yuhara, M., Orihashi, Y., Yoneda, S., Shimizu, H., Kunimaru, T., Takahashi, K., Yanagi, T., Nakano, T., Fujimaki, H., Shinjo, R., Asahara, Y., Tanimizu, M. and Dragusanu, C. (2000). JNdi-1: a neodymium isotopic reference in consistency with LaJolla neodymium. *Chemical Geology,* 168(3–4), 279-281.

Tarnocai C., Kettles, I.M., and Lacelle, B. (2005). Peatlands of Canada Database Research Branch, Agriculture and Agri-Food Canada, Ottawa, Ontario, Canada, digital database.

Tarnocai, C. and Stolbovoy, V. (2006). Chapter 2: Northern peatlands: their characteristics, development and sensitivity to climate change In: *Peatlands: Evolution and Records of Environmental and Climate Changes.* (Martini, IP, Martınez-Cortïzas, A. and Chesworth, W. (eds) Vol. 9, p. 17-51). Amsterdam: Elsevier.

Tegen, I. et Fung, I. (1994). Modeling of mineral dust in the atmosphere: Sources, transport, and optical thickness. *Journal of Geophysical Research: Atmospheres,* 99(D11), 22897-22914.

Thibault, S. and Payette, S. (2009). Recent permafrost degradation in bogs of the James Bay area, northern Quebec, Canada. *Permafrost and Periglacial Processes,* 20(4), 383-389.

Tolonen, K. (1984). Interpretation of changes in the ash content of ombrotrophic peat layers. *Bulletin of the Geological Society of Finland,* 56, 207-219.

van Bellen, S., Garneau, M. and Booth, R.K. (2011). Holocene carbon accumulation rates from three ombrotrophic peatlands in boreal Quebec, Canada: Impact of climate-driven ecohydrological change. *The Holocene,* 21(8), 1217-1231.

Vanneste, H., De Vleeschouwer, F., Martínez-Cortizas, A., von Scheffer, C., Piotrowska, N., Coronato, A. and Le Roux, G. (2015). Late-glacial elevated dust deposition linked to westerly wind shifts in southern South America. *Scientific Reports,* 5

Vanneste, H., De Vleeschouwer, F., Bertrand, S., Martinez-Cortizas, A., Vanderstraeten, A., Mattielli, N., Coronato, A., Piotrowska, N., Jeandel, C. et Le Roux G. (Submitted). Elevated dust deposition in Tierra del Fuego (Chile) resulting from Neoglacial Darwin Cordillera glacier fluctuations. *Journal of Quaternary Science*.

Viau, A.E., Gajewski, K., Fines, P., Atkinson, D.E. and Sawada, M.C. (2002). Widespread evidence of 1500 yr climate variability in North America during the past 14000 yr. *Geology,* 30(5), 455-458.

Viau, A.E., Gajewski, K., Sawada, M.C. and Fines, P. (2006). Millennial-scale temperature variations in North America during the Holocene. *Journal of Geophysical Research: Atmospheres,* 111(D9).

Viau, A.E. et Gajewski, K. (2009). Reconstructing Millennial-Scale, Regional Paleoclimates of Boreal Canada during the Holocene. *Journal of Climate,* 22(2), 316-330.

Wang, T., Surge, D. and Walker, K.J. (2013). Seasonal climate change across the Roman Warm Period/Vandal Minimum transition using isotope sclerochronology in archaeological shells and otoliths, southwest Florida, USA. *Quaternary International,* 308–309, 230-241.

Wanner, H., Beer, J., Bütikofer, J., Crowley, T.J., Cubasch, U., Flückiger, J., Goosse, H., Grosjean, M., Joos, F., Kaplan, J.O., Küttel, M., Müller, S.A., Prentice, I.C., Solomina, O., Stocker, T.F., Tarasov, P., Wagner, M. and Widmann, M. (2008). Mid- to Late Holocene climate change: an overview. *Quaternary Science Reviews,* 27(19–20), 1791-1828.

Wanner, H., Solomina, O., Grosjean, M., Ritz, S.P. and Jetel, M. (2011). Structure and origin of Holocene cold events. *Quaternary Science Reviews,* 30(21–22), 3109-3123.

Wedepohl, K.H. (1995). The composition of the continental crust. *Geochimica et Cosmochimica Acta,* 59(7), 1217-1232.

Weiss, D., Shotyk, W., Rieley, J., Page, S., Gloor, M., Reese, S. et Martinez-Cortizas, A. (2002). The geochemistry of major and selected trace elements in a forested peat bog, Kalimantan, SE Asia, and its implications for past atmospheric dust deposition. *Geochimica et Cosmochimica Acta,* 66(13), 2307-2323.

Woodland, W.A., Charman, D.J. et Sims, P.C. (1998). Quantitative estimates of water tables and soil moisture in Holocene peatlands from testate amoebae. *The Holocene,* 8(3), 261-273.

Yafa, C., Farmer, J.G., Graham, M.C., Bacon, J.R., Barbante, C., Cairns, W.R.L., Bindler, R., Renberg, I., Cheburkin, A., Emons, H., Handley, M.J., Norton, S.A., Krachler, M., Shotyk, W., Li, X.D., Martinez-Cortizas, A., Pulford, I.D., MacIver, V., Schweyer, J., Steinnes, E., Sjobakk, T.E., Weiss, D., Dolgopolova,

A. and Kylander, M. (2004). Development of an ombrotrophic peat bog (low ash) reference material for the determination of elemental concentrations. *Journal of Environmental Monitoring,* 6(5), 493-501.

Yin, Y., Wurzler, S., Levin, Z. et Reisin, T.G. (2002). Interactions of mineral dust particles and clouds: Effects on precipitation and cloud optical properties. *Journal of Geophysical Research: Atmospheres,* 107(D23), 19-14.

Yu, Z., Campbell, I.D., Campbell, C., Vitt, D.H., Bond, G.C. and Apps, M.J. (2003). Carbon sequestration in western Canadian peat highly sensitive to Holocene wet-dry climate cycles at millennial timescales. *The Holocene,* 13(6), 801-808.

Zdanowicz, C.M., Zielinski, G.A., Wake, C.P., Fisher, D.A. and Koerner, R.M. (2000). A Holocene record of atmospheric dust deposition on the Penny Ice Cap, Baffin Island, Canada. *Quaternary Research,* 53(1), 62-69.